Multi-dimensional mycelia interactions

A thesis submitted to Cardiff University for the degree of Doctor of Philosophy

By

Jade O'Leary, B.Sc (Hons)

February 2018

DECLARATION

This work has not been submitted in substance for any other degree or award at this or any other university or place of learning, nor is being submitted concurrently in candidature for any degree or other award.

Signed …… (candidate) Date ……

STATEMENT 1

This thesis is being submitted in partial fulfilment of the requirements for the degree of PhD.

Signed …… (candidate) Date ……

STATEMENT 2

This thesis is the result of my own independent work/investigation, except where otherwise stated. Other sources are acknowledged by explicit references. The views expressed are my own.

Signed …… (candidate) Date ……

STATEMENT 3

I hereby give consent for my thesis, if accepted, to be available for photocopying and for inter-library loan, and for the title and summary to be made available to outside organisations.

Signed …… (candidate) Date ……

STATEMENT 4: PREVIOUSLY APPROVED BAR ON ACCESS

I hereby give consent for my thesis, if accepted, to be available for photocopying and for inter-library loans **after expiry of a bar on access previously approved by the Academic Standards & Quality Committee.**

Signed …… (candidate) Date ……

Acknowledgements

I would like to thank my supervisors, Dr Carsten Müller and Professor Dan Eastwood for all their time and advice, and especially Professor Lynne Boddy for her tireless dedication and infectious enthusiasm. Thanks to the Natural Environment Research Council (NERC) for studentship NE/L00243/1 and for funding UHPLC-MS analyses at the NERC Biomolecular Analysis Facility, Birmingham (NBAF-B). Many thanks also to all the technical staff, bioinformaticians and statisticians at NBAF-B: Professor Mark Viant, Dr Ulf Sommer, Dr Clement Heude, Dr Jasper Engle and Kas Houthujis, for all their hard work and for teaching me that MS data needn't be scary.

I will always be grateful to the fungal ecology group: Dr Jen Hiscox, Dr Mel Savoury, Sarah Johnston, Emma Gilmartin, Marta Misiak and Yu Fukasawa, for all their assistance, teachings and advice, and to Katie Journeaux for being a brilliant project student. Huge thanks go to 6th floor office friends: Fred Windsor, Hisham Razi, Ifan Jâms, Willow Smallbone, Rhidian Thomas, Katie Dunkley and Mike Reynolds, for many laughs over the last three years. Thank you to all my non-science friends, especially Fi, Lizzie, Stew and Dave, for always providing me with an adventure buddy when times have gotten hard, and massive thanks to Pat, who has never failed to put a smile on my face. Finally, I'd like to thank my brothers, Rhys and Sam, for always humbling me with their own ridiculous achievements, and of course, Mum and Dad, for their life time of support and encouragement.

Statement of contributions

The contributions of colleagues and students to the work presented in this thesis are explicitly detailed below:

Chapter 3: Dr Jen Hiscox and Dr Mel Savoury collaborated on experimental set up, field work and harvesting procedures. Andrew Langley and Stewart McDowell assisted Dr Jen Hiscox with enzyme assays.

Chapter 7: Katie Journeaux collaborated on practical lab work and bioinformatics.

Chapter 8: Professor Mark Viant provided invaluable advice on experimental design. Dr Ulf Sommer ran UHPLC-MS analyses and conducted bioinformatics and metabolome annotation. Dr Jasper Engle and Kas Houthuijs collaborated on statistical analysis.

Table of contents

Summary

The activities of competing wood decay fungi bring about the decomposition of deadwood. The rate of decomposition is determined by the community composition, which is shaped by competitive interactions. Fungi compete with one another for territory and resources within 3-dimensional space via the production of an arsenal of inhibitory chemical compounds, yet interspecific interactions and chemical warfare within communities have never before been studied in 3-dimensional resources. This thesis, therefore, aims to determine how interactions cause metabolic processes to change, and, by the use of novel 3-dimensional systems, how those processes are affected by increased species diversity and spatial heterogeneity. Overarching hypotheses which have driven investigations are: (1) secondary metabolism and interaction outcome are inherently linked, both of which are affected by environmental conditions, (2) changes to spatial distributions and increased species diversity cause interaction outcomes and community dynamics to alter, and (3) changes to metabolic strategies for antagonism and resource utilisation will reflect alterations to community dynamics.

Transitive interactions in pair-wise 2-dimensional systems often became intransitive in species richer 3-dimensional systems, and the extent of patch fragmentation determined the length of coexistence of individuals within communities. Production of secondary metabolites comprising the fungal chemical weaponry, namely extracellular lignocellulolytic enzymes and volatile organic compounds (VOCs), was significantly different between 2- and 3-dimensional systems, between systems of varied species diversity, and between different spatial distributions of fungi, reflecting the observed changes to community dynamics. Furthermore, the production of intracellular metabolites which function in the biosynthesis pathways of antimicrobial compounds and agents of decay, was affected by species diversity, spatial distributions and territory fragmentation. Additionally, secondary metabolism and interaction outcome were found to be inherently linked, and affected by abiotic conditions. Specifically, interaction

outcomes changed under different temperatures, and when wood was pre-colonised for different lengths of time. Changes to the production of both enzymes and VOCs reflected the different outcomes, as either the cause or effect of outcome changes. These conclusions not only confirm the thesis hypotheses, but also demonstrate the importance of environmental conditions, species diversity and spatial dynamics to fungal community dynamics and forect ecosystem functioning.

List of figures

List of tables

List of abbreviations

ABTS	2,2'-Azino-bis(3-ethylbenzothiazoline-6-sulfonic acid)
ANOVA	Analysis of variance
ASCA	ANOVA simultaneous component analysis
Ba	*Bjerkandera adusta*
C	Carbon
CAS	Chemical abstracts service
Cp	*Coniophora puteana*
CRS	Competitive, stress-tolerant, ruderal
D	Deadlock
DIMS	Direct infusion mass spectrometry
DMAB	3-(Dimethyl amino)-benzoic acid
DOCs	Diffusible organic compounds
DVB	Divinylbenzene
EDTA	Ethylene diamine tetraacetate
EI	Electron impact
ESI	Electron spray ionization
FC	Fold change
FDR	False discovery rate
FT-ICR	Fourier transform ion cyclotron resonance
FT-ICR	Fourier transform
GAPDH	D-glycealdehyde-3-phosphate dehydrogenase
GC	Gas chromatography
GC-MS	Gas chromatography and mass spectrometry
GH	Glycoside hydrolase
GLM	Generalized linear model

HE	Hydrocarbon equivalents
Hf	*Hypholoma fasciculare*
IMS	Ion mobility spectrometry
IZ	Interaction zone
KEGG	Kyoto Encyclopedia of Genes and Genomes
KNN	K-nearest neighbour
LC	Liquid chromatography
LC-MS	Liquid chromatography and mass spectrometry
LDAs	Lignin-degrading auxiliary enzymes
Lip	Lignin peroxidases
LMEs	Lignin modifying enzymes
m/z	Mass-charge ratio
MA	Malt agar
MBTH	3-Methyl-2-benzothialone-hydrazone hydrochloride
Mn	Manganese
MnP	Manganese peroxidases
MS	Mass spectrometry
MUF	4-Methylumbelliferol
NIST	National Institute of Standards and Technology
NMR	Nuclear magnetic resonance
OPLS-DA	Orthogonal projection to latent structures-discriminant analysis
PCA	Principal components analysis
PDMS	Polydimethylsiloxane
Pi	Inorganic phosphate
Po	*Pleurotus ostreatus*

PQN	Parallel quasi-Newton
PR	Partial replacement
PTR-MS	Proton transfer reaction mass spectrometry
Pv	*Phanerochaete velutina*
QC	Quality control
QQQ	Triple quadrupole
R	Replacement
RI	Retention index
ROS	Reactive oxigen species
SEM	Standard error of the mean
SESI-MS	Secondary electrospray ionization mass spectrometry
Sg	*Stereum gausapatum*
Sh	*Stereum hirsutum*
SPME	Solid phase microextraction
TD	Thermodesorption
TD-GC-TOF-MS	Thermal desorption time-of-flight mass spectrometry
TOF	Time-of-flight
Tv	Trametes versicolor
UHPLC-MS	Ultra-high performance liquid chromatography mass spectrometry
Vc	*Vuilleminia comedens*
VOCs	Volatile organic compounds
VP	Versatile peroxidases

List of publications

Sections of Chapter 2, specifically '2.3.2 Multispecies interactions' and Figure 2.1, form part of the following review paper which has been accepted for publication:

Hiscox, J., O'Leary, J. & Boddy, L. (2018) Fungus Wars: basidiomycete battles in wood decay. *Studies in Mycology*, 89, 117-124.

A version of Chapter 5 has been accepted for publication as:

O'Leary, J., Eastwood, D.C., Müller, C.T. & Boddy, L. (2018) Emergent properties arising from spatial heterogeneity influence fungal community dynamics. *Fungal Ecology*, 33, 32-39.

Chapter 1. General introduction

1.1 Temperate forest ecosystems and the accumulation of dead wood

Forest ecosystems cover approximately a third of the total global land mass, with tropical, boreal and temperate forests accounting for 48, 30 and 22 % of global forested areas respectively (Keenan et al. 2015). The forests of Central and Western Europe are primarily temperate, and temperate forest is also located in some regions of North America, the Mediterranean and north-eastern Asia, as well as some parts of New Zealand and southern Chile (Lal & Lorenz 2012). These regions are characterised by warm wet summers and mild winters, supporting a species rich biota (Martin et al. 2001). They comprise a highly diverse mixed flora of conifers, broad-leaved deciduous and broad-leafed evergreen trees, such as alder (*Alnus glutinosa*), birch (*Betula pendula*), oak (*Quercus robur*), elm (*Ulmus minor*) and beech (*Fagus sylvatica*) (Ciesla 2002). Temperate forest trees reduce carbon dioxide during photosynthesis, fixing carbon (C) within their biomass, some of which is lost through oxidation processes during photo- and autotrophic respiration (approximately 560 g m^{-2} per annum). 15 kg m^{-2} of C, however, is accumulated and stored as plant biomass within temperate forests every year (Martin et al. 2001).

There is a volume of between 8 and 20 m^3/ha of dead wood in European temperate forest ecosystems that arrives on the forest floor every year (Forest Europe 2012). It is a vital element, storing sequestered C, minerals and nutrients. It provides habitats for a range of organisms including mammals, birds, invertebrates, bryophytes, lichens and fungi (Humphrey et al. 2004), functions as a rooting substrate for seedlings (Narukawa & Yamamoto 2002), contributes to the stability of soils by preventing surface water runoff (Kraigher et al. 2002), and increases forest productivity (Debeljak 2006). The activities of dead wood decomposers release organic molecules from the substrate, 'unlocking' stored nutrients and making them available for plants

(Merganičová et al. 2012), and releasing C which is fed into the carbon cycle (Allison & Treseder 2008).

1.2 Wood decomposers – drivers of the carbon cycle

A relatively narrow range of saprotrophic basidiomycete fungi, and even fewer ascomycetes, are the major agents of wood decomposition (Hibbet et al. 2007). They are able to breakdown the recalcitrant lignocellulose, the primary component of wood, and convert it into monomeric compounds (Eriksson et al. 1990; Doddapaneni et al. 2013). These fungi may arrive at a resource as spores, or spread from other resources as mycelium. Fungi that are only able to spread to new resources as spores are termed resource-unit-restricted, and are, therefore, usually less combative than mycelial spread non-resource-unit-restricted fungi, which can form patches of dense mycelial aggregates, or cords, allowing them to access and utilise larger quantities of nutrients (Boddy & Hiscox 2016). Individual fungi may fall into a defined category of ecological strategy (CRS: competitive, ruderal, stress-tolerant), or a combination of strategies, which may vary during different life cycle stages, or between physiologically different regions of the same mycelia (Boddy & Hiscox 2016). The differences in life history strategies largely determine the ability of individuals to initiate primary resource colonisation, to compete against subsequent resource colonisers, and to retain captured territory within the resource (Boddy 2000). Community development, therefore, is dependent on individual colonisation ability and antagonistic potential against other invaders during interactions. The shape of the community determines the rate at which dead wood is decomposed, since different individuals decompose wood at different rates, thus, community composition determines the rate at which C is unlocked and fed into the C cycle.

1.3 Thesis aims

This thesis describes a study which set out to explore the interactions of wood decay fungi, and the metabolic processes that govern fungal interactions during decomposition. Traditionally,

interactions have been studied by pairing fungi, a method which allows easy manipulation and produces highly valuable information regarding interaction dynamics. In nature, however, multiple fungal individuals interact with each other within 3-dimensional resources, resulting in communities whose compositions are constantly changing. This study set out to determine how interactions cause metabolic processes to change, and, by the use of novel 3-dimensional systems (Figure 1.1), how those processes are affected by increased species diversity and spatial heterogeneity. Overarching hypotheses which have driven investigations are: (1) secondary metabolism and interaction outcome are inherently linked, both of which are affected by environmental conditions, (2) changes to spatial distributions and increased species diversity cause interaction outcomes and community dynamics to alter, and (3) changes to metabolic strategies for antagonism and resource utilisation will reflect alterations to community dynamics.

Chapter 2 reviews the literature on interactions between wood decay fungi and describes the mechanisms by which antagonism takes place. It discusses secondary metabolism by fungi, including the enzymatic strategies by which fungi compete with one another and decompose lignocellulose, the ecological role of volatile organic compounds (VOCs), and the role of intercellular metabolism during interactions. Throughout Chapter 2, the main thesis hypotheses outlined in the current chapter are justified.

Chapter 3 investigates the link between enzyme activity in decaying wood and the outcomes of interactions between the well characterised fungus *Trametes versicolor* and six other wood decay basidiomycetes, and assesses the stability of that relationship under environmental change. Microclimatic effects on interaction outcomes and enzyme activity were investigated by performing experiments at two controlled temperatures in the laboratory, and in the field, and the length of time that a fungus had been exploiting the substrate was considered by using wood pre-colonised for different lengths of time.

Chapter 4 directly follows by exploration of VOC evolution during pair-wise interactions, and its relationship with interaction outcomes. Experiments were conducted at two controlled temperatures in the laboratory, and wood was pre-colonised for different lengths of time. VOC extracts were analysed by thermal desorption gas chromatography time-of-flight mass spectrometry (TD-GC-TOF-MS), a more sensitive VOC detection method than the solid phase microextraction (SPME) fibres that have been used previously.

Chapter 5 examines the dynamics of a three species community with comparisons between 2- and 3-dimensional systems. Spatial distributions and patch size dynamics were investigated for their roles in species coexistence, and how interactions change over different spatial dimensions was determined.

Chapter 6 begins to unravel the functional physiology of wood decay during interactions within 2- and 3-dimesnional competitive systems. Activity of 12 lignin and cellulose decomposing enzymes by a three species community competing within 3-dimensional systems of varying patchiness was quantified. The competitive network of the community within each 3-dimensional spatial pattern was determined and compared to the competitive hierarchy determined by pair-wise competition, and enzyme activity was assessed throughout.

Chapter 7 directly follows by investigating VOC production by the community described in Chapter 6. Again, production during 2-dimensional pair-wise interactions was compared with production by the community within 3-dimensional resources. The coexistence potential of the community, largely mediated by patch fragmentation, was linked to VOC production, and possible ecological roles of specific compounds are discussed.

Chapter 8 further investigates metabolism during interactions in 2- and 3-dimesnional systems by quantifying the production of the full set of wood breakdown products, small non-diffusible secondary metabolites, hormones and signalling molecules by *T. versicolor* in the systems studies in Chapters 6 and 7. Non-targeted ultra-high performance liquid chromatography mass

spectrometry (UHPLC-MS) was used to maximum coverage of the metabolome, and, where possible, LC-MS spectra were putatively identified and metabolites of importance linked to metabolic pathways.

Chapter 9 reflects on the findings of the previous chapters and contextualises them as a whole within the broader literature. It discusses the successes within experimental design whilst highlighting the limitations. Finally, it outlines research priorities for the future, and concludes the thesis studies.

Figure 1.1 Photographs of interaction set ups used within the studies of this thesis. (A) Paired *F. sylvatica* blocks, as in Chapters 3 and 4, containing *T. versicolor* (right hand-side block) and *H. fasciculare* (left hand-side block). *H. fasciculare* mycelial fans can be seen starting to surround the *T. versicolor* block. (B) Ecologically relevant 3-dimensional 27-block experimental systems, as used in Chapters 5, 6, 7 and 8. Aggregated mycelium of *V. comedens* can be seen where it occupied a larger adjacent volume of territory, but same total territory as its competitors, *T. versicolor* and *H. fasciculare*, which are dispersed throughout the remainder of the cube.

Chapter 2. Wood decay basidiomycetes: their interactions and metabolism

2.1 Abstract

The combined activities of individuals within a community of wood decay fungi bring about decomposition. Within these communities, fungi are constantly competing for space and resources, battling with their neighbours which shapes the structure of the community. Chemical warfare is initiated when competitive fungi meet, and a vast number of lignocellulose degrading extracellular enzymes and volatile organic compounds (VOCs) are produced for both antagonistic and defensive purposes. The mechanisms by which fungi antagonistically interact with one another and their enzymatic attack of lignocellulose are well reviewed, what is not known is the role of intracellular metabolites during interactions in wood, and the pathways that regulate them. The literature regarding interspecific competition, extracellular enzyme and VOC production is reviewed below, and the potential application of metabolomics to the study of decomposition processes is discussed.

2.2 Introduction

Wood decay fungi rarely decompose wood alone, instead they reside within complex communities of interacting individuals, the structure of which is constantly changing, driving ecosystem dynamics (Deacon et al. 2006; Hansen et al. 2008). Since different species decay wood at different rates and in different ways, for example, in their physical alteration of wood, suite of chemicals produced and the relative proportion of substrate used (Hiscox et al. 2015b), understanding the interactions of fungi is vital to comprehend fully wood decay processes. During the decomposition process, extracellular enzymes are deployed which facilitate the breakdown of deadwood (Lundell et al. 2010), VOCs that function in interspecific signalling and antagonism are released (Wheatley 2002; El Ariebi et al. 2016), and individuals regulate themselves internally, likely protecting against attack (Peiris et al. 2008). The production of extracellular enzymes and VOCs change during interactions (Evans et al. 2008; Hiscox et al. 2010a; Hiscox et al. 2010b; El Ariebi et al. 2016), and it is vital to understand how fungi chemically modify and decay wood in order to understand the importance of secondary metabolism in fungal antagonism. Fungal mechanisms of combat, the role of enzymes in wood decay, and the ecological role of VOCs and intracellular metabolites are considered below. The function of secondary metabolites during antagonism is also discussed.

2.3 Interspecific fungal interactions

Wood decay basidiomycetes participate in a whole spectrum of interaction types, including mutualism and commensalism, but the most common type when interacting within wood is competition (Boddy 2000). Fungi interacting with one another within a woody resource are competing for territory, since a fungus that occupies a particular region can potentially occupy and utilise all of the resources within that territory (Hiscox et al. 2015a). Interference competition (combat) may result in deadlock (neither fungus gains territory held by another fungus), replacement (one fungus gains the territory held by another), partial replacement (one

fungus partially gains territory of another) or even mutual replacement (both fungi partially gain territory held by the other) (Boddy 2000). The K-selected characteristics of later stage resource colonisers (secondary colonisers) frequently lend them greater combative fitness than the early resource colonisers (primary colonisers) (Boddy 2000). This often results in a hierarchy of combative ability between specific species combinations which is usualy transitive, where species A is more combative than species B which is more combative than species C: late-secondary colonisers > early-secondary colonisers > primary colonisers. However, small changes to environmental conditions can cause interactions to become intransitive (Woodward & Boddy 2008), where no one species is most dominant, like in a game of rock-paper-scissors. Chapter 5 outlines intransitive interactions in more detail.

2.3.1 Mechanisms of combat

The mechanisms by which fungi antagonistically interact occur following contact, but they can also occur at a distance. Following contact and non-self-recognition, a particular fungus might employ a single mechanism, or a variety of mechanisms depending on the identity of the competitor and conditions. Hyphal interference results in cytoplasmic damage and finally the death of the section of the opponent's hypha or spore that was contacted by the hypha of the more combative fungus (Boddy 2000). For example, in interactions between *Phlebiopsis gigantea* and *Heterobasidion annosum*, *P. gigantea* hyphae caused vacuolation of the cytoplasm of contacted *H. annosum* hyphae (Ikediugwu et al. 1970; Ikediugwu 1976), and a similar observation was made during biocontrol trials of *Grosmannia clavigera* in pulpwood by *P. gigantea* (Behrendt & Blanchette 2001). When the basidiomycete *Coprinopsis cinerea* and the ascomycetes *Podospora* spp. were confronted with the mycelia of antagonists, peroxidases were accumulated in large quantities at the interaction zone and linked to hyphal interference. Other studies suggest that secreted proteins with antifungal activity are involved in this mechanism (Kaiserer et al. 2003; Deacon 2013). It is possible that hyphal interference occurs by the

synergistic activity of several species-specific substances. Enzymes involved in antagonism are discussed more thoroughly in section 2.4.

A few species of wood decay fungi are able to parasitise others. Mycoparasitism is a species-specific interaction involving host recognition by a lectin-carbohydrate interaction, penetration of the host hypha and production of cell wall-lytic enzymes and secondary metabolites (Section 2.4), and finally bio- or necrotrophic assimilation of host nutrients (Whipps 1987; Chet et al. 1997; McQuilken et al. 2003). The most widely studied mycoparasites, *Trichoderma* species, are invasive necoparasites (i.e. unspecialised parasites with a broad host range) whose hyphae coil around and penetrate host hyphae releasing toxic metabolites and enzymes (Lorito et al. 2010). They therefore serve as important biological control agents of soil-borne plant-pathogens (López-Mondéjar et al. 2011). Usually, parasitism by wood decay fungi is a temporary strategy which facilitates the capture of large domains held by the mycelia of competitors (Rayner et al. 1987). The mycoparasite can then utilise the nutrients within its now larger domain of wood, and interact with competitive fungi by gross mycelial contact (see next paragraph for details) (Boddy 2000).

Gross mycelial contact is characterised by a change in the morphology of interacting mycelia (Boddy 2000; Donnelly & Boddy 2001). This is clearly visualised in agar culture and across soil trays where morphological changes such as pigmentation (Woodward & Boddy 2007), physical barrages, mycelial fans, invasive cords and rhizomorphic structures (Boddy 2000) are easily identified (Figure 2.1). The redox activities of phenoloxidase, laccase and peroxidase are associated with gross mycelial contact (Section 2.4), as has been demonstrated during interactions between *Trametes versicolor* and five wood decay basidiomycetes (Hiscox et al. 2010a).

A fascinating and unusual method of combat, though common in the Fungal Kingdom, occurs at a distance in the absence of mycelial contact. It is mediated by diffusible organic compounds

(DOCs) or VOCs (Sonnenbichler et al. 1994) which are usually non-fatal, instead inhibiting growth rate and enzyme activity (Mackie & Wheatley 1998), and effects can be transient as a decrease in antagonist growth rate is often followed by recovery (Humphris et al. 2002). DOCs and VOCs are also important in many antagonistic interactions following hyphal/mycelial damage. Section 2.5 reviews VOCs in more detail.

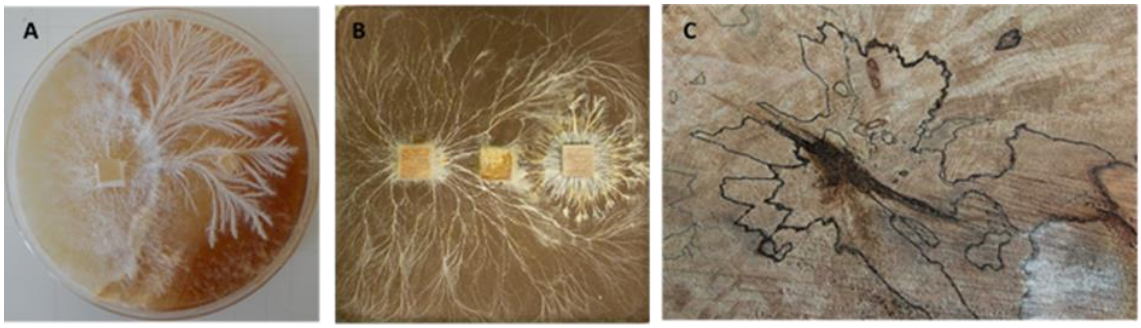

Figure 2.1 Fungal interactions in agar culture (A), across soil trays (B) and in wood (C). A: *Resinicium bicolor* (left) and *Phanerochaete velutina* (right) interacting on 2 % malt extract agar. *R. bicolor* can be seen producing mycelial cords. B: Wood blocks colonised with *P. velutina* (left), *Sterium hirsutum* (middle) and *Hypholoma fasciculare* (right) were placed onto trays of compacted non-sterile soil. *P. velutina* and *H. fasciculare* produced foraging mycelial cords. Pigmentation associated with antagonistic enzyme production surrounds the *H. fasciculare* colonised wood block. C: Fungal interactions within beech wood produce interactions zone lines and pseudosclerotial plates.

2.3.2 Multispecies interactions

The physical structure of fungal communities is often visible in cross-sections of decaying logs and branches, as different mycelia often stain the wood in different ways, or surround themselves with melanised barriers called pseudosclerotial plates (Figure 2.1). Most research on interactions has focused on pair-wise combinations of fungi due to the challenges of working with multispecies systems. Pair-wise combinations, however, are not always accurate predictors of outcomes of multispecies interactions, and outcomes are often less consistent in systems with multiple competitors (Hiscox et al. 2017). On the few occasions that multispecies interactions have been studied they have usually been conducted within 2-dimensional systems (Schoeman et al. 1996; Boddy & Abdalla 1998; White et al. 1998; Sturrock et al. 2002; A'Bear et al. 2013; Toledo et al. 2016; Maynard et al. 2017a). For example, Toledo *et al*. (2016) compared three-species interactions with pair-wise interactions in agar culture revealing differences in outcomes due to additional competition and the positioning of individuals within the three-species system, and A'Bear *et al.* (2013) assessed the effects of elevated temperature and invertebrate grazing on three-way fungal interactions across 2-dimensional soil trays. The spatial orientation of competitors, especially whether or not a competitor is surrounded by others, also affects outcomes in wood block interactions (White et al. 1998; Hiscox et al. 2017). Additionally, multispecies interactions may result in increased species coexistence within the resource. For example, pair-wise interactions in beech (*Fagus sylvatica*) wood blocks between the secondary coloniser *T. versicolor* and the late secondary colonisers *Hypholoma fasciculare* and *Phanerochaete velutina*, resulted in replacement of *T. versicolor* and *H. fasciculare* by *P. velutina*, and deadlock between *T. versicolor* and *H. fasciculare*. However, when all three species interacted simultaneously, *T. versicolor* retained its original territory and coexisted with its competitors for longer (Hiscox et al. 2017).

Overall, the increased species diversity and inconsistency of outcomes resulting from multispecies interactions makes community development within decaying wood very difficult to predict. Furthermore, fungal communities in the natural environment interact within 3-dimensional resources, and spatial heterogeneity within substrates alters community dynamics, e.g. may promote coexistence, by providing spatial refuges and reducing the rate at which individuals encounter one another (Huffaker 1958; Brockhurst et al. 2005) (discussed in detail in Chapter 5). Yet differences between interactions in 2-dimensions and more heterogeneous 3-dimensions have not previously been tested. Specifically, how community dynamics are altered as a result of increased species diversity (e.g. pair-wise verses three or more species interactions), and by changes to the spatial location/distribution of individuals within 3-dimensional structures (hypothesis 2: Chapter 1) should be tested (Chapter 5).

2.4 Fungal secondary metabolism and enzymatic decay

Fungi readily produce a large variety of secondary metabolites, such as enzymes, that, unlike primary metabolites, are not directly involved in organism growth. Secondary metabolites are usually low molecular weight, bioactive compounds derived from polyketides and non-ribosomal peptides (Keller et al. 2005; Brakhage 2013). Given the dynamic ecosystems where fungi reside and the complex nature of interspecific competition and interactions with other microorganisms, it is probable that secondary metabolites evolved for use as chemical signals in communication, antagonism, and for resource defence (Yim et al. 2007: Brakhage & Schroeckh 2011), as well as for resource utilisation (Lynd et al. 2002). Despite major efforts to identify biosynthetic genes for these compounds in light of recently available fungal genome sequences (Grigoriev et al. 2014), the exact role of secondary metabolites in fungal ecology and the pathways that regulate them are still largely unknown. Production has been linked to genes encoding the regulation of sexual and asexual reproduction (Fox & Howlett 2008) and

morphological differentiation processes (Calvo et al. 2002), however, the mechanisms behind these remain relatively unclear.

2.4.1 Wood, and the role of extracellular enzymes in lignocellulose decomposition

Lignin, cellulose and hemicellulose comprise three main polymeric constituents of lignocellulose (Higuchi et al. 1997). Cellulose is composed of β-1,4-linked D-glucopyransosyl units (Nevell & Zeronian 1985) that form linear, long chain homopolymers and constitute over 50 % of woody weight (Martíinez et al. 2005). Hemicelluloses differ in their molecular structure between plant species but retain the common feature of a "decorated" main chain preventing the hemicellulose molecules aggregating, with side groups often containing a carboxylic acid group. A complex structure of dimethoxylated, monomethoxylated and non-methoxylated phenylpropanoid units derived from p-hydroxycinnamyl alchohols make up the three-dimensional network that is lignin (Martíez et al. 2005). Lignin is often distributed with hemicelluloses in the spaces between intercellulose microfibrils in primary and secondary plant cell walls. This recalcitrant polymer is found in its highest concentration, however, in the middle lamella where it acts as a cementing agent connecting cells and hardening xylem tissue cell walls, hence contributing to the mechanical resistance of wood to chemical and biological degradation (Fengel & Wegener 1984; Higuchi 1990).

The oxidative systems of wood decay fungi and their methods of enzymatic decay of lignin classify them broadly into three rot types: soft-rot, white-rot and brown rot (Goodell et al. 2008; Martinez et al. 2009; Floudas et al. 2012). White-rot fungi, which account for over 90 % of all wood decay fungi (Janusz et al. 2017), possess a decomposition pathway whereby they extracellularly secrete oxidative enzymes, breaking down the recalcitrant lignin polymer either simultaneously with all other woody constituents (as occurs in hardwood wood types), selectively in the absence of cellulose (as occurs in hardwood and softwood), or a combination of both (Higuchi 1993). Brown-rot fungi, which mainly grow on softwoods, only partially modify

lignin by demethylation. Genome sequencing of the brown-rot fungi *Postia placenta* (Martinez et al. 2009) and *Serpula lacrymans* (Eastwood et al. 2011) concluded that brown-rot fungi lack the necessary enzymes for lignin depolymerisation, termed lignin modifying enzymes (LMEs), namely lignin peroxidases (LiP), manganese peroxidases (MnP), versatile peroxidases (VP) and laccases (Maciel et al. 2010). Instead, a strategy is employed which breaks down cellulose by hydrolysis and causes the demethylation of lignin, leaving a residue of modified lignin which is not decomposed (Tang et al. 2013). Soft-rot typically occurs in wood with a low lignin content by Ascomycota fungi and related asexual taxa, and is characterised by biconical, cylindrical cavities in the secondary wood cell wall (Blanchette et al. 2004). Compared to white-rot and brown-rot fungi, little is known about the enzymatic machinery that contributes to decomposition by soft-rot fungi (Goodell et al. 2008).

Genomic studies have revealed that glycoside hydrolase (GH) families GH6 and GH7 endoglucanase, which include the crystalline cellulose attacking cellobiohydrolase genes (Baldrian & Valásková 2008), are present in all white-rot lineages but absent in brown-rot lineages (Martinez et al. 2009; Eastwood et al. 2011; Floudas et al. 2012). GH5 endoglucanase encoding genes and pectinases, however, are present in greater abundances in brown-rot species, implying that GH5 endoglucanases may be involved in intracellular enzyme diffusion (Eastwood et al. 2011). This suggests that brown-rot fungi may use easily diffused low molecular weight chemicals to breakdown cellulose in the absence of lignin degrading enzymes (Kubicek 1990). However, despite the collective comparative analyses of white- and brown-rot gene repertoires and expression profiles revealing substantial variation between the two rot types, there is still considerable uncertainty regarding the precise mechanisms of rot employed by different fungal species (Hori et al. 2013). Additionally, the results of a phylogenetically informed principal-components analysis (PCA) of 33 basidiomycete genomes (Riley et al. 2014), suggest little dichotomy between the two models of enzymatic wood decay, suggesting that the categorisation of rot-types is not as clear cut as once thought.

It is important to note that strategies for the enzymatic attack of lignocellulose are also used by fungi as mechanisms of antagonism, i.e. extracellular enzymes are produced during hyphal interference, mycoparasitism and gross mycelial contact (Section 2.3.1). Specific examples are given in sections 2.4.2 and 2.4.3.

2.4.2 Lignin modifying enzymes (LMEs)

LMEs are essential for lignin decay, oxidatively catalysing its breakdown to CO_2 and H_2O (Lundell et al. 2010). Mineralization of lignin, however, often requires simultaneous action by additional enzymes known as lignin-degrading auxiliary enzymes (LDAs) (da Silva Coelho-Moreira et al. 2013; Janusz et al. 2017) which cannot decay lignin alone.

The main LME peroxidases, namely lignin peroxidases (LiP), manganese peroxidases (MnP) and versatile peroxidases (VP), belong to the superfamily catalase-peroxidases (Zamocky et al. 2014) which is divided into three sub-classes: class I catalase-peroxidases, prokaryotic and eukaryotic organelle-localised heme peroxidases, class II extracellular fungal secreted heme peroxidases, and class III plant secreted heme peroxidases (Passardi et al. 2007; Kamocky et al. 2009; Janusz et al. 2017). Class II peroxidases contain a prosthetic group of protoporphyrin IX (Pollegioni et al. 2015) and function via a catalytic cycle to oxidise a range of organic and inorganic compounds (Box 1). Hydrogen peroxide acts as a primary catalyst during this reaction, where oxidised substrate molecules gradually reduce the enzyme back to its native state, releasing two water molecules and organic radicals that subsequently form oxidised end-products (Lundell et al. 2010).

Box 1. LME peroxidase catalytic cycle.

LME peroxidase + H_2O_2 → Compound 1 + H_2O

Compound 1 + reduced substrate → Compound 2 + oxidised substrate

Compound 2 + reduced substrate → LME peroxidase + oxidised substrate + H_2O

LiP that is capable of depolymerising lignin is relatively non-specific, oxidising both aromatic phenolic molecules and a range of non-phenolic molecules in lignin, as well as a variety of other organic compounds (Wong 2009). LiPs were first described in the extensively studied white-rot fungus *Phanerochaete chrysosporium* (Tien and Kirk 1983; Paszczynski et al. 1986; Kirk and Farrell 1987), and more recently in *Phlebia tremellosa* (Dosdall et al. 2017) and *Pleurotus ostreatus* (Fernández-Fueyo et al. 2014). They are secreted as sets of various isozymes and isoforms (Santhanam et al. 2012) and are able to oxidise substrates that other peroxidases cannot due to their high redox potential (approximately 1.2 V at pH 3) (Sigoillot et al. 2012). However, LiP activity is variable and often not detected during wood decomposition, even when LiP gene expression is detected (Hiscox et al. 2010a; Hiscox et al. 2010b).

MnP oxidises Mn (II) to Mn (III), which is able to oxidise phenolic compounds in lignin (Forrester et al. 1988), but not non-phenolic compounds (Kirk & Farrell 1987). Mn (III) diffuses from the enzyme into the lignocellulose substrate where it is chelated with organic acids such as fumarate, malate and oxalate (Sigoillot et al. 2012), and functions as a low molecular weight redox mediator, oxidising organic compounds (Goszczynski et al. 1994).

VPs are glycoproteins that are secreted as several isoenzymes and were first detected in *Pleurotus* species (Ruiz-Duenas et al. 1999; Ruiz-Duenas et al. 2001) and more recently in *Bjerkandera fumosa* (Rodakiewicz-Nowak et al. 2006). The hybrid nature of these enzymes allow them to efficiently oxidase substrates that MnP and LiP alone cannot (Eriksson & Bermek 2009).

They are essentially a hybrid of the molecular architecture of LiP and MnP. They can transfer electrons from aromatic donors and consequently oxidise non-phenolic compounds without Mn ions, similar to LiPs (Perez-Boada et al. 2005), however, they also contain a Mn-blinding site allowing them to efficiently oxidise Mn (II) to Mn (III) (Ruiz-Dueñas & Martínez 2009).

Another group of LMEs are laccases, also known as phenol oxidases, which function in the oxidation of a range of phenolic and low-redox potential compounds using molecular oxygen as an electron acceptor (Janusz et al. 2017). Overall, phenolic substrate compounds donate four electrons, and the resultant reactive phenoxy radicals undergo subsequent chemical reactions which oxidise quinones or oligomeric products (Box 2; Lundell et al. 2010). Laccases are multicopper oxidases containing four copper atoms located within two metal centres (Garavaglia et al. 2004). Laccase may be secreted extracellularly or intracellularly, functioning intracellularly in the transformation of phenolic compounds within the cell (Baldrian 2006).

Box 2. Laccase catalytic cycle.

$$\text{Laccase} + O_2 \rightarrow \text{Laccase-O-O-H}$$

$$\text{Laccase-O-O-H} + 2\ H \rightarrow \text{Laccase-OH} + H_2O$$

$$\text{Laccase-OH} + 4\ \text{Phenolic substrate compounds} \rightarrow \text{Laccase} + 4\ \text{reactive phenoxy radicals} + H_2O$$

In addition to decomposition processes, LME production is also associated with interspecific interactions between fungi. Reactive oxygen species (ROS), produced by laccase, oxidases and peroxidases, often increase in abundance and accumulate in localised regions where fungi meet, termed the interaction zone (Eyre et al. 2010). For example, laccase activity in the interaction zone of *T. versicolor* and *Stereum gausapatum* increased by 14-fold that of monocultures (Hiscox et al. 2010a). The exact role of ROS' is unclear, but it has been suggested that they may function

directly in the oxidative damage of competitor mycelia (Silar 2005), increase resource utilisation aiding combat, or detoxify VOCs and diffusible compounds produced by competitors (Baldrian 2004).

2.4.3 Non-ligninolytic enzymes

Cellulose is depolymerised by the synergistic activities of glycosyl hydrolase enzymes, which cleave glycosidic bonds with a water molecule (Davies & Henrissat 1995), yielding glucose as the sole product (Horn et al. 2012). The synergistic activities involve the cleavage of internal cellulose chain bonds by endo-1,4-β-glucanases, attack of the reducing and/or non-reducing end of the cellulose polymer by exo-1,4-β-glucanases, and the conversion of cellobiose by β-glucanases (Horn et al. 2012). Exo-glucanase enzymes involved in this process may be processive, meaning they thread a single polysaccharide chain through the enzyme's catalytic site continuously, yielding multiple disaccharides (Horn et al. 2006). Processive exo-1,4-β-glucanases, termed cellobiohydrolases, are hugely important as approximately 70 % of cellulases produced by fungi are cellobiohydrolases belonging to GH6 and GH7 families (Annamalai et al. 2016).

Enzymes involved in nutrient acquisition are also produced during wood decay. For example, chitinases, which hydrolyse β1–4 bonds in N-acetylglucosamine monomers found in chitin chains, were produced when *H. fasciculare*, *R. bicolor* and *Coniophora arida* were synergistically decaying wood with *Fomitopsis pinicola* (Lindahm & Finlay 2006), likely functioning in the breakdown and nitrogen uptake of opponent fungal chitinous walls (Patil et al. 2000). Additionally, acid phosphatase, which releases inorganic phosphate (Pi) from organophosphates in mycelia (Reys et al. 1990), was produced during interactions of 10 basidiomycetes against *T. versicolor* on wood (Hiscox et al. 2010b). Enzyme activity of both LMEs and non-lignin modifying enzymes, therefore, appear to be important mechanisms of interspecific antagonism during decay, and it would be logically hypothesised that interaction outcome and enzyme

activity are inherently linked (hypothesis 1: Chapter 1). A previous study which paired five basidiomycetes against *T. versicolor* found that while interaction outcomes differed between different pairings, there was no clear link between outcomes and enzyme activity (Hiscox et al. 2010a). However, outcomes of interactions between identical pairings are known to change under different environmental conditions (Hiscox et al. 2016a), but differences in enzyme activity between pairings whose outcomes changed under different conditions is not known. The relationship between interaction outcome and enzyme activity, therefore, should be further investigated by assessing enzyme activity during interactions under a variety of abiotic conditions (as in Chapter 3).

Investigations into enzyme activity during interactions have commonly been performed on artificial media (Eyre et al. 2010; Hiscox et al. 2010a), however, a study that assessed enzyme activity in fungi grown on agar and beech (*F. sylvatica*) wood blocks found that production varies extensively between the two substrates (Hiscox et al. 2010b). Additionally, all other previous studies assessed enzyme production during interspecific pairings. However, as interaction outcomes alter when species diversity is increased (Toledo et al. 2016; Hiscox et al. 2017), and spatial heterogeneity causes changes to community dynamics (Brockhurst et al. 2005), enzyme activity and the consequential rate of decomposition is likely to differ during community interactions within more complex 3-dimensional structures, compared to pair-wise interactions (hypothesis 3: Chapter 1). Enzyme activity, and the production of other secondary metabolites, should therefore be compared between 2- and 3-dimensional systems of varied species diversity and spatial dynamics (Chapters 6,7,8).

2.5 Fungal secondary metabolism: volatile organic compounds

During secondary metabolism a range of side products are produced by fungi including VOCs. VOCs are low molecular weight aliphatic and aromatic chemicals that readily vaporise at 0.01 kPa and 20 °C (Pagans et al. 2006). In excess of 1000 microorganism-derived organic

compounds have currently been identified (Lemfack et al. 2014), and more than 300 of those recognised in fungi (Hung et al. 2015). Volatile production by fungi has been described (Rapior et al. 2000; Rosecke et al. 2000; Konuma et al. 2015; Isidorov et al. 2016; Isaka et al. 2017), with their functions linked to a variety of processes including hormone signalling (Bennett et al. 2012), semiochemical attraction and deterrence of saproxylic insects (Leather et al. 2014), signals for host plant interactions (Lee et al. 2016) and interspecific antagonism and defence (Hynes et al. 2007; Evans et al. 2008; El Ariebi et al. 2016). For example, the fungivorous beetle, *Bolitophagus reticulatus*, was able to differentiate between different VOCs produced by the basidiomycete *Fomes fomentarius* in order to assess host quality (Holighaus et al. 2014), and metabolism by *Arabidopsis thaliana* was inhibited by the VOCs of three ascomycete fungi (Splivallo et al. 2007). Elucidating the function of individual compounds is not usually possible as VOCs are commonly extracted from the headspace of microcosms. Additionally, a specific bouquet of complementary compounds are often required for the facilitation of different functions (Morath et al. 2012), and so testing the effects of lots of chemicals singly is not usually beneficial. Some studies, however, have investigated individual synthetically produced VOCs, e.g. 1-octen-3-ol, and determined their functional roles in antagonism and growth suppression. 1-Octen-3-ol, the most commonly reported fungal VOC, is produced as a product of linoleic acid breakdown (Bennett et al. 2012) and significantly supressed conidia germination frequency of *Penicillium paneum* (Ascomycota) in a self-inhibitory mechanism of regulatory spore germination (Chitarra et al. 2004). Also, when grown in the presence of 1-octen-3-ol, *A. thaliana* expressed known defence genes, indicating recognition of the fungal produced antagonistic chemical (Kishimoto et al. 2007).

Research on VOC production by interacting wood decay fungi has shown that profiles change differentially in response to the presence of specific competitors. For example, the interaction between *T. versicolor* and *S. gausapatum* yielded eight VOCs that were not produced by either fungus singly, but in the interaction between *T. versicolor* and *H. fasciculare* there were no

interaction-specific VOCs produced (Evans et al. 2008). Additionally, specific compounds produced by *H. fasciculare* and *R. bicolor* when interacting were not produced when *H. fasciculare* was interacting with *P. velutina* and *vice versa*, and inhibitory effects of VOCs on mycelial extension rate were species specific, highlighting the role of VOCs in carbon cycling processes as mediators of community development (El Ariebi et al. 2016).

More than 30,000 terpenoid compounds have been reported (Connolly & Hill 1991), and a diverse range of terpenoids, in particular sesquiterpenes, are produced by fungi (El Ariebi et al. 2016), often functioning during antagonistic interactions. The structural diversity of sesquiterpenes arises from the assembly of their 15-carbon backbone and the distinct arrangement of functional groups and substituents upon the structural scaffold (Chappell & Coates 2011). Sesquiterpene hydrocarbons were associated with toxin synthesis by the ascomycete *Penicillium roqueforti* (Jeleń 2002), and the sesquiterpene α-cadinol and derivatives synthesised from it showed antifungal activity against three wood decay basidiomycetes (Wu et al. 2005). Also, the sesquiterpene heptelidic acid, which inhibits D-glycealdehyde-3-phosphate dehydrogenase (GAPDH) therefore altering ATP generation (Siddiquee 2014), was isolated from three ascomycetes, *Gliocladium virens*, *Chaetomium globosum*, and *Trichoderma viride*, and was antimicrobial against the bacterium *Bacteroides fragilis* (Itoh et al. 1980).

Although biotic effects on VOCs have been investigated, of all the studies on VOC production by wood decay fungi during interactions, none have assessed the influence of abiotic factors, such as temperature, which does cause microbial VOC profiles to change (Schade & Custer 2004; Asensio et al. 2007). Since VOC production by wood decay fungi is complex and species specific, complete understanding of VOC production by fungi decaying wood alone and how that changes when faced with a range of competitors under different environmental conditions is vital for understanding fully the role of VOCs within forest carbon dynamics. Whilst assessing these changes in pairs of fungi will produce crucially important information (Chapter 4), VOC

production by communities of fungi should also be assessed (Chapter 7), as the knowledge regarding the relationship between species diversity and the role of VOCs is simply missing at present.

The production of VOCs is biologically dynamic imposing constraints to the technological and methodological sampling of these compounds, an impediment that has contributed to the limited scope of study of VOCs compared with other fungal metabolites, e.g. enzymes (Morath et al. 2012). That being said, advances in the field have been made. For example, carbon coated thermal desorption (TD) tubes have proven to be far superior in their collection of a wider range of compounds than the solid phase microextraction (SPME) fibres used in the past (discussed in Chapter 4). However, the field is not without its challenges, and accurate identification of collected compounds is still a difficult process. Methods of VOC collection and analytical instrumentation are discussed in detail in Supplementary Material 2.1.

2.6 Metabolomics

Metabolomics is defined as the combined qualitative and quantitative analysis of the full complement of naturally occurring small molecules (metabolites) required by an organism, or group of organisms, for maintenance, growth and cellular function. The 'metabolome' of an organism is made up of thousands of these metabolites including lipids, amino acids, sugars, vitamins, organic acids and nucleotides, that are products of cellular metabolism (Jones et al. 2013), and as the final product downstream of the genome, an organism's metabolome most closely reveals the phenotype or function of the cell (Dunn 2008). The field of metabolomics is relatively young compared to other well established 'omics techniques (i.e. genomics, transcriptomics, proteomics), and was only applied to environmental sciences at the beginning of the 21st century with, for example, the use of nuclear magnetic resonance (NMR) spectroscopy combined with multivariate statistical analyses to diagnose disease in shellfish (Viant et al. 2003) and examine invertebrate responses to environmental toxins (Warne et al.

2000). While metabolomics is increasingly being applied to biological systems, to our knowledge, analytical techniques have not been applied to a comprehensive metabolomics project in fungal mediated wood decay. Metabolomics has, however, been applied to fungal cultures in natural products research (Bertrand et al. 2013), in the study of fungal phytopathogens (Low et al. 2009; Tan et al. 2009), and interacting basidiomycetes on agar (Peiris et al. 2008; Luo et al. 2017) and in liquid medium (Xu et al. 2018). Previously, it was shown that wood decay fungi alter intracellular metabolite production differently during interactions compared to monocultures. For example, *Stereum hirsutum* increased metabolite production when it was losing to a competitor, and decreased metabolite production when it was winning (Peiris et al. 2008; more details in Chapter 8), and novel metabolites were produced when *T. versicolor* was interacting with a variety of competitors compared to monocultures (Luo et al. 2017; Xu et al. 2018; details in Chapter 8). However, no previous metabolomics project has been conducted on wood decay fungi in wood. It is well known that both gene expression of wood decay fungi (Cánovas et al. 2017) and metabolite production (Hiscox et al. 2010b) differ substantially when fungi are growing on artificial media compared to natural wood substrates. Therefore, in order to fully characterise intracellular metabolism and its role in interspecific competition during wood decay, a large-scale metabolomics study must be performed on wood decay fungi interacting in wood (this is done for the first time in Chapter 8). Furthermore, as with the production of enzymes and VOCs, it is not known how resource heterogeneity (2- or 3-dimensions), species diversity and distribution patterns of individuals within 3-dimensional resources affects intracellular metabolism (hypothesis 3: Chapter 1), and experiments testing these variables should be carried out (Chapter 8).

Within the field of metabolomics, there is a vast array of analytical instrumentation. The relative benefit and limitation of each instrument type can vary depending on sample type, polarity of metabolites, and on whether a targeted (quantification of pre-selected, known metabolites) or non-targeted (quantification of the entire metabolome of an organism, often with a lot of

uncharacterised/unknown metabolites) experimental approach is used (Viant & Sommer 2012). The emergence of new technologies, such as ultra-high performance metabolomics, are hugely exciting in their potential for novel discoveries regarding wood decay fungal physiology, given the scale of data generated by these techniques and the fact that they have not previously been applied to wood decay fungi during decay. Analytical instrumentation for the study of metabolomics is discussed in more detail in Supplementary Material 2.2.

2.7 Conclusions

Despite the wealth of knowledge regarding interspecific fungal interactions, their enzymatic attack of lignocellulose and the function of VOC production, very little is known regarding the production of secondary metabolites under environmental change. Further, fungal decay occurs by the combined activities of multiple individuals within 3-dimensional resources, yet the effects of species diversity and spatial distributions within resources have never been tested on the production of extracellular enzymes or VOCs. This thesis aims to address these knowledge gaps. Additionally, a large scale metabolomics study of the metabolic processes that regulate cellular function during decay by wood decay fungi has never before been conducted. Excitingly, new technologies are emerging that have the potential to fill this void and produce novel findings regarding cellular processes and organism physiology. Chapter 8 presents the first study of this kind and assesses the metabolic pathways that regulate interspecific interactions during decay.

Chapter 3. Abiotic conditions alter metabolic processes during the competitive interactions of wood decay fungi: Extracellular enzyme production

3.1 Abstract

The terrestrial carbon cycle is largely facilitated by the metabolic activities of saprotrophic fungal decomposers that enzymatically breakdown dead wood in forest ecosystems, releasing sequestered carbon. Dynamic fungal wood decay community contribution to forest biogeochemical processes is expected to be critical in response to increasing global temperatures. To understand how decomposition processes drive community structure and substrate utilisation in forest systems under environmental change, pair-wise interactions of a community of basidiomycete fungi were assed under 3 different microclimate conditions (15 °C and 25 °C controlled laboratory conditions, and a field site setting), with wood pre-colonised for longer used in some cases. The activities of 12 lignin/cellulolytic enzymes and the rate of decomposition were assessed. Abiotic conditions influenced outcomes of interactions which were reflected by changes to enzyme activity, and enzyme activity altered throughout the course of interactions reflecting interaction progression and changes to territory occupation. Wood that was pre-colonised for longer prior to interactions decayed most slowly, while temperature had little impact on the rate of decomposition. However, altered temperature did cause changes to individual dominance and the suite and activity of lignocellulose degrading enzymes, underlining the importance of understanding the impact of community structure on carbon cycling in forest ecosystems under a changing climate.

3.2 Introduction

Sequestration of CO_2 in forest ecosystems is pivotal to the global carbon cycle. The Intergovernmental Panel on Climate Change (IPCC 2007) estimated that between 1993 and 2003, 3,300 Mt CO_2 yr^{-1} were stored within terrestrial forest sinks in soils and dead wood (Post et al. 1982; Venugopal et al. 2016). Wood decay basidiomycete fungi play an essential role in these ecosystems, decomposing 120 t km^{-1} yr^{-1} of wood and releasing the fixed carbon and nutrients therein (White 2003), resulting in CO_2 efflux (Cox et al. 2000). The community composition of wood decay fungi and the rate at which they decompose wood vary with temperature (Hiscox et al. 2016a), and likely regulate climate feedbacks to the carbon cycle (Allison & Treseder 2008). The average global temperature has increased by 0.8 °C since 1900 (Hansen et al. 2006) and is predicted to increase a further 1.5-2.0 °C by 2100 (IPCC 2013), which is predicted to increase the rate of wood decomposition (Davidson & Janssens 2006).

Fungal communities are dynamic systems, the composition of which is constantly changing (Boddy 2001). A high species diversity of wood decayers can enhance the rate of decomposition (Maynard et al. 2017b), especially under changing temperature regimes (Toljander et al. 2006). In the natural environment, complete wood mineralisation is achieved by complex communities, rather than individual species (Boddy 2000), and increased production of extracellular enzymes occurs during competitive interactions between wood decay fungi (Hiscox et al. 2010a; Hiscox et al. 2010b; Crowther et al. 2011; Hiscox & Boddy 2017). The ability of wood decay fungi to produce different extracellular enzymes varies between species and individuals (Eichlerová et al. 2015). Furthermore, enzyme production and activity varies considerably between different combinations of fungi (Hiscox et al. 2010a).

Metabolic processes during wood decay vary depending on environmental conditions. For example, the activity of nine lignin and cellulose decomposing enzymes increased in angiosperm forest soil samples as temperature increased from -5 °C to 30 °C, with 63-69 % total annual

enzyme activity being recorded during the warmest period of the year (Baldrian et al. 2013). The outcomes of interactions also vary with changes in temperature, and historical occupancy (Hiscox et al. 2017) leading to changes in community composition and, therefore, the local enzyme pool. Environmentally induced alterations to lignin/cellulolytic enzyme production during competitive interactions, however, has not previously been assessed. Yet in a constantly changing microenvironment, and with climate change and other global environmental stressors imposed on top of this, understanding fungal interactions and enzyme production under varied environmental conditions is crucial to fully comprehending wood decomposition processes and decay, and how these might alter in the future.

In this study, wood blocks colonised by six wood decay basidiomycetes were paired against *Trametes versicolor* under three different microclimates (15 °C and 25 °C controlled laboratory conditions, and a field site setting experiencing variable temperature regimes). Wood that had been pre-colonised for different lengths of time was used in some cases, mimicking decay-induced structural and chemical modifications to the resource. The outcomes of interactions and rate of decomposition were assessed. The hypothesis that the outcomes of interactions would be affected by environmental conditions and that changes in enzyme activity would reflect those changes, was tested by (1) assessing the activity of four ligninolytic and eight cellulolytic enzymes in the actively competing region (interaction zone) of interactions with a range of interaction outcomes, in laboratory versus field conditions; (2) quantifying enzyme activity in samples where interaction outcomes changed as a result of environmental conditions; and (3) measuring enzyme activity in the interaction zone and non-interacting region of *T. versicolor* and *Hypholoma fasciculare* blocks over the time taken for the interaction to fully resolve. It was also hypothesised that changes to substrate utilisation in blocks pre-colonised for different lengths of time would mean interaction outcomes would differ between blocks colonised for a longer or shorter time.

3.3 Methods

3.3.1 Colonisation of wood blocks

Seven species of native, beech (*Fagus sylvatica*)-inhabiting fungi, typical of different successional stages of wood decay (Table 3.1), were used to colonise 30 x 30 x 30 mm beech wood blocks. The blocks were sterilised by autoclaving three times, with 48 h intervals between autoclave cycles, then placed onto cultures of single strains on 0.5 % malt agar (MA; 5 g l^{-1} malt extract, 15 g l^{-1} agar; Lab M, UK) and incubated in the dark at 20 °C for 12 or 24 weeks. At the end of the pre-colonisation period, block densities were determined for each strain as dry weight/fresh volume (g cm^{-3}; 10 replicates).

3.3.2 Interactions set up

Blocks that had been pre-colonised for 12 weeks were scraped free of adhering mycelium 48 h before interactions were established. Immediately after scraping, blocks were marked on the corners of each block using a pyrography iron to indicate the identity of the strain colonising the block (Figure 3.1). Blocks were paired together with cut vessels touching so that the wood grain ran in the same direction, and with markings on the corners furthest from the region of contact, and held together using a sterile elastic band, or plastic coated garden wire (Poundland, UK) to which an aluminium forestry tag had been attached for blocks that were placed in the field. Interactions were set up between the *T. versicolor* heterokaryon and *Vuilleminia comedens*, *Coniophora puteana*, *Bjerkandera adusta*, *Pleurotus ostreatus*, *Hypholoma fasciculare*, or *Phanerochaete velutina*, and between the *T. versicolor* homokaryon and *V. comedens* or *C. puteana*. Self-pairings of all strains used were also set up.

For controlled temperature experiments, blocks were placed onto perlite (30 ml; Homebase, UK) moistened with sterile distilled water to achieve a water potential of -0.012 kPa (determined by the method of Fawcett & Collins-George 1967), in plastic 200 ml lidded pots (Cater4you, UK).

A hole in the pot wall (1x2 mm diameter) covered in microporous surgical tape (3M, UK) allowed aeration. Five replicates of each pairing combination were incubated at 15 °C, or 25 °C and were harvested 1, 14, 28, 56, and 84 d after interactions were established.

Paired blocks were also placed in a mixed deciduous (predominantly beech) woodland site in Whitestone Woods, Tintern (lat/lon 51.723105/-2.691886), in a 10 x 10 m area divided into 25 grid squares. Each grid square contained one replicate of each pairing for a certain time point (i.e. each square contained one replicate of 16 different pairing combinations). Hourly temperature readings were taken using dataloggers distributed randomly across the site (3 replicates; TinyTag, UK; Supplementary Figure 3.1). Pairings were assorted randomly within each grid square and held in position with tent pegs. Five replicates of each pairing combination were collected 1, 14, 28, 56, and 84 d after interactions were established.

The effect of pre-colonisation time on interaction progress and outcomes was assessed by pairing blocks pre-colonised for either 12 or 24 weeks (densities of blocks sacrificed after pre-colonisation are given in Supplementary Figure 3.2). Interaction combinations studied in this experiment included *T. versicolor* heterokaryon with *V. comedens*, *H. fasciculare*, or *P. velutina*. Pairings were incubated at 15 °C. Interactions were established where: (1) *T. versicolor* blocks were pre-colonised for 12 weeks and competitor blocks for 24 weeks, (2) *T. versicolor* blocks were pre-colonised for 24 weeks and competitor blocks for 12 weeks, and (3) both *T. versicolor* and competitor blocks were pre-colonised for 24 weeks. Self-pairings of all fungi in blocks pre-colonised for 24 weeks were also set up. Interactions and self-pairings where both *T. versicolor* and the competitor had been pre-colonised for 12 weeks were performed as part of the temperature experiment.

Table 3.1 Details of experimental species. Cultures were obtained from isolated mycelia from wood or fruit bodies and their identifications confirmed by ITS rRNA sequencing.

Species	Abbreviation	Isolate ID	Provenance	Successional role	Rot type	Homo/heterokaryon
Trametes versicolor	TvM	TvAW-H	Cardiff University Culture Collection	Secondary coloniser	White	Homokaryon
	Tv	TvAW-HxFP	Mated strain: TvAW-H with TvFP664-SSI from Clark University, MA, USA	Secondary coloniser	White	Heterokaryon
Vuilleminia comedens	Vc	VcWVJH1	Cardiff University Culture Collection	Primary coloniser	White	Heterokaryon
Coniophora puteana	Cp	Cp EMPA#62	EMPA, Switzerland	Primary coloniser	Brown	Homokaryon
Bjerkandera adusta	Ba	BaSS1	Cardiff University Culture Collection	Secondary coloniser	White	Heterokaryon
Pleurotus ostreatus	Po	Po-JWHW2014	Public University of Navarre	Secondary coloniser	White	Heterokaryon
Hypholoma fasciculare	Hf	HfGTWV2	Cardiff University Culture Collection	Late secondary coloniser/cord former	White	Heterokaryon
Phanerochaete velutina	Pv	Pv29	Cardiff University Culture Collection	Late secondary coloniser/cord former	White	Heterokaryon

3.3.3 Harvest and re-isolation procedures

For the field experiment, blocks were returned to the laboratory and cleaned, and any unusual surface features (e.g. production of fruit bodies) were noted. For all experiments, blocks were split into quarters perpendicular to the point of contact with the paired block (along the grain) using a surface-sterilised chisel (Figure 3.1A). Contacting quarters from both blocks involved in the interaction were wrapped in foil; three matched quarters were flash frozen in liquid nitrogen and stored at -80 ^{o}C, whilst the remaining quarters were used for re-isolation and density determination. For re-isolations, the quarter-blocks were split into two perpendicular to the point of contact, and pieces of wood (~2 mm^3) excised 3.75, 11.25, 18.75 and 26.25 mm from the point of contact. These wood chips were inoculated onto 2 % MA and incubated at 20 °C until mycelia had emerged and could be identified morphologically. The other half of the quarter-blocks were used to determine final density from fresh volume and oven dry weight (mg mm^{-3}) (blocks collected at 84 d only) and weight loss was determined by comparison with a sample of 10 blocks per species sacrificed at the start of the experiment. The rate of weight loss (mg d^{-1}) for each species was calculated as the change in block densities between the end of the colonisation period, and interaction harvest. Using the territory occupied by each species at the end of the experiment, the expected contribution of each species to weight loss in each interaction was calculated. These expected values were then compared with the actual weight losses determined from each block following harvest to calculate the effect of interaction processes on block decomposition.

3.3.4 Enzyme extraction and assays

Specific interactions and regions of interactions were chosen for enzyme analysis based on the interaction outcomes determined after re-isolation onto agar (Figure 3.1). These were: (1) the pooled interaction zones of interactions of *T. versicolor* with *B. adusta*, *H. fasciculare*,

P. ostreatus and *P. velutina* and all relevant self-pairings in the field and at 15 °C (chosen because this was the highest temperature recorded by loggers during the field experiment), 14 d after interaction set-up; (2) specific regions of blocks from interactions of *T. versicolor* with *H. fasciculare* and *P. velutina* chosen based on interaction stage, at 15 °C, 25 °C and in the field (see Supplementary Table 3.1 for details of regions); and (3) all regions of interacting *T. versicolor* and *H. fasciculare* blocks over 84 d (total time taken for interaction to fully resolve). Statistical comparisons were made within these groups.

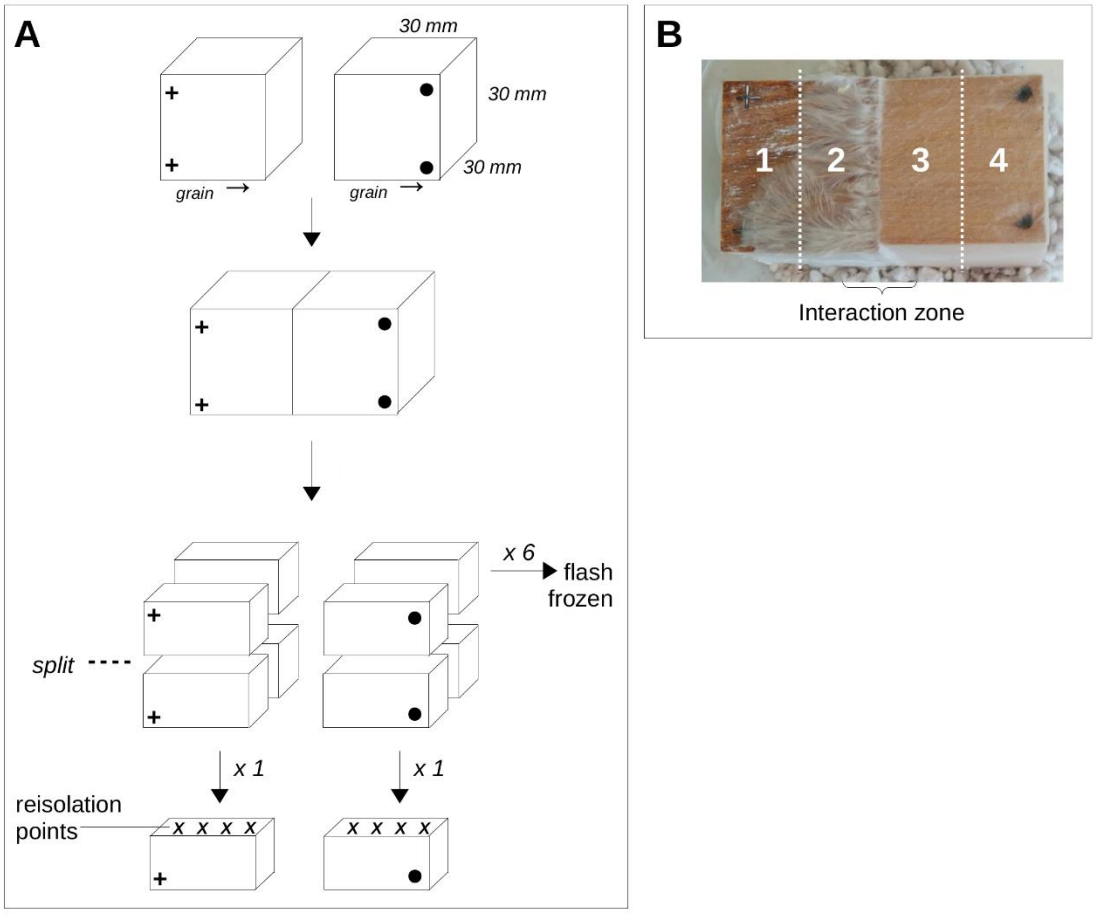

Figure 3.1 Experimental set up of interactions. (A) Wood block interactions under different conditions. (B) Regions from which extracts were taken for enzyme assays for interactions with *H. fasciculare* and *P. velutina* (See Supplementary Table 3.1 for specific details on sampled regions).

Blocks were removed from storage at -80 °C and freeze dried for 48 h (Edwards Modulyo, UK). Sawdust was generated from different regions of the blocks using a 4 mm drill bit. Enzyme activity assays were performed as per the protocol of Hiscox *et al*. (2010a). First, 0.5 g sawdust was shaken in 5 ml of 50 mM sodium acetate buffer (pH 5.0) at 4 °C overnight. The activities of the following terminal hydrolases were measured using 4-methylumbelliferol (MUF)-based substrates as described previously (Baldrian 2009; Šnajdr et al. 2011): β-glucosidase (EC 3.2.1.21), α-glucosidase (EC 3.2.1.20), cellobiohydrolase (EC 3.2.1.91), β-xylosidase (EC 3.2.1.37), N-acetylglucosaminidase (EC 3.2.1.30), phosphodiesterase (EC 3.1.4.1), phosphomonoesterase (EC 3.1.3.2) and arylsulfatase (EC 3.1.6.1). Briefly, substrates (40 µl in dimethylsulphoxide) at final concentration of 500 mM were combined with three technical replicates of 200 µL of samples (diluted 1:10) in a 96 well plate. Background fluorescence was determined by combining 200 µL sample (diluted 1:10) with 40 µl MUF standards. The 96 well plates were incubated at 40 °C and fluorescence recorded at 5 and 125 min using a Tecan Infinite microplate reader (Tecan, Switzerland) with an excitation wavelength of 355 nm and an emission wavelength of 460 nm. Quantitative enzymatic activities were calculated after blank subtraction based on a standard curve of MUF. One unit of enzyme activity was defined as the amount of enzyme releasing 1 mM of MUF min^{-1}.

Laccase (phenoloxidase; EC 1.10.3.2) activity was determined by monitoring the oxidation of 2,2'-azino-bis(3-ethylbenzothiazoline-6-sulfonic acid) diammonium salt (ABTS) in citrate-phosphate buffer (100 mM citrate, 200 mM phosphate, pH 5.0; according to Bourbonnais & Paice 1990), by monitoring the formation of green colouration spectrophotometrically at 420 nm. Three technical replicates were performed for each sample.

Manganese peroxidase (MnP; EC 1.11.1.13) activity was determined by monitoring spectrophotometrically at 595 nm the purple colouration from oxidative coupling of 3-methyl-2-benzothialone-hydrazone hydrochloride (MBTH) and 3-(dimethyl amino)-benzoic

acid (DMAB) in succinate-lactate buffer (100 mM, pH 4.5). Three technical replicates were performed for each sample. The results were corrected by activities of samples without manganese, and with ethylene diamine tetraacetate (EDTA) to chelate any Mn^{2+} present in the samples, allowing detection of Mn^{2+}-independent peroxidases (versatile peroxidase). The results were also corrected by activities of samples in the absence of H_2O_2, allowing detection of oxidase (but not peroxidase) activity.

Activities of enzymes within a sample were normalised to the protein content of that sample, determined using Qubit™ fluorometric assays (ThermoFisher Scientific Inc., UK).

3.3.5 Statistical analysis

All statistical analyses were conducted using R statistical software (R Core Team 2014). Mean enzyme activities (from 5 replicates) were compared using one-way analysis of variance (ANOVA) in combination with Tukey *post hoc* tests when data were normally distributed. Kruskal-Wallis tests followed by a Dunn's test *post hoc* procedure was used when data were non-normally distributed. The actual and expected weight losses following interaction harvest were compared using a one-way t-test (where the hypothesis was that the difference was significantly different to 0).

3.4 Results

3.4.1 Interaction outcomes change under different abiotic conditions

Generally, the combative ability of *T. versicolor* increased with temperature, and in some cases interaction outcomes were reversed under the different temperature regimes (Figure 3.2). For example, *T. versicolor* heterokaryon was partially replaced by *H. fasciculare* and *P. velutina* at 15 °C, but at 25 °C it deadlocked with *H. fasciculare* and partially replaced it in some replicates, and fully replaced *P. velutina*. The *T. versicolor* heterokaryon only partially replaced *V. comedens* and *P. ostreatus* at 15 °C but fully replaced both at 25 °C (Figure 3.2B). Interactions involving

T. versicolor against *C. puteana* and *B. adusta* were more consistent between the two temperatures, with *T. versicolor* replacing and deadlocking with the competitors in the majority of replicates respectively, although outcomes were more variable between replicates at the higher temperature. At 15 °C, the *T. versicolor* homokaryon was less combative than the heterokaryon: the homokaryon deadlocked with *V. comedens* and resulted in a variety of outcomes when interacting with *C. puteana* including partial replacement by *C. puteana* (Figure 3.2A), however, the heterokaryon deadlocked with *C. puteana* and partially replaced *V. comedens* in all replicates (Figure 3.2B). At 25 °C, interactions with *V.* comedens and *C. puteana* against both the *T. versicolor* heterokaryon and homokaryon were more similar to those at 15 °C involving the heterokaryon: *T. versicolor* fully replaced *V. comedens* and resulted in a variety of outcomes with *C. puteana* including total replacement by *T. versicolor* and deadlock (Figure 3.2B).

Under field conditions, outcomes of interactions of the *T. versicolor* heterokaryon with *B. adusta* and *H. fasciculare* and between the *T. versicolor* homokaryon and *V. comedens* more closely resembled those at 15 °C than at 25 °C (Figure 3.2). During interactions with all other competitors, *T. versicolor* was less combative in the field compared to either laboratory condition, gaining only small amounts of territory from its competitors and was fully replaced by *P. velutina* when in the field (Figure 3.2).

3.4.2 Pre-colonisation time alters combative abilities

T. versicolor was most combative when it had colonised the wood for the same or shorter time than its competitors (Figure 3.2B). For example, *T. versicolor* replaced *P. velutina* when it had colonised the resource for the same time or a shorter time than *P. velutina*, but it deadlocked and was replaced in two replicates when *P. velutina* had colonised the wood for a shorter time than it (Figure 3.2B). *T. versicolor* partially replaced *V. comedens* in all replicates when it was in

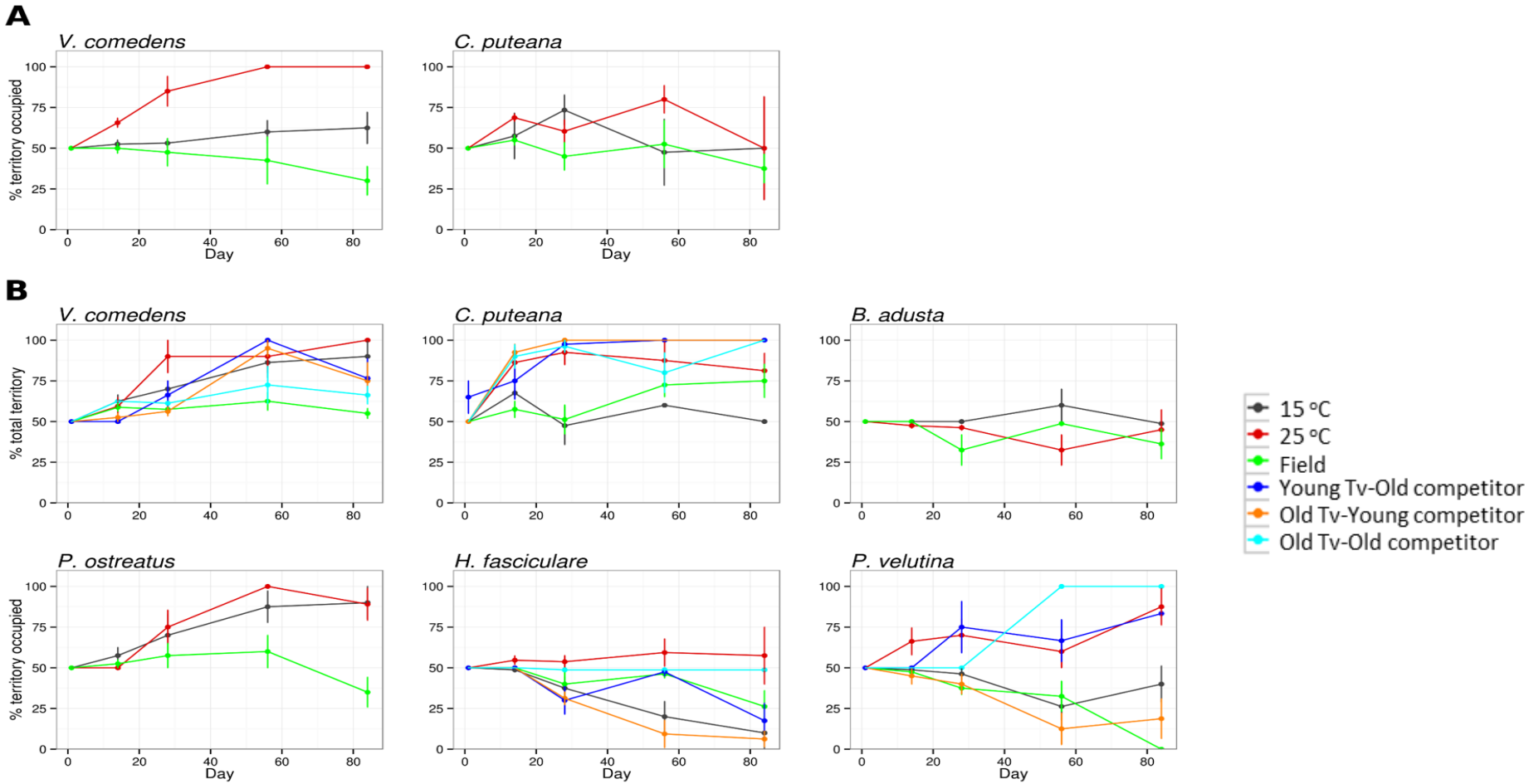

Figure 3.2 Percentage territory of resource occupied by *T. versicolor* homokaryon (A) and heterokaryon (B) throughout the duration of the interaction period (84 d). See Supplementary Table 3.2 for interaction outcomes and scores of combative ability.

less well decayed wood than *V. comedens*. When *T. versicolor* was in more decayed wood than *V. comedens*, however, interaction outcomes were more variable across replicates (as indicated by the error bars) and it replaced, partially replaced and deadlocked with *V. comedens* in 2, 1 and 1 replicates respectively. When paired with *C. puteana*, *T. versicolor* consistently fully replaced it regardless of pre-colonisation length (Figure 3.2B).

3.4.3 Competition affects enzyme activity during interactions in wood at 15 °C and in the field

Activity of some enzymes was significantly higher in wood block interactions that had been kept at a constant 15 °C compared to field interactions. This was observed in the *T. versicolor*, *B. adusta* and *H. fasciculare* self-pairing controls, and for the interaction between *T. versicolor* and *B. adjusta* (Table 3.2; Supplementary Figure 3.3). Of all the affected enzymes, β-glucosidase had the highest activity and in *T. versicolor* self-pairings it was significantly higher (3-fold increase) in the lab (15 °C) compared to in the field. Cellobiohydrolase, phosphodiesterase and β-xylosidase activity was also higher for *T. versicolor* self-pairings in the lab, with 9-, 4- and 5-fold differences in activity compared to in the field, respectively. Phosphodiesterase activity was also significantly higher at 15 °C than in the field in *H. fasciculare* self-pairings (4-fold difference), and MnP and cellobiohydrolase activity was significantly higher at 15 °C than in the field in *B. adusta* self-pairings and in the interaction between *T. versicolor* and *B. adjusta* respectively (60- and 4-fold differences respectively) (Table 3.2; Supplementary Figure 3.3).

Enzyme activity was sometimes affected by competition. For example, activity during the *T. versicolor* and *B. adusta* interaction was higher under both 15 °C and field conditions than in the *B. adusta* controls, although there was no difference compared to the *T. versicolor* controls in this case (Table 3.2; Supplementary Figure 3.3). In the interaction between *T. versicolor* and *P. ostreatus* at constant 15 °C, a greater number of enzymes were significantly affected by competition than in any other interaction, with α-glucosidase, β-glucosidase, phosphodiesterase, and β-xylosidase activity significantly lower than in the *T. versicolor* control,

Table 3.2 Enzyme activity of pooled interaction zones of *T. versicolor* and competitor blocks from the 15 °C laboratory experiment and the field experiment. Values are means of 5 replicates. ǂ Significant difference ($p < 0.05$) in activity compared with the same interactions under laboratory conditions. ϕ Significant difference ($p < 0.05$) in activity compared with the *T. versicolor* self-pairing control under corresponding environmental condition. Ω Significant difference ($p < 0.05$) in activity compared with competitor self-pairing control under corresponding environmental condition. (-) represents a failed assay.

	Activity mU g-1																	
	Tv-Tv		Ba-Ba		Tv-Ba		Hf-Hf		Tv-Hf		Po-Po		Tv-Po		Pv-Pv		Tv-Pv	
	Lab	Field	Lab	Field	Lab	Field	Lab	Field	Lab	Field	Lab	Field	Lab	Field	Lab	Field	Lab	Field
Laccase	76.23	32.52	3.07	0.98	48.18	48.61	5.48	0.00	333.40	63.37	3.03	4.25	91.70	57.53	0.00	0.00	119.66	49.43
MnP	12.43	0.00	60.37	0.00 ǂ	16.31	6.40	3.56	0.00	14.19	2.70	0.00	0.00	7.64	0.00	0.00	0.31	11.73	7.80
Peroxidase	0.00	1.40	1.17	1.00	1.63	0.25	0.00	10.42	2.35	0.00	3.87	19.53	1.25	1.34	0.00	6.17	1.34	6.95
α-glucosidase	99.60	64.49	0.94	0.00	47.19 Ω	16.19 Ω	3.30	2.98	13.75 ϕ	32.34	0.00	0.00	12.48 ϕΩ	7.29 ϕ	22.65	13.44	26.27	36.84
Cellobiohydrolase	55.40	5.96 ǂ	19.72	10.03	16.80	3.77 ǂ	2.29	2.24	7.41 ϕ	3.58	1.26	1.80	3.93 ϕ	3.13	24.92	7.01	9.90 ϕ	12.29
β-glucosidase	1142.86	362.92 ǂ	403.65	403.66	543.44	280.09	62.65	38.17	295.85 ϕ	200.18	85.48	74.52	305.94 ϕ	215.38	410.31	243.75	313.81 ϕ	363.88
Exochitinase	72.46	36.83	48.00	24.60	72.99	21.46	34.39	13.53	54.18	21.68	29.37	24.00	32.27	22.12	27.10	21.22	59.54	63.25
Acid phosphatase	2047.29	1230.11	173.67	209.33	2015.48 Ω	758.34	243.04	154.21	818.55	776.33	91.03	101.25	515.31 Ω	466.23	1435.57	1644.76	825.13	1164.58
Phosphodiesterase	132.27	33.37 ǂ	61.33	28.25	161.67	18.73	16.91	4.83 ǂ	67.13	21.16 Ω	5.11	4.76	12.51 ϕ	16.98	64.56	49.39	20.59 ϕΩ	17.30 Ω
Arylsulfatase	188.70	-	57.08	6.43	146.43	114.85	25.32	119.72	46.87	0.00	0.00	37.08	0.00	178.01	63.55	44.73	2.25	30.76
β-xylosidase	78.40	16.90 ǂ	15.40	9.64	23.52 ϕ	10.87	21.25	7.39	27.25	10.62	3.15	2.88	11.31 ϕ	8.25	10.85	7.97	13.88 ϕ	14.50

and α-glucosidase and acid phosphatase activity significantly higher than in the *P. ostreatus* control (Table 3.2; Supplementary Figure 3.3).

3.4.4 Enzyme activity reflects changes to interaction outcome caused by abiotic condition

Acid phosphatase was consistently the most active enzyme in the field and at constant 15 °C, particularly when *T. versicolor* was interacting with *P. velutina* (Table 3.3A,C; Supplementary Figure 3.4). Under both of these conditions, the outcome of interaction had no effect on acid phosphatase activity. Outcomes of the interaction between *T. versicolor* and *H. fasciculare* at 25 °C did effect acid phosphatase activity: activity was significantly higher ($p < 0.05$) when competitors deadlocked compared to when *H. fasciculare* was partially replaced. Similarly, β-glucosidase activity was higher when deadlock occurred (either early or late in the interaction process) between *T. versicolor* paired with *H. fasciculare* and paired with *P. velutina* under both controlled temperature treatments, compared to when partial replacement of a competitor occurred, although there were no significant differences in activity between deadlock and partial replacement in the field (Table 3.3; Supplementary Figure 3.4).

MnP activity was significantly associated with interaction outcome in all three environmental conditions. For both interactions tested (*T. versicolor* against *H. fasciculare* and *P. velutina*), different outcomes were associated with significantly different MnP, except when *T. versicolor* and *H. fasciculare* interacted in the field (Table 3.3; Supplementary Figure 3.4). Most notably, there was little or no activity when there was deadlock, whether early or late in the interaction process, but activity significantly increased when partial replacement of a competitor occurred during the interaction between *T. versicolor* and *P. velutina* at 15 °C and 25 °C. α-Glucosidase activity also significantly increased when *P. velutina* partially replaced *T. versicolor* at 15 °C, compared to when the competitors were in deadlock under the same conditions.

Table 3.3 Enzyme activity of interactions with *T. versicolor* against *H. fasciculare* and *P. velutina*. Different outcomes occurred as interactions progressed and specific replicates were sampled accordingly (see Supplementary Table 3.1 for details). (A) Activity in the 15 °C experiment. (B) Activity in the 25 °C experiment. (C) Activity in the field. Values are means of 5 replicates. ǂ Significant difference ($p < 0.05$) in activity compared with corresponding interaction at 15 °C. ϕ Significant difference ($p < 0.05$) in activity compared with corresponding interaction at 25 °C. Ω Significant difference ($p < 0.05$) in activity compared with corresponding interaction under field conditions. (-) represents a failed assay.

A	Activity mU g-1											
	Hf-Hf		Pv-Pv		Tv-Tv		Tv-Hf			Tv-Pv		
	Initial	Late	Initial	Late	Initial	Late	Initial deadlock	PR of Tv	R of Tv	Initial deadlock	PR of Tv	Late deadlock
Laccase	0.02	0.00	1.22 ϕΩ	1.05 ϕΩ	1.53 a	0.00 b	1.84	7.25	1.79	0.00 a	10.37 b Ω	0.26 a
MnP	5.85	21.20	15.69	15.79 Ω	7.82 Ω	3.08	0.00 a	13.77 b	9.18 ab	0.00 a	26.00 b	0.00 a
Peroxidase	1.22	24.80 ϕ	3.19 Ω	-	0.00	28.74	2.53	2.99	0.00	0.98	4.83	0.00
α-glucosidase	0.00 Ω	0.00	5.82	14.47 ϕΩ	43.69 ϕ	63.25	0.00 Ω	1.34 Ω	6.28	10.67 b	41.90 a	8.53 b
Cellobiohydrolase	0.00 Ω	0.00	0.00 a	16.98 b	7.75 ϕ	0.00 Ω	0.00	8.38	11.81	0.00 a	20.89 b	0.00 a
β-glucosidase	30.58	2.12 ϕΩ	71.34	0.38 ϕΩ	271.40	121.07	119.95 a ϕ	26.07 b ϕΩ	45.02 b	149.10 a ϕΩ	29.83 b Ω	145.97 a
Exochitinase	32.32	16.64	9.23	19.70 Ω	40.81 ϕ	27.83	29.15 ϕ	16.16	26.26	23.31 ab ϕ	62.58 a	11.46 b
Acid phosphatase	88.73 ϕ	68.78 Ω	979.04	1698.41 Ω	1339.15 ϕ	1711.30	332.30 ϕ	198.16	274.22	510.29 ϕ	806.31	423.92
Phosphodiesterase	1.16	0.00 Ω	56.78 ϕ	82.72 ϕΩ	84.41 ϕ	91.32	14.05 ϕ	0.00 Ω	0.82	25.32 ϕ	21.31	33.86
Arylsulfatase	0.00	9.11	9.27	14.59	0.00	0.00	0.00	3.58	4.00	9.08	4.03	3.05
β-xylosidase	70.00 a	0.00 b Ω	0.00	6.42 ϕ	37.56	15.09	10.60 ϕ	7.87	12.14	1.62 a	16.82 b	1.85 a
Oxidase	0.83	0.00	4.83	23.40	10.78	0.00	0.14	0.95	8.26	0.00	3.32	4.34

Table continues over page.

B	Activity mU g-1											
	Hf-Hf		Pv-Pv		Tv-Tv		Tv-Hf			Tv-Pv		
	Initial	Late	Initial	Late	Initial	Late	Initial deadlock	PR of Hf	Late deadlock	Initial deadlock	PR of PV	R of PV
Laccase	0.00	0.00	0.00 ǂ	0.00 ǂ	0.00	2.30 Ω	19.42 Ω	17.22	0.34	2.19 Ω	4.36	5.06
MnP	1.52	3.11	1.04	2.45 Ω	4.43	2.68	2.01 a	0.65 ab	0.00 b	0.00 a	11.20 b	0.53 a
Peroxidase	1.83 a Ω	0.00 b ǂ	0.77 Ω	0.00	0.48	0.00	0.90 a	0.03 ab	4.92 b	1.74	0.00	0.61
α-glucosidase	0.00	0.00	0.53	3.36 ǂ	1.10 ǂΩ	38.88	0.76	0.00	0.00 Ω	0.00	0.00	0.00
Cellobiohydrolase	0.00 Ω	0.00	0.00	2.75	0.00 ǂΩ	0.00 Ω	0.00	0.00	3.40	0.00	0.00	0.00
β-glucosidase	13.15	12.15 ǂ	51.25	112.23 ǂ	76.53	100.94	57.20 ab ǂ	8.71 a ǂ	86.32 b	42.567 a ǂ	12.47 b	35.03 ab
Exochitinase	7.70	5.11	3.36 a Ω	11.13 b	6.07 ǂΩ	17.41	7.74 ǂ	2.83	4.42 Ω	1.38 ǂΩ	0.00	2.32
Acid phosphatase	33.24 ǂΩ	43.74 Ω	408.72	1280.09	390.75 ǂΩ	1061.02	106.41 a ǂΩ	35.46 b	51.19 ab Ω	88.63 ǂΩ	65.31	73.35
Phosphodiesterase	0.00	0.00 Ω	15.58 ǂ	47.98 ǂΩ	11.27 ǂΩ	82.65	1.13 ǂΩ	0.51	0.07	4.94 ǂΩ	1.44	0.85
Arylsulfatase	0.00	0.00	5.41	0.00	-	14.39	0.00	1.66	0.38	4.05	0.00	0.00
β-xylosidase	0.83	0.00	0.18	0.00 ǂ	0.00 a	9.28 b	2.82 a ǂ	0.00 b	0.00 b Ω	0.00 Ω	0.00	0.00
Oxidase	1.98	1.61	1.00	0.16	3.52	2.91	7.11	9.86	0.00	0.08	4.21	6.01
C	Hf-Hf		Pv-Pv		Tv-Tv		Tv-Hf			Tv-Pv		
	Initial	Late	Initial	Late	Initial	Late	Initial deadlock	PR of Tv	Late deadlock	Initial deadlock	PR of Tv	R of Tv
Laccase	0.00	-	0.00 ǂ	0.00 ǂ	0.00	0.00 ϕ	4.25 a ϕ	2.10 ab	0.00 b	0.00 ϕ	0.00 ǂ	3.57
MnP	1.12	-	3.23 a	0.00 b ǂϕ	0.00 ǂ	2.88	3.42	5.38	2.47	3.50 a	5.17 ab	12.00 b
Peroxidase	1.24 ϕ	51.77	0.00 ǂϕ	0.00	8.69	0.00	1.17 a	3.51 ab	0.00 b	2.23 ab	9.79 a	4.34 b
α-glucosidase	0.28 ǂ	-	5.63	2.39 ǂ	129.70 ϕ	94.66	7.69 ǂ	21.30 ǂ	19.14 ϕ	19.75	60.01	48.29
Cellobiohydrolase	0.00 ǂϕ	-32.13	4.18	4.16	20.97 ϕ	26.92 ǂϕ	0.59	3.13	5.79	7.35	10.49	7.66
β-glucosidase	15.36	291.74 ǂ	114.19	76.59 ǂ	270.11	282.49	105.54	124.65 ǂ	152.81	185.23 ǂ	235.37 ǂ	162.92
Exochitinase	17.07	101.89	13.70 ϕ	11.80 ǂ	75.50 ϕ	55.43	18.57	45.70	34.43 ϕ	28.54 ϕ	116.44	74.97
Acid phosphatase	174.03 ϕ	4909.68 ǂϕ	975.51	951.24 ǂ	1830.82 ϕ	936.01	344.51 ϕ	322.27	248.73 ϕ	779.66 ϕ	1679.15	1437.30
Phosphodiesterase	3.58 a	66.92 b ǂϕ	41.41	20.08 ǂϕ	77.23 ϕ	76.91	12.58 ϕ	10.61 ǂ	6.19	25.02 ϕ	33.88	31.22
Arylsulfatase	0.00	-	0.00	0.00	0.00	0.00	0.00	-	0.00	0.00	-	0.00
β-xylosidase	6.59	85.34 ǂ	2.12	1.99	39.02	28.22	7.66	8.47	11.97 ϕ	13.78 ϕ	17.94	10.15
Oxidase	0.84	0.00	1.07	0.97	2.43	3.25	2.81	2.19	0.61	0.00	0.00	2.16

β-glucosidase activity was significantly higher ($p < 0.05$) when *H. fasiculare* partially replaced *T. versicolor* at 15 °C, compared to when *H. fasiculare* was partially replaced in the same interaction at 25 °C (Table 3.3A,B; Supplementary Figure 3.4). Differences in activity also occurred between treatments in pairings with the same outcomes. For example, activity of α-glucosidase, β-glucosidase and phosphodiesterase was significantly higher in field samples that resulted in partial replacement of *T. versicolor* by *H. fasciculare*, compared to samples where *T. versicolor* was also partially replaced by *H. fasciculare* at 15 °C (Table 3.3A,C; Supplementary Figure 3.4).

3.4.5 Enzyme production can be tracked throughout the interaction between T. versicolor and H. fasciculare over 84 days

Changes in activity levels of six and eight enzymes in the interaction zone (the *T. versicolor* block and *H. fasciculare* block respectively) occurred over time, however, the activity of only three enzymes (laccase, arylsulfatase and β-xylosidase) changed when *T. versicolor* was growing alone, and the activity of only one enzyme (laccase) changed over time when *H. fasciculare* was growing alone (Table 3.4; Supplementary Figure 3.5). Acid phosphatase was the most active enzyme during the interaction of *T. versicolor* and *H. fasciculare*. Its production was linked to *T. versicolor* as it was produced in an equally high amount, relative to other enzymes, in the *T. versicolor* side of the interaction in both the interaction zone and non-interaction zone region, and in the *T. versicolor* self-pairing after 1 d, and then decreased over time. Activity of acid phosphatase on the *H. fasciculare* side of the interaction was significantly lower; it increased at 14 d, when *H. fasciculare* began the process of replacement of *T. versicolor* (Figure 3.2B), before returning to pre-interaction levels (Table 3.4; Supplementary Figure 3.5).

The second most active enzyme was β-glucosidase. Activity on the *T. versicolor* side of the interaction decreased over the timecourse in both the interaction zone and non-interaction

zone region of the block (Table 3.4; Supplementary Figure 3.5). The *H. fasciculare* side of the interaction had the greatest activity level at 14 d, as with acid phosphatase, and then decreased over the remainder of the timecourse. *T. versicolor* produced phosphodiesterase and α-glucosidase in greater quantities than *H. fasciculare* in both self-pairing controls and when the two fungi were interacting, in fact α-glucosidase was only produced on the *H. fasciculare* side of the interaction at 14 d.

Arylsulfatase activity was relatively high at 1 d compared to other enzymes when the fungi were interacting but was not produced by either fungus at 14 d. Activity resumed on both sides of the interaction at 28 – 84 d although it was lower than that at 1 d. There was no arylsulfatase activity in the non-interaction zone region of either block until the very end of the timecourse. Laccase activity was significantly higher at 1 d than at 84 d on both sides of the interaction zone, with a gradual decrease between time points. Laccase activity in the *T. versicolor* interaction zone was significantly higher at 28 d than in the non-interaction zone region, and this was the only time that the interaction zone had a significantly different amount of activity to the non-interaction zone region, for any enzyme.

3.4.6 Rate of decay is slower during interactions than monocultures

Decay rate was lower than expected, based on the rate of decay of respective self-pairings, in almost all interspecific interactions, with decay rate significantly lower in 10 of the pairings, compared to single fungus control cultures (Figure 3.3). The exception to this was the interaction between *T. versicolor* and *P. velutina* at 25 °C, which lost significantly more weight than was expected based on decay rate when the fungi were growing alone (Figure 3.3).

Table 3.4 Enzyme activity in both the interaction zone, and non-interaction region of *T. versicolor* (Tv) and *H. fasciculare* (Hf) blocks at 1, 14, 28 and 84 d under 15 °C controlled temperature. Values are means of 5 replicates. ǂ Significant difference ($p < 0.05$) in activity compared with additional region of block (interaction zone (IZ) – non-interaction region (Non-IZ)). ϕ Significant difference ($p < 0.05$) in activity compared with competitor side of the interaction zone. Square bracket indicates side of the interaction zone sampled. (-) represents a failed assay.

	Activity mU g-1													
	Tv-Tv							Hf-Hf						
	IZ				Non-IZ			IZ				Non-IZ		
	1 d	14 d	28 d	84 d	14 d	28 d	84 d	1 d	14 d	28 d	84 d	14 d	28 d	84 d
Laccase	30.10 a	8.85 ab	12.82 ab	2.92 b	13.76 a	14.87 ab	1.87 b	15.30 a	0.00 b	47.02 a	0.50 b	1.43	14.61	21.86
MnP	21.40	14.47	24.25	13.67	17.79	14.79	11.45	6.37	3.83	8.67	2.14	4.59	5.64	0.00
Peroxidase	2.64	0.44	0.00	0.61	0.00	1.03	1.32	0.85	1.64	2.57	0.00	4.46	2.45	1.15
α-glucosidase	212.51	81.78	94.13	111.62	75.00	98.50	111.33	5.49	0.17	0.00	0.00	0.00	0.00	0.00
Cellobiohydrolase	65.00	57.90	15.79	11.28	44.26	23.55	13.75	0.85	0.36	0.00	0.00	0.00	0.00	0.00
β-glucosidase	1201.84	1193.52	602.23	441.01	978.71	635.96	522.27	213.42	89.43	85.33	61.85	108.61	105.59	70.01
Exochitinase	120.48	62.19	60.93	47.75	56.55	57.49	42.37	46.71	57.28	36.28	32.07	54.22	39.68	32.96
Acid phosphatase	3081.74	1615.79	1804.10	2062.95	1350.40	1598.02	2010.78	549.18	159.00	151.86	225.14	158.69	160.70	210.21
Phosphodiesterase	174.80	131.61	117.89	114.57	128.57	102.12	105.64	18.57	11.14	3.46	6.29	8.34	7.06	9.26
Arylsulfatase	-	5.89 ab	241.78 b	17.57 b	42.45	67.51	-	113.40	-	-	35.23	117.00	32.03	20.59
β-xylosidase	92.37 a	60.54 ab	33.59 b	29.83 b	58.95	34.55	30.62	28.73	31.22	14.67	13.27	30.25	21.59	15.65

Table 3.4 *Continued.*

	Activity mU g-1													
	[Tv]-Hf							Tv-[Hf]						
	IZ				Non-IZ			IZ				Non-IZ		
	1 d	14 d	28 d	84 d	14 d	28 d	84 d	1 d	14 d	28 d	84 d	14 d	28 d	84 d
Laccase	79.93 a	41.06 ab	28.81 ab ǂϕ	24.03 b	14.69	6.04 ǂ	7.20	18.13 a	19.70 ab	6.33 ab ϕ	3.74 b	4.66	21.33	9.13
MnP	22.35	10.68	11.05	9.16	8.23	23.61	5.01	11.86 a	8.19 ab	30.56 ab	2.07 b	7.23	34.90	2.42
Peroxidase	10.46 a	5.59 ab	5.42 ab	2.40 b	0.71	6.57	4.80	12.76 a	4.16 ab	1.66 bc	0.00 c	3.17	0.94	0.02
α-glucosidase	103.40 ϕ	24.01	17.86	0.00	18.66	24.58	0.00	0.00 ϕ	20.62	0.00	0.00	13.46	0.00	0.00
Cellobiohydrolase	24.53	17.79	10.67	2.54	25.73	25.50	11.92	0.93	8.69	4.32	0.14	10.87	0.80	0.00
β-glucosidase	639.32 ab	531.88 a	423.21 ab	121.99 b	665.39 a	588.06 a	199.49 b	41.87 a	422.51 b	173.04 ab	101.17 ab	472.73	183.90	93.71
Exochitinase	52.35	68.15	33.55	19.32	42.98	37.19	17.02	22.63	56.83	16.46	17.04	48.41	15.32	16.73
Acid phosphatase	2512.58 a ϕ	583.71 ab	342.44 ab	225.56 b	621.07	437.00	220.81	131.68 ϕ	663.93	262.11	189.77	726.16	262.41	228.75
Phosphodiesterase	125.38 a	24.09 ab	14.01 b	12.75 b	31.18	19.31	10.45	12.32	40.75	10.94	7.54	40.46	11.67	7.84
Arylsulfatase	448.21 a	-	14.14 ab	63.79 ab	-	-	97.27	731.70 a	-	106.59 ab	16.75 ab	-	-	59.09
β-xylosidase	52.49 ab	34.94 a	12.53 b	16.70 b	37.41 a	19.59 b	14.22 b	25.05 ab	35.51 a	12.45 b	19.15 ab	34.51 a	10.65 b	15.36 ab

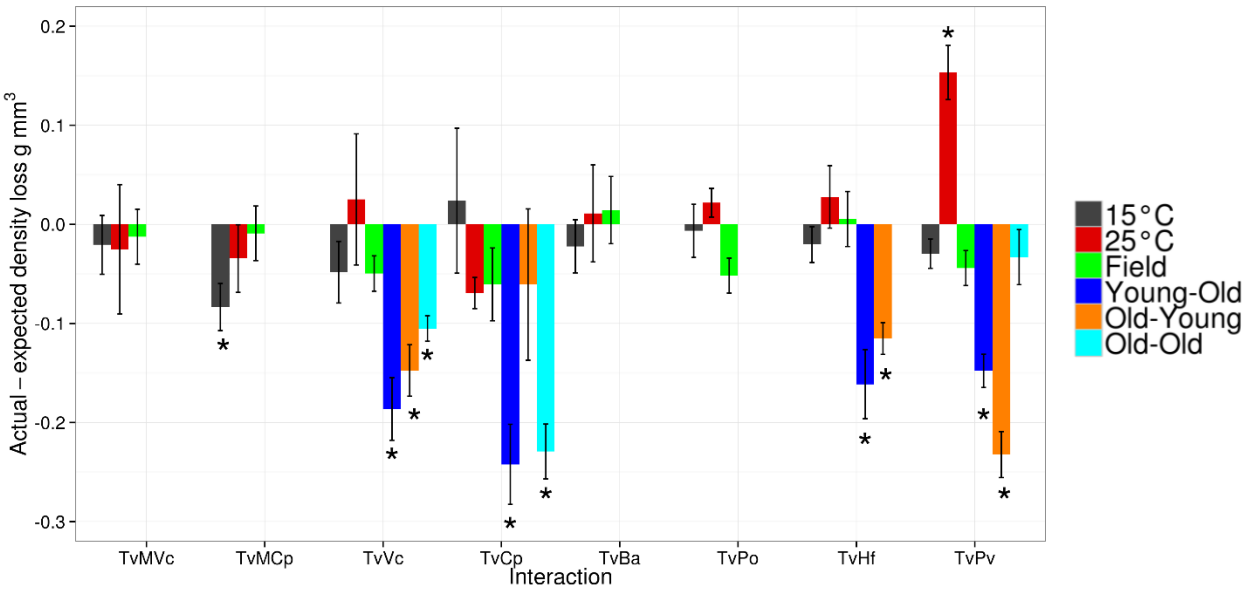

Figure 3.3 Changes in decomposition rate of blocks following interactions. The bars represent replicate mean ± 95 % confidence interval. * indicates actual density loss minus expected density loss was significantly (p < 0.05) different to 0. % density losses are shown in Supplementary Table 3.2.

3.5 Discussion

This study is the first of its kind to assess the effects of changing temperature on extracellular enzyme production during the antagonistic interactions of wood decay basidiomycetes. The combative abilities of fungi altered under different temperature regimes, affecting the outcomes of interactions, which was reflected by changes in enzyme activity.

3.5.1 Reversal of outcomes at different temperatures is reflected in enzyme activity

Changes to the relative combative ability of wood decay fungi and reversal of outcomes under different temperature regimes has been reported previously (Hiscox et al. 2016a), and may partly be attributed to the different temperature optima for growth rate of individual

competitors. A previous study found no link between the activity of wood decay-associated enzymes and differences in interaction outcome (Hiscox et al. 2010a). However, in that study, different outcomes examined arose from combinations of different competitors, rather than from the same pair of competitors under different conditions, the latter being the case in the present study. Changes to enzyme activity in self-pairings under different environmental conditions were observed in the present study, suggesting that changes to enzyme activity are temperature-induced, supporting the study hypotheses. However, it is possible that the change in enzyme activities under the different conditions may be either a direct or indirect cause of changes to the combative abilities of fungi.

However, in some cases interaction outcome did not appear to be closely correlated with enzyme activity. For example, the final outcome of interaction between *T. versicolor* versus *H. fasciculare* was deadlock both at 25 °C and in the field, but the activity of acid phosphatase, α-glucosidase, exochitinase and β-xylosidase were significantly different between the two environmental conditions. This would suggest that interaction outcomes are not the cause or effect, or not the sole cause or effect, of diverging enzymatic profiles, and that more complex metabolic processes are responsible. Furthermore, in the natural environment fungi frequently interact simultaneously with several different species. Recent studies of the interactions with three species of wood decay fungi interacting simultaneously revealed that the relative position of individuals within an interaction affects interaction outcomes (Hiscox et al. 2017; Chapter 5). So while the present study provides valuable information regarding the relationship between interaction outcomes and enzyme activity, it is important to remember that in nature metabolic mechanisms may be more complex.

3.5.2 Terminal hydrolase enzyme activity is greatest during deadlock, but reactive oxygen species generating enzyme activity is lower

When competitors are combatively unevenly matched, initially high levels of antagonistic compounds are deployed before one of the fungi successfully makes headway and begins the process of replacement (Hiscox & Boddy 2017). The successful antagonist then utilises the mycelium of the displaced competitor and metabolic products functioning in the breakdown of mycelia increase in the region of displacement (Hiscox & Boddy 2017). This was seen in the present study where activity of enzymes throughout the course of the interaction between *T. versicolor* and *H. fasciculare* was generally highest soon after the interaction began, then decreased throughout the remainder of the experiment. Activities of some enzymes were highest after 14 d in the *H. fasiculare* block interaction zone, reflecting the start of the gradual replacement of *T. versicolor* by *H. fasciculare* after 14 d, then returned to pre-interaction levels. Mycelial damage is linked to the oxidative activities of reactive oxygen species (ROS) such as laccase, peroxidases and NADPH oxidase (Hiscox & Boddy 2017), and while in the present study laccase production was significantly higher in the *T. versicolor* pre-colonised block following territory loss, peroxidase and MnP were not. Additionally, interactions with *H. fasciculare* and *P. velutina* sometimes resulted in replacement of *T. versicolor* and sometimes in deadlock. However, changes in the activity of ROS-generating enzymes between interactions with different outcomes only occurred in the interaction with *P. velutina* at 15 ^{o}C, where laccase and MnP production was lower during deadlock compared with partial replacement of *T. versicolor*. This suggests that these enzymes are not always determinants of interaction outcome, and that other metabolic processes are occurring.

3.5.3 Pre-colonisation length and environmental condition affect metabolic activity

T. versicolor was less combative when it had pre-colonised wood for longer (six months rather than three months), supporting the second study hypothesis. This is likely due to more extensive chemical and physical modifications, including changes to pH and water potential, accumulation of secondary metabolites, depletion of nutrients (Hiscox et al. 2016a) and decreased VOC production (Chapter 4). Additionally, though subtle, *T. versicolor* was often slightly less combative when in the field compared to under controlled environmental conditions in the laboratory. Moreover, the production of some enzymes in the *T. versicolor* self-pairing and in interspecific interactions were significantly lower in the field, possibly contributing to the reduction in combative success. Many factors are likely responsible for the reduction in enzymatic activity when in the field including fluctuating temperature and humidity (A'Bear et al. 2014), changes to pH (Gadd 1999), and competition from additional microbes (including fungi and bacteria) and invertebrates (Crowther et al. 2011). It is probable that different metabolic processes take place when under controlled and environmental conditions (Benjamin et al. 2002), and that less energy is put into decomposition strategies and the production of wood degrading enzymes when in the field, rather more emphasis being given to innate survival processes.

3.5.4 The heterokaryon of T. versicolor was more combative than the homokaryon

The heterokaryon of *T. versicolor* was more combative than the homokaryon during interactions at 15 ^{o}C, but the two were similarly matched during interactions at 25 ^{o}C. Homokaryons are often considered to be weaker combatants due to their theoretical short phase within the life cycle (Kauserud et al. 2006), but while the homokaryon phase is often short (Williams et al. 1981), homokaryons (including *T. versicolor*) have been found to persist in the field for many years (Coates & Rayner 1985; Garbelotto et al. 1997; Redfern et al. 2001). Two previous studies have assessed the combative abilities of a range of different homo- and heterokaryon isolates

and found that homokaryons of *Hericium coralloides* are more combative than heterokaryons (Crockatt et al. 2008), while those of *T. versicolor* did not differ in their combative abilities (Hiscox et al. 2010b). Both findings are in contrast to the current study indicating that the homokaryon used here was not representative of most. This was shown further by differences in the rate of decay between the two karyotic states in the present study, which previous studies did not find (Crockatt et al. 2008; Hiscox et al. 2010b).

3.5.5 Decomposition processes are more sensitive to pre-colonisation length than climate effects

Throughout the study, blocks decayed more slowly during interactions where a competitor had pre-colonised the resource for a longer time period, perhaps reflecting the change in metabolic mechanisms following extensive chemical modification of the resource. However, temperature had little effect on the rate of decomposition. Changing temperatures form the basis of many global change projection models (IPCC 2013), yet these results suggest that temperature may not be the predominant factor affecting fungal driven ecosystem processes, and that other factors such as community succession and individual life cycles should be considered when predicting climate change effects. Different temperatures did affect individual combative success, however, which resulted in changes in the dominant species present and was reflected in the quantities of lignin and cellulose decomposing enzymes. It would seem then that the decomposition of organic matter may be indirectly affected by climate change via changes to the suite of decomposition agents within the community, as well as by direct effects of temperature on metabolism. Other factors such as humidity are also likely to play important roles in climate effects on fungal driven processes (Venugopal et al. 2016) and should also be considered in projection models.

3.6 Conclusions

Abiotic variables affect metabolic processes during wood decomposition by interacting fungi. Temperature was important in determining the outcomes of interactions between competing individuals, and changes in extracellular enzyme production reflected those outcomes. However, there were also differences in enzyme production between pairings under different environmental regimes but with identical outcomes, suggesting enzyme activity is more sensitive to microclimate than biotic variables. Activity of enzymes generally reflected the progression of outcomes over time: terminal hydrolase activity was greatest during deadlock, and decreased as territory occupation changed. *T. versicolor* was less combative in the field and also when it had pre-colonised wood for longer before the experiment, probably due to greater variability of environmental conditions and chemical changes to the resource, respectively. The rate of decay was more sensitive to the effects of longer pre-colonisation (i.e. more decayed wood) than it was to direct climate effects. However, changes in microclimate altered which individual dominated wood blocks, and the quantities of lignin and cellulose decomposing enzymes reflected those changes, underlining climate change effects on fungal community succession and productivity.

Chapter 4. Abiotic conditions alter metabolic processes during the competitive interactions of wood decay fungi: Production of volatile organic compounds

4.1 Abstract

Wood decay fungi promote the decomposition of dead wood in forest ecosystems, during which, individuals within the fungal community interact with each other, and employ a variety of antagonistic mechanisms including production of volatile organic compounds (VOCs). The effects of two major variables on VOC production by interacting wood decay fungi were tested: temperature and state of decay. *Fagus sylvatica* (beech) blocks colonised by six different basidiomycetes were paired with *Trametes versicolor* colonised blocks, and VOC production was measured throughout interactions, and analysed by thermal desorption gas chromatography time-of-flight mass spectrometry (TD-GC-TOF-MS). A total of 78 metabolites were detected, and the principal groups of VOCs comprised sesquiterpenes, alkanes and esters. VOC profiles altered as a result of changing temperature, but the extent of decay in wood prior to interactions was found to have a more pronounced effect on VOC production than direct climate variables. Furthermore, the suite of VOCs and abundance of particular compounds altered as a result of antagonism, compared to single species self-pairings. Abiotic conditions clearly mediate metabolic processes, which under predicted climate change conditions are likely to alter the rate of decomposition of dead wood in forest ecosystems.

4.2 Introduction

A variety of secondary metabolites are released during decomposition, including extracellular enzymes, VOCs and small diffusible and non-diffusible metabolites, some of which have roles in the breakdown of the recalcitrant lignocellulose (Hynes et al. 2007; Riley et al. 2014; Konuma et al. 2015). Enzymes are the most widely studied agents of wood decomposition (Martínez et al. 2005; Hiscox et al. 2010a; Hiscox et al. 2010b; Baldrian & Lindahl 2011; Chapter 3), but specific VOCs are also produced during decay (Konuma et al. 2015; El Ariebi et al. 2016), functioning as important infochemicals (Morath et al. 2012) and antimicrobial agents (Abraham 2010). Yet VOC production during combative interactions has received comparatively limited attention. The suite of compounds produced by wood decay fungi include alcohols, aldehydes, ketones, esters, terpenes, and volatile sesquiterpenoids, a group that has received much attention in the study of fungal VOCs (Hynes et al. 2007; Evans et al. 2008; Kramer & Abrahman 2012; El Ariebi et al. 2016). Many factors influence VOC profiles including temperature, pH, humidity, the availability of nutrients and resource competition (Korpi et al. 2009; El Ariebi et al. 2016), and profiles can change substantially over time (Hynes et al. 2007; Evans et al. 2008; El Ariebi et al. 2016). VOC evolution during competitive interactions of wood decay fungi under different environmental conditions has not yet, however, been assessed.

The majority of studies of fungal and other microbial VOCs have been conducted for economical purposes for the food production and packaging industries (e.g. Broekaert et al. 2013; Lippolis et al. 2014), and the ecological role of VOCs produced by fungi has been relatively under researched. That being said, the ecological potential of fungal VOCs has been described (Morath et al. 2012) and changes in profiles assessed during fungal-fungal competition over time (Hynes et al. 2007; Evans et al. 2008; El Ariebi et al. 2016). However, under predicted global warming scenarios community VOC profiles may change, thus the assessment of changes in VOC profiles under different environmental conditions is crucial for fully understanding the ecological function of VOCs.

The aim of the present study was to assess changes to VOC profiles produced during interactions of *T.* v*ersicolor* with six other wood decay basidiomycetes in wood blocks at two ecologically relevant temperatures: 15 °C and 25 °C and in response to varying wood decay. VOC production was assessed by thermal desorption gas chromatography time-of-flight mass spectrometry (TD-GC-TOF-MS) of samples extracted from the headspace of interacting fungi. It builds upon the study presented in Chapter 3 which quantified the activity of 12 lignin/cellulolytic enzymes during these interactions, and the rate of decomposition.

4.3 Methods

4.3.1 Experimental design

Beech (*F. sylvatica*) wood blocks were colonised with seven individual fungi, and paired together as in Chapter 3 (details of experimental species are given in Table 3.1, n.b. only the *T. versicolor* heterokaryon was used in this study). Briefly, sterilised wood blocks were placed onto 7 d old cultures of individual fungi on 0.5 % malt agar (MA; 5 g l^{-1} malt extract, 15 g l^{-1} agar; Lab M, UK) and were incubated in the dark at 20 °C for 12 or 24 weeks.

Following pre-colonisation, and 48 h before interaction pairings, blocks were scraped free of excess mycelium. They were paired together with cut vessel ends touching and held together with a sterile elastic band (removed after 5 d). Paired blocks were placed into 200 ml lidded pots (Cater4you, UK) containing 30 ml of perlite (Homebase, UK) moistened with sterile distilled water to achieve a water potential of -0.012 kPa (determined by the method of Fawcett & Collins-George 1967), and pots were aerated via a 1×2 mm diameter hole which was covered with microporous surgical tape (3M, UK) (three replicates per treatment and per timepoint).

The effect of temperature on VOC production was assessed by incubating pairings (pre-colonised for 12 weeks prior to experiment) at 15 °C or 25 °C. Interactions were set up between *T. versicolor* and *Vuilleminia comedens*, *Coniophora puteana*, *Bjerkandera adusta*,

Pleurotus ostreatus, *Hypholoma fasciculare*, or *Phanerochaete velutina*. Self-pairings of all species were also set up.

The effect of pre-colonisation length on VOC production was assessed by pairing blocks pre-colonised for either 12 or 24 weeks (densities of blocks sacrificed after pre-colonisation are detailed in Supplementary Table 4.1). Interactions studied in this experiment were *T. versicolor* against *V. comedens*, *H. fasciculare*, and *P. velutina*. Pairings were incubated at 15 °C. The following interactions were set up; (1) *T. versicolor* blocks were pre-colonised for 12 weeks and competitor blocks for 24 weeks; (2) *T. versicolor* blocks were pre-colonised for 24 weeks and competitor blocks for 12 weeks; and (3) both *T. versicolor* and competitor blocks were pre-colonised for 24 weeks. Self-pairings of all species in blocks pre-colonised for 24 weeks were also set up. Interactions and self-pairings where both *T. versicolor* and the competitor had been pre-colonised for 12 weeks were performed as part of the temperature experiment.

4.3.2 Sampling of VOCs

Production of VOCs was measured via an adaptation of the protocol of Spadafora *et al.* (2016) 1, 14, and 28 d after interactions between fungi in colonised wood blocks were set up. Three replicates of each pairing were chosen at random, and VOCs collected prior to block harvest and fungal re-isolation. Pots were inserted, singly and lidless, into a multi-purpose roasting bag (46 x 56 cm; Lakeland, UK), which was sealed and stored at 15 °C or 25 °C (i.e. the same as the experimental incubation temperature) for 30 min to allow VOCs to equilibrate in the headspace. Headspace (500 ml) gas was collected with an EasyVOC manual pump (Markes International Ltd., UK) onto SafeLok™ thermodesorption (TD) tubes (Tenax TD & Sulficarb; Markes International Ltd., UK). Control samples comprised a pot containing uncolonised sterile beech wood blocks.

VOCs were desorbed using a TD100 thermodesorption system (Markes International Ltd., UK) with the following settings: tube desorption 10 min at 280 °C, at a trap flow of 40 ml min^{-1}; trap

desorption and transfer 40 °C s^{-1} to 300 °C, with a split flow of 20 ml min^{-1} into gas chromatograph (GC; 7890A; Agilent Technologies Inc., USA). VOCs were separated over 60 m, 0.32 mm I.D., 0.5 µm Rx5ms (Restek, UK) with 2 ml min^{-1} helium as carrier gas under constant flow conditions using the following temperature program: 35 °C for 5 min, 5 °C min^{-1} to 100 °C, hold 5 min. Mass spectra were recorded from *m/z* 30 to 350 on a time-of-flight mass spectrometer (BenchTOF-dx, Markes International Ltd., UK). C8-C20 alkane standard (0.5 µl, Supelco) was loaded onto a blank thermodesorption tube as a retention standard and quality control (QC).

Following VOC extraction, blocks were sacrificed and the outcomes of interactions, rate of decay and extracellular enzyme activity was determined (results reported in Chapter 3).

4.3.3 Data processing

GC-MS data were initially processed using MSD ChemStation software (E.02.02.1177; Agilent Technologies Inc., USA) and deconvoluted and integrated with AMDIS (National Institute of Standards and Technology 11 (NIST)) using a custom retention-indexed mass spectral library. Compounds which were not present in all three replicates were excluded from statistical analyses, as were compounds abundant in controls. MS spectra from deconvolution were searched against the NIST 2011 library (Software by Stein, version 2.0 g, 2011). Putative identifications were based on matches of mass spectra (>80 %) and retention index (RI +/− 15).

Using MetaboAnalyst 3.0 (Xia & Wishard 2016), all data were normalized by constant sum, g-log transformed and mean centred, missing value imputation was performed by replacement with half of the data matrix's reported minimum peak area, and interquantile range estimation was used to filter near-constant peaks. QCs were excluded from the matrix (see Supplementary Figure 4.1 for QC clustering) and the standardised binned data were used for statistical analysis.

4.3.4 Statistical analysis

All GC-MS data statistical analyses were conducted using Metaboanalyst 3.0 (Xia & Wishard, 2016). Principal component analysis (PCA) was used to check the unsupervised segregation of the entire GC-MS data set and clustering of the QCs (see Supplementary Figure 4.1). QCs were deemed as sufficient enough quality and were removed from the data set. Orthogonal projection to latent structures-discriminant analysis (OPLS-DA) was then applied to each sample group separately: 15 °C, 25 °C and pairings with different pre-colonisation lengths (i.e. 3 OPLS-DA models), and to each time point for each sample group (i.e. 9 OPLS-DA models). Compounds contributing most to fluctuation in the discriminant models were identified from the modelled covariance and correlation (loadings plot). Then, univariate one-way analysis of variance (ANOVA) with a 5 % Benjamini-Hochberg false discovery rate (FDR) correction for multiple comparisons (Benjamini & Hochberg 1995) was applied to significant compounds, with Tukey *post hoc* tests.

4.4 Results

4.4.1 VOC bouquet composition

After noise reduction, over all a total of 78 compounds were detected, 70 of which were putatively identified by comparison to the NIST library of mass spectra and a further 9 unidentified compounds were also detected (Table 4.1). Compound classes included sesquiterpenes (19), alkanes (15), esters (9), ketones (6), alkenes (6), alcohols (4), aldehydes (3), monoterpenes (2), terphenyls (1) quinones (1), amides (1), ethers (1), arenes (1), and alkenols (1).

Table 4.1 VOC compounds putatively identified by TD-TOF-GC-MS. Retention index (RI), CAS registry number, chemical group and reference of previous reporting are given.

	Compound name	RI	CAS	Chemical group	Reference
C1‡	4-epi-α-Acoradiene	1474	729602-94-2	Sesquiterpene	
C2‡Φ	β-Alaskene	1502.7	99529-78-9	Sesquiterpene	
C3ΦΩ	α-Barbatene	1415.5	53060-59-6	Sesquiterpene	
C4‡ΦΩ	β-Barbatene	1441	72346-55-5	Sesquiterpene	
C5‡	Azulene	1532.2	395070-76-5	Sesquiterpene	
C6Φ	[1,1':3',1''-Terphenyl]-2'-ol	2275	2432-11-3	Terphenyl	
C7‡Φ	Phthalic acid	2299	84-64-0	Aldehyde	Yan et al. 2008
C8‡	(+)-Sativen	1396.2	3650-28-0	Sesquiterpene	Paul & Park 2013; Savel'eva et al. 2014
C9Φ	1-Dodecanone, 2-(imidazol-1-yl)-1-(4-methoxyphenyl)-	2742	2432-11-3	Ketone	
C10Ω	α-Himachalene	1405	3853-83-6	Sesquiterpene	
C11Ω	β-Himachalene	1524	1461-03-6	Sesquiterpene	Elamparithi et al. 2014
C12‡	2-Methyl-1-heptene	782	15870-10-7	Alkene	Schalchli et al. 2013
C13‡	2-Butyl-1-octanol	1277	3913-02-8	Alcohol	
C14‡Φ	2-Ethyl-4-methyl-1-pentanol	931	106-67-2	Alcohol	
C15‡Ω	1S-à-Pinene	942	7785-26-4	Monoterpene	Rivas da Silva et al. 2012; Paul & Park 2013
C16‡Ω	2,4-Dimethyl-1-heptene	819	19549-87-2	Alkene	Cordero et al. 2014; Suwannarach et al. 2015
C17‡	2,4-Dimethyl-1-hexene	720	16746-87-5	Alkene	
C18Ω	p-Benzoquinone	1633	719-22-2	Chinone	Raza et al. 2009
C19‡	2-Butanone	555	78-93-3	Ketone	Isidorov et al. 2016
C20‡Φ	3-Methyl-2-butanone	590	563-80-4	Ketone	Savel'eva et al. 2014; Konuma et al. 2015
C21	(Z)-6-methyl-2-decene	1059	74630-31-2	Alkene	
C22Φ	2-Ethylhexyl trans-4-methoxycinnamate	2322	83834-59-7	Ester	Fernandez de Simon et al. 2014
C23‡Ω	2-Propenoic acid ester 1	2188	5466-77-3	Ester	
C24‡	2-Propenoic acid ester 2	2336	5466-77-3	Ester	
C25Φ	3-Octanone	966	106-68-3	Ketone	Isidorov et al. 2016
C26‡	3-Pentanol	681	584-02-1	Alcohol	Wihlborg et al. 2008
C27‡Ω	β-Patchoulene	1356	514-51-2	Sesquiterpene	
C28	5,5-Dimethyl-1,3-hexadiene	730	1515-79-3	Alkene	
C29Φ	Methyl acetate	487	79-20-9	Ester	Sharip et al. 2016
C30Φ	Acetone	455	67-64-1	Ketone	Isidorov et al. 2016
C31‡	α-Longipinene	1422	59-89-08-2	Sesquiterpene	Isidorov et al. 2016
C32Ω	α-Pinene	943	7785-70-8	Monoterpene	Isidorov et al. 2016
C33‡Φ	Cuparene	1556	16982-00-6	Sesquiterpene derivative	Konuma et al. 2015
C34‡	Benzoic acid, tetradecyl ester	2213	-	Ester	
C35‡	Isocaryophyllene	1434	118-65-0	Sesquiterpene	Sanchez-Fernandez et al. 2016
C36Φ	Unknown1	1026	-	-	
C37‡	Unknown2	1312	-	-	
C38‡	Unknown3	1084	-	-	

Table 4.1 *Continued*

	Compound name	RI	CAS	Chemical group	Reference
C39ϕ	Unknown4	1235	-	-	
C40‡Ω	Unknown5	1245	-	-	
C41‡ϕΩ	Unknown6	1250	-	-	
C42‡ϕΩ	Cedrene	1403	469-61-4	Sesquiterpene	Konuma et al. 2015
C43‡	Cetene	1889	629-73-2	Alkene	Kolayli et al. 2009; Usha Nandhini et al. 2015
C44‡ϕ	cis-Thujopsene	1454	470-40-6	Sesquiterpene	Konuma et al. 2015
C45Ω	Decanal	1186	112-31-2	Ketone	Ho et al. 2010
C46‡	2,9-Dimethyldecane	1086	1002-17-1	Alkane	
C47‡	4,6-Dimethyldodecane	1285	61141-72-8	Alkane	Geethalakshmi & Sarada 2013
C48‡	Methylformamide	607	123-39-7	Amide	Chen et al. 1989
C49	2,3-Dimethylheptane	788	3074-71-3	Alkane	
C50ϕ	4-Methylheptane	752	589-53-7	Alkane	Sinha et al. 2015
C51ϕ	5-Ethyl-2-methylheptane	887	13475-78-0	Alkane	Zerinque & Bhantnagar 1994
C52‡	Hexadecanoic acid, methyl ester	1878	112-39-0	Ester	Kong et al. 2004
C53‡ϕΩ	2,3,5-Trimethylhexane	724	1069-53-0	Alkane	Borjesson et al. 1989
C54	Isopropyl palmitate	2013	110-27-0	Ester	Pan et al. 2016
C55‡ϕ	Longifolene	1428	475-20-7	Sesquiterpene	Konuma et al. 2015
C56	1-Heptadecanol	1954	1454-85-9	Alcohol	Qadri et al. 2017
C57‡	2,5-Dimethylnonane	1027	17302-27-1	Alkane	Lippolis et al. 2014
C58‡Ω	Octyl ether	1665	629-82-3	Ether	Pernak etal. 2004
C59ϕ	2,7-Dimethyloctane	933	1072-16-8	Alkane	Schaeffer et al. 1979
C60‡	4-Methyloctane	872	2216-34-4	Alkane	Ahearn et al. 1997
C61‡Ω	6-ethyl-2-methyloctane	1158	62016-19-7	Alkane	Sen at al. 2016
C62‡	β-Chamigrene	1504	18431-82-8	Sesquiterpene	Mun & Prewitt 2011
C63Ω	α-Chamigrene	1533	19912-83-5	Sesquiterpene	Mun & Prewitt 2011
C64Ω	Toluene	786	108-88-3	Arene	Isidorov et al. 2016
C65‡ϕ	4,8-Dimethylundecane	1218	17301-33-6	Alkane	
C66‡	Unknown7	1161	-	-	
C67‡	1,2-Benzenedicarboxylic acid, butyl 2-ethylhexyl ester	2370	85-69-8	Aldehyde	Sun et al. 2015
C68	6-Methyl-5-hepten-2-ol	964	1569-60-4	Alkenol (aliphatic alkenone)	Liouane et al. 2010
C69	Benzoic acid ester	2392	-	Ester	
C70	Benzoic acid, tridecyl ester	2300	-	Ester	
C71ϕ	Unknown8	900	-	-	
C72	Unknown9	695	-	-	
C73	2-Methylheptane	752	592-27-8	Alkane	Zerinque & Bhatnagar 1994
C74‡	2,5-Dimethylhexane	688	592-13-2	Alkane	Micheluz et al. 2016
C75	γ-Cadinene	1538	39029-41-9	Sesquiterpene	Konuma et al. 2015
C76	Palmitic acid	1968	57-10-3	Aldehyde	Gutierrez et al. 2002
C77	3,6-Dimethyloctane	940	15869-94-0	Alkane	
C78	2,8-Dimethylundecane	1225	17301-25-6	Alkane	Jiani et al. 2015

‡ Compounds identified by ANOVA as significant ($p < 0.05$) in 15 ºC experiment; ϕ 25 ºC experiment; Ω pre-colonisation length experiment.

A total of 58 VOCs were detected in the head space of 15 °C experimental samples (competitive interactions and same species controls) (Supplementary Table 4.2). The scores plot from the supervised OPLS-DA showed obvious separation between the three sampling days accounting for 20 % of the variance (T score [1] axis; Figure 4.1A), although the greatest degree of separation occurred between different interactions (Figure 4.1B-D). From the corresponding loadings plots, 45 compounds were identified as contributing significantly (ANOVA: $p < 0.05$; Supplementary Table 4.3) to the separation (Supplementary Figure 4.2A). Of these, there were 14 sesquiterpenes, 8 alkanes, 5 alkenes, 5 esters, 5 unidentified compounds, 3 alcohols, 2 aldehydes, 1 ketone, 1 amide and 1 monoterpene. VOC profiles of individual pairings were most distinct from each other after 14 d, with *V. comedens* self-pairings and interactions between *T. versicolor* and *B. adusta* forming clusters distinctly separate from any other groups (Figure 4.1C).

At 25 °C, 47 compounds were detected in the head space of interactions (Supplementary Table 4.4). Of these, 25 VOCs significantly contributed (ANOVA: $p < 0.05$; Supplementary Table 4.5) to the separation between different interactions, and the temporal separation (orthogonal T score [1] axis: 41 % of the variance and T score [1] axis: 10 % of the variance, respectively; Figure 4.1E; Supplementary Figure 4.2E). These 25 compounds comprised 7 sesquiterpenes, 5 alkanes, 4 ketones, 4 unidentified compounds, 2 esters, 1 alcohol, 1 aldehyde and 1 terphenyl. Separation between profiles of individual pairings changed amongst each time point (Figure 4.1F-H), and replicates of the interaction of *T. versicolor* against *V. comedens*, and *C. puteana* and *P. ostreatus* self-pairings clustered into groups disparately different to any others after 28 d (Figure 4.1H).

During the course of the experiment with wood blocks at different decay stages, 25 compounds were detected (Supplementary Table 4.6). Of these, 19 had significant effects (ANOVA: $p < 0.05$; Supplementary Table 4.7) on the variance between interaction types, though profiles were not

separated by time: 35 % along the orthogonal T score [1] axis and 26 % along the T score [1] axis (Figure 4.2A; Supplementary Figure 4.2I). These 19 compounds consisted of 7 sesquiterpenes, 2 monoterpenes, 2 esters, 2 alkanes, 2 unidentified compounds, 1 alkene, 1 ketone, 1 arene, and 1 quinone.

4.4.2 Single species (self-pairing) production of VOCs

At 15 °C, acetone (C30) was the most abundant compound for four of the species (*T. versicolor*, *H. fasciculare*, *P. ostreatus* and *P. velutina*) on average across the three time points accounting for 37 %, 39 %, 43 %, and 44 % of the total peak area respectively, and was the second most abundant compound produced by *B. adjusta* and *V. comedens* with 18 % and 32 % respectively of the total peak area (Supplementary Table 4.2). 2-Propenoic acid (C24) had the highest peak area for *B. adusta* (31 %) and *C. puteana* (32 %). For *V. comedens*, β-barbatene (C4) was the most abundant accounting for 39 % of the total peak area (Figure 4.3A).

Acetone (C30) was also the most consistently abundant compound at 25 °C accounting for 60 % of the total peak area across all time points produced by *T. versicolor*, 29 % for *B. adjusta*, 49 % for *H. fasciculare*, 35 % for *P. ostreatus*, 47 % for *P. velutina* and 24 % for *V. comedens*. 2-Ethylhexyl trans-4-methoxycinnamate (C22) was the most abundant compound produced by *C. puteana* (17 % total peak area), and was second most abundant in *H. fasciculare*, *P. ostreatus*, *P. velutina* and *V. comedens* (18 %, 28 %, 20 %, and 18 % respectively) (Supplementary Table 4.4).

After 6 months pre-colonisation, acetone (C30) was the most highly abundant compound for all species (*T. versicolor* (48 % of total peak area), *P. velutina* (93 %) and *H. fasciculare* (84 %)) except *V. comedens* where β-barbatene (C4) was the most abundant (76 %) and 2,3,5-trimethylhexane (C53) the second most abundant (9 %). β-Barbatene (C4) was the second highest abundant compound in *T. versicolor* (40 %) and *H. fasciculare* (13 %), and for *P. velutina* cetene (C43) was second most abundant (6 %) (Supplementary Table 4.6).

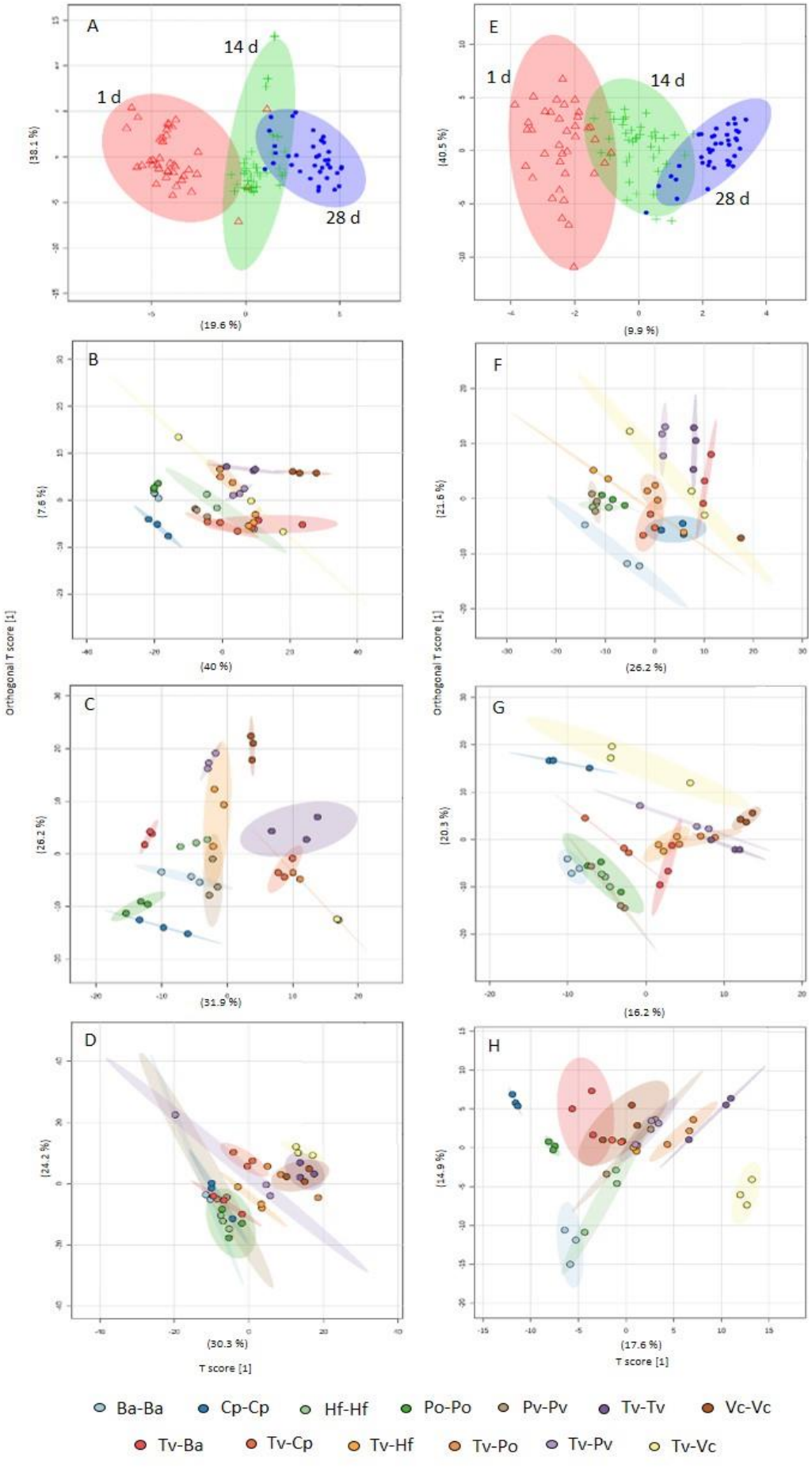
A
1 d
14 d
28 d
(38.1 %)
(19.6 %)
E
1 d
14 d
28 d
(40.5 %)
(9.9 %)
B
(7.6 %)
(40 %)
F
(21.6 %)
(26.2 %)
Orthogonal T score [1]
C
(26.2 %)
(31.9 %)
G
(20.3 %)
(16.2 %)
D
(24.2 %)
(30.3 %)
T score [1]
H
(14.9 %)
(17.6 %)
T score [1]
Ba-Ba
Cp-Cp
Hf-Hf
Po-Po
Pv-Pv
Tv-Tv
Vc-Vc
Tv-Ba
Tv-Cp
Tv-Hf
Tv-Po
Tv-Pv
Tv-Vc

Figure 4.1 OPLS-DA scores plots derived from the GC-MS spectra of interactions at 15 °C (A-D) and 25 °C (E-H). A-D: (A) samples from all three time classes at 15 °C, (B) individual pairings at 15 °C 1 d after interaction set up, after 14 d (C), and after 28 d (D). E-H: (E) samples from all three time classes at 25 °C, (F) Individual pairings at 25 °C after 1 d, after 14 d (G), and after 28 d (H). Points represent individual samples (three independent biological replicates per pairing), and 95 % confidence intervals of the means of sample groups are fitted onto the spatial ordination. See Supplementary Figure 4.2 for corresponding loadings plots.

4.4.3 Change in production of VOCs during interspecific interactions

A total of 36 VOCs were detected across all samples involving *T. versicolor* paired against a competitor (i.e. excluding same species controls) at 15 °C, and 35 were detected at 25 °C. At both temperatures, many compounds were produced during competitive interactions which were not produced in controls, and some which were produced in self-pairings were not produced during interactions. For example, 2-ethyl-4-methyl-1-pentanol (C14) was produced when *T. versicolor* was interacting with *P. ostreatus* at 15 °C and with *C. puteana* at 25 °C, but was not produced in self-pairings of any of those fungi, and the same compound was produced by *V. comedens* and *B. adusta* self-pairings at 25 °C but was not produced when either fungus was interacting with *T. versicolor* (Supplementary Tables 4.2,4). The loss of compounds during interactions compared to self-pairings was higher at 25 °C, except during the interaction between *T. versicolor* and *B. adusta* where 19 VOCs were absent at 15 °C compared to 15 at 25 °C (Supplementary Tables 4.2,4). Similarly, appearance of new VOCs during competitive interactions compared to self-pairings was higher at 25 °C than it was at 15 °C.

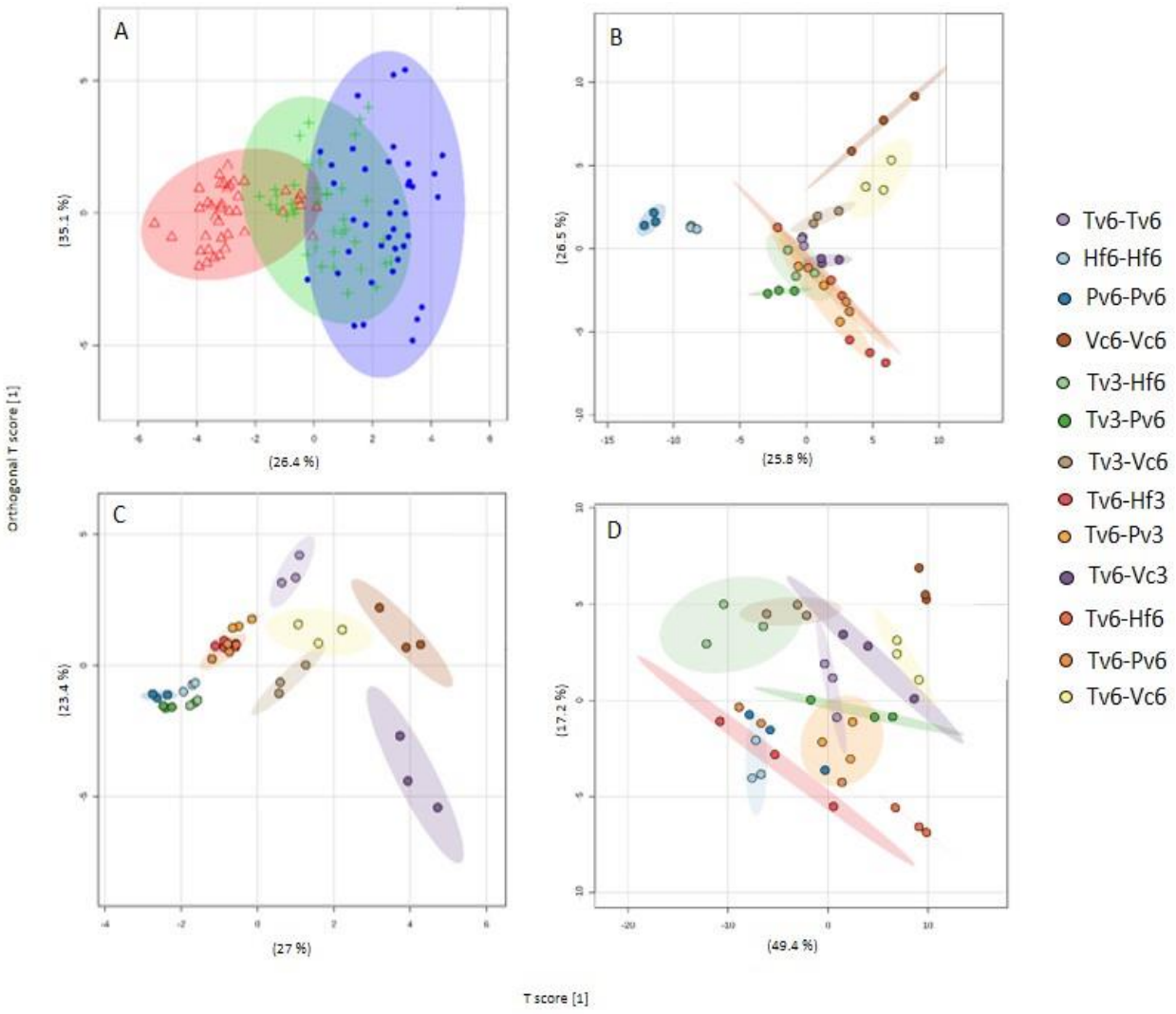

Figure 4.2 OPLS-DA scores plots derived from the GC-MS spectra of interactions in the pre-colonisation length experiment. (A) Samples from all three time classes, (B) individual pairings 1 d after interaction set up, after 14 d (C), and after 28 d (D). Points represent individual samples (three independent biological replicates per pairing), and 95 % confidence intervals of the means of sample groups are fitted onto the spatial ordination. Numbers in legend indicate length of pre-colonisation: three or six months. See supplementary Figure 4.2 for corresponding loadings plots.

In addition to being lost or gained, the abundance of many compounds was reduced or increased in interspecific interactions compared to self-pairings, though there were no discernible patterns to this change. For example, the abundance of -methoxy cinnamate (C23) was reduced across all time points in the interspecific interaction between *T. versicolor* and *B. adusta* at 25 °C, but its abundance increased at all time points when *T. versicolor* was interacting with *C. puteana* at 25 °C (Supplementary Table 4.4), and α-barbatene (C3) was present in *T. versicolor* and *V. comedens* self-pairings at 15 °C, but was absent when the two fungi were together (Figure 4.3A).

Acetone (C30) was consistently highly abundant in both self-pairings and interspecific interactions under all 3 experimental conditions. At 15 °C when *T. versicolor* was paired against *B. adjusta* it accounted for 50 % of the total peak area, 34 % when against *C. puteana*, 52 % against *H. fasiculare*, 46 % against *P. ostreatus*, 55 % against *P. velutina* and 33 % against *V. comedens* (Figure 4.3A; Supplementary Table 4.2), and was similarly high when *T. versicolor* was paired against *B. adjusta*, *H. fasciculare*, *P. ostreatus* and *V. comedens* at 25 °C (33 %, 55 %, 33 %, and 44 % total peak area respectively: Supplementary Table 4.4). When *T. versicolor* had colonised wood for 3 months and was paired against competitors which had pre-colonised wood for 6 months, acetone was consistently the most abundant compound and β-barbatene (C4) was the second most abundant. This was reversed when wood blocks that had been pre-colonised for six months with *T. versicolor* were paired against competitors that had been pre-colonised for three months: β-barbatene (C4) was the highest and acetone (C30) the second most highly abundant (Supplementary Table 4.6). α-Barbatene (C3) and β-barbatene (C4) were consistently highly significant, and were the most significant compounds that occurred under all three experimental conditions (Figure 4.3A-C).

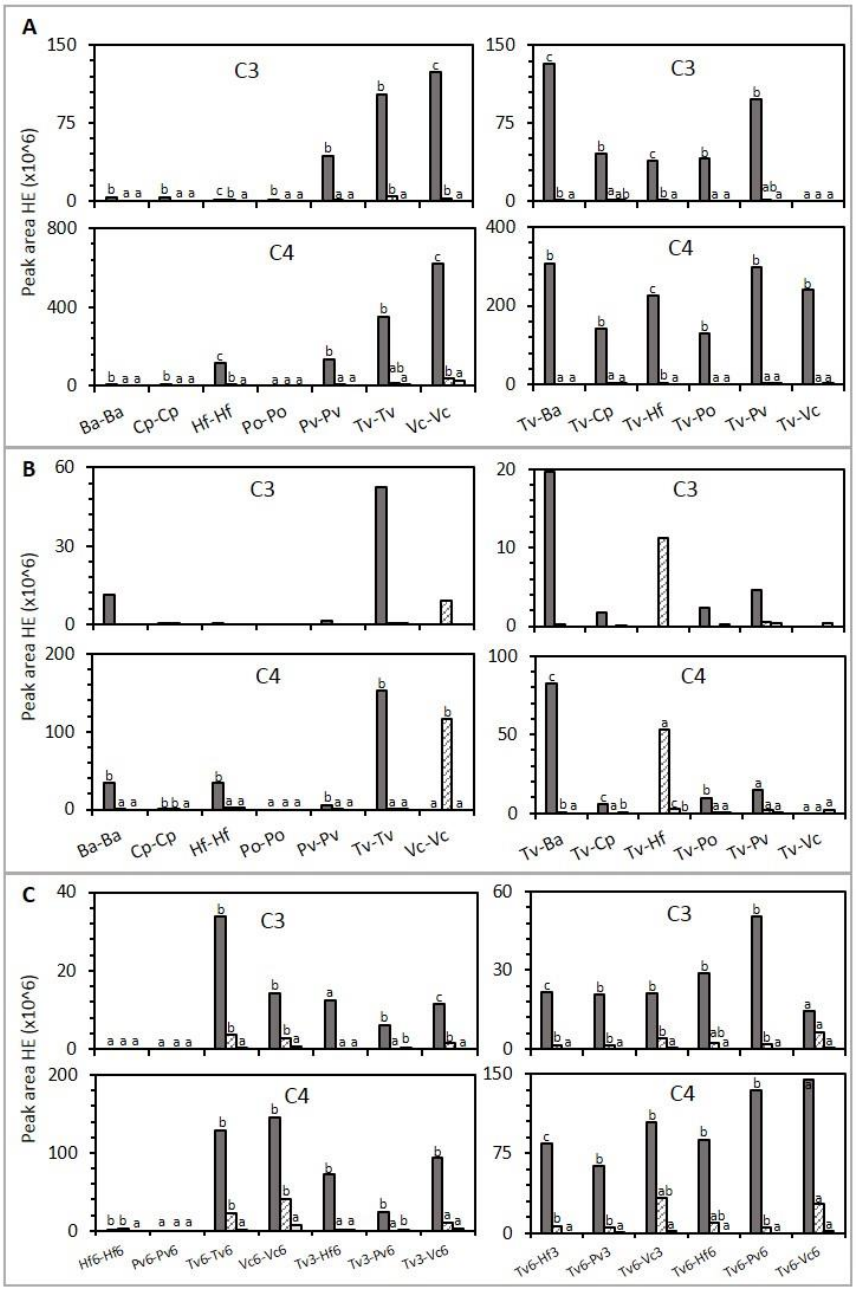

Figure 4.3 Peak area abundance of highly significant (p < 0.001) compounds detected in all three experiments: (A) 15 °C; (B) 25 °C; and (C) pre-colonisation length experiment. Bars represent the abundance of compounds, expressed in hydrocarbon equivalents (HE), 1 d (dark grey bars), 14 d (stripped bars) and 28 d (pale grey bars) after interaction set-up. Abundance is calculated from the mean of 3 replicates and error bars displaying SEM are omitted due to values being less than 1 % of the mean (see Supplementary Table 4.8 for SEM). Compounds chosen were in the top 40 % most significant compounds in the 15 °C and 25 °C experiment (C3: p = 2.46e-20 and p = 286e-9 respectively; C4: p = 147e-10 and p = 171e-5), and were also highly abundant in the pre-colonisation length experiment (C3: p = 2.7e-7; C4: p = 7.67e-6). C3: α-barbatene, C4: β-barbatene. Tv: *T. versicolor*, Ba: *B. adusta*, Cp: *C. puteana*, Hf: *H. fasciculare*, Po: *P. ostreatus*, Pv: *P. velutina*, Vc: *V. comedens*. Numbers in (C) indicate pre-colonisation length (3 or 6 months).

4.5 Discussion

This study revealed that significant changes to VOC profiles occur when fungi interact with each other. Although this has been seen previously during interactions on artificial media (Hynes et al. 2007; Evans et al. 2008), across soil and in wood (El Ariebi et al. 2016), a novel finding here was that VOC profiles during interactions change as a result of temperature and extent of wood decay (colonisation time).

4.5.1 Environmental conditions and pre-colonisation length affect VOC production

Generally, VOC profiles for all pairings differed between temperature regimes and more VOCs were detected at the lower temperature. For example, 2,7-dimethyloctane (C59), an iso-branched *n*-alkane that is readily degraded by some fungal and bacterial strains (Schaeffer et al. 1979), was not detected in any pairing at 15 °C but was detected in every interaction and self-pairing at 25 °C. The outcomes of interactions amongst wood decay fungi and the rates at which they occur are affected by temperature (Schoeman et al. 1996; Hiscox & Boddy 2017), and the changes in VOC emissions may be a consequence of, or even causal in, these changes. However, in the present study, increased production of some compounds including 2,7-dimethyloctane (C59) also occurred in self-pairing controls, indicating temperature induced changes to innate metabolic processes as well.

VOC profiles were more similar to self-pairing controls in interactions where both blocks had been colonised for six months, compared to interactions where either one or both blocks had been colonised for a shorter time. A time series experiment of VOC production by *T. versicolor* and *Fomitopsis palustris* grown separately on wood chips found that increased VOC production was associated with the active phase of wood decay (Konuma et al. 2015), possibly explaining the reduction in VOC production during interactions, relative to self-pairings, in wood at a later stage of decomposition. The relative combative abilities of individuals alter depending on state of decay of wood (Hiscox et al. 2016a; Chapter 5). It is therefore probable that alterations in the

combative mechanisms employed by fungi during different phases of wood decay contribute to the change in VOC profiles.

4.5.2 Relationship between interaction outcome and the production of VOCs

The outcomes of some interactions and the enzyme activity have previously been shown to differ at different temperatures (Chapter 3). For example, at 15 °C *T. versicolor* was partially replaced by both *H. fasciculare* and *P. velutina* but at 25 °C it deadlocked with *H. fasciculare* and fully replaced *P. velutina*. In the present study there were large differences in the quantity of certain compounds emitted during these confrontations, compared to the self-paired controls. For example, abundance of methyl acetate (C29) was much greater in the interaction between *T. versicolor* and *P. velutina* at 25 °C, while acetone (C30) abundance was lower, compared to the self-pairings. The change in interaction outcome and, therefore, the change in dominant individual, may have been responsible for the change in VOC profiles. Conversely, the different outcomes of the interaction may have been mediated by different VOC profiles and enzyme activities, as the specific suite of antagonistic compounds produced by each fungus individually changed in response to temperature.

4.5.3 Temporal VOC production and species specificity

Changes in the abundance of compounds at 14 d and 28 d compared to that after 1 d of interaction was compound and pairing specific, with no clear patterns of temporal VOC production. This is in contrast with the enzyme activity which generally decreased after 14 d (Chapter 3), and earlier studies of VOC production, where production decreased after 14 d (Hynes et al. 2007; Evans et al. 2008; El Ariebi et al. 2016). All of the aforementioned earlier studies sampled VOCs using solid phase microextraction (SPME) fibres which are particularly efficient at absorbing sesquiterpenes but are limited by their poor absorption of non-sesquiterpene compounds (Hynes et al. 2007). The carbon coated TD tubes used for VOC

collection in the current study are superior in their absorption of a far wider spectrum of compounds than just sesquiterpenes. As a result, more compounds were detected which likely included many that are not affected by biotic/abiotic factors, and so patterns of decreasing VOC production over time were more difficult to discern. Although the sesquiterpenes detected in this study did generally decrease with time.

The abundance of specific VOCs was also highly variable amongst species, and the relative quantity of common compounds also differed, as found in other studies. For example, only ten VOCs out of a total of 75 were commonly produced by all eight ascomycete and zygomycete leaf litter decomposing fungi studied (Isidorov et al. 2016), and only three compounds out of a total of 55 detected were produced by all seven selected ascomycete fungal species studied (Micheluz et al. 2016).

4.5.4 Ecological functions of VOCs

Of the 78 volatile compounds detected in the present study, 19 were sesquiterpenes, comprising the biggest class of aliphatic organic compounds. Sesquiterpenes, and structurally diverse sesquiterpenoids, are produced in their thousands by bacteria, fungi and plants (Schmidt-Dannert 2015), and are generally thought to play a role in signalling, e.g. with insects (Davis et al. 2013), while others are linked to enzyme inactivation via cell membrane disturbance and inhibition of gene expression (Davidson 2001). Sesquiterpenes produced by fungi have antimicrobial properties (Viiri et al. 2001; Hynes et al. 2007; El Ariebi et al. 2016; Sánchez-Fernández et al. 2016; Isaka et al. 2017) and their production is often higher during interspecific interactions. For example, during interactions between *H. fasciculare* and *Resinicium bicolor* the production of 19 sesquiterpenoids increased compared with self-pairing controls (Hynes et al. 2007). In the current study, the sesquiterpene β-himachalene (C11), which has previously been linked to antifungal activity against plant pathogenic and saprotropic fungi (Schalchli et al. 2011), increased 14 d after the start of the interaction between *T. versicolor* and

V. comedens when at different states of decay (colonised for 6 and 3 months respectively) compared to self-pairing controls. Also, β-chamigrene (C62) and cedrene (C42) (identified in the current study) have antifungal activity against *T. versicolor* and *Gloeohyllum trabeum* from Eastern red cedar (*Juniperus virginiana*) (Mun & Prewitt 2011), and in the present study they increased 28 d after the start of the interaction between *T. versicolor* and *C. puteana* at 15 °C. In the interaction with *V. comedens*, increased production began as *T. versicolor* was beginning to gain territory from the competitor, and when against *C. puteana* greater production began once *T. versicolor* had fully replaced its opponent suggesting production of the antimicrobial compounds by *T. versicolor* in order to gain and maintain territory.

Production of the ketone acetone (C30) was highly conserved in all interspecific interactions and in the majority of single species profiles. Acetone is a major constituent of the VOC profiles of decaying plant material (Warneke et al. 1999), and is highly abundant in decaying litter of Douglas fir (*Pseudotsuga menziesii*) (Copeland et al. 2014), Scots pine (*Pinus sylvestris*) and Norway spruce (*Picea abies*) (Isidorov et al. 2016). Of 75 organic carbon compounds emitted by eight isolated coniferous leaf litter fungi, acetone was consistently the most highly abundant and was one of only ten compounds that was produced by all eight fungi (Isidorov et al. 2016). This is similar to the current study, where acetone was produced abundantly in every pairing except the *C. puteana* self-pairings at 15 °C.

Six of the compounds detected in the present study, namely 3-methyl-2-butanone (C20), cuparene (C33), cedrene (C42), cis-thujopsene (C44), longifolene (C55) and γ-cadinene (C75), have been reported previously in a study where wood decay fungi were cultivated on potato dextrose agar (PDA) and wood chips (Konuma et al. 2015). Cuparene was produced by *T. versicolor* on wood chips but not on PDA, suggesting that cuparene derives from wood decomposition, perhaps reflecting the precursor availability in wood. Isocaryophyllene (C35) was previously detected in an intraspecific interaction of the endophyte *Nodulisporium* sp., and

in the interspecific interaction between *Nodulisporium* sp. and the plant pathogen *Pythium aphanidermatum* (Sánchez-Fernández et al. 2016). Other compounds, such as (+)-sativen (C8) and 3-methyl-2-butanone (C20), have been reported and suggested for use as chemical biomarkers (Savel'eva et al. 2014), while some have been reported in plants, e.g. 1,2-benzenedicarboxylic acid, butyl cyclohexyl ester (C7) (Yan et al. 2008), and some have antimicrobial properties, e.g. α-himachalene (C10) (Elamparithi et al. 2014) and p-benzoquinone (C18) (Raza et al. 2009). The ester methyl acetate (C29) has been reported previously in a suite of breakdown products of lignocellulose which, when collected and emitted in the presence of fungi, caused inhibition of spore germination and suppression of mycelia growth (Sharip et al. 2016). Thus the inference that at least some of the VOCs reported here may have an important influence on the outcome of interactions, and on changes in these interactions at different temperatures and on wood of differing decay states, is supported by their role in other systems.

4.6 Conclusions

This study demonstrates changes in the antagonistic metabolic processes of wood decay basidiomycetes as a result of environmental change. Abiotic conditions altered VOC production, with relatively small changes in temperature and state of decay of wood resources impacting the suite of VOCs produced and the abundance of individual compounds. Fewer compounds were produced by interacting fungi at a higher temperature, and VOC production during interactions was more similar to self-pairings in resources pre-colonised for a longer period (i.e. more decayed). Additionally, the alteration in interaction outcomes of some pairings as a result of changing temperature (Chapter 3), was reflected in changes in the abundance of specific compounds. Several VOCs with antifungal properties were produced, possibly as antagonistic weaponry, and the quantities of these compounds changed during the course of interactions reflecting the progression of individual territory gain/loss, which in turn is affected by abiotic condition. The findings for VOCs are reflected in the study on enzyme activity

(Chapter 3), further demonstrating the effects of environmental variables on innate metabolic processes. Under predicted climate change conditions these changes in metabolic processes together with the shifts in fungal community structure which they promote, are likely to affect the rate of decomposition of dead wood in forest ecosystems.

Chapter 5: Emergent properties arising from spatial heterogeneity influence fungal community dynamics

5.1 Abstract

Community dynamics are mediated by species interactions, and within communities spatial heterogeneity and intransitive relationships promote coexistence. However, few experimental studies have assessed effects of heterogeneity on the interactions of competing individuals. Most studies have only used simplistic pair-wise interactions in a 2-dimensional plane, but this chapter investigates a three-species community in an environmentally realistic novel 3-dimensional system. It shows how spatial heterogeneity and patch size dynamics are important for coexistence, and how competitive interactions change over different spatial dimensions. Emergent properties arose with increased spatial heterogeneity: the weakest competitor co-occurred with the community when its territory was less fragmented, and interactions became intransitive.

5.2 Introduction

Spatial variation in natural ecosystems affects all aspects of ecology from the level of individual behaviour, to whole population and community dynamics (Holmes et al. 1994). Since interactions between individuals of a community play a pivotal role in shaping the structure of the community, understanding interactions in the context of spatial variation is critical to explaining community development and its contribution to the functioning of the wider ecosystem.

Spatial heterogeneity promotes coexistence by providing spatial refuges and reducing the encounter rate of individuals, hence reducing the risk of attack (Huffaker 1958; Brockhurst et al. 2005). The classical study by Luckinbill (1973) demonstrated that the unstable interaction between *Didinium nasutum* and *Paramecium aurelia* (where *P. aurelia* is driven to extinction by *D. nasutum*) was stabilised and coexistence occurred following an increase in viscosity of culture medium. More recently, theoretical models have predicted that the spatial distribution of individuals affects community stability such that greater dispersion of species will result in greater niche partitioning, which promotes coexistence over evolutionary time (Wang et al. 2015). Additionally, long-term investigations of habitat fragmentation show that patchiness has drastic negative effects on biodiversity (Lovejoy et al. 1986; Laurance et al. 2011). Little experimental work, however, has been conducted on the combined effects of spatial variability and patch size or quality on species interaction stabilisation (Daugherty 2011).

Intransitivity is a key mechanism in maintaining species coexistence and biodiversity by satisfying an interaction relationship similar to that in a game of 'rock-paper-scissors' (Kerr et al. 2002; Reichenbach et al. 2007). Intransitive interactions often occur in species-rich communities and result in the survival of combatively weaker individuals (Gallien et al. 2017; Maynard et al. 2017a). A study which paired 18 basidiomycetes against each other to investigate the structure of their competitive network, found that diverse communities with high intransitivity showed a

positive diversity-function relationship (Maynard et al. 2017b), which in the real world would translate to decomposition processes and carbon cycling.

Fungal community dynamics have been well studied in the past (Caruso et al. 2012; Hannula et al. 2013; Hiscox et al. 2015a; Peršoh 2015; Arnstadt et al. 2016; Van Der Wal et al. 2016), with some attention given to the effects of spatial patterns and individual patch size on interaction outcomes (White et al. 1998; Sturrock et al. 2002; Hiscox et al. 2017). All of these studies, however, have been conducted across essentially a 2-dimensional plane, yet in the real world decomposer communities operate in heterogeneous, 3-dimensional space, and at larger scales emergent properties may arise (Halley et al. 1996). The aim of the present study was to test the effect of spatial distributions and patch size on community interactions in 3-dimensional space, and to determine the effect of such spatial variability on the ecosystem service provided by the community, namely resource decay rate.

Using wood decay basidiomycetes as experimental organisms, the outcomes of multiple species competitive interactions were tested in both 2- and 3-dimensional systems. The effect of (1) the orientation of woody vessels (an aspect of resource structural complexity), (2) patch size and (3) spatial patterns on species interactions and decay rate were investigated, and the following hypotheses tested: (1) substratum orientation causes combative strength to change; (2) patch fragmentation negatively affects an individual's competitive success; and (3) spatial heterogeneity in a three-species community causes changes to the ecosystem function, in this case wood decay, provided by the community compared to dual-species competitive systems.

5.3 Methods

5.3.1 Fungal strains

Three fungal species were selected based on their ecological roles and successional order in the natural environment: a primary resource coloniser (*Stereum gausapatum*), and two early secondary colonisers (*Stereum hirsutum* and *Trametes versicolor*) (Supplementary Table 5.1). Specific strains were chosen based on their expected combative hierarchy: *T. versicolor* > *S. hirsutum* > *S. gausapatum* (Hiscox et al. 2015a; Hiscox et al. 2015b; Hiscox et al. 2016b).

5.3.2 Experimental design

Interactions were performed by combining pre-colonised wood blocks (three species, one per block) with different levels of complexity (Figure 5.1): (experiment 1) two wood blocks; (experiment 2) three wood blocks; (experiment 3) a 3x3 (i.e. nine) matrix of blocks; (experiment 4) a 3x3x3 (i.e. 27) matrix of blocks. (1) With pairs of blocks, all combinations of the three species were made, i.e. three combinations. (2) With triplicates, all three combinations of three species were made, each with a different species in the middle. (3) In the nine block matrix arrangement, three blocks pre-colonised with each species were arranged with the constraint that two blocks containing the same species never had faces adjacent to each other; three combinations were made. (4) In the 27-block cube, nine blocks of each individual species were combined such that blocks containing the same species were not adjacent to one another. There are nine possible combinations, but only three, randomly selected combinations, were made. In (1) and (2) blocks were arranged with cut vessel ends touching (Figure 5.2a). In (3) and (4) blocks were joined such that some cut vessel ends were touching but others were not, but all vessels were parallel. (Experiment 5) Effect of vessel orientation was investigated with vessels laid parallel (Figure 5.2b), and compared with outcomes of blocks joined with cut vessels touching in (1), (2) and (3).

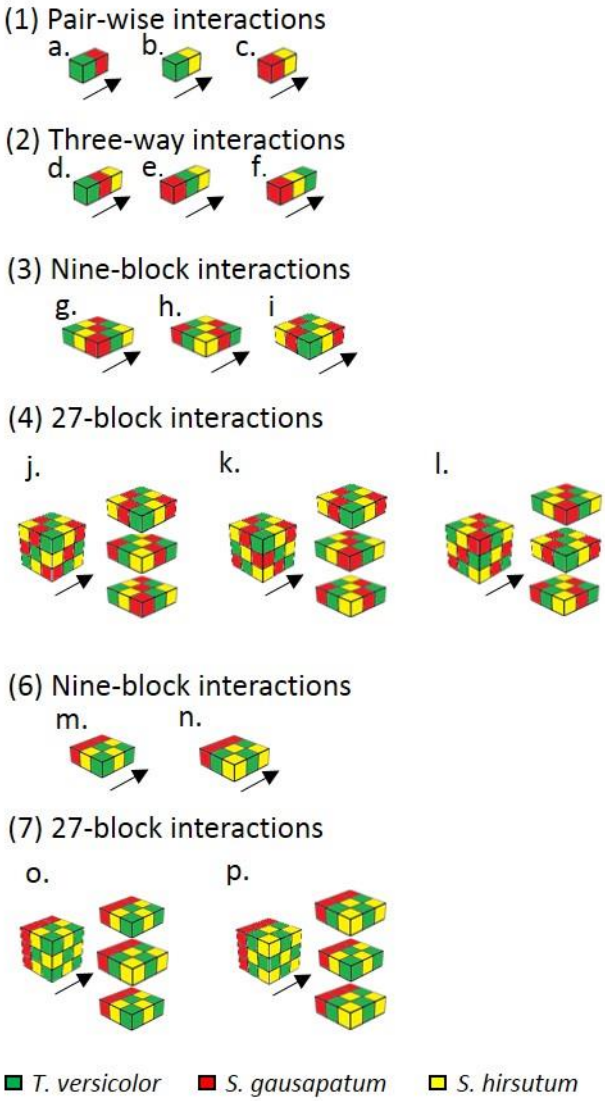

Figure 5.1 Spatial distribution of species within experimental design. Blocks coloured red indicate *S.gausapatum*, green indicates *T. versicolor* and yellow blocks are indicative of *S. hirsutum*. Dispersal patterns of nine-way and 27-block interactions were arranged such that blocks containing the same species do not have adjacent faces. Arrows indicate xylem directional flow.

The effect of one fungus (the primary coloniser *S. gausapatum*) occupying a larger adjacent volume of wood (but still a total volume equal to the other two species) was investigated in (experiment 6) 3x3 combinations and (experiment 7) 3x3x3 cubes. In (6) *S. gausapatum* blocks were placed with cut vessel ends adjacent, and the other two species positioned in all combinations such that no two blocks containing the same species were adjacent, touching the *S. gausapatum* wood blocks with vessels lying parallel. In (7) a 3x3 "wall" was constructed with cut vessels adjacent, and vessels lying parallel, with the other two species arranged in both possible combinations with vessels lying parallel to those of *S. gausapatum*, but never with blocks of the same species (*T. versicolor* or *S. hirsutum*) touching each other.

5.3.3 Wood block colonisation and interaction assembly

Beech (*Fagus sylvatica*) blocks (2x2x2 cm) were pre-colonised by placing on 0.5 % agar (MA: 5 gL^{-1} malt extract, 15 gL^{-1} agar; Lab M, UK) cultures of the appropriate fungus (*S. gausapatum*, *S. hirsutum* and *T. versicolor*) and then incubated for 12 weeks at 20 °C in the dark. Mycelia and agar were scraped from the surface of each wood block, using a sterile scalpel, 3 d prior to interaction set-up. Wood blocks were joined (by securing with elastic bands, which were removed after 7 d) and placed in polypropylene pots (70 ml, 340 ml, 340 ml, 500 ml for pair-wise, triplet, nine-block and 27-block interactions respectively; Cater4You Ltd) containing perlite (20 ml, 40 ml, 60 ml and 85 ml respectively; medium grade, 3-6 mm). 2 ml, 3 ml, 6 ml and 12 ml of dH_20 was added to the perlite respectively. Each pot plus wood blocks was weighed and dH_20 added to the perlite every 14 d to maintain moisture. Each pot had a < 1 mm hole covered with microporous tape for aeration. For pair-wise, three-way and nine-way interactions 10 replicates were set-up and four replicates of each 27-block cube, but a few replicates were lost due to contamination.

5.3.4 Determination of interaction outcome

Interacting wood block systems were incubated for 119 d. Then, they were deconstructed and each individual block split along the grain into thirds using a sterile (flamed in 70 % ethanol) chisel. The middle third was used for density measurements (to estimate decay rate), while four chips (approximately 3-5 mm) were taken from the inside-face of the remaining two thirds (eight chips in total per block) and were placed onto 2 % (w/v) malt agar (MA; 20 gL^{-1} malt extract, 15 gL^{-1} agar). Plates were incubated at 20 °C for 6 d before morphological identification of the species finally present in each block.

5.3.5 Estimation of decay rate

The mean initial density (g cm^{-3}) of 10 blocks pre-colonised with each species individually was determined as dry weight (80 °C for in excess of 72 hr) per fresh volume (cm^3), measured with digital callipers. Following cube deconstruction at the end of the experiment, the density of a third of each individual block was determined to estimate rate of decay by comparing with density at the start.

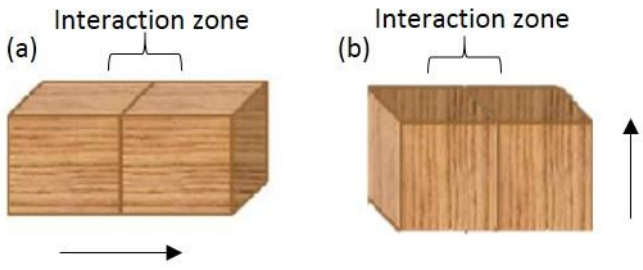

Figure 5.2 Xylem vessel orientations of wood blocks. (a) Cut vessel ends touching; (b) vessels laid parallel. Arrows indicate xylem directional flow.

5.3.6 Statistical analysis

All statistical analyses were conducted using R statistical software (R Core Team 2014). The rate of decay of wood in all configurations of the experimental set-up was compared using a one-way ANOVA followed by Tukey *post hoc* tests.

For every interaction, each species was assigned a score of combative ability as a percentage of the total system colonised at the end of the experiment. Each competitor scored between 0 and 8 (since eight regions were isolated) for each block within a system (0 indicates no recovery of a species from any isolation point, 8 indicates full recovery of a species from all eight isolation points). Individual species scores were combined for all blocks within a system, normalised to the number of replicates performed and converted to a percentage of the blocks colonised by each species. The data were analysed using a GLM followed by Tukey *post hoc* tests. The position of a given block within a system and, therefore, the number of faces of that block involved in direct combat was incorporated as a factor within the model. The effect of vessel orientation was tested by assigning each individual block a category based on the number of adjacent blocks whose vessels were touching, or laid parallel. For example, in pairs and triplets, blocks were either laid with vessel ends touching, or with vessels laid parallel to their neighbours. However, in nine-block systems where blocks were laid with vessel ends touching, blocks also had neighbours whose vessels were parallel, as did blocks in 27-block interactions. Vessel orientation was, therefore, a factor within the model. Water was always added to the perlite, as such, with 27-block interactions the layer laid on the perlite had greatest access to water, and the layer furthest from the perlite had least access to water. This was statistically accounted for by assigning each block to a category (greatest, moderate or least access to water), and was incorporated into the model.

5.4 Results

5.4.1 Combative ability in 2, 3, 9 and 27 block systems

Overall, *T. versicolor* consistently had the greatest score of combative ability ($F_{2, 42}$ = 89.84, $P < 0.001$). *S. hirsutum* scored second highest, however, overall this was not significantly different from *S. gausapatum* ($p > 0.05$).

In pair-wise experiments (experiment 1), interactions concluded with complete replacement of *S. gausapatum* by *T. versicolor*, partial replacement (36 % of territory) of *S. hirsutum* by *T. versicolor* (Table 5.1; Supplementary Table 5.2), and deadlock between *S. hirsutum* and *S. gausapatum* consistently across all replicates (Figure 5.3a).

The position of a fungus (relative to the number of surrounding competitor held blocks) within 3-way interactions (experiment 2) affected the territory held in a manner that was specific to individual fungi. *T. versicolor* obtained more territory after 119 d when placed between its competitors: when placed centrally it occupied 100 % of *S. gausapatum's* territory and 90 % of *S. hirsutum's* territory, whereas when placed on the edge next to *S. gausapatum* it occupied 100 % of *S. gausapatum's* territory but only 19 % of *S. hirsutum's* territory, and when placed on the edge next to *S. hirsutum* it captured none of *S. gausapatum's* territory and only 19 % of *S. hirsutum's* territory (Table 5.1). *S. gausapatum* was more successful (100 % territory retention in every replicate) when placed on the edge of an interaction next to *S. hirsutum* (arrangement pattern f; Figure 5.1) with whom it was in deadlock with (neither fungus captured territory held by the other), however, when positioned next to *T. versicolor* (as in arrangements d and e; Figure 5.1), *S. gausapatum* was constantly replaced by *T. versicolor* (Figure 5.3b). *S. hirsutum* lost 19 % of its territory to *T. versicolor* when both positioned between competitors (pattern f; Figure 5.1) and when placed on the edge next to *S. gausapatum* (pattern d; Figure 5.1) but it only managed to retain 10 % of its original territory when placed on the edge next to *T. versicolor* (pattern 3; Figure 5.1; Table 5.1).

Table 5.1 Total occupancy of systems at the end of the experiment. Individual occupancy is expressed as the percentage of a system occupied by an individual and is taken from the mean of each replicate set. Patterns are coded as per Fig. 1. *Denotes interactions where vessels are laid parallel**.**

	Total system occupancy (%)		
Pattern	*S. gausapatum*	*S. hirsutum*	*T. versicolor*
a	0.00	-	100.00
a*	12.50	-	87.50
b	-	14.00	86.00
b*	-	40.00	60.00
c	50.00	50.00	-
c*	50.00	50.00	-
d	0.00	27.00	73.00
d*	0.00	29.00	71.00
e	0.00	3.33	96.67
e*	0.00	30.00	70.00
f	33.33	27.00	39.67
f*	28.33	26.67	45.00
g	5.22	10.67	84.11
g*	9.67	20.22	70.11
h	3.00	11.11	85.89
h*	11.00	20.33	68.67
i	0.00	10.56	89.44
i*	0.00	13.17	86.83
j	5.59	6.37	88.07
k	5.48	5.70	88.82
l	3.67	0.00	96.33
m	33.33	10.56	56.11
n	30.00	12.11	57.89
o	33.33	1.67	65.00
p	33.15	3.41	63.44

The extent of replacement of individuals in nine-block systems (experiment 3) was rather more variable across replicates although an overall hierarchy could still be discerned: *T. versicolor* > *S. hirsutum* > *S. gausapatum* (Figure 5.3c). After 119 d, *T. versicolor* occupied an average of 84 % of the total system in arrangement g (Figure 5.1), 86 % in arrangement h and 89 % in arrangement i. *S. hirsutum* lost 68 % of its original territory to *T. versicolor* in arrangement g, 67 % in arrangement h and 68 % in arrangement i, and *S. gausapatum* lost 84 %, 91 % and 100 % of its original territory respectively to *T. versicolor* (Table 5.1). Any given block could be positioned centrally and therefore have four faces directly engaged in combat, on a corner so that two faces were engaged in combat, or on the edge of a system between two corner blocks (three faces engaged in combat). The position that a block occupied within the system, however, had no significant effect on the combative fitness of individuals ($F_{21, 42} = 0.389$, $p > 0.05$).

For 27-block interactions (experiment 4; Figure 5.1), a given block could have all six faces engaged in combat if positioned centrally, three if positioned on a corner, four if on the edge between two corner blocks, or five if positioned in the centre of an outside layer. The position of blocks within the system had no significant effect ($F_{21, 42} = 0.389$, $p > 0.05$) on the interaction outcome. *T. versicolor* consistently replaced its competitors, finally occupying 88, 89 and 96 % of the system in patterns j, k and l (Figure 5.1) respectively, regardless of relative position (Table 5.1).The amount of territory occupied by *S. gausapatum* and *S. hirsutum* was not significantly different from each other in patterns j, k and l (Figure 5.1), both always occupied < 6 %.

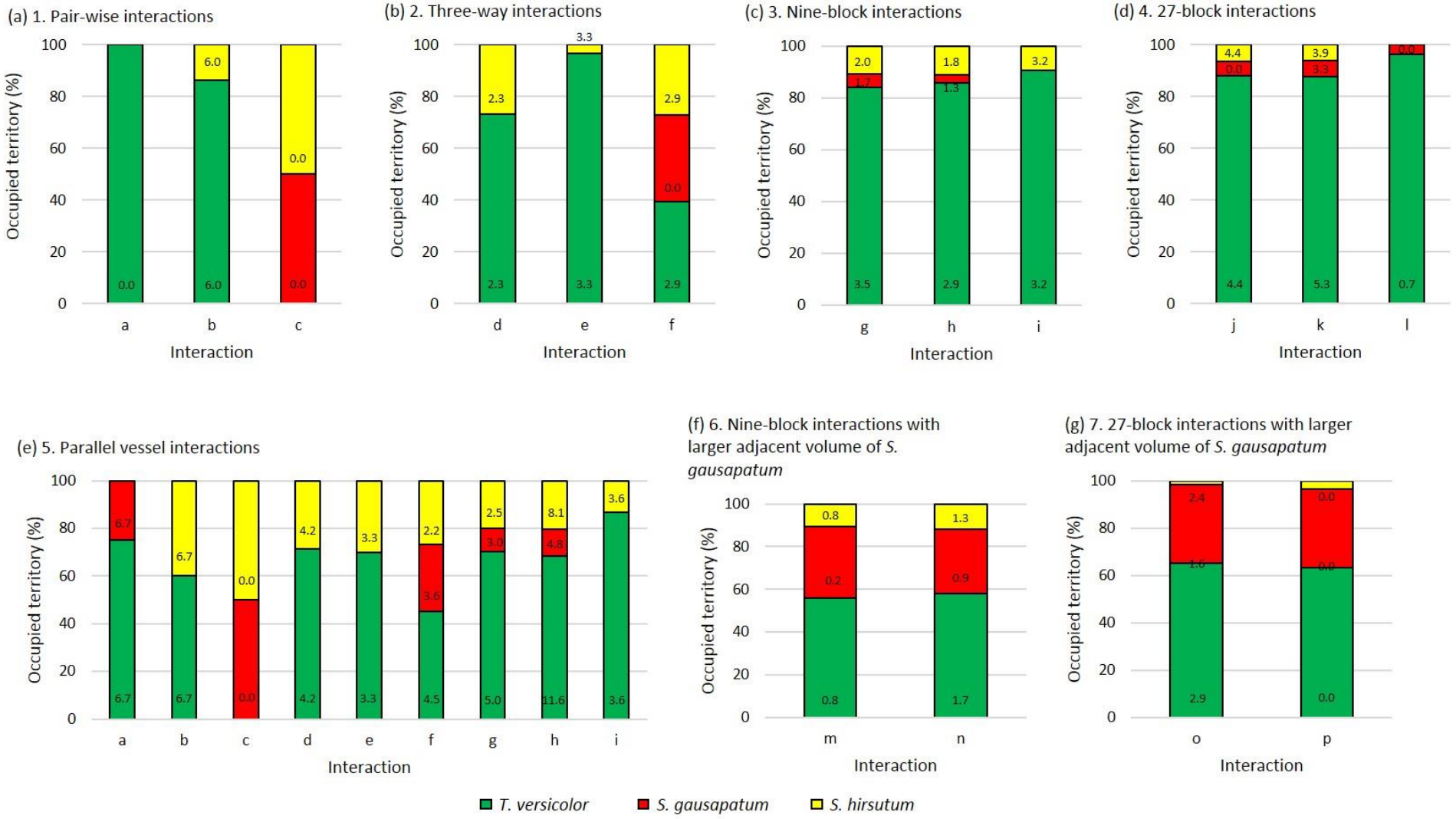
(a) 1. Pair-wise interactions
(b) 2. Three-way interactions
(c) 3. Nine-block interactions
(d) 4. 27-block interactions
(e) 5. Parallel vessel interactions
(f) 6. Nine-block interactions with larger adjacent volume of S. gausapatum
(g) 7. 27-block interactions with larger adjacent volume of S. gausapatum
Occupied territory (%)
Interaction
T. versicolor
S. gausapatum
S. hirsutum

Figure 5.3 Combative ability scores of fungi during pair-wise (experiment 1), three-way (experiment 2), nine-block (experiment 3), 27-block (experiment 4) interactions, interactions with a parallel vessel alignment (experiment 5), and interactions with a larger adjacent volume of *S. gausapatum* in nine-block (experiment 6) and 27-block (experiment 7) systems. Colours represent combative ability scores of each species per each interaction type and are expressed as a percentage of each interaction system occupied by a species at the end of the experiment, normalised to the replicate number. Numbers within bars are ± SEM. Numbers in brackets refer to treatment number indicated in Figure 5.1. N.B. blocks in a, b, c, d and f are laid with vessel ends touching. For significant differences ($p < 0.05$) between groups see Supplementary Figure 5.1.

5.4.2 Effect of vessel orientation on outcome of interaction

The orientation of vessels sometimes affected combative success (experiment 5: effect of vessel orientation). When *T. versicolor* was paired with *S. gausapatum* (pattern a; Figure 5.1), the latter defended 25 % of its territory when vessels were laid parallel to those of *T. versicolor*, but was fully replaced when cut vessel ends were touching. Combative ability of *S. hirsutum* was greater ($F_{14, 1665} = 3.29$, $p < 0.001$) against *T.* versicolor when in wood with vessels laid parallel compared to when vessel ends touched (Figure 5.3e). For example, in the three-block interaction arrangement e (Figure 5.1), *S. hirsutum* lost 90 % of its territory to *T. versicolor* when cut vessel ends were touching, but only lost 10 % of its original territory when vessels were laid parallel (Table 5.1).

5.4.3 Effect of patch size on outcome of interactions

Consistently, *S. gausapatum* was far more combative when its initial adjacent patch size was greater than that of competitors, despite total initial volume being identical (experiments 6

and 7). In nine-block systems where competitors were evenly dispersed (experiment 3), *S. gausapatum's* maximum final occupancy was 11 % (arrangement I; Figure 5.1) and it was fully replaced in arrangement h (Figure 5.3c). However, when *S. gausapatum* was arranged such that it occupied a larger adjacent volume, but with the same total volume as its competitors (experiment 6), it managed to retain 100 % ($F_{24, 1682}$ = 87.85, p < 0.001) of its original territory (33 % of the entire system) (arrangement m; Figure 5.3f). Similarly, in evenly dispersed 27 cube systems (experiment 4) the maximum amount of territory held by *S. gausapatum* at the end of the experiment was 6 % (arrangement k; Figure 5.3d), but when *S. gausapatum* occupied a larger initial adjacent volume (experiment 7), it retained 100 % of its original territory (Figure 5.3g) ($F_{24, 1682}$ = 87.85, p < 0.001).

The territory finally occupied by the other competitors was consequently reduced when *S. gausapatum* occupied a larger adjacent patch size in comparison to when all three species were evenly dispersed (Figure 5.3f,g). The average final occupancy of *T. versicolor* in nine-block systems across all spatial arrangements dropped significantly from 81 % when evenly dispersed (experiment 3) to 57 % ($F_{24, 1682}$ = 50.36, p < 0.001) when *S. gausapatum* occupied a larger adjacent volume (experiment 6; Figure 5.3f), and in 27 cube systems it fell from 91 % when evenly dispersed (experiment 4) to 64 % ($F_{24, 1682}$ = 50.36, p < 0.001) when *S. gausapatum's* initial adjacent patch size was greater (experiment 7; Figure 5.3g). The allocation of water within 27-block interactions had no effect (*T. versicolor*: $F_{2, 1665}$ = 2.32, p > 0.05; *S. hirsutum*: $F_{2, 1665}$ = 1.28, p > 0.05; *S. gausapatum*: $F_{2, 1665}$ = 1.24, p > 0.05) on outcome of interaction.

5.4.4 Effect of community composition on decay

Wood colonised by all species decayed significantly during the experiment. *T. versicolor* and *S. hirsutum* decayed wood at a similar rate (18 and 13 % total weight loss respectively), and blocks originally colonised by *S. gausapatum* had a significantly faster rate of decay than both *T. versicolor* and *S. hirsutum* (Supplementary Figure 5.2). The pair-wise permutation of

S. gausapatum and *S. hirsutum* (treatment c) in both wood vessel orientations resulted in a rate of decay that was significantly slower (12 and 14 % weight loss for each vessel orientation respectively; $F_{25, 1752} = 8.85$, $p < 0.01$; Supplementary Table 5.3) than any other arrangement (Figure 5.4). Neither the number of blocks interacting nor systems with larger adjacent *S. gausapatum* volume significantly affected the rate of decay.

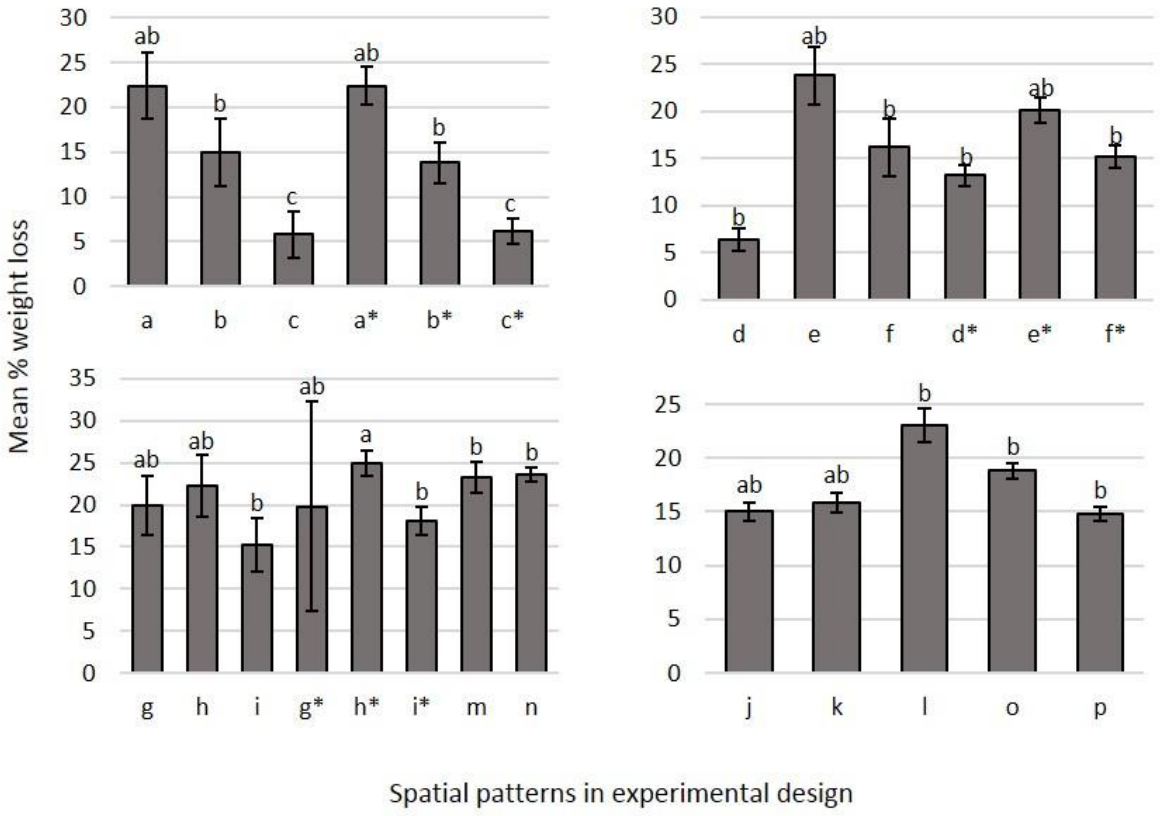

Figure 5.4 Mean % weight loss after 119 d of all blocks within each interaction type. Error bars denote SEM and statistical difference between group means are shown. Spatial patterns are coded as per Figure 5.1. * Denotes parallel vessel alignment.

5.5 Discussion

5.5.1 Patch size, fragmentation and emergent properties

The study showed, for the first time, that extent of fragmentation of fungal territory, and substratum complexity influenced community dynamics of wood decay fungi. In macroecology, patch fragmentation, or "patchiness" has a profound effect on species interactions and subsequent community structure and ecosystem functioning (Kareiva 1987; Didham 2010), and as hypothesised in the present study patchiness negatively impacted combative ability (hypothesis 2). Increased patch size, but unchanged total territory of the weakest competitor, *S. gausapatum*, resulted in a dynamic shift in the competitive hierarchy of this simple community (Figure 5.3f,g). The ability of *T. versicolor* to invade and capture the territory of *S. gausapatum* was inhibited, resulting in *S. gausapatum* retaining more of its territory.

Emergent properties have been demonstrated to arise in forest plots, e.g. mycorrhizal networks facilitate greater seedling establishment of Douglas-fir (*Pseudotsuga menziesii*) (Teste et al. 2009), and increased combativeness by *S. gausapatum* and resulting coexistence with its competitors when occupying a greater adjacent volume (Figure 5.3f,g) is a clear emergent property in the present study. Relative combative ability increases when larger volumes of wood are occupied (Holmer & Stenlind 1993), however, total volume remained the same in the present study. Exactly which mechanisms lead to this emergent property are unclear; the overall perimeter to defend is lower in large patch sizes than with the distributed blocks and the availability of extra resources that can be translocated from elsewhere in its territory to the antagonistic mycelial front is likely to be important (Lindahl & Olsson 2004; Hiscox & Boddy 2017). Additionally, anastomosis, or hyphal fusion, of genetically identical hyphae (i.e. that of the same individual) occurs following self-recognition and results in enhanced communication and resource pooling throughout the mycelium (Rayner 1991). The production of extracellular enzymes, diffusible and volatile organic compounds (VOCs) and non-diffusible metabolites are

mediators of antagonistic interactions (Hiscox et al. 2010b; El Ariebi et al. 2016), and changes in these need further study.

While *S. gausapatum* maintained a greater proportion of its territory when occupying a greater adjacent volume (experiments 6 and 7; Figure 5.3f,g), concomitantly *S. hirsutum* lost more territory to *T. versicolor* suggesting a faster rate of replacement of *S. hirsutum* by *T. versicolor* which was not the case when *S. gausapatum* was less combative (i.e. *S. gausapatum* was replaced first when fungi were dispersed). This same phenomenon of initial replacement of the weakest competitor before all others by the stronger was seen previously in an experiment when the aggressive *Phanerocheate velutina* grew from wood across the surface of soil to three wood blocks each colonised by a different species: the weaker combatant of the three was attacked and replaced first (Abdalla & Boddy 1996).

5.5.2 Relative positioning of individuals affects outcomes

The pair-wise outcomes were transitive (*T. versicolor* > *S. hirsutum* > *S. gausapatum*; Figure 5.3a), as in earlier studies (Hiscox et al. 2015b; Hiscox et al. 2016a) and reflects the life history strategies (Andrews 1992) of the species: secondary colonisers > primary colonisers. If fed into a community model, this would likely result in fast replacement of *S. gausapatum* by *T. versicolor*, followed by later replacement of *S. hirsutum* and collapse of the community to a single species. When spatial heterogeneity was increased in 3-dimensional structures and patchiness decreased (i.e. when *S. gausapatum* occupied a larger adjacent volume), however, the community network loop closed, which is characteristic of intransivity and promotes co-existence (Laird & Schamp 2006), with *T. versicolor* successfully attacking *S. hirsutum*, and *S. gausapatum* deadlocking with both of the other competitors. The survival rate of less competitive species is thought to increase with environmental heterogeneity due to the provision of permanent spatial refuges (Brockhurst et al. 2005). Given a longer interaction time and following resource depletion, it is probable that the relationships in the 3-dimensional cube

would de-stabilise and the relative volume of territory occupied by each species would change, with *S. hirsutum* likely becoming extinct from the community and *T. versicolor* establishing dominance within it. The latter, most ecologically dominant species, would then occupy even more territory, and ultimate replacement of *S. gausapatum* would be predicted. While the outcomes of interactions in three-species 2-dimensional systems were largely reflective of those in pairs (Figure 5.3a,b,c), scaling up of spatial dynamics into larger systems and altering the patchiness of species distributions, resulted in outcomes that were not expected. Changes in community structure are commonly predicted from pair-wise experimental data (Veech 2012), however, the current study indicates why caution should be taken when making such extrapolations.

The position of individual fungi relative to their competitors affected outcomes in three-block interactions (Figure 5.3b), but this was not evident in more complex nine-block and 27-block interactions (Figure 5.3c,d). *T. versicolor* was most combative when positioned between its competitors, *S. gausapatum* fared better when it was not positioned next to *T. versicolor* (i.e. on the edge next to *S. hirsutum*), and *S. hirsutum* was equally combative when placed next to *S. gausapatum* in both arrangements (edge position next to *S. gausapatum* and when placed centrally between the two) but lost the majority of its territory when placed on the edge next to *T. versicolor* (Figure 5.3b). The greater success of *T. versicolor* when placed centrally probably relates to its ability to rapidly extend its territory by capturing that of *S. gausapatum*, making it then relatively more combative than *S. hirsutum* by virtue of the large resource to which it then had access. This aligns with the reason for the greater success of *S. gausapatum* when territory was not fragmented, increased competitive advantage when larger territory is occupied (Holmer & Stenlid 1993) and to a previous study (Hiscox et al. 2017) with combinations of three beech wood blocks that found fungi were most successful when positioned next to an un-colonised resource, and thus able easily to obtain additional territory.

5.5.3 Xylem vessel orientation influences community structure

S. hirsutum and *S. gausapatum* were less successful when they met the most combative opponent, *T. versicolor*, 'head on' growing towards one another along vessels whose cut ends were in contact (Figure 5.3a,b), than when they were in parallel xylem alignments (Figure 5.3e), showing effects of resource structural complexity (support of hypothesis 1). This probably relates to the different combative mechanisms that fungi employ simultaneously, and how these are affected by wood architecture. Interference competition (combat) can occur at a distance from the antagonist, as a result of VOCs and/or diffusible organic compounds (DOCs) and enzyme activity, and following hyphal contact with these chemicals and other mechanisms (Boddy 2000; Boddy & Hiscox 2016b). When mycelia meet 'head on', all mechanisms can be brought to bear, and in large quantity. When mycelia are in columns of decay parallel to one another, antagonistic chemicals and hyphae themselves can only reach the target opponent hyphae via natural pores in wood cell walls or decay cavities produced by fungal breakdown of the wood cell wall, and breaching of any barriers (such as pseudosclerotial plates) formed by opponents. This presumably allows a smaller 'invasive force', at least at early stages of decay. When traversing parallel decay columns, spatial refuges may occur which may account for the greater competitive strength of *Stereum* spp. when interacting in this orientation. *T. versicolor* was unaffected by substratum orientation. Its dominance in real-world communities, before the arrival of cord-forming species, may be partially explained by its ability to compete efficiently regardless of substratum complexity as natural resources often exhibit non-uniformity in the form of wounds, burrs and knots.

5.5.4 Effect of interactions and community dynamics on community productivity

The rate of wood decomposition often increases during interactions, as evidenced by weight loss after several months (Hiscox et al. 2016a) and 'instantaneous' CO_2 evolution (Hiscox et al. 2015b) presumably reflecting increased metabolic cost of the production of enzymes, VOCs,

reactive oxygen species *etc*., required for attack and defence (Woodward & Boddy 2008). In the present study the rate of decomposition varied under different scenarios, but notably the decay rate of wood colonised by both *S. hirsutum* and *S. gausapatum* paired together (Figure 5.4c), was much slower than in other combinations. This interaction resulted in deadlock with no further metabolic demand for attack and defence chemicals. Hiscox *et al.* (2017) similarly reported a lack of change in the rate of decay when outcomes were deadlock. When *T. versicolor* interacted with *Bjerkandera adusta* decay rate varied depending on whether the fungus had access to an extra, uncolonised resource.

It was hypothesised (hypothesis 3) that spatial heterogeneity in a multi-species community would cause changes to community performance due to species complementarity and resource partitioning (Wagg et al. 2015; Hiscox et al. 2015b). Although the dimensionality of interactions and the effect of the primary coloniser's larger adjacent volume were not of direct significance to the rate of decomposition, spatial structure caused changes to community dynamics. Since different species decay wood at different rates, community composition has a major impact on decay rate. In the real-world where decay communities are made up of many more species and individuals of the same species, the rate of productivity, therefore, is likely to change depending on the specific suite of species comprising the community. Additionally, as spatial heterogeneity and reduction in patch fragmentation lead to intransitive relationship networks which support biodiversity, over a longer period, i.e. sufficient time for decomposition to progress, community productivity should be influenced (Maynard et al. 2017b).

5.6 Conclusions

This study is the first to assess the combative interactions of multiple fungi in wood with comparisons between 2- and 3-dimensional experimental systems. These results provide an insight into the mechanisms of species coexistence, and how interactions change over different spatial scales. Competitive outcomes observed in 3-dimensional systems were not reflective of

the transitive interactions (*T. versicolor* > *S. hirsutum* > *S. gausapatum*) exhibited in 2-dimensional systems. This highlights the importance of 3-dimensional decay systems with multi-species interactions for ecologically pertinent study of community dynamics. Spatial heterogeneity was important for coexistence of all individuals within the community, while the weakest individuals were outcompeted in more fragmented, and spatially simpler systems. The exact mechanisms responsible for this change in coexistence potential are unclear, and investigation into VOCs, extracellular enzyme and metabolite production during 2- and 3-dimensional community interactions of differing spatial dynamics should be conducted. Whether fungi met and interacted with each other 'head on' growing towards each other along xylem vessels or whether decay columns were parallel with each other (i.e. complexity of the resource) affected the outcome of interactions such that an increase in the weaker competitor's combativeness was positively correlated with substratum complexity. Dimensionality did not have a direct effect on the rate of decomposition, however, spatial distributions altered the dynamics of the community, which in the real-world is likely to be reflected by changes to decomposition and nutrient cycling.

Chapter 6: Extracellular enzyme production during community interactions in spatially heterogeneous structures

6.1 Abstract

Fungal decay of dead wood is facilitated by the oxidative activities of extracellular lignocellulose decomposing enzymes. Enzyme production by pairs of interacting fungi has been well studied, but production of enzymes by multiple species within spatially complex resources has been overlooked. In this study, the activity of 12 lignocellulose decomposing enzymes by the decay fungi *Trametes versicolor* and *Vuilleminia comedens* were investigated during pair-wise interactions in 2 cm^3 beech (*Fagus sylvatica*) blocks, with comparisons to community interactions with *Hypholoma fasiculare* within 3-dimensional 27-block assemblages. The effect of territory fragmentation on enzyme activity was assessed by arranging the fungi in different spatial positions. Species diversity, resource heterogeneity and territory fragmentation altered the profiles of wood decay enzymes, specifically, activity was greatest in 3-dimensional community interactions where territory was less fragmented. This highlights the importance of species diversity and distributions to community function.

6.2 Introduction

The primary role of lignin and cellulolytic enzymes is in the decomposition of wood which occurs through the oxidation and hydrolysation of the recalcitrant lignocellulose (Chapter 2). Certain enzymes, however, may function in a variety of roles due to their non-specific nature. For example, laccase production by the white-rot fungus *Pleurotus ostreatus* increased in the presence of heavy metals (Baldrian et al. 2000; Baldrian & Gabriel 2002; Baldrian et al. 2005), enzyme production altered depending on temperature (Chapter 3), and invertebrate grazing effected fungal enzyme activity (Crowther et al. 2011). Large differences in enzyme activity also occur as a result of interspecific interactions, as was evidenced in Chapter 3. Laccase and peroxidases may function defensively during interactions by producing protecting melanins in hyphae which breakdown toxic compounds and reactive oxygen species (Henson et al. 1999). For example, laccase produced by *Fusarium oxysporum* detoxifies heavy metals in aqueous solution (Sanyal et al. 2005), so may be successful at detoxifying an opponent's antagonistic chemicals. They may also function antagonistically during interactions.

Previous studies which have investigated the role of wood decay enzyme activity during interactions have focused their attention on bi-species 2-dimensional systems (Hiscox et al. 2010a; Hiscox et al. 2010b; Chapter 3). These systems have produced highly valuable information regarding, for example, the localisation of enzyme production within mycelia (Hiscox et al. 2010a), differences in enzyme production between mono- and dikaryons during growth on artificial media and in natural wood substrates (Hiscox et al. 2010b), and enzyme activity under different environmental conditions (Chapter 3). It is known, however, that increased species diversity within interactions causes outcomes to change, and that the spatial orientation of individuals within competitive systems also affects individual combative ability (White et al. 1998; Toledo et al. 2016; Hiscox et al. 2017). Additionally, multispecies interactions within spatially heterogeneous systems have resulted in increased species coexistence, which

combative hierarchies determined from pair-wise interactions did not predict (Hiscox et al. 2017; Chapter 5). It appears then, that while providing useful information regarding innate enzyme production during spatially simple pair-wise interactions, investigations of multispecies interactions within structurally complex systems are needed to comprehend fully the metabolic processes of fungal communities within naturally complex resources in forest ecosystems.

The aim of this study was to investigate the production of extracellular enzymes by a community of wood decay fungi during decomposition, with comparisons between 2- and 3-dimensional systems. Pair-wise interactions between *H. fasciculare*, *T. versicolor* and *V. comedens* were compared with 27-block assemblages containing all three fungi, in two different spatial arrangements. Arrangements were such that all three fungi were evenly dispersed throughout the system, or with the weakest competitor, *V. comedens*, occupying a larger adjacent volume, but same total volume as its competitors, and the other two fungi dispersed throughout the remainder of the system. It was hypothesised that: (1) the combative ability of *V. comedens* would drastically increase when it was occupying a larger adjacent volume causing the competitive hierarchy to change, as was seen in a similar system (Chapter 5) because resource size occupied by a mycelium alters combative ability (Holmer & Stenlid 1997), (2) spatial heterogeneity and species diversity in a multispecies community would cause metabolic process to differ from those in bi-species 2-dimensional decay systems since enzyme production changes depending on the identity of competitors (Chapter 3), and (3) metabolic processes would differ between the two spatial orientations in 27-block interactions as increased resource pooling within the mycelium of *V. comedens* when occupying a larger adjacent volume (Rayner 1991) would contribute to its change in combative strength, and would be reflected by changes to enzyme activity.

6.3 Methods

6.3.1 Fungal isolates and cultivation

Strains of three wood decay basidiomycetes were obtained from the culture collection of the Cardiff University Fungal Ecology Group (Table 6.1) and were maintained on 0.5 % (w/v) malt agar (MA; 5 gL^{-1} malt extract, 15 gL^{-1} agar; Lab M, Lancs, UK) at 20 ^{o}C. Beech (*F. sylvatica*) wood blocks (2 x 2 x 2 cm) were autoclaved and colonised as in Chapter 5 (Section 5.3.3), for 12 weeks. After pre-colonisation, block densities were determined for each fungus as dry weight/fresh volume (g cm^{-3}; 10 replicates).

Table 6.1 Details of experimental species. Cultures were obtained from isolated mycelia from wood or fruit bodies. All isolates used were heterokaryons.

Species	Acronym	Ecological role	Strain ID	Source	Rot type
Hypholoma fasciculare	Hf	Late secondary coloniser	DD3	Fruit body tissue	White
Trametes versicolor	Tv	Secondary coloniser	Tv CCJH1	Fruit body/wood	White
Vuilleminia comedens	Vc	Primary coloniser	VcWvJH1	Fruit body/ wood	White

6.3.2 System interactions

Wood blocks colonised by individual species were arranged in: (1) pairs in all possible combinations, i.e. three combinations, plus single species self-pairings, with cut vessel ends touching (Figure 6.1, a-f); and (2) 3-dimensional 27-block 3x3x3 lattices containing nine blocks of each species (Figure 6.1). Lattices were arranged so that all three fungi were distributed evenly throughout the lattice with no two blocks of the same species touching (one combination was randomly chosen out of a possible nine) (Figure 6.1g); or (3) where *V. comedens* occupied a

larger adjacent volume (a 3x3 exterior "wall") but the same total volume as its competitors (nine blocks), and the other two fungi, *T. versicolor* and *H. fasciculare* were dispersed (Figure 6.1h). 27-block systems comprising each species singly were also set up (Figure 6.1, i-j). For all interactions, excess mycelium was scraped from each colonised wood block three days prior to interaction set-up. Once joined and secured with a sterile elastic band (removed after 5 d), wood blocks were placed in polypropylene pots (70 ml and 500 ml for pair-wise and 27-block interactions respectively; Cater4You Ltd.) containing medium grade 3-6 mm sized perlite (20 ml and 85 ml respectively; Homebase) and 2 ml and 12 ml of sterile dH_2O respectively. Total weight of each interaction was measured and moisture levels maintained accordingly. An aeration hole was punctured in each pot and covered with surgical microporous tape (3M, Bracknell, UK). Interacting systems were incubated at 20 °C, and five replicates destructively sampled 1 d and 28 d after interaction set up.

6.3.3 Destructive sampling, re-isolation and decay rate estimation

After 1 d and 28 d, volatile organic compounds (VOCs) were extracted from the headspace of interactions as described in Chapter 7 (Section 7.3.2). Following VOC extraction, interactions were deconstructed and each block split along the grain into quarters using a sterile chisel. Three quarters of each block were foil wrapped, flash frozen in liquid nitrogen and stored at -80 °C. For the remaining quarter, two chips (~2 mm^3) were taken from an inside face and inoculated onto 2 % MA, incubated at 20 °C then emerging mycelia identified morphologically. The chip-excised face was then removed from the quarter by splitting with a chisel, and final density determined as dry weight (80 °C for in excess of 72 hr) per fresh volume (cm^3) (blocks sampled at 28 d only), and the rate of decay estimated by comparison with density at the start.

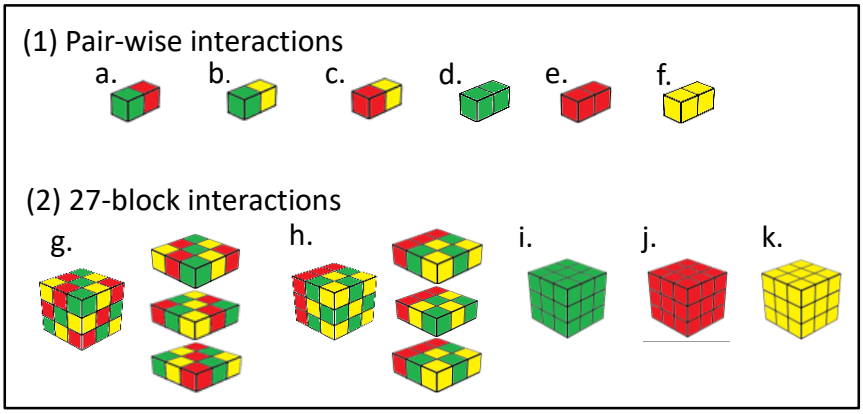

Figure 6.1 Spatial distribution of species in pair-wise (1) and 27-block (2) interactions. Green blocks: *T. versicolor*; yellow blocks: *H. fasciculare*; red blocks: *V. comedens*. a-c: pair-wise interactions in all conceivable combinations; d-f: single species self-pairings; g: dispersal cube (fungi were dispersed throughout the system and arranged so that no two blocks containing the same species had adjacent faces); h: "wall" distribution cubes (*V. comedens* occupied a larger adjacent volume, while the other two competitors were arranged so that no two blocks containing the same species had adjacent faces); i-k: single species "self" 27-block cubes.

6.3.4 Enzyme assays

Frozen blocks (-80 °C) were removed from storage and freeze dried for 48 h (Edwards Modulyo, UK), then ground to sawdust using a spice and coffee grinder (Wahl James Martin, UK). 0.5 g of sawdust was added to 5 ml of 50 mM sodium acetate buffer and shaken overnight at 4 °C. For pair-wise interactions, *T. versicolor* and *V. comedens* blocks from all interactions and one block from their respective self-pairings were used (five replicates). In 27-block assemblages, a given block could have all six faces engaged in combat if positioned centrally, three if positioned on a corner, four if positioned on the edge of a cube between two corners, or five if positioned centrally within an outside layer, and each species occupied a maximum of 3 different spatial positions within each community assemblage. Five replicates of each spatial position for

T. versicolor and *V. comedens* blocks within 27-block systems were used for assays (three pseudoreplicates per system), full details of which can be found in Supplementary Table 6.1.

The activities of laccase (EC 1.10.3.2), MnP (EC 1.11.1.13), oxidases, manganese independent peroxidases (peroxidase), β-glucosidase (EC 3.2.1.21), α-glucosidase (EC 3.2.1.20), cellobiohydrolase (EC 3.2.1.91), β-xylosidase (EC 3.2.1.37), N-acetylglucosaminidase (EC 3.2.1.30), phosphodiesterase (EC 3.1.4.1), phosphomonoesterase (EC 3.1.3.2) and arylsulfatase (EC 3.1.6.1) were measured as per the method of Hiscox *et al.* (2010a) (described in Chapter 3 (Section 3.3.5)).

Three technical replicates were assayed for each enzyme, and the protein content of each sample was determined using Qubit™ fluorometric assays (ThermoFisher Scientific Inc., UK), to which all enzyme activities were normalised.

6.3.5 Statistical analysis

The rate of decay and progression of interactions were analysed using R statistical software (R Core Team 2014). For each interaction, every species was assigned an individual score of combative ability, expressed as the percentage of the total system that it finally occupied. Briefly, each competitor scored between 0 and 2 for each block within a system (since two regions of every block were isolated; no outgrowth of a competitor from either isolation point scored 0, outgrowth from one isolation point scored 1, outgrowth from both isolation points scored 2). Scores for all blocks within a system were combined for each competitor individually, normalised to the number of replicates and converted to a percentage of the total system colonised. The data were analysed using a GLM combined with Tukey *post hoc* tests. The position of a given block within 27-block systems and, therefore, the number of faces of that block that were directly in combat with others was incorporated as a factor into the model. In 27-block interactions, water was unevenly distributed as it was always added to the perlite, as such, the

layer laid on the perlite had greatest access to water and the furthest most layer from the perlite had least access. To statistically account for this, each block was assigned to a category (greatest, moderate or least access to water), and was incorporated into the model. The rate of decay of wood in all interactions was compared using a one-way ANOVA followed by Tukey *post hoc* tests.

One-way ANOVA with Tukey *post hoc* tests were used to compare mean enzyme activities (from five replicates), or Kruskal-Wallis tests followed by a Dunn's test *post hoc* procedure was used when data were non-normally distributed. All statistical analyses were conducted using R statistical software (R Core Team 2014).

6.4 Results

6.4.1 Combative ability

In pair-wise interactions, an overall hierarchy of combative ability was exhibited where *H. fasciculare* > *T. versicolor* > *V. comedens*. When paired together, *H. fasciculare* and *T. versicolor* were evenly matched ($F_{59, 48} = 2$, $p > 0.05$), and neither gained any territory held by the other (deadlock). When paired against *V. comedens*, *T. versicolor* invaded and gained 40 % of the territory originally held by *V. comedens*, and *H. fasciculare* gained 80 % of the original territory of *V. comedens* (Figure 6.2).

In 27-block interactions where all three fungi were dispersed, *H. fasiculare* was the most combative, finally occupying 60 % of the system (80 % territory gain), *T. versicolor* was second most combative finally occupying 30 % of the system (9 % territory loss), and *V. comedens* was the least combative finally occupying just 10 % of the total system (69 % territory loss) (Figure 6.2).

When *V. comedens* occupied a larger adjacent volume it was able to defend its territory more effectively and retained almost all of it, losing just 6 % (Figure 6.2). *T. versicolor* lost 45 % of its

original territory making it the least combative competitor, and *H. fasciculare* captured 51 % of the total system territory from its competitors, making it the most combative (Figure 6.2).

When arranged in 27-block configurations, individual blocks had different numbers of faces touching and engaged in direct combat with other blocks, depending on spatial location within the system. There were no significant effects ($F_{59, 48} = 2$, $p > 0.05$) to the combative abilities of fungi due to the position of blocks within systems. Additionally, the allocation of water within 27-block interactions did not significantly affect fungal combative ability.

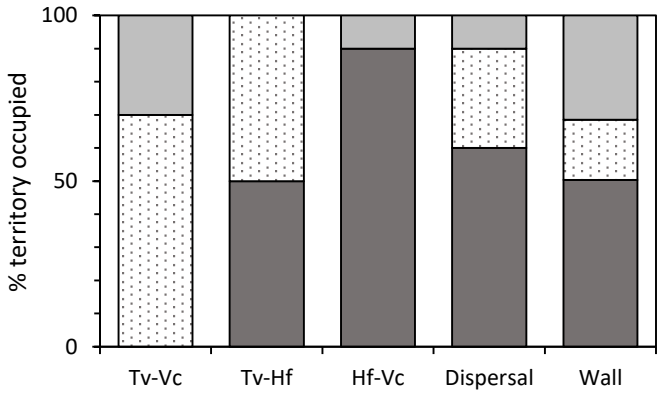

Figure 6.2 Interaction progression after 28 d in pair-wise (*T. versicolor* (Tv) against *V. comedens* (Vc); *T. versicolor* against *H. fasiculare* (Hf); *H. facifculare* against *V. comedens*), and 27-block (where all three species were evenly dispersed (Dispersal; Figure 1g), and where *V. comedens* occupied a larger adjacent volume (Wall; Figure 1h) interactions. Bars show the proportion of territory occupied by each species at the end of the experiment (means of five replicates). Dark grey, *H. fasiculare*; spotted, *T. versicolor*, pale grey: *V. comedens*.

6.4.2 Enzyme activity during pair-wise interactions

After 1 d, the only significant difference ($p < 0.05$) to enzyme activity during pair-wise interactions occurred to the activity of cellobiohydrolase in self-pairings of *T. versicolor* blocks: activity was significantly lower when paired against *H. fasiculare* than when paired with its self. After 28 d, the production of α-glucosidase, cellobiohydrolase, β-xylosidase, exochitinase, arylsulfatase and phosphodiesterase by *T. versicolor* was significantly increased when it was paired against both competitors (*V. comedens* and *H. fasiculare*) compared to its self-pairing control. Cellobiohydrolase production by *V. comedens* significantly decreased in blocks that were paired against *T. versicolor* for 28 d, compared to its self-pairing control (Table 6.2).

6.4.3 Enzyme activity in 27-block interactions

There were no significant differences ($p > 0.05$) in enzyme production by either fungus assayed between pseudoreplicates occupying different spatial locations within 27-block assemblages. As a result of this, activities of all pseudoreplicates within systems were pooled, and "mean enzyme activity" from here on refers to the means of all 15 replicates (3 pseudoreplicates x 5 biological replicates).

Enzyme activity was often greater in "wall" configuration cubes compared to cubes where all three fungi were dispersed. For example, in *T. versicolor* colonised blocks from "wall" configuration cubes, 1 d after interaction set up β-glucosidase, cellobiohydrolase, exochitinase, acid phosphatase and arylsulfatase activity was significantly increased ($p < 0.05$) compared to *T. versicolor* blocks in cubes where all three fungi were fully dispersed (Table 6.3; Supplementary Figure 6.1). Similarly, activity of β-glucosidase, α-glucosidase, cellobiohydrolase, β-xylosidase, exochitinase, acid phosphatase and phosphodiesterase by *V. comedens* in cubes where *V. comedens* colonised blocks that formed the "wall" of larger adjacent volume, was increased

28 d after interaction set up compared to cubes where fungi were dispersed (Table 6.3; Supplementary Figure 6.1). Increased enzyme activity when fungi were dispersed only occurred for laccase, specifically in *V. comedens* colonised blocks 28 d after interaction set up (Table 6.3; Supplementary Figure 6.1).

Activity in *T. versicolor* blocks was generally higher 28 d after interaction set up than after 1 d. For example, exochitinase activity was 3.7-fold higher after 28 d in *T. versicolor* self-cubes, than after 1 d. For *V. comedens* temporal change was more variable, with, for example, a 2.3-fold increase in α-glucosidase activity after 28 d in "wall" distribution cubes, but a 2.4-fold decrease in oxidase activity in the same blocks after 28 d (Table 6.3; Supplementary Figure 6.1).

6.4.4 Differences in enzyme activity between 2- and 3-dimensions

Generally, enzyme production was higher when fungi were arranged within 27-block assemblages, compared to when paired. For example, acid phosphatase activity was 140 mU g-1 in the *V comedens* self-pairing after 28 d, but was 11 fold more active (1516 mU g-1) after 28 d when *V. comedens* comprised a 27-block cube (Tables 6.2,3). Laccase activity, however, was usually higher in pairings, for example 34 mU g-1 in *T. versicolor* self-pairings compared to 5 mU g-1 in 27-block cubes solely comprising *T. versicolor* after 28 d (Tables 6.2,3).

6.4.5 Rate of decay

Overall, *H. fasciculare* decayed wood significantly ($p < 0.001$) slower than *T. versicolor* and *V. comedens*. There were no significant differences ($p > 0.05$) between competitor blocks within individual interactions, nor were there any differences between same species blocks across interactions (Supplementary Figure 6.2).

Table 6.2 Enzyme activity in pair-wise interactions 1 d and 28 d after interaction set up. Square brackets indicate which competitor block was used for assays, and values represent the mean of five replicates. Tv: *T. versicolor*, Hf: *H. fasciculare*, Vc: *V. comedens*. Significant differences ($p < 0.05$) between means of samples 1 d and 28 d after interaction set up are indicated by different letters, and ǂ indicates a significant difference between the means of interactions and corresponding self-pairing. (-) represents a failed assay.

	Activity mU g-1											
	[Tv]-Tv		[Tv]-Hf		[Tv]-Vc		[Vc]-Vc		[Vc]-Tv		[Vc]-Hf	
	1 d	28 d	1 d	28 d	1 d	28 d	1 d	28 d	1 d	28 d	1 d	28 d
Laccase	17.30 a	34.28 a	14.65 a	20.52 a	24.92 a	9.67 a	92.55 a	50.61 a	81.20 a	59.47 a	110.22 a	59.40 a
Oxidase	3.51 a	6.92 a	5.83 a	10.06 a	5.34 a	11.54 a	12.61 a	9.35 a	11.24 a	8.77 a	11.88 a	11.39 a
Peroxidase	0.00 a	0.00 a	0.69 a	4.03 a	0.00 a	0.00 a	0.00 a	1.49 a	0.49 a	0.42 a	0.00 a	0.00 a
MnP	36.99 a	30.08 a	31.78 a	30.72 a	34.46 a	51.54 a	9.71 a	11.14 a	9.78 a	6.74 a	6.07 a	6.37 a
β-glucosidase	0.56	-	-	344.85	9.98 a	293.53 b	101.06 a	103.55 a	89.96 a	68.16 a	84.92 a	75.25 a
α-glucosidase	23.93 a	18.19 a	12.11 a	691.39 bǂ	29.03 a	653.61 bǂ	129.62 a	102.64 a	91.02 a	88.35 a	95.55 a	150.27 a
Cellobiohydrolase	17.92 a	9.46 a	3.29 aǂ	404.04 bǂ	14.93 a	395.77 bǂ	115.47 a	103.44 a	97.13 a	58.56 aǂ	88.08 a	100.39 a
β-xylosidase	18.02 a	6.88 a	2.96 a	509.18 bǂ	13.83 a	451.78 bǂ	108.10 a	110.65 a	110.16 a	65.69 a	75.79 a	86.90 a
Exochitinase	19.00 a	2.09 a	3.01 a	440.34 bǂ	11.77 a	332.40 bǂ	90.29 a	93.28 a	101.70 a	50.75 a	73.43 a	70.22 a
Arylsulfatase	1813.13 a	231.45 a	125.12 a	53782.63 bǂ	836.35 a	46922.39 bǂ	17010.33 a	15750.99 a	14822.10 a	9756.11 a	9239.22 a	13945.88 a
Acid phosphatase	70.73	-	-	2398.01	-	2325.66	125.81 a	140.07 a	136.24 a	73.34 a	73.34 a	9.37 a
Phosphodiesterase	52.55 a	10.33 a	7.12 a	1031.78 bǂ	18.8 a	998.66 bǂ	406.69 a	286.91 a	320.33 a	177.97 a	237.46 a	283.75 a

Table 6.3 Enzyme activity 27-block interactions 1 d and 28 d after interaction set up. Values represent the mean of all assayed *T. versicolor* (Tv) or *V. comedens* (Vc) blocks within 27-block cubes (3 different positions (not significantly different to each other, $p > 0.05$) X 5 replicates = 15 replicates per cube). Self-cube: 27-block cubes comprising each species singly, wall cube: 27-block interaction where *V. comedens* occupied a larger adjacent volume, dispersal cube: 27-block interaction where all three fungi were dispersed. Significant differences ($p < 0.05$) between means of samples 1 d and 28 d after interaction set up are indicated by letters, and ǂ indicates a significant difference between the means of interactions and corresponding self-cubes. (-) represents a failed assay.

	Activity mU g-1											
	Tv self-cube		Tv wall cube		Tv dispersal cube		Vc self-cube		Vc wall cube		Vc dispersal cube	
	1 d	28 d	1 d	28 d	1 d	28 d	1 d	28 d	1 d	28 d	1 d	28 d
Laccase	2.62 a	5.01 a	8.24 a	3.20 a	11.80 a	0.26 a	43.15 a	17.45 a	52.87 b	0.00 a	110.39 bǂ	55.27 a
Oxidase	1.84 a	2.74 a	3.59 aǂ	7.18 aǂ	4.91 aǂ	4.05 a	16.11 a	12.61 a	31.99 aǂ	13.51 a	18.84 a	10.90 a
Peroxidase	2.40 a	2.25 a	3.37 a	1.71 a	0.00 a	2.84 a	-	20.45	7.22 a	10.68 a	7.01 a	5.84 a
MnP	7.63 a	16.61 a	5.91 a	7.81 a	1.74 a	1.30 aǂ	-	60.99	24.94 a	31.99 aǂ	18.46 a	10.05 aǂ
β-glucosidase	75.03 a	167.06 b	133.67 a	68.29 aǂ	35.14 a	37.81 aǂ	87.38 a	231.19 b	307.77 aǂ	231.89 a	127.51 b	31.82 aǂ
α-glucosidase	210.10 a	632.86 a	265.78 a	100.85 a	101.38 a	80.41 a	201.69 a	387.57 a	530.92 a	1238.10 b	361.80 b	60.04 aǂ
Cellobiohydrolase	91.81 a	248.38 b	155.32 a	78.43 aǂ	56.97 a	54.16 aǂ	98.01 a	247.37 b	409.09 aǂ	317.28 aǂ	169.10 b	44.77 aǂ
β-xylosidase	154.14 a	465.45 a	172.78 a	80.20 aǂ	64.63 a	66.94 aǂ	123.64 a	299.51 a	382.68 a	335.64 a	181.51 b	33.91 aǂ
Exochitinase	129.88 a	479.99 b	492.47 bǂ	54.79 aǂ	24.24 aǂ	30.98 aǂ	91.41 a	247.31 b	308.29 aǂ	229.80 a	117.62 b	30.06 aǂ
Arylsulfatase	33924.66 a	131992.13 a	66989.54 b	12449.33 aǂ	24801.63 a	14329.59 aǂ	1270.26 a	2776.28 a	4394.65 a	4959.88 a	2655.74 b	487.96 a
Acid phosphatase	1453.02 a	5545.51 a	2412.03 b	96.06 aǂ	137.14 aǂ	88.86 aǂ	649.70 a	1516.46 a	2074.45 a	2085.83 a	1080.72 b	184.31 aǂ
Phosphodiesterase	522.03 a	1572.85 a	885.34 a	241.72 a	376.57 a	238.11 aǂ	313.26 a	652.05 a	1151.92 a	1031.47 a	674.32 a	105.74 aǂ

6.5 Discussion

This study is novel in its approach of testing the metabolic processes that govern interspecific interactions during decomposition by its use of ecologically pertinent 3-dimensional systems. This resulted in the discovery that extracellular enzyme activity reflects changes to community dynamics that are caused by extent of territory fragmentation and spatial distributions.

6.5.1 Combative ability is reflected in enzyme activity

When fungi were paired for 28 d, *T. versicolor* and *H. fasciculare* deadlocked but both partially replaced *V. comedens*. When fungi initially encounter each other, vast quantities of antagonistic compounds are generated and exerted as combative weaponry with roles in both aggression and defence (Hiscox & Boddy 2017). After 1 d, cellobiohydrolase activity by *T. versicolor* was lower when interacting with *H. fasciculare*, perhaps due to an initial lag in combative mechanisms at such an early stage in the interaction process. By 28 d, however, cellobiohydrolase activity as well as activity of β-glucosidase, α-glucosidase, β-xylosidase, exochitinase and phosphodiesterase was greater when *T. versicolor* was paired with *H. fasciculare* and with *V. comedens*, compared to self-pairings. Chitinases and glucanases directly target competitor mycelium and hydrolyse the cell wall (Lindahl & Finlay 2006), leading to commencement of the process of replacement by the successful combatant, and the breakdown of the displaced competitor's mycelium (Hiscox & Boddy 2017; Chapter 3). In the present study, cell wall-hydrolysing enzyme production increased when *T. versicolor* was in deadlock, not just when it was successfully gaining territory, i.e. against *V. comedens*. A previous study also found that activity of certain enzymes increased when *T. versicolor* and *H. fasciculare* were in deadlock, namely β-glucosidase and acid phosphatase (Chapter 3), which is likely due to the combatively similar individuals deploying antagonistic chemicals in an attempt to overcome the other.

6.5.2 Territory fragmentation and individual competitive success is mediated by metabolic processes

Enzyme activity was often higher in 27-block interactions when *V. comedens* occupied a larger adjacent volume, compared to when fungi were evenly dispersed. As hypothesised, the competitive hierarchy displayed in pair-wise interactions (*H. fasciculare* > *T. versicolor* > *V. comedens*) was also exhibited when the interacting community was dispersed, but not when *V. comedens* occupied a larger adjacent volume. When its territory was adjacent, *V. comedens* drastically increased its competitive ability in this study, thus supporting hypothesis 1. Similarly, when the relatively weak competitor, *S. gausapatum*, was present as a 'wall' its relative combative ability increased, allowing it to coexist with *T. versicolor* and S*tereum hirsutum* (Chapter 5). Fungi are known to increase enzyme production during antagonism (Hiscox et al. 2010a; Chapter 3), and constitutive defences are often created to obstruct competitor mycelium from invading and capturing colonised territory (Hiscox & Boddy 2017). Such defences may take the form of melanised tissue, known as pseudosclerotial plates, which surround the occupied territory acting as a physical barrier (Rayner & Boddy 1988), or the accumulation of secondary metabolites, such as diffusible and volatile organic compounds (DOCs and VOCs) which often possess antimicrobial properties and may inhibit competitor growth (El Ariebi et al. 2016; Chapter 4). Some fungi, however, defend their territory by modifying the resource and making it unfavourable or inhospitable for potential invaders, by, for example, lowering the water content or pH (Hiscox & Boddy 2017). Furthermore, anastomosis of an individual's mycelia results in enhanced translocation of resources required for antagonism throughout the mycelial network (Rayner 1991), likely improving the combative ability of *V. comedens* when occupying a larger adjacent volume, and may also be responsible for the homologous combative ability and enzyme activity of *V. comedens* and *T. versicolor* occupying different spatial locations within 3-dimensional cubes. In the present study, lignin and cellulose decomposing enzymes,

specifically β-glucosidase, α-glucosidase, cellobiohydrolase, β-xylosidase, exochitinase, acid phosphatase and phosphodiesterase, were produced in large quantities by *V. comedens* when it occupied a larger adjacent patch size relative to when fungi were evenly dispersed (supporting hypothesis 3), perhaps modifying the lignocellulose resource in a manner favourable to itself, or damaging the opponent's mycelia, resulting in the inability of its competitors to invade and displace it. Additionally, increased production of enzymes is thought to facilitate nutrient acquisition during interactions, antagonism being energetically expensive (Hiscox & Boddy 2017; Hiscox et al. 2017). The increased nutrients available to *V. comedens* as a result may act as precursors for the production of inhibitory secondary metabolites, increasing its defensive arsenal further.

Laccase production by *V. comedens* significantly increased after 28 d when all fungi were dispersed compared to when *V. comedens* occupied a larger adjacent volume: the only time increased production in dispersed systems occurred. Laccase is an enzyme involved in generating reactive oxygen species (Baldrian 2006) whose oxidative activities detoxify competitor metabolites (Hiscox & Boddy 2017). *H. fasiculare* had replaced 69 % of the mycelium of *V. comedens* after 28 d, so it is probable, therefore, that the increased laccase production was in fact caused by *H. fasciculare* when it was displacing *V. comedens*.

T. versicolor also increased production of specific enzymes when *V. comedens* occupied a larger adjacent volume, relative to when all three fungi were evenly dispersed, which was not necessarily predicted. This is suggestive of an increased metabolic response of *T. versicolor* towards the heightened defensive capabilities of *V. comedens*. A change in metabolic mechanisms as a result of enhanced competitive threat was seen previously when the outcome of the interaction between *T. versicolor* and *Phanerochaete velutina* was reversed at different temperatures (Chapter 3). When interacting at 25 °C *T. versicolor* partially replaced *P. velutina*, at 15 °C, however, *P. velutina* was more combative and partially replaced *T. versicolor*. The

metabolic strategy of *T. versicolor* differed between the two temperatures, with greater production of extracellular laccase, MnP, peroxidase, α-glucosidase, cellobiohydrolase, β-glucosidase, exochitinase, acid phosphatase, phosphodiesterase, arylsulfatase and β-xylosidase when faced with the increased combative force of *P. velutina* at the lower temperature.

6.5.3 Spatial heterogeneity and species diversity influence metabolic function

Enzyme activity was often greatest when fungi were arranged within 3-dimensional space with all three species interacting simultaneously, particularly when *V. comedens* occupied a larger adjacent patch size, supporting hypothesis 2. In nature, fungi interact with each other within 3-dimenionsal resources, and the differences in metabolic activity between system interactions of varied heterogeneity and species diversity, highlights the limitations of traditional bi-species pair-wise study of naturally occurring species interaction processes. The increased expenditure of metabolic products may be caused by a change in combative mechanisms as a result of resource structural complexity (Chapter 5), or due to the greater number of competing individuals within community assemblages (Hiscox et al. 2017). A previous study which paired 18 basidiomycete fungi against each other, found that the effects of species diversity alone on community function (measured as respiration, carbon use efficiency and biomass production) were negligible, but that a diverse community comprising weak competitors with high intransitivity exhibited a positive diversity-function relationship, and transitive communities of highly combative competitors showed a negative diversity-function relationship (Maynard et al. 2017b). In the present study, extracellular enzyme production was generally highest in systems where *V. comedens* occupied a larger adjacent volume, and presumably as a result was more combative leading to coexistence of the three individuals and a closed community network loop (characteristic of intransitivity). When individuals were dispersed, there was a transitive hierarchy of combative ability, which given a longer interaction length would likely have resulted

in the extinction of the weakest competitor, *V. comedens*, from the community (Chapter 5). The production of enzymes was generally lower when individuals were dispersed, compared to the system of coexisting individuals. The differences in enzyme production between the community exhibiting intransitive characteristics, and the transitive community comprising the strongest competitors may, therefore, be reflective of the positive/negative diversity-function relationship.

6.6 Conclusions

Never before have the effects of territory fragmentation on enzyme production by a community of wood decay fungi been tested, nor have comparisons been made between enzymes in 2- and 3-dimensional systems. Cell-wall hydrolysing enzymes were produced during pair-wise interactions both when a successful combatant was attacking and displacing its competitor, and when competitors were in deadlock. Enzyme activity was usually greatest during community interactions when the weakest competitor, *V. comedens*, occupied a larger adjacent volume compared to when individuals were dispersed, and its combative ability considerably improved. Increased production of enzymes by *V. comedens* when occupying a larger adjacent patch size was most likely due to increased metabolic investment in constitutive defensive mechanisms. *T. versicolor* also increased enzyme production in response to the increased defensive arsenal of *V. comedens*. When the fungal community was dispersed, a transitive hierarchy of combative ability was exhibited mirroring that of pair-wise interactions. Enzyme activity in systems where all three individuals were dispersed was reduced compared to 3-dimenionsal systems where the three fungi coexisted, emphasising the importance of species distributions and species diversity to community function. Despite different enzymatic profiles and activity levels between different system interactions, significant differences in the rate of decay were not detected. However, in the natural environment over a longer time frame, the production of lignin and cellulose degrading enzymes is likely to increase the rate of decomposition.

Chapter 7: Production of volatile organic compounds in 3-dimensional model wood decay communities

7.1 Abstract

Fungal produced volatile organic compounds (VOCs) function in a range of processes including interspecific antagonism. While VOC production during pair-wise interactions of wood decay fungi has been well characterised, multispecies production of volatiles in spatially complex resources has received little attention, yet species diversity and resource heterogeneity has been shown previously to affect metabolic processes. This study, therefore, investigated VOC production by a community of three fungal species arranged in 3- dimensional structures, and compared this with single species and bi-species production across a 2- dimensional plane. VOCs were extracted from the headspace of interactions and analysed by thermal desorption gas chromatography time-of-flight mass spectrometry (TD-GC-TOF-MS). Sesquiterpenes comprised the biggest group of aliphatic compounds, and a high proportion of esters, alkenes and ketones were also detected. Profiles of VOCs differed between 2- and 3-dimensional systems, and the suite and abundance of certain compounds changed as a result of increased species diversity and spatial orientation of individuals within community assemblages.

7.2 Introduction

Volatile emissions by fungi have been well described in the past (Rapior et al. 2000; Rosecke et al. 2000; Konuma et al. 2015; Isidorov et al. 2016; Isaka et al. 2017), with their functions linked to a variety of processes including hormone signalling (Bennett et al. 2012), semiochemical attraction and deterrence of saproxylic insects (Leather et al. 2014), signals for host plant interactions (Lee et al. 2016) and interspecific antagonism and defence (Jeleń 2002; Sánchez-Fernández et al. 2016; Chapter 4). For example, VOCs produced by the ascomycete *Fusarium oxysporum* inhibit mycelial growth of *F. oxysporum formae speciales* (Minerdi et al. 2008), and *Trichoderma* species suppress the growth of the basidiomycete *Phellinus noxius* and its rate of decomposition by inhibitory VOC production (Schwarze et al. 2012). Furthermore, studies such as El Ariebi *et al.* (2016) highlight the antagonistic properties of VOCs against other fungi during competition for resources.

Despite the considerable role of VOCs in fungal antagonism, only a few studies have considered the effects of interspecific interactions on VOC production by decay fungi (Hynes et al. 2007; Evans et al. 2008; El Ariebi et al. 2016; Chapter 4). Additionally, most studies fail to investigate fungal VOC production within naturally heterogeneous substrates, and have assessed VOCs during pair-wise interactions, negating the effects of resource structural complexity and species diversity on volatile production, both of which have resulted in changes to individual combative ability and metabolic processes previously (Chapters 5,6).

In the present study, VOCs were extracted from the headspace of pair-wise interactions between *Hypholoma fasciculare*, *Trametes versicolor* and *Vuilleminia comedens*, and 3-dimensional 27-block assemblages containing all three fungi. The hypothesis that resource heterogeneity and species diversity would alter VOC profiles was tested by comparisons between 2- and 3-dimensional systems, and the hypothesis that changes to VOC profiles would occur as a result of territory fragmentation was investigated by altering species distributions

within 27-block interactions: species were either dispersed so that no two blocks containing the same species were adjacent, or *V. comedens* occupied a larger adjacent area, but same total area as its competitors (as in Chapter 6). VOC extracts were analysed by thermal desorption gas chromatography time-of-flight mass spectrometry (TD-GC-TOF-MS), and the suite and abundance of volatile metabolites produced during interactions determined.

7.3 Materials and methods

7.3.1 Fungal cultures and system interactions

Three wood decay basidiomycetes, *H. fasciculare*, *T. versicolor* and *V. comedens* were cultivated and pair-wise and 27-block interactions arranged as in Chapter 6 (Section 6.3.1; 6.3.2). Briefly, 2x2x2 cm beech (*Fagus sylvatica*) blocks were colonised by each fungus individually and placed into polypropylene pots arranged in: (1) pairs in all possible combinations plus single species self-pairings; and (2) 27-block (3x3x3) 3-dimensional lattices containing nine blocks of each species. 27-block assemblages were arranged so that all three fungi were dispersed throughout the system with no two blocks of the same species touching, or so that *V. comedens* occupied a larger adjacent area (3x3 "wall") but the same total area as its competitors (nine blocks), and the other two fungi were dispersed.

7.3.2 VOC analysis

Three replicates of each interaction were sampled for VOCs 1 d and 28 d after interaction set-up. The method of Spadafora *et al.* (2016) was adapted, where for each interaction the lid was removed and the pot placed into a plastic roasting bag (3 L; Lakeland, UK) which was sealed with a 1 ml Eppendorf tube with its end cut off attached to the nape of the bag. Headspace was allowed to equilibrate by incubation of sample bags at 20 ^{o}C for 30 min, and 500 ml of headspace was collected onto a thermodesorption (TD) tube (Tenax TA & Sulficarb, Markes International

Ltd.) using a manual EasyVOC pump (Markes International Ltd.). Headspace was collected from bags containing a polypropylene pot, perlite, water and uncolonised *F. sylvatica* blocks to control for environmental fluctuation, and 0.5 µL C8-C20 alkane standard loaded onto a blank TD tube for retention standard and quality control (QC).

Tubes were desorbed following the listed settings on a TD100 thermodesorption system (Markes International Ltd.): 10 min at 280 °C, trap flow of 40 ml/min and trap desorption and transfer: 40 °C/s to 300°C, split flow of 20 ml/min^{-1} into GC (7890A; Agilent Technologies, Inc). Separation of samples occured over 60 m, 0.32 mm ID, 0.5 µm Rxi-5ms (Restek) at 2 ml constant flow of helium using the following temperature program: Initial temperature 35 °C for 5 min, 5°C/min^{-1} to 100 °C, then 15 °C to 250, final hold 5 min. Mass spectra were recorded from *m/z* 30 – 350 on a time-of flight mass spectrometer (BenchTOF-dx, Almasco International).

Initially, GC-MS data were processed using MSD ChemStation software (E.02.02.1177; Agilent Technologies Inc., USA) then deconvoluted and integrated against a custom retention-index mass spectral library with AMDIS (National Institute of Standards and Technology 11 (NIST)) library, and putative identifications were based on matches of mass spectra (>80 %) and retention index (RI +/− 15). Compounds not present in all replicates and compounds present in controls were excluded from statistical analyses. Data were normalized by constant sum, g-log transformed and mean centered, and missing values were imputed with half of the data matrix's reported minimum peak area (MetaboAnalyst 3.0; Xia & Wishard 2016). Housekeeping (near constant) peaks were filtered using an interquantile range estimation.

7.3.3 Statistical analysis

Mass spectra of the entire data set were analysed by principal components analysis (PCA) to check for clustering of the QCs and, therefore, robustness of the data set (see Supplementary Figure 1 for QC clustering). QCs were then removed from the matrix and orthogonal projection

to latent structures-discriminant analysis (OPLS-DA) was applied to the standardised binned data to determine the degree of separation between the four major sample groups: pair-wise samples 1 d and 28 d after interaction set up, and 27-block samples 1 d and 28 d after interaction set up. The data were then separated into pair-wise and 27-block sample groups, and OPLS-DA was applied to each group separately. The modelled covariance and correlation (loadings plot) was used to identify the compounds contributing most to the discriminant model separation, and one-way analysis of variance (ANOVA) with a 5 % Benjamini-Hochberg false discovery rate (FDR) correction for multiple comparisons (Benjamini & Hochberg 1995), and Tukey *post hoc* tests were applied to those compounds (MetaboAnalyst 3.0 (Xia & Wishard 2016)).

7.4 Results

7.4.1 Composition of VOC profiles

A total of 67 VOCs were detected after noise reduction, 66 of which were putatively identified by comparison of their mass spectra to the NIST library (Table 7.1). Putatively identified compounds belonged to the following classes of compounds: sesquiterpenes (27), esters (10), alkenes (6), ketones (6), aldehydes (4), alkanes (2), alcohols (2), carboxylic acids (2), terpenes (1), terpenoids (1), ethers (1), alkenones (1), alkenols (1), terphenols (1), and arenes (1).

39 compounds were detected overall in pair-wise experimental samples (Table 7.1) and the scores plot from the OPLS-DA shows distinct separation between different pairings, except *T. versicolor* against *V. comedens* and *V.comedens* self-pairings whose confidence intervals overlap (Figure 7.1A). 37 compounds were identified from the loadings plot (Figure 7.7.1B) as contributing significantly (ANOVA: $p < 0.05$; Supplementary Table 7.1) to the separation between groups. The significant compounds comprised 9 sesquiterpenes, 9 esters, 5 ketones, 3 alkenes, 2 aldehydes, 2 alcohols, a terphenol, an alkane, an ether, a carboxylic acid, an alkenol, an arene, and an unidentified compound.

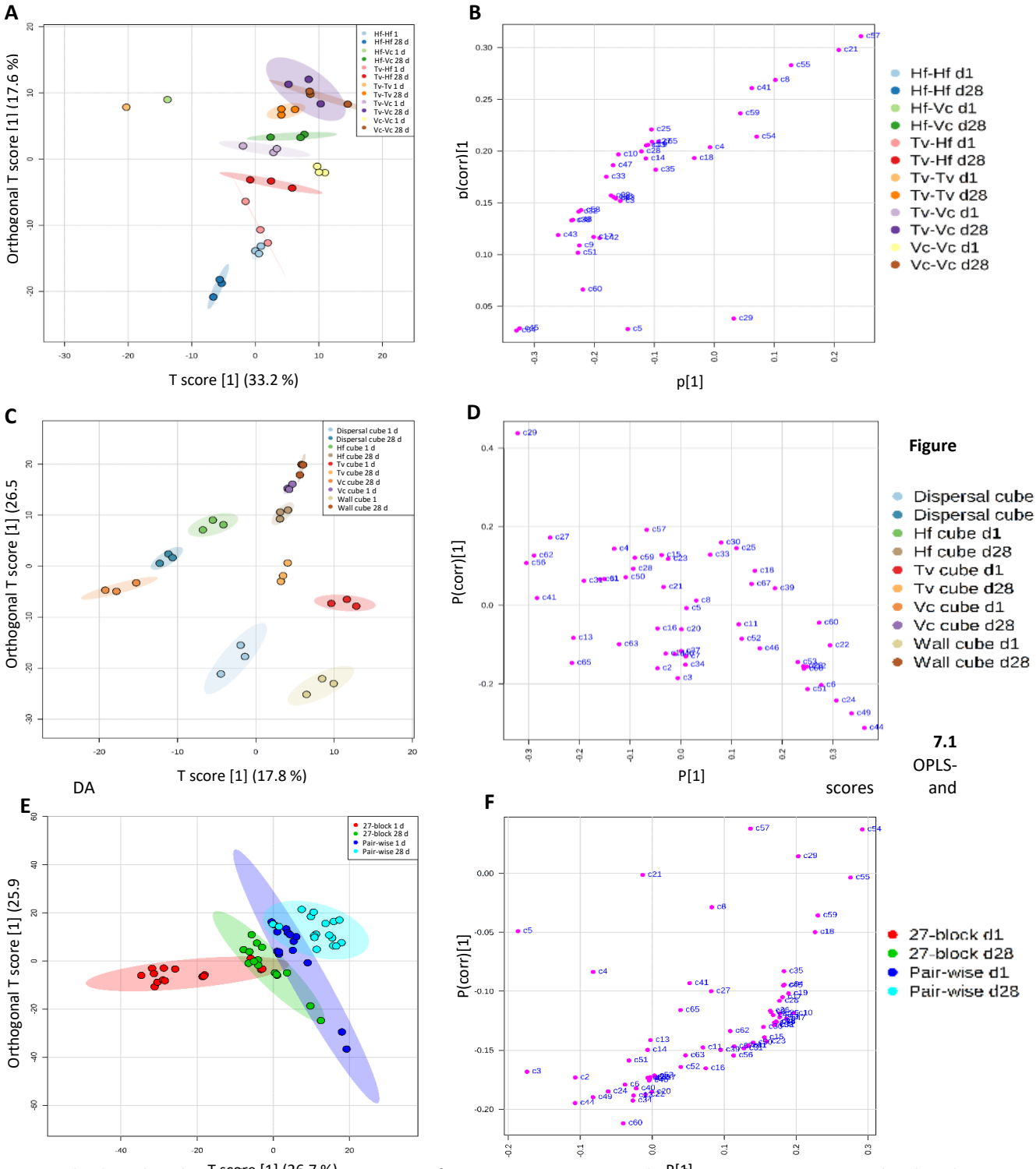

Figure 7.1 OPLS-DA scores and loadings plots derived from the GC-MS spectra of interactions. A-B: scores plot of pair-wise interactions 1 d and 28 d after interaction set up (A) and loadings plot (B) showing VOCs significantly contributing (ANOVA: $p < 0.05$) to the spatial arrangement of A. C-D: scores plot of 27-block interactions 1 d and 28 d after interaction set up (C) and loadings plot of significant features (D). E-F: scores plot showing pair-wise and 27-block interactions 1 d and 28 d after interaction set up combined into four sample groups (E), and the loadings plot of significant features (F). For scores plots, points represent individual samples (three independent biological replicates per interaction), with 95 % confidence intervals of the means of groups fitted onto the spatial ordination. For loadings plots, significant features are labelled as per compounds in Table 1, and data were acquired from three independent biological replicates.

Table 7.1 VOC compounds putatively identified by TD-ToF-GC-MS. Retention index (RI), CAS registry number, chemical group and reference of previous reporting are given.

	Compound name	RI	CAS	Chemical group	Reference
c1[ϕ]	4-epi-α-Acoradiene	1474	729602-94-2	Sesquiterpene	Chapter 4
c2[ϕ]	Spiro[4.5]dec-7-ene		729602-94-2	Sesquiterpene	Faraldos et al., 2010
c3[‡ϕ]	α-Alaskene	1502.7	99529-78-9	Sesquiterpene	Chapter 4
c4[‡ϕ]	α-Barbatene	1415.5	53060-59-6	Sesquiterpene	Chapter 4
c5[‡ϕ]	β-Barbatene	1441	72346-55-5	Sesquiterpene	Chapter 4
c6[ϕ]	Azulene	1532.2	395070-76-5	Sesquiterpene	Chapter 4
c7[ϕ]	δ-Cuprenene		98093-94-8	Sesquiterpene	
c8[‡ϕ]	[1,1':3',1''-Terphenyl]-2'-ol	2275	2432-11-3	Terphenol	Chapter 4
c9[‡]	Phthalic acid ester1	2370	85-69-8	Aldehyde	Sun et al., 2015
c10[‡]	Phthalic acid ester2	2299	84-64-0	Aldehyde	Yang et al., 2011
c11[ϕ]	(+)-Sativen	1396.2	3650-28-0	Sesquiterpene	Chapter 4
c12[ϕ]	α-Himachalene	1405	3853-83-6	Sesquiterpene	Soidrou et al., 2013; Chapter 4
c13[‡ϕ]	β-Himachalene	1524	1461-03-6	Sesquiterpene	Schalchli et al., 2011; Chapter 4
c14[‡ϕ]	2-Butyl-1-octanol	1277	3913-02-8	Alcohol	Schalchli et al., 2011; Sen et al., 2017; Chapter 4
c15	Isobutene	386	115-11-7	Alkene	Fukuda et al., 1984; Klein et al., 2000
c16	2-(1-Cyclopent-1-enyl-1-methylethyl)cyclopentanone	1497	-	Alkenone	-
c17[‡]	2,6-Dimethyl-6-trifluoroacetoxyoctane	1067	-	Ester	-
c18[‡ϕ]	2-Butanone	555	78-93-3	Ketone	Isidorov et al., 2016; Chapter 4
c19[‡]	2-Butanone, 3-methyl-	590	563-80-4	Ketone	Savel'eva et al., 2014; Konuma et al., 2015; Chapter 4
c20[ϕ]	(E)-2-Dodecene	1222	7206-13-5	Alkene	Mansour et al., 2017
c21[‡ϕ]	2-Ethylhexyl trans-4-methoxycinnamate	2322	83834-59-7	Ester	Fernandez de Simon et al., 2014; Chapter 4
c22[ϕ]	Isolongifolene	1402	1135-66-6	Sesquiterpene	Du et al., 2011
c23[ϕ]	3-(4-methoxyphenyl)-2-propenoic acid		830-09-1	Carboxylic acid	Yu et al., 2009
c24[ϕ]	Daucene		16661-00-0	Sesquiterpene	Ho et al., 2011; Yelle et al., 2011
c25[‡ϕ]	3-Octanone	966	106-68-3	Ketone	Isidorov et al., 2016; Chapter 4
c26[ϕ]	β-Patchoulene	1356	514-51-2	Sesquiterpene	Chapter 4
c27[‡ϕ]	5,5-Dimethyl-1,3-hexadiene	730	1515-79-3	Alkene	Chapter 4
c28[‡ϕ]	6-Methyl-5-hepten-2-ol	964	1569-60-4	Alkenol (aliphatic alkenone)	Liouane et al., 2010; Chapter 4
c29[‡ϕ]	Acetone	455	67-64-1	Ketone	Isidorov et al., 2016; Chapter 4
c30[ϕ]	á-Longipinene	1422	5989-08-2	Sesquiterpene	Isidorov et al., 2016; Chapter 4
c31[ϕ]	Benzaldehyde	982	100-52-7	Aldehyde	Ho et al., 2011
c32[‡]	Benzoic acid, tetradecyl ester	2213	-	Ester	Chapter 4
c33[‡]	Unknown compound	-	-	-	
c34[ϕ]	Caryophyllene	1504	87-44-5	Sesquiterpene	Soidrou et al., 2013
c35[‡]	Cedrene	1403	469-61-4	Sesquiterpene	Konuma et al., 2015; Chapter 4
c36[‡]	cis-Thujopsene	1454	470-40-6	Sesquiterpene	Konuma et al., 2015
c37[ϕ]	Copaene	1391	3856-25-5	Sesquiterpene	Soidrou et al., 2013; Konuma et al., 2015
c38[‡]	Butyl isobutyl phthalate	1973	17851-53-5	Ester	Wang et al., 2009

Table 7.1 *Continued*

	Compound name	RI	CAS	Chemical group	Reference
c39ϕ	β-Elemene	1494	515-13-9	Sesquiterpene	Soidrou et al., 2013
c40ϕ	(-)-limonene	1032	5989-54-8	Terpene	de Lima et al., 2015
c41‡ϕ	Decanal	1186	112-31-2	Ketone	Ho et al., 2010; Chapter 4
c42‡	2,6,7-Trimethyldecane	1058	62108-25-2	Alkane	Strobel et al., 2008
c43‡	Diisooctyl phthalate	2525	27554-26-3	Ester	Kudalkar et al., 2012
c44ϕ	Germacrene D	1480	23986-74-5	Sesquiterpene	Ho et al., 2011; Soidrou et al., 2013
c45‡	2-Monopalmitin	2498	23470-00-0	Ester	Özer & Arin, 2014
c46ϕ	2,3,5-Trimethylhexane	813	1069-53-0	Alkane	Boerjesson et al., 1989
c47‡	Homosalate	2037	118-56-9	Ester	-
c48‡	Isopropyl palmitate	2013	110-27-0	Ester	Pan et al., 2016; Chapter 4
c49ϕ	Linalool	1082	78-70-6	Terpenoid	Soidrou et al., 2013
c50ϕ	Longifolene	1428	475-20-7	Sesquiterpene	Konuma et al., 2015; Chapter 4
c51‡ϕ	γ-Cadinene	1512	39029-41-9	Sesquiterpene	Ho et al., 2010
c52ϕ	Calamenene	1510	483-77-2	Sesquiterpene	Wang et al., 2012
c53ϕ	δ-Cadinene	1530	483-76-1	Sesquiterpene	Ho et al., 2011; Wang et al., 2012
c54‡	1-Heptadecanol	1954	1454-85-9	Alcohol	Qadri et al., 2017; Chapter 4
c55‡	Palmitic Acid	1968	57-10-3	Carboxylic acid	Peiris et al., 2008; Du et al., 2011
c56ϕ	Nonanal	1084	124-19-6	Aldehyde	Ho et al., 2010
c57‡ϕ	Octyl ether	1688	629-82-3	Ether	Polizzi et al., 2012
c58	Octocrylene	2871	6197-30-4	Ester	Nguyen et al., 2013
c59‡ϕ	Pentanoic acid	1581	-	Ester	-
c60‡ϕ	Propene	310	115-07-1	Alkene	Yu et al., 2013
c61ϕ	p-Xylene	848.4	106-42-3	Alkene	Rouches et al., 2017
c62‡ϕ	β-Chamigrene	1474	18431-82-8	Sesquiterpene	Ho et al., 2011; Mun & Prewitt, 2011
c63‡ϕ	α-Chamigrene	1507	19912-83-5	Sesquiterpene	Mun & Prewitt, 2011
c64‡	Squalene	2914	111-02-4	Alkene	Gutierrez et al., 2002
c65‡ϕ	Toluene	786	108-88-3	Arene	Isidorov et al., 2016; Chapter 4
c66ϕ	Longipinene	1368	5989-08-2	Sesquiterpene	Chapter 4
c67ϕ	Undecanal	1303	112-44-7	Ketone	Ho et al., 2010

‡ Compounds identified by ANOVA as significant ($p < 0.05$) in pair-wise interactions; ϕ 27-block interactions.

Overall in 27-block interactions, 50 compounds were detected (Table 7.1) of which 47 contributed significantly (ANOVA: $p < 0.05$; Supplementary Table 7.2) to the differences between groups (Figures 7.1c,d). Replicates within each system interaction (single species cubes, "wall" distribution cubes and dispersed distribution cubes) formed clusters distinct from each other and showed clear temporal separation (Figure 7.1c), and the compounds responsible for this included 25 sesquiterpenes, 5 ketones, 4 alkenes, 2 aldehydes, 2 esters, a terpenoid, a terphenol, an alcohol, an alkane, an ether, a carboxylic acid, and alkenol, a terpene, and an arene.

7.4.2 Pair-wise VOC production

For every pairing, fewer VOCs were produced after 1 d compared to after 28 d, and interacting fungi produced more VOCs than fungi growing alone (Supplementary Table 7.3). Compounds that were most highly abundant were pairing specific: β-barbatene (C5) was the most abundant compound during interactions between *T. versicolor* and *V. comedens*, and *T. versicolor* and *H. fasciculare* after 1 d, accounting for 62 and 83 % of their total peak areas respectively; 2-butanone (C18) was the most abundant in interactions between *H. fasciculare* and *V. comedens* after 1 d (33 % total peak area) and *T. versicolor* self-pairings (22 % total peak area); and acetone (C29) was the most abundant compound in *V. comedens* and *H. fasciculare* self-pairings after 1 d (95 and 88 % total peak area respectively) (Supplementary Table 7.3).

Out of the 39 compounds produced during pair-wise interactions, 15 of them were only produced during interspecific interactions, i.e. they were not produced by fungi singly (Supplementary Table 7.3). For example 2-monopalmitin (C45) was produced during the interactions of *T. versicolor* against *V. comedens,* and *T. versicolor* against *H. fasciculare* after 1 d, but not by any fungus growing alone (Figure 7.2). Conversely, some compounds which were produced by self-pairings were not produced when fungi were interacting with other species,

e.g. 1,2-benzenedicarboxylic acid, butyl cyclohexyl ester (C10) which was produced by *T. versicolor* growing alone (Supplementary Table 3). Neither 2-ethylhexyl trans-4-methoxycinnamate (C21) nor octyl ether (C57) were produced by any pairing after 1 d, but both were produced after 28 d by all self-pairings and interspecific interactions (Figure 7.2; Supplementary Table 7.3).

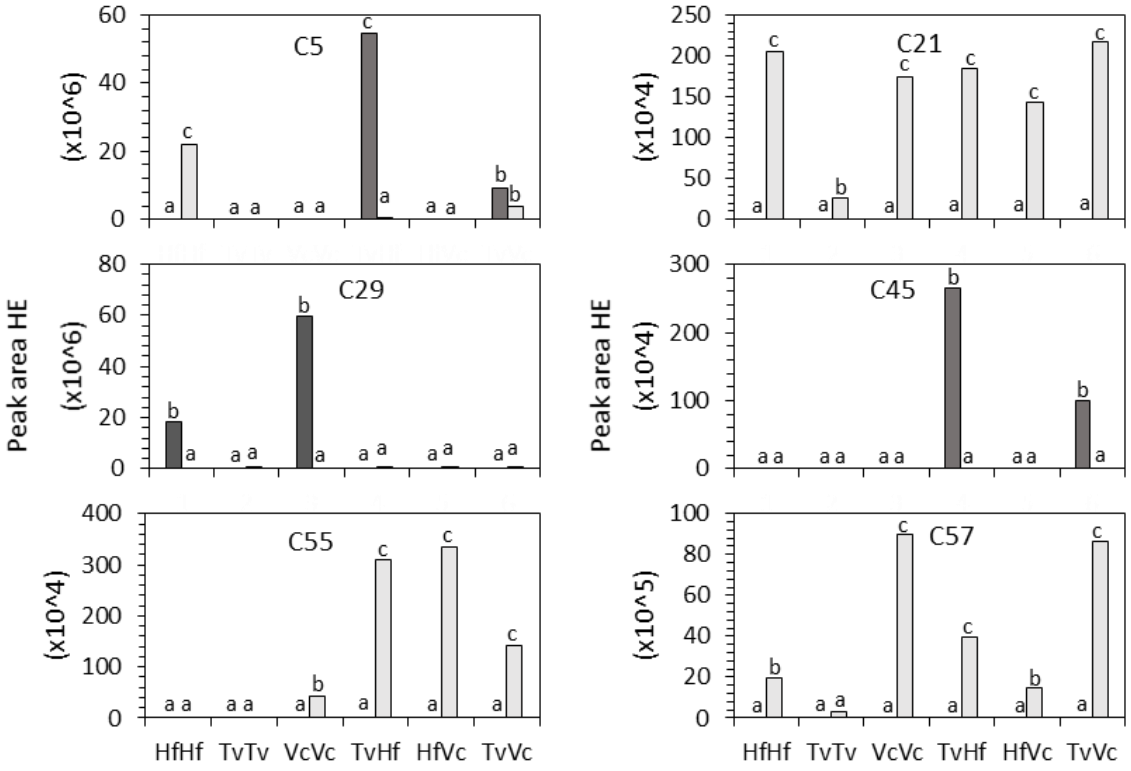

Figure 7.2 Peak area abundance of the six most highly significant compounds (ANOVA: $p < 0.001$; Supplementary Table 1) in pair-wise interactions 1 d (dark grey) and 28 d (pale grey) after interaction set up, expressed in hydrocarbon equivalents (HE). Abundancies are calculated from the mean of three replicates and SEM was always less than 1 % of the mean (see Supplementary Table 5). C5: β-barbatene, C21: 2-ethylhexyl trans-4-methoxycinnamate, C29: acetone, C45: 2-monopalmitin, C55: palmitic acid, C57: octyl ether. Tv: *T. versicolor*, Hf: *H. fasciculare*, Vc: *V. comedens*. Different letters indicate a significant difference ($p < 0.05$) in abundance between samples. Statistical comparisons were made separately for each compound.

7.4.3 VOC production in 27-block assemblages

β-Barbatene (C5) was the most highly abundant compound in 27-block interactions: it was produced during every interaction except 27-block cubes solely comprising *T. versicolor* after 28 d, and was the most abundant in all other interactions except cubes where fungi were dispersed after 28 d where acetone (C29) was produced in a greater quantity (Supplementary Table 7.4). 2-Butanone (C18), 6-methyl-5-hepten-2-ol (C28), á-longipinene (C30) and an unidentified compound (C33) were produced during the 3-species community interactions but not by any fungus singly, and 4-epi-α-acoradiene (C1), isobutene (C15), 3-octanone (C25), benzaldehyde (C31), β-elemene (C39), longifolene (C50), nonanal (C56), p-xylene (C61) and undecanal (C67) were produced by fungi singly, but were not produced when all three fungi were interacting (Supplementary Table 7.4).

After 1 d, 10 compounds were produced in significantly different quantities (ANOVA: $p < 0.05$) during 3-species interactions in cubes where *V. comedens* occupied a larger adjacent volume, compared to cubes where all three fungi were dispersed (Supplementary Table 7.4). For example, propene (C60) was highly abundant in the dispersal distribution cubes after 28 d (peak area of 13×10^6 hydrocarbon equivalents (HE)) but decreased in abundance when *V. comedens* occupied a larger adjacent volume (3.5×10^6 HE; Figure 7.3). 5,5-Dimethyl-1,3-hexadiene (C27), decanal (C41), octyl ether (C57) and toluene (C65) also showed this pattern, and the reverse was true for α-himachalene (C12), 2-butanone (C18), (E)-2-dodecene (C20), caryophyllene (C34) and α-chamigrene (C63): production was significantly higher in cubes where *V. comedens* occupied a larger adjacent volume (Supplementary Table 7.4). After 28 d, 13 compounds had significantly different abundancies (ANOVA: $p < 0.05$) between the two distribution patterns: production of δ-cuprenene (C7), 3-(4-methoxyphenyl)-2-propenoic acid (C23), 6-methyl-5-hepten-2-ol (C28), decanal (C41), calamenene (C52), pentanoic acid (C59), propene (C60) and toluene (C65) significantly increased when fungi were dispersed, and α-barbatene (C4), β-barbatene (C5),

2-butanone (C18), 2-ethylhexyl trans-4-methoxycinnamate (C21) and á-longipinene (C30) production significantly increased when *V. comedens* occupied a larger adjacent volume.

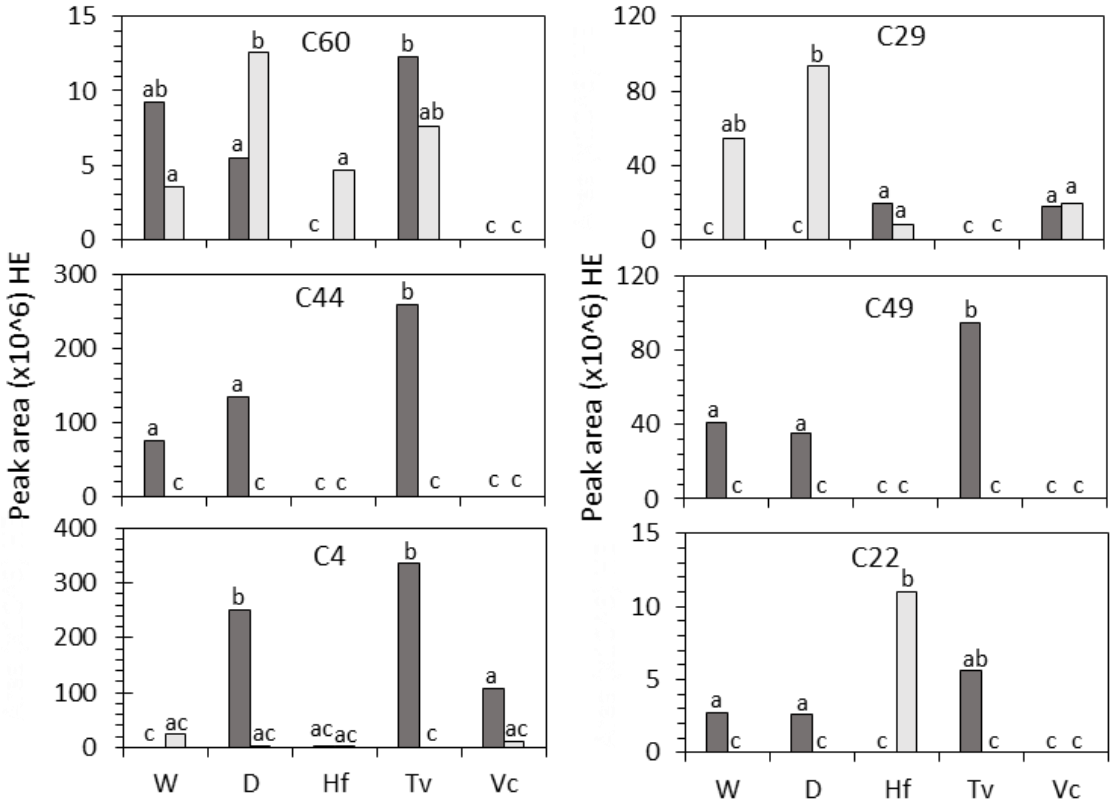

Figure 7.3 Peak area abundance of the six most highly significant compounds (ANOVA: $p < 0.001$; Supplementary Table 2) in 27-block interactions 1 d (dark grey) and 28 d (pale grey) after interaction set up, expressed in hydrocarbon equivalents (HE). Abundancies are calculated from the mean of three replicates, SEM values were always less than 1 % of the mean (see Supplementary Table 5). C60: propene, C29: acetone, C44: germacrene D, C49: linalool, C4: α-barbatene, C22: isolongifolene. W: "wall" distribution cubes; D: cubes where all fungi are evenly dispersed; Tv: cubes comprised solely of *T. versicolor,* Hf: cubes comprised solely of *H. fasciculare*, Vc: cubes comprised solely of *V. comedens*. Different letters indicate a significant difference ($p < 0.05$) in abundance between samples. Statistical comparisons were made separately for each compound.

7.4.4 2-dimensional vs 3-dimensional comparisons

The pair-wise interactions after 1 d and 28 d, and 27-block interactions after 28 d had similar profiles (Figure 7.1e,f). The difference in VOC profiles between 1 d and 28 d was more distinct for 27-block interactions than for the pair-wise interactions. Some compounds produced by fungi growing singly within 3-dimensional structures were not produced by self-pairings growing in 2-dimensions, and *vice versa*. For example, α-barbatene (C4) and β-barbatene (C5) were the most highly abundant compounds in whole 27-block *T. versicolor* cubes after 1 d (accounting for 20 and 39 % of the total peak area respectively) but neither were produced by *T. versicolor* self-pairings, and 2-butanone (C18) and 3-octanone (C25) were highly abundant in *T. versicolor* self-pairings after 28 d (both accounting for 22 % of the total peak area) but were not produced when *T. versicolor* was growing alone in 27-block interactions (Supplementary Tables 7.3,4).

7.5 Discussion

VOC production by wood decay fungi alters in response to changes in competitor identity (Chapter 4). In the present study, VOC profiles differed extensively between pairs and 27-block arrangements, and many compounds were only produced by monocultures, or during community interactions. This shows for the very first time that species diversity, spatial distribution of individuals, and resource structural heterogeneity influence the suite and abundance of the arsenal of VOCs used in chemical warfare.

7.5.1 VOC production is influenced by resource heterogeneity and species diversity

When fungi were paired with a competitor, more VOCs were produced compared to when fungi were decomposing wood alone, production of compounds during both paired and 27-block interactions, that were not produced in single species controls, often occurred, and profiles differed when three species were interacting simultaneously compared to when fungi were paired. For example, the ester 2-monopalmitin (C45), which was detected previously in the

profiles of two soil dwelling ascomycete fungi that inhibited the spread of black mould disease (*Aspergillus niger*) (Özer & Arin 2014), was produced when *T. versicolor* was paired with *V. comedens* and when paired with *H. fasciculare*, but was not produced by any fungus singly. Production of specific compounds has also been reported during the interactions of six basidiomycetes against *T. versicolor* during wood decay (Chapter 4), demonstrating the effects of competition and species diversity on VOC production. Conversely, however, certain compounds were produced by specific fungi when growing alone, but were not produced when fungi were interacting. E.g. longifolene (C50), a sesquiterpene reported previously during independent growth on wood chips by *T. versicolor* and *Fomitopsis palustris* (Konuma et al. 2015), was detected when *V. comedens* was growing alone in a 27-block configuration but not when the three fungi were interacting. It is possible, therefore, that some compounds function in resource modification or intraspecific signalling when decaying wood alone.

In addition to greater species diversity, increased spatial heterogeneity and resource structural complexity affected VOC production, supporting the first study hypothesis. The sesquiterpenes α-barbatene (C4) and β-barbatene (C5) constituted the most highly abundant compounds produced by *T. versicolor* when arranged within a 3-dimensional structure but were not produced by *T. versicolor* when paired with itself in a 2-dimensional system. Metabolic processes were found to change previously as a result of increased structural heterogeneity when the specific profiles of lignin and cellulose degrading enzymes differed between 2-dimensional pairings and 3-dimensional community assemblages (Chapter 6). 3-dimensional resources, as are found in nature, are more dynamic in their architecture with an array of interlinking xylem vessels that fungi traverse, with many aligned parallel to each other separated by wood cell walls. Fungi must navigate the structurally complex resource, perhaps producing a greater diversity of intraspecific info-chemicals than when in a more structurally simple substrate, attributing to the change in the metabolic mechanisms deployed during decay.

7.5.2 Territory fragmentation is responsible for divergent VOC profiles

VOC profiles from the headspaces of the two spatially different community assemblages differed in the suite and abundance of specific compounds they comprised, even after 1 d, thus supporting the second study hypothesis. Individual fungi produce distinct VOC profiles (Chapter 4; El Ariebi et al. 2016), therefore, the divergent profiles may have reflected the proportions of individuals present at the time of extraction: *V. comedens* became extinct from the community when fungi were dispersed, but coexisted with its competitors when it occupied a larger adjacent volume (Chapter 6). However, the profiles were drastically different after just 1 d, so it is more likely that metabolic processes were altered as a direct result of individual spatial location in relation to competitors. Spatial variation occurs in all natural ecosystems, and considerably affects species interactions, community structure and subsequent ecosystem functioning (Kareiva 1987; Didham 2010; Chapters 5,6). A change in metabolic mechanisms was evidenced in the divergent enzymatic profiles of fungi interacting within the same assemblages (Chapter 6), and was likely due to the construction of constitutive defences (e.g. accumulation of secondary metabolites) by *V. comedens* when more combative, and a metabolic response by *T. versicolor* to the increased antagonistic force. In the present study, while clearly demonstrating altered metabolic mechanisms, since samples were extracted from the headspace of interactions, it is not possible to discern which fungus was responsible for the production of specific compounds.

7.5.3 Roles of volatile compounds

Sesquiterpenes comprised the biggest group of aliphatic compounds, and the sesquiterpene β-barbatene (C5) was the most highly abundant compound. Sesquiterpenes are produced by fungi in large quantities (Hynes et al. 2007; El Ariebi et al. 2016; Chapter 4) and often function as antimicrobial agents (Viiri et al. 2001; Sánchez-Fernández et al. 2016; Isaka et al. 2017). For

example, a broth culture of the basidiomycete *Inonotus* sp., produced nine sesquiterpenoids including inonoalliacane B and inonoalliacane F which exhibited antimicrobial activity against herpes simplex virus, and *Baccillus cereus* respectively (Isaka et al. 2017). Sesquiterpenes are also produced by other organisms including plants, and can provide enormous economic benefits to the commercial forestry and timber industries. γ-Cadinene (C51) was produced by *Machilus pseudolongifolia* whose leaf oils were antifungal against four wood decay basidiomycetes which are problematic to the timber industry (Ho et al. 2010). Similarly, extracts from the heartwood of three *Juniperus* species contained sesquiterpenes including thujopsene (C36) that were antifungal against four basidiomycete decay fungi (Tumen et al. 2013).

The ester 2-ethylhexyl trans-4-methoxycinnamate (C21) was constantly abundant, appearing in the profiles of all 27-block assemblages except whole *T. versicolor* cubes after 28 d, and was present in large quantities in the profiles of every pair-wise interaction after 28 d. This ester was produced in large quantities previously during pair-wise interactions (Chapter 4), and was detected in extracts of acacia (*Robinia pseudoacacia*), ash (*Fraxinus excelsior* L. and *F. americana* L.), chestnut (*Castanea sativa*) and cherry (*Prunus avium*) that had been heated for cooperage treatment for the storage of alcoholic beverages (Fernández de Simón et al. 2014).

Of the 67 compounds identified in this study, 26 of them were detected previously in the headspace of pair-wise interactions between six basidiomycetes and *T. versicolor* (Chapter 4). The three fungal species assessed in the present study were also used previously, and the experimental procedures including wood block colonisation, the method of interaction set up, VOC extraction and GC-MS analysis were identical. The temperature of incubation in the present study (20 ^{o}C) differed to that of the previous experiment (15 ^{o}C and 25 ^{o}C), the spatial orientation of interactions, i.e. pairs verses 27-block assemblages, and the diversity of species within interactions (bi-species pairs verses 3-species interactions) differed between the two studies, probably contributing to the divergence of compounds between the two studies. Additionally,

in the previous study a greater number of VOCs were detected over all, likely reflecting the assortment of species used and the species specific nature of VOC production.

7.6 Conclusions

The profiles of VOCs produced by fungi during wood decomposition differ as a result of spatial variation, species diversity and territory fragmentation. Highly abundant compounds produced by fungi growing alone across a 2-dimensional plane were not produced when the same fungi grew singly within structurally more complex 3-dimensional structures, and *vice versa*, indicating metabolic changes resulting from resource structural complexity. The quantity of VOCs and also the abundance of synonymous compounds changed with a change in species diversity, i.e. fungi growing alone, two species interacting or three species interacting simultaneously, and the fragmentation of territory led to alterations to metabolic mechanisms which resulted in divergent VOC profiles. Various sesquiterpenes with antimicrobial properties were produced, comprising the largest chemical group of detected compounds, and compounds belonging to a range of other chemical families were also produced, with known functions as antimicrobial agents.

Chapter 8: Differential metabolomics analysis of the wood decay fungus *Trametes versicolor* reveals metabolic pathways associated with intracellular regulation of antagonism

8.1 Abstract

Genome sequencing projects of wood decay fungi have been vital in their elucidation of the mechanics of decomposition processes, but are limited by their lack of functional characterisation resulting in knowledge gaps regarding, for example, how mechanisms change during interactions. This chapter presents the very first large-scale functional metabolomics study of interacting fungi during decomposition. Intracellular metabolite production by *Trametes versicolor* when interacting within 3-dimensional wood decay community systems and structurally simpler 2-dimensional pair-wise interactions was analysed by ultra-high performance liquid chromatography, coupled with Orbitrap mass spectrometry (UHPLC-MS). The UHPLC-MS profiles were extremely rich in information, totalling 2825 metabolic peaks across the entire dataset of which 1597 were putatively identified. Distinct metabolic profiles were formed as a result of competition, compared to when *T. versicolor* was decaying wood alone, and alterations to species diversity and spatial distributions within systems caused discrimination between profiles. Metabolites associated with the biosynthesis and metabolism pathways of antibiotics were particularly affected, as well as those involved in metabolic pathways linked to decay processes. Dimensionality of the resource did not directly affect the metabolome, and is instead proposed as a moderator of the diversity-function relationship.

8.2 Introduction

Decomposition of dead-wood is the central process in nutrient cycling in forest ecosystems and is brought about by the activities of wood decay basidiomycetes. While the fundamental enzymatic depolymerisation of lignocellulose has been relatively well described (Valášková et al. 2007; Baldrian 2008; Chapters 3,6), the intracellular processes that regulate these mechanisms remain uncertain. Genome sequencing efforts have been expanded in recent years (Floudas et al. 2012; Grigoriev et al. 2014; Riley 2014), providing an exceptional volume of information regarding the genomic basis of decomposition processes. However, the physical blueprint of genes and transcripts provided by genome sequencing does not sufficiently reveal the functional characteristics of those genes (Werner 2010). This is where functional projects, such as metabolomics, play a vital role.

Characterisation of the metabolome provides an unrivalled view of the functional physiology of an organism's cellular response to environmental stimuli (Zhang et al. 2013), and reveals connections between metabolic pathways that operate within the cell (Wang et al. 2011). While the metabolome of interacting wood decay fungi has been investigated on agar (Peiris et al. 2008; Luo et al. 2017) and in liquid medium (Xu et al. 2018), a large-scale metabolomics project has never before been applied to wood decay fungi interacting within their natural substrate, wood. Previously, GC-TOF-MS showed that *Stereum hirsutum* decreased production of intracellular metabolites when interacting with *Coprinus micaceus*, a competitor against whom *S. hirsutum* wins, and increased production of metabolites when it was losing against *C. disseminates*, compared to monocultures (Peiris et al. 2008). Additionally, metabolites involved in carbohydrate, amino acids and lipid metabolism super pathways were produced in significantly greater abundance during interactions between *T. versicolor*, *P. ostreatus* and *Dichomitus squalenes* compared to monocultures in a UHPLC-MS and GC-MS study (Luo et al. 2017). Similarly, LC-MS revealed novel metabolites, with potential properties that may be

important in the synthesis of new drugs, were produced when *T. versicolor* and *Ganoderma applanatum* were interacting, but not when they were growing alone (Xu et al. 2018). These studies excitingly show that intracellular metabolites, not just those that are extracellularly secreted (e.g. enzymes and VOCs), function in metabolic pathways involved in stress responses to antagonism. However, the lack of characterisation of the metabolome of wood decay fungi in wood is an oversight, given that it is known that gene expression and metabolic strategies often differ hugely between natural and non-natural substrates (Hiscox et al. 2010b; Cánovas et al. 2017).

To study the differential metabolic response of competitive fungi in their natural substrate for the very first time, metabolomics analysis was performed on *T. versicolor* colonised beech (*Fagus sylvatica*) blocks from a 3-dimensional three species community decay system. Comparisons were made with pair-wise 2-dimensional systems of the individuals within the community (*T. versicolor*, *H. fasciculare* and *V. comedens*), and territory fragmentation within 3-dimensional systems was used as an experimental variable by arranging the fungi in two spatial arrangements, as in Chapters 6 and 7. Fungi were spatially arranged either so that all three fungi were dispersed with no two blocks of the same species adjacent, or such that the weakest competitor, *V. comedens*, occupied a larger adjacent volume of territory, but same total volume of territory as its competitors, with the other two fungi dispersed throughout the rest of the system. The nature of metabolomics as a discipline and the lack of previous study of metabolomics in wood decay drove this study with an exploratory approach, rather than a hypothesis testing approach. That being said, the findings of the previous chapters did lead to the prediction that intracellular metabolism would be influenced by competition, species diversity and spatial dynamics. Metabolites were analysed by UHPLC coupled with Orbitrap MS using an established metabolomics approach, and finally, important metabolites were assigned likely regulatory pathways and their possible functions discussed.

8.3 Methods

8.3.1 Culture conditions and system interactions

Strains of three wood decay basidiomycetes, *H. fasiculare*, *T. versicolor* and *V. comedens* were cultured and arranged in pairs and 27-block assemblages as described in Chapter 6 (Section 6.3.1; 6.3.2). Briefly, beech (*F. sylvatica*) wood blocks (2x2x2 cm) colonised by individual fungi were arranged in : (1) pairs in all combinations plus single-species self-pairings; and (2) 27-block (3x3x3) interactions where either all fungi were dispersed with no two blocks of the same species in contact, or with *V. comedens* occupying a larger adjacent volume (or "wall"), but same total volume (9 blocks) as its competitors, and the other two fungi were randomly dispersed, again with the constraint that none of the blocks of the same species were adjacent.

8.3.2 Metabolite extraction

Following VOC extraction after 1 d and 28 d (Chapter 7), interacting combinations of wood blocks were deconstructed and individual blocks split into quarters, then three quarters of each block were flash frozen, and stored at -80 ^{o}C (Chapter 6: 6.3.3). Frozen blocks (-80 ^{o}C) of *T. versicolor* and *V. comedens* were removed from storage, freeze dried and ground to sawdust for enzyme assays (Chapter 6: 6.3.4). Remaining material from *T. versicolor* blocks were used to extract metabolites (5 replicates; see Supplementary Table 8.1 for specific blocks) following an adaptation of the previously described protocol (Sana & Fischer 2007). 0.5 g of sawdust was added to 1666 µl of each of H_2O, methanol and chloroform, vigorously vortexed and sonicated for 15 min (Elmasonic S150, Singen, Germany). Extracts were rested to allow chloroform separation, then 1500 µl of extract was removed, without chloroform. Extracts were centrifuged for 5 min at 17,000 x g (Biofuge, Thermo Fisher Scientific, MA, USA), and 200 µl of supernatant

removed and dried *in vacuo* (Thermo Savant, NY, USA) for ca. 3 h. Extracts were stored at -80 ^{o}C until analysis.

8.3.3 Ultra-high performance liquid chromatography-mass spectrometry (UHPLC-MS)

First, a quality control (QC) sample was pooled from all samples, then dried down (20,000 x g for 10 min at 4 °C, Biofuge) for UHPLC-MS. Chromatography (20 µl per sample) was performed on a Thermo Dionex Ultimate 3000 RS system with a Thermo Scientific Q Exactive Orbitrap mass spectrometer as detection. Samples (10 µl) were separated over a 100 x 2.1 mm, 1.9 µm particles, C18 column (Thermo Hypersil Gold) at a flow rate of 400 µl min^{-1} using a 14 min linear gradient programme from 0.1 % formic acid in water to 0.1 % formic acid in methanol. MS acquisition started at 0.1 min, with the flow up to 0.45 min directed towards waste. Data were acquired in positive ion and profile mode from *m/z* 100-1000 at 70,000 resolution. Samples were run in a controlled randomised order, with QC samples equidistantly between them.

8.3.4 UHPLC-MS data processing

The Thermo.raw data files in profile mode were converted into mz/ML format in centroid mode using MSConvert (Proteowizard 3.0.7665). Data were aligned using an R (3.2.0) based XCMS and CAMERA script (both R packages: Brown et al. 2009; Dunn et al. 2011) and resulted in a csv file intensity matrix (9309 features). The matrix was imported into MatLab and inserted into a direct infusion mass spectrometry (DIMS) SIMStitch pipeline (Kirwan et al. 2014) where a blank filter of > 2x sample over blank signal was applied, and a sample filter of peak-presence of at least 50 % of all samples. The matrix was further processed by normalisation using the parallel quasi-Newton (PQN) algorithm and missing value imputation using K-nearest neighbour (KNN) with k = 5 for univariate statistics including fold-changes. For multivariate statistics, data were g-log transformed after optimisation on QC samples.

8.3.5 Statistical analysis, and identification of metabolites and metabolic pathways

Initially, principle component analysis (PCA) was applied to the g-log transformed data to explore the unsupervised separation between control samples (*T. versicolor* growling alone), interaction samples and QCs. The median RSD for the QC samples was 11.15 %, indicating that the MS data were of sufficiently high quality for further statistical analysis (see Supplementary Figure 8.1 for QC clustering). Analysis of variance simultaneous component analysis (ASCA) was applied to the standardised binned data minus the QCs, and the model was permutation tested (5000 permutations) to determine the significance of factors (sample day, and block position within systems). An additional ASCA model was tested to determine the significance of species distribution patterns within cubes, i.e. species being dispersed, *V. comedens* occupying a larger adjacent volume, or *T. versicolor* comprising the entire system, but did not include spatial location within assemblages as a factor. Pair-wise comparisons using ASCA were carried out for *post hoc* testing of significant effects, and the *p*-values were adjusted for multiple testing using a 5 % Benjamini Hochberg false discovery rate (FDR) correction (Benjamini & Hochberg 1995). Univariate analysis of variance (ANOVA) was applied to the whole normalised matrix with a 5 % FDR correction (Benjamini & Hocherg 1995) to test for significant metabolites. Finally, fold changes (FC) between significant groups were determined.

Peaks were putatively identified by inputting *m/z* values and their associated mean intensities into MI-Pack software version 2 beta (Weber & Viant 2010), where metabolites were compared against the Kyoto Encyclopaedia of Genes and Genomes (KEGG) database. A set of highly significant metabolites (ANOVA: $p < 0.001$) were further searched against the KEGG database to determine possible roles within metabolic pathways.

8.4 Results

8.4.1 UHPLC-MS metabolomics

The processed LC-MS data yielded a peak list and data matrix of 2825 signals, of which 1597 have been putatively identified. PCA allowed the visualisation of metabolic differences, and the scores plot revealed that the largest metabolic differences occurred temporally (along the PC 1 axis, 28 % of the variance) between 1 d and 28 d, while smaller metabolic differences occurred between individual interactions (PC 2 axis, 12 % of the variance) (Supplementary Figure 8.1).

Table 8.1 Full ASCA model results. *p*-values for experimental factors and their interaction is given, and significance ($p < 0.05$) indicated (*). Model factors include: (1) position of analysed block within systems (i.e. number of directly adjacent competitors) and sample day (1 d and 28 d) for self-pairings, paired interactions, 27-block assemblages comprised solely of *T. versicolor* (Tv), 27-block assemblages where fungi were dispersed (Dispersal cube), and 27-block assemblages where *V. comedens* occupied a larger adjacent volume (Wall cube); and (2) type of 27-block assemblage (distribution pattern) and sample day for dispersal cubes, wall cubes and 27-block assemblages comprised of *T. versicolor*.

	Block position	**Sample day**	**Interaction**
Self-pairings	< 0.001 *	< 0.001 *	0.064
Paired interactions	< 0.001 *	< 0.001 *	< 0.001 *
Tv 27-block assemblage	0.736	< 0.001 *	0.961
Dispersal cube	0.12	< 0.001 *	0.175
Wall cube	0.057	< 0.001 *	0.339
	Assemblage	**Sample day**	**Interaction**
27-block assemblages	< 0.001 *	< 0.001 *	< 0.001 *

Following confirmation that metabolic profiles differ between sampling days and between individual interactions, the supervised multivariate ASCA analysis revealed more detailed differences. Results of the statistical significance of the two categorical factors (sampling time and block position, i.e. specific spatial position within interactions) to each group of interactions is summarised in Table 8.1. The metabolome of *T. versicolor* differed significantly between 1 d and 28 d in every interaction demonstrating a strong effect of time of sampling. The effect of block position relative to neighbours was significant in pair-wise interactions but not in 27-block assemblages, where the metabolome of *T. versicolor* was homogenous within each cube. From here on, therefore, metabolite production by *T. versicolor* within 27-block cubes refers to the average metabolite intensities from all block positions within a cube (15 replicates: 5 biological replicates x 3 block positions (pseudoreplicates)).

8.4.2 Competition affects metabolite production during pair-wise interactions

In pair-wise interactions, the metabolome of *T. versicolor* was always significantly different (Adj. $p < 0.05$) between the two sampling days (1 d and 28 d after interaction set up) (Figure 8.1A-C). After 1 d, the metabolic profiles of all pair-wise interactions were undistinguishable from each other ($p > 0.05$; Figure 8.2A), however, after 28 d, *H. fasciculare* affected the metabolome of *T. versicolor* such that production of 670 metabolites was significantly increased and of 620 was decreased compared to self-pairings of *T. versicolor* (Table 8.2; Figure 8.1D). *V. comedens* had no significant effect on the metabolome of *T. versicolor*, even after 28 d (Table 8.2; Figure 8.1E).

The most statistically significant metabolites (ANOVA: $p < 0.05$) produced during pair-wise interactions are listed in Supplementary Table 8.2. Metabolites that were putatively identified are involved in alkaloid and coenzyme A biosynthesis pathways, as well as aromatic hydrocarbon degradation pathways (Table 8.3). All of these metabolites were produced in greater abundance

in the interaction between *T. versicolor* and *H. fasciculare* compared to *T. versicolor* monocultures after 1 d, but their production decreased in the same interaction after 28 d (Supplementary Table 8.2).

Table 8.2 *Post hoc* pair-wise comparisons between significant interactions as identified by ASCA. Comparisons are made temporally between 1 d and 28 d of specific interactions, e.g. 'Tv-Tv: 1 d - 28 d', or comparisons are made between interactions at specific times, e.g. '28 d: Tv-Tv – Tv-Hf'. *p*-values of the ASCA model and adjusted *p*-values (Benjamini-Hochberg) are given, as well as the number of significant features (determined by ANOVA: $p < 0.05$) and the number of significant features that are increased and decreased in the sample group given after the (-), compared to that given before the (-). Tv: *T. versicolor*, Hf: *H. fasciculare*, Vc: *V. comedens*, Tv cube: 27-block cube comprised solely of *T. versicolor*, Wall cube: 27-block cube where *V. comedens* occupied a larger adjacent volume, Dispersal cube: 27-block cube where all three fungi are dispersed throughout the cube.

	ASCA		ANOVA		
	p-value	Adj. *p*-value	Sig. features	Increased	Decreased
Tv-Tv: 1 d - 28 d	0.004	0.012	924	402	522
Tv-Hf: 1 d - 28 d	0.005	0.015	337	153	184
Tv-Vc: 1 d - 28 d	0.007	0.021	849	402	447
28 d: Tv-Tv - Tv-Hf	0.008	0.048	1290	670	620
28 d: Tv-Tv - Tv-Vc	0.172	0.762	11	11	0
28 d: Tv-Hf - Tv-Vc	0.005	0.03	1394	660	734
Tv cube: 1 d -28 d	< 0.001	< 0.001	1115	483	632
Wall cube: 1 d -28 d	< 0.001	< 0.001	1683	735	948
Dispersal cube: 1 d -28 d	< 0.001	< 0.001	1853	1012	841
1 d: Tv cube - Wall cube	< 0.001	< 0.001	539	381	158
1 d: Tv cube - Dispersal cube	< 0.001	< 0.001	1425	486	939
1 d: Wall cube - Dispersal cube	< 0.001	< 0.001	993	428	565
28 d: Tv cube - Wall cube	< 0.001	< 0.001	1781	892	889
28 d: Tv cube - Dispersal cube	< 0.001	< 0.001	1667	880	787
28 d: Wall cube - Dispersal cube	0.007	0.042	14	9	5
28 d: Tv-Hf - Wall cube	< 0.001	< 0.001	97	36	61
28 d: Tv-Hf - Dispersal cube	< 0.001	< 0.001	350	151	199

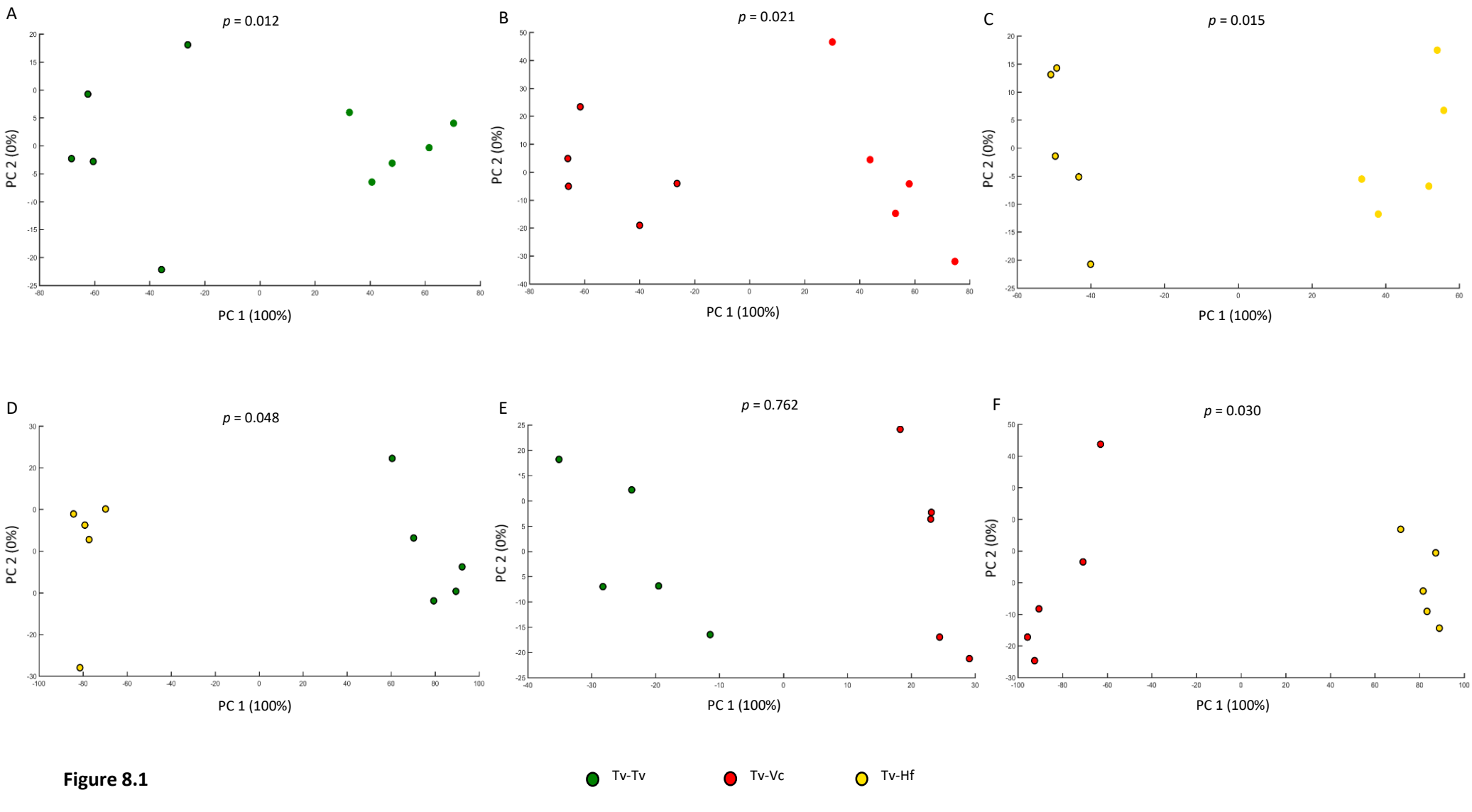
A
p = 0.012
PC 2 (0%)
PC 1 (100%)
B
p = 0.021
PC 2 (0%)
PC 1 (100%)
C
p = 0.015
PC 2 (0%)
PC 1 (100%)
D
p = 0.048
PC 2 (0%)
PC 1 (100%)
E
p = 0.762
PC 2 (0%)
PC 1 (100%)
F
p = 0.030
PC 2 (0%)
PC 1 (100%)
Tv-Tv
Tv-Vc
Tv-Hf

Figure 8.1

Figure 8.1 ASCA scores plots showing pair-wise comparisons of sample groups, derived from the UHPLC-MS spectra of *T. versicolor* blocks within pair-wise interactions, with adjusted p-values given. A-C: temporal separation of interactions where no outline around points indicates samples 1 d after interaction set up, and an outline around points indicates samples after 28 d of interacting. D-F: separation between different interactions 28 d after interaction set up. Tv: *T. versicolor*, Vc: *V. comedens*, Hf: *H. fasciculare*.

8.4.3 Species diversity and spatial distribution of individuals affects metabolism in community interactions

The metabolome of *T. versicolor* was significantly different (Adj. $p < 0.001$) after 28 d compared to after 1 d in all 27-block assemblages (Figure 8.3A-C). When all three fungi were dispersed more metabolites were produced in greater abundance by *T. versicolor* after 28 d than were produced in lower abundance, compared to after 1 d, but when *V. comedens* occupied a larger adjacent volume and when cubes were comprised solely of *T. versicolor* more metabolites decreased after 28 d, compared to after 1 d (Table 8.2).

In contrast to pair-wise interactions, the metabolome of *T. versicolor* differed significantly between assemblage types even after 1 d (Adj. $p < 0.001$; Figure 8.3D-I), though the difference between 27-block interactions when all fungi were dispersed and when *V. comedens* occupied a larger adjacent volume was not as pronounced after 28 d (Adj. $p = 0.042$; Figure 8.2B; Figure 8.3I). Relative to single-species controls (cubes comprised solely of *T. versicolor*), there was a greater number of metabolic differences when all three fungi were dispersed (1425 and 1667 after 1 d and 28 d respectively, ANOVA: $p < 0.05$), than when interacting in cubes where *V. comedens* occupied a larger adjacent volume (539 and 1781 after 1 d and 28 d respectively; Table 8.2) (Figure 8.3D-E, G-H).

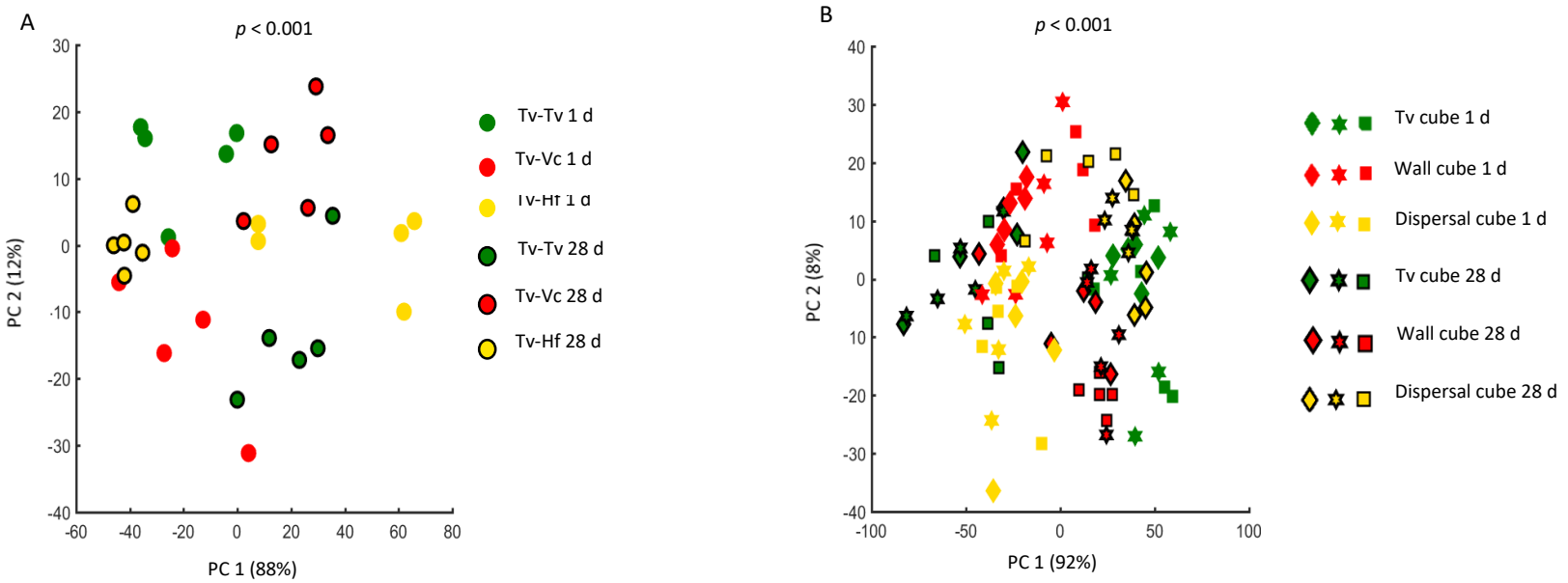

Figure 8.2 ASCA scores plots derived from the UHPLC-MS spectra of *T. versicolor* blocks within pair-wise (A) and 27-block (B) interactions, with adjusted *p*-values given. Shapes in B represent the different spatial positions of blocks (pseudoreplicates) within each assemblage which were not significantly different to each other. Tv: *T. versicolor*, Vc: *V. comedens*, Hf: *H. fasciculare*, Tv cube: 27-block assemblage comprised solely of *T. versicolor*, Wall cube: 27-block cube where *V. comedens* occupies a larger adjacent volume, Dispersal cube: 27-block cube where all three fungi are dispersed.

When interacting in cubes where all fungi were dispersed, the metabolome of *T. versicolor* was altered to a greater degree than when interacting in cubes where *V. comedens* occupied a larger adjacent volume, relative to cubes comprised solely of *T. versicolor* (Figure 8.3D-E, G-H): there was a higher number of metabolic differences (ANOVA: $p < 0.05$) when dispersed (1425 and 1667 after 1 d and 28 d respectively), than when interacting in cubes where *V. comedens* occupied a larger adjacent volume (539 and 1781 after 1 d and 28 d respectively; Table 8.2). Metabolites contributing to these differences involved those associated with the metabolism and biosynthesis of antimicrobial compounds such as streptomycin, all of which were produced in greater abundance compared to monocultures (Table 8.3; Supplementary Table 8.3).

Between the two community assemblages, after 1 d the abundance of 993 metabolites were produced in significantly different quantities (Table 8.2; 8.3F). After 28 d, however, only 14 metabolites were produced in significantly different quantities between cubes where fungi were dispersed and cubes where *V. comedens* occupied a larger adjacent volume (Table 8.2; Figure 8.3I). These metabolites included those involved in purine, pyrimidine and sulphur metabolism pathways, as well as the biosynthesis pathways of numerous antibiotic compounds (e.g. neomycin and kanamycin), and the metabolism pathways of antimicrobials (Table 8.3; Supplementary Table 8.4).

8.4.4 Dimensionality alone does not affect metabolism

There was no significant difference between the metabolome of *T. versicolor* when it was paired against itself and when it comprised a whole 27-block cube, after 1 d or after 28 d ($p = 0.156$ and $p = 0.210$ respectively; Figure 8.4A). The metabolome did, however, differ between 2- and 3-dimenions when *T. versicolor* was interacting with other fungi: after 28 d the metabolome of *T. versicolor* was significantly different when it was paired with *H. fasciculare* compared to when it was arranged in both community 3-dimensional assemblages (Figure 8.4B-D). Production of

Table 8.3

Metabolite	KEGG no.	Pathway	Possible function	Reference
Swainsonine	C10173	Tropane, piperidine and pyridine alkaloid biosynthesis	Antimicrobial activity	Lee et al. 2001
Pantothenol	C05944	Coenzyme A biosynthesis	Organism growth; antimicrobial activity	Spry et al. 2008
Retronecine	C06177	Tropane, piperidine and pyridine alkaloid biosynthesis	Antimicrobial activity	Lee et al. 2001
N2-Acetyl-L-aminoadipate semialdehyde	C12988	Lysine degredation	Defence	Ljunggren, 2015
(S)-5-Oxo-2,5-dihydrofuran-2-acetate	C14610	Benzoate degredation	Decomposition	Martinez et al. 2009
Hydroxyatrazine	C06552	Atrazine degradation	Nitrogen acquisition	Singh et al. 2008
Xylobiose	C01630	ABC transporters	Cellular transport	Wilkens 2015
1-Guanidino-1-deoxy-scyllo-inositol	C04280	Streptomycin biosynthesis	Antimicrobial activity	Popova et al. 2009
D-Lysopine	C04020	Lysine degredation	Defence	Ljunggren 2015
dethiobiotin	C01909	Biotin metabolism	Defence	Bleuler-Martinez et al. 2012
(+)-7-Isojasmonic acid	C16317	alpha-Linolenic acid metabolism	Defence	Walters et al. 2004
GMP	C00144	Purine metabolism	Carbon uptake	Rineau et al. 2013
11-Dehydro-thromboxane B2	C05964	Arachidonic acid metabolism	Defense	Ells et al. 2012
AMP	C00020	Purine metabolism	Carbon uptake	Rineau et al. 2013
L-alpha-Acetyl-N-normethadol	C16661	Drug metabolism - cytochrome P450	Lignin decomposition; xenobiotics detoxification	Ichinose 2013
Nicotinamide	C00153	Nicotinate and nicotinamide metabolism	Nutrient acquition	-
Homocystine	C00155	Cysteine and methionine metabolism; Sulphur metabolism	Enzyme metabolism; Decomposition	Tuor et al. 1995; Blanchette 1995
CMP	C00055	Pyrimidine metabolism	Carbon uptake	Rineau et al. 2013
Decylubiquinol	C15495	Sulphur metabolism	Decomposition	Blanchette 1995
Spironolactone	C07310	Glucocorticoid and mineralocorticoid receptor agonists/antagonists	Antimicrobial activity	-
N6-Acetyl-L-lysine	C02727	Lysine degredation	Defence	Ljunggren 2015
Mannopine	C16692	ABC transporters	Cellular transport	Wilkens 2015
5'-Phosphoribostamycin	C18004	Neomycin, kanamycin and gentamicin biosynthesis	Antimicrobial activity	Popova et al. 2009
4alpha-formyl-4beta-methyl-5alpha-cholesta-8,24-dien-3beta-ol	C15808	Steroid biosynthesis; Biosynthesis of antibiotics	Antimicrobial activity	Popova et al. 2009
Mitomycin	C06681	Biosynethesis of antibiotics	Antimicrobial activity	Popova et al. 2009
Deoxynupharidine	C09945	Biosynthesis of alkaloids derived from terpenoid and polyketide	Antimicrobial activity	Geris & Simpson 2009
Swainsonine	C10173	Tropane, piperidine and pyridine alkaloid biosynthesis	Antimicrobial activity	Lee et al. 2001
Fructoselysine	C16488	Phosphotransferase system (PTS)	Carbohydrate uptake by bacteria	Kotrba et al. 2001
AMP	C00020	Purine metabolism	Carbon uptake	Rineau et al. 2013
L-alpha-Acetyl-N,N-dinormethadol	C16662	Drug metabolism - cytochrome P450	Lignin decomposition; xenobiotics detoxification	Ichinose 2013
1-Guanidino-1-deoxy-scyllo-inositol	C04280	Streptomycin biosynthesis	Antimicrobial activity	Popova et al. 2009
GMP	C00144	Purine metabolism	Carbon uptake	Rineau et al. 2013
Pantothenol	C05944	Coenzyme A biosynthesis	Organism growth; antimicrobial activity	Spry et al. 2008
Mannopine	C16692	ABC transporters	Cellular transport	Wilkens 2015
Cytosine	C00380	Pyrimidine metabolism	Carbon uptake	Rineau et al. 2013

Table 8.3 Most significant putatively identified metabolites from ANOVA analysis (Supplementary Tables 8.1,2,3,4) in pair-wise and 27-block interactions. Possible metabolic pathways and the functional outcome of those pathways are given, as well as references of previous reports in fungi or relevant pathway.

151 metabolites significantly increased and 199 significantly decreased when the three fungi were dispersed in 3-dimensional cubes compared to when *T. versicolor* was paired with *H. fasciculare*. Furthermore, production of 36 metabolites significantly increased and 61 significantly decreased when *T. versicolor* was interacting in a cube where *V. comedens* occupied a larger adjacent volume, compared to when it was paired with *H. fasciculare* (Table 8.2). These included metabolites involved in alkaloid biosynthesis, streptomycin biosynthesis and metabolism of wood constituents pathways (Table 8.3; Supplementary Table 8.5).

8.5 Discussion

This very first metabolomics analysis of the interactions between fungi in decomposing wood exposes the influence of interspecific competition on intracellular metabolism. The metabolome of *T. versicolor* was altered in pair-wise and community interactions as a result of competition, and also differed between 3-dimensional assemblages of different spatial arrangements. Previous chapters have described the roles of extracellularly secreted enzymes and VOCs in antagonism (Chapters 6,7), but this study shows that intracellular metabolism also plays a vital role.

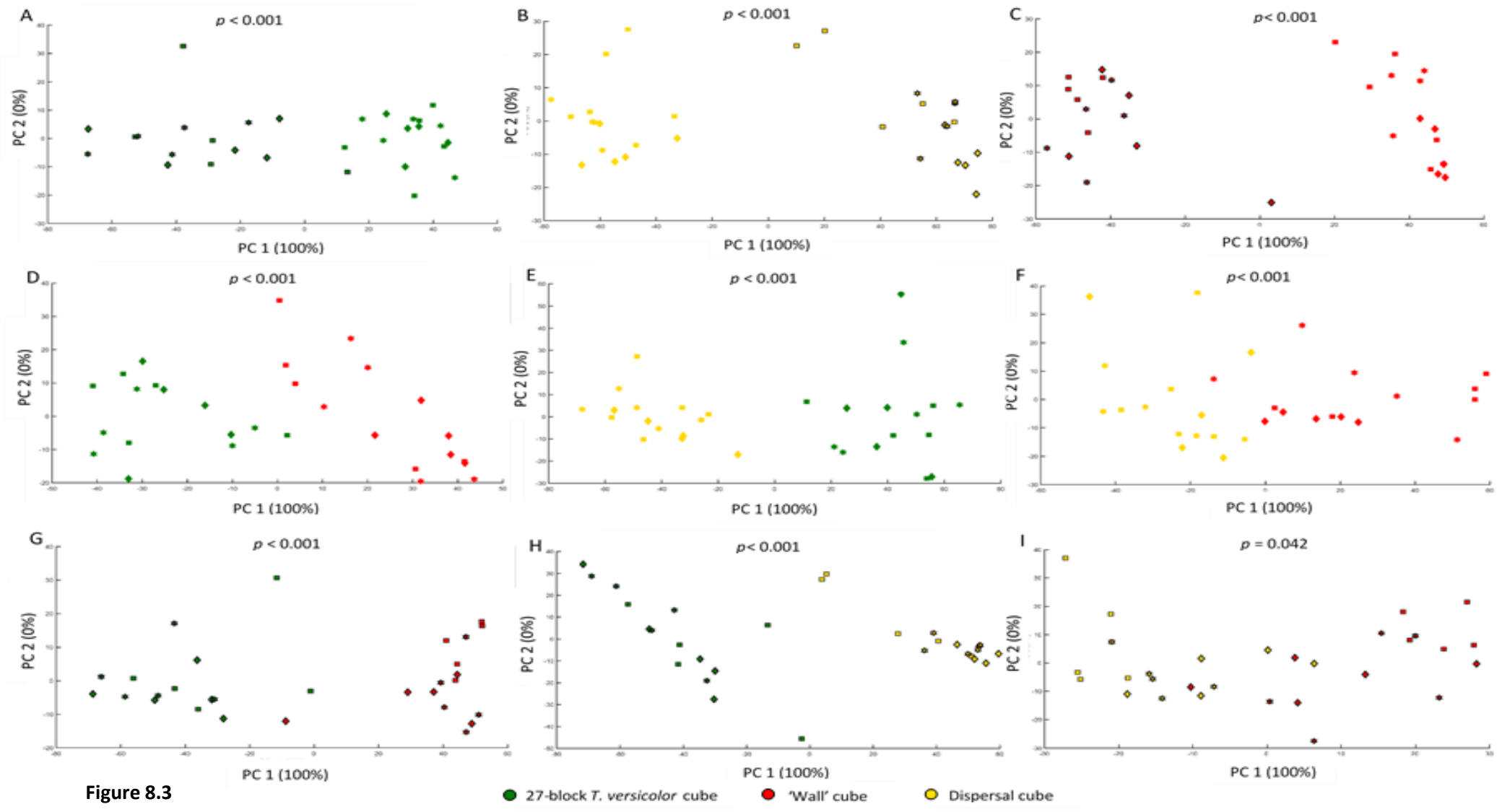
A
p < 0.001
PC 2 (0%)
PC 1 (100%)
B
p < 0.001
PC 2 (0%)
PC 1 (100%)
C
p< 0.001
PC 2 (0%)
PC 1 (100%)
D
p < 0.001
PC 2 (0%)
PC 1 (100%)
E
p < 0.001
PC 2 (0%)
PC 1 (100%)
F
p< 0.001
PC 2 (0%)
PC 1 (100%)
G
p < 0.001
PC 2 (0%)
PC 1 (100%)
H
p< 0.001
PC 2 (0%)
PC 1 (100%)
I
p = 0.042
PC 2 (0%)
PC 1 (100%)
27-block T. versicolor cube
'Wall' cube
Dispersal cube

Figure 8.3

Figure 8.3 ASCA scores plots showing pair-wise comparisons of sample groups derived from the UHPLC-MS spectra of *T. versicolor* blocks within 27-block assemblages, with adjusted *p*-values given. A-C: temporal separation of 27-block assemblages where no outline on points indicates samples 1 d after interaction set up, and an outline on points indicates samples after 28 d of interacting. D-F: separation between different cubes 1 d after interaction set up. G-I: separation between different cubes 28 d after interaction set up. Shapes represent the different spatial positions of blocks (pseudoreplicates) which within each cube are not statistically different ($p > 0.05$) from each other.

8.5.1 Intracellular metabolites function in pathways vital for antagonism

The metabolome of *T. versicolor* was altered compared to monocultures when it was paired against *H. fasciculare*, a competitor against which it deadlocked, but it did not change when it was paired against *V. comedens*, whom *T. versicolor* displaced from 40 % of its territory (Chapter 6). When against *H. fasciculare*, the metabolome changed such that production of significantly affected (ANOVA: $p = 0.05$) metabolites decreased in the interaction after 1 d, but increased after 28 d, even though the interaction had not progressed from deadlock during that time. This would suggest that intracellular processes involved in antagonism are active even during deadlock, perhaps reflecting an effort by *T. versicolor* to gain an advantage, and/or defend its territory (Hiscox et al. 2017). The most significantly affected metabolites included swainsonine and retronecine, which are both involved in the biosynthesis pathway of alkaloids such as piperidine, and N2-acetyl-L-aminoadipate semialdehyde which is involved in lysine metabolism. Piperidine, which is a derivative of lysine (Kukula-Koch & Widelski 2017), previously showed intense fungicidal activity against the basidiomycete *Puccinia recondita*, a phytopathogen of wheat and rye (Lee et al. 2001), and lysine was produced during the

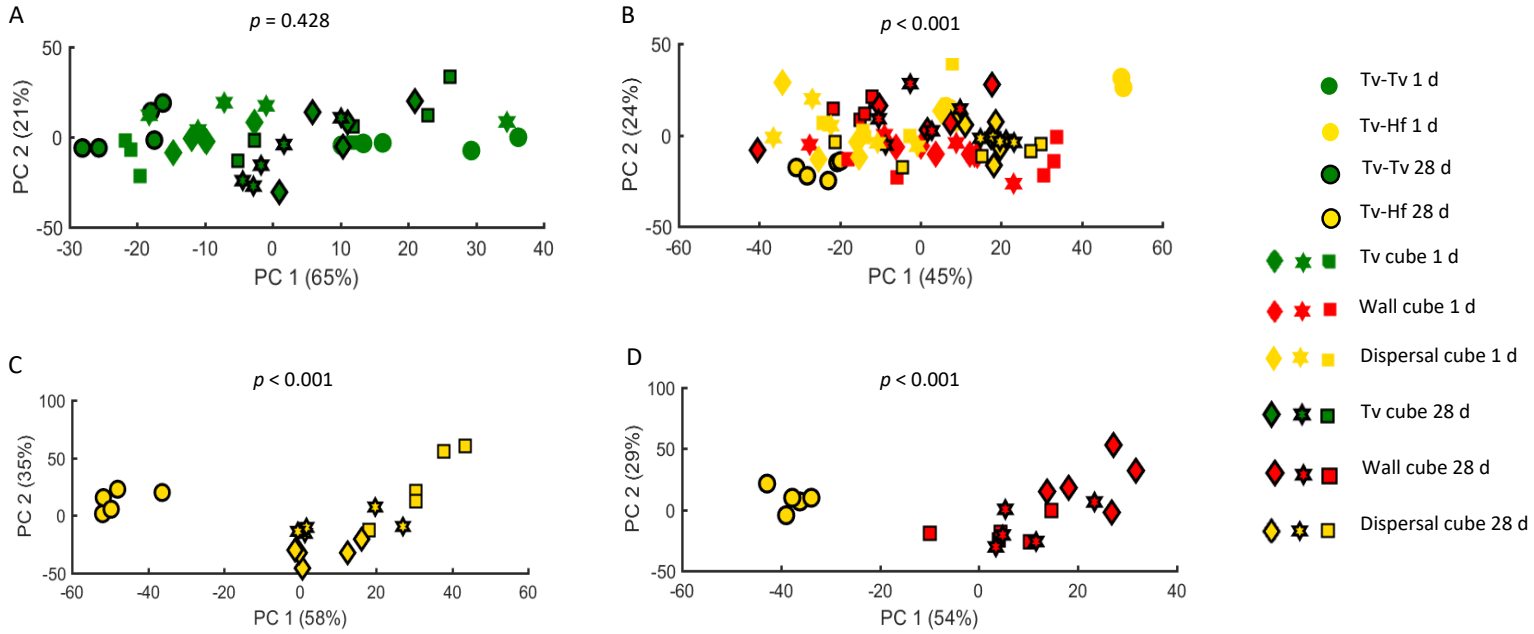

Figure 8.4 ASCA scores plots displaying comparisons between 2- and 3-dimensional systems. Data are derived from the UHPLC-MS spectra of *T. versicolor,* and comparisons are made between interactions of: (A) *T. versicolor* self-pairings and 27-block assemblages comprised solely of *T. versicolor*, 1 d and 28 d after interaction set up; (B) *T. versicolor* paired with *H. fasciculare*, and 3-D cubes of both spatial orientations, 1 d and 28 d after interaction set up; (C) *T. versicolor* paired with *H. fasiculare*, and 3-D cubes where the three fungi were dispersed, after 28 d; and (D) *T. versicolor* paired with *H. fasiculare*, and 3-D cubes where *V. comedens* occupied a larger adjacent volume, after 28 d. Shapes representing points in 3-D cubes indicate different spatial positions of blocks (pseudoreplicates) which were not significantly different from each other. Tv: *T. versicolor*, Tv cube: 27-block cube comprised solely of *T. versicolor*, Wall cube: 27-block cube where *V. comedens* occupied a larger adjacent volume, Dispersal cube: 27-block cube where all fungi were dispersed, Hf: *H. fasciculare*.

interaction between the decay fungi *Heterobasidion parviporum* and *Gloeophyllum sepiarium* but not when either fungus was growing alone (Ljunggren 2015). Intracellularly produced lysine clearly seems to have a role in antagonism, or at the very least is produced as a precursor for other inhibitory secondary metabolites (Ljunggren 2015). The role of N2-acetyl-L-aminoadipate semialdehyde in lysine metabolism is likely a response to lysine production by the other two competitors, or could also be produced by *T. versicolor* as a defensive compound to guard against its own lysine production (Hiscox & Boddy 2017).

8.5.2 Spatial heterogeneity as a moderator of the diversity-function relationship?

Species diversity and spatial heterogeneity were previously shown to impact extracellular metabolite production significantly with both the suite and abundance of ligninolytic enzymes and VOCs differing between two- and three-species interactions, and between 2-dimensional *T. versicolor* self-pairings and 3-dimensional cubes comprised solely of *T. versicolor* (Chapters 6,7). Thus, the proportional influence of each factor on secondary metabolism was difficult to quantify. However, in the current study whilst the metabolome of *T. versicolor* differed between pair-wise interactions and 3-species community interactions, it did not differ significantly between 2- and 3-dimensional *T. versicolor* controls, which would suggest that species diversity has a greater influence on metabolism than does spatial heterogeneity. Theoretical research has suggested that resource heterogeneity can determine the strength of the diversity-function relationship (Cardinale et al. 2000) through resource and spatial-niche partitioning (Dimitrakopoulos & Schmid 2004), leading to the promotion of coexistence (Wang et al. 2015). Further, species richness can affect the rate of decomposition, with communities with an intermediate level of diversity (less than 10 species) often causing greatest decay (Cardinale et al. 2006; Toljander et al. 2006), while communities of greater diversity may inhibit decomposition if competition is a stronger effector than complementarity (Nielsen et al. 2011). Within the current studies, there was greater coexistence in more heterogeneous and

species-diverse systems (Chapter 6), with the production of enzymes (Chapter 6), VOCs (Chapter 7) and intracellular metabolites differing compared to structurally simpler systems with a lower species diversity. This perhaps explains the role of spatial heterogeneity within complex communities as a moderator of the diversity-function relationship, rather than a direct effector of metabolism.

8.5.3 The metabolome responds to a change in competitor antagonistic strategy

The position of blocks within 3-dimesional cubes did not affect the metabolome of *T. versicolor*, neither did it affect its combative ability or enzyme activity (Chapter 6). This is surprising, considering that spatial location within 3-block interactions does significantly affect combative ability (Hiscox et al. 2017; Chapter 5), but could be due to a stochastic influence occurring in 3-block interactions since, in theory, larger scale systems will balance out the effects of stochasticity and operate more uniformly (White et al. 1998). The metabolome of *T. versicolor* did differ between 3-dimensional cubes where all three fungi were dispersed, and cubes where *V. comedens* occupied a larger adjacent volume, however. The antagonistic strategy of *V. comedens* altered between the two arrangements with its production of extracellular enzymes significantly changing which in part resulted in the vast improvement of its combative ability when arranged with conspecifics adjacent (Chapter 6). The homogenous nature of metabolite production by *T. versicolor* within each 3-dimesional cube arrangement indicates that metabolic changes between the two community interactions are a direct response to the increase in combative ability and change of antagonistic mechanisms by *V. comedens*.

Metabolites functioning in the biosynthesis pathways of antibiotics and, interestingly, antibacterial compounds, e.g. neomycin, kanamycin and gentamicin, were affected by species distributions within 3-dimensional cubes. Fungi have been long known to produce antibacterial chemicals when in the presence of bacteria (Brian 1951; de Boer et al. 2005), however, in the

present study seemingly ‘pure’ fungal cultures were used without the addition of any bacterial strains. It is possible that these well-known antibacterial compounds also operate as antifungal agents as some non-specific compounds do inhibit both bacteria and fungi (Modiya & Patel 2012; Swain et al. 2017), or are products of a more general response by the fungus, e.g. a signal cascade causing a whole suite of metabolites to be produced (Hicks et al. 1997). Additionally, however, fructoselysine which functions as part of the phosphototransferase system (PTS) for carbohydrate uptake in bacteria (Kotrba et al. 2001) was significantly produced during this experiment, even though the PTS pathway has only ever been described in bacteria. It seems unlikely that this system of carbohydrate metabolism has been overlooked in the extensive genomic and functional characterisation of wood decay (e.g. Martinez et al. 2009; Eastwood et al. 2011; Floudas et al. 2012; Riley et al. 2014), instead it is more probable that fungal-associated bacteria are residing within or on the hyphae of what we believed to be our ‘pure’ fungal cultures (Johnston et al. 2016).

It is no surprise that metabolites involved in pathways that function in carbon and nitrogen uptake, and general decomposition processes were produced during this experiment. Purine, pyrimidine and sulphur metabolism, which involve GMP (guanosine 5'-monophosphate) and AMP (adenosine 5'-monophosphate), CMP (cytidine 5'-monophosphate), and decylubiquinol in their metabolic pathways respectively, are vital for carbon utilisation by fungi (Blanchette 1995; Rineau et al. 2012). Additionally, cytochrome P450s, the metabolism of which require L-alpha-acetyl-N-normethadol, are an extensively characterised family of enzymes that are directly involved in lignin decay (Doddapaneni et al. 2005; Ichinose 2013). The abundance of metabolites involved in these pathways were significantly affected in different interactions in the present study, indicating that species diversity and spatial patterns affect innate decomposition processes.

8.6 Conclusions

This very first metabolomics study of the interactions of wood decay fungi during decomposition showed that the metabolome of *T. versicolor* is altered as a result of competition, species diversity, and spatial distributions within resources. In pair-wise interactions, *H. fasiculare* influenced the intracellular metabolic processes of *T. versicolor* such that metabolites involved in the biosynthesis of alkaloids and the metabolism of lysine, both of which are associated with antagonism, were produced in greater abundance compared to monocultures. Spatial heterogeneity of resources (2- or 3-dimensions) did not directly affect the metabolome of *T. versicolor*, but metabolite production did differ between 2- and 3-dimensional systems with different species richness. Spatial heterogeneity is, therefore, proposed as a mediator of the diversity-function relationship, rather than a direct effector of the metabolome. Spatial distributions of individuals, specifically whether fungi were dispersed or whether a competitor occupied a larger adjacent volume, resulting in its enhanced combative ability (Chapter 6), caused the metabolome of *T. versicolor* to change, particularly affecting metabolites involved in antibiotics biosynthesis pathways. Finally, the production of metabolites associated with wood decay processes, such as carbon and nitrogen utilisation, differed between specific system setups, highlighting the impact of competition, species diversity and spatial distributions on decomposition processes.

Chapter 9: General discussion

9.1 Synthesis

The work presented in this thesis adds to the current knowledge of interspecific fungal interactions during wood decay, specifically the functional mechanisms of chemical warfare utilised by fungi during pair-wise interactions, and community interactions in 3-dimensional resources. This is the first time that multispecies interactions have been examined with comparisons between 2- and 3-dimensions, and elucidates the importance of species diversity and spatial distributions of individuals to community dynamics. Furthermore, it revealed the link between fungal secondary metabolism and outcomes of competitive interactions, and investigated the stability of that relationship under environmental change. This work also furthers our knowledge of the intracellular processes that regulate interactions during decay, by presenting the first metabolomics study on interacting fungi in wood.

This chapter revisits the primary thesis hypotheses outlined in Chapter 1, and synthesises the main findings of the experimental work across Chapters 3-8 into the context of those hypotheses. Particular triumphs and downfalls in the experimental design of studies presented in this thesis are considered, and finally, future research priorities for the advancement of the field are discussed.

9.1.1 Hypothesis 1: secondary metabolism and interaction outcome are inherently linked, both of which are affected by environmental conditions

The relationship between interaction outcome and secondary metabolism, and the stability of that relationship under environmental change was elucidated in Chapters 3 and 4. The major finding of Chapter 3 was that abiotic conditions, specifically temperature and pre-colonisation length, are important influencers on interaction outcome, and different outcomes are reflected

by extracellular enzyme production. It has been reported previously that temperature causes interaction outcomes to change (Hiscox et al. 2016a), but the present study is the first to show that enzyme activity is linked to changes in outcomes. Furthermore, tracking terminal hydrolase activity throughout the interaction between *Trametes versicolor* and *Hypholoma fasciculare*, revealed that its activity was greatest during deadlock and then returned to pre-interaction levels when *H. fasciculare* started the process of replacement of *T. versicolor* and territory occupation changed. Environmental conditions also significantly affect VOC production (Chapter 4). It was revealed that interactions whose outcomes, and enzymatic profiles, changed under different temperatures (Chapter 3), also differed in their suite and/or abundance of specific VOCs (Chapter 4). This finding was novel as previous studies have found competition causes changes to VOC profiles (Hynes et al. 2007; Evans et al. 2008; El Ariebi et al. 2016), but temperature and the extent of resource decay had not previously been linked to VOC production by wood decay fungi. While differences in enzyme and VOC profiles between interactions with different outcomes may be incidental, it is possible that both enzymes and VOCs actually contribute to diverging combative abilities and outcomes through antimicrobial activities (El Ariebi et al. 2016). The relationship between secondary metabolite production and interaction outcome, therefore, may be explained as (1) temperature causes relative combative abilities to alter, resulting in a change in interaction outcome, a switch in dominant individual and the resulting species-specific suite of metabolites to change, or (2) temperature directly affects the production of enzymes and VOCs, and the change in metabolite production mediates interaction outcomes. Either scenario explains the vital role of fungal secondary metabolism to forest ecosystem dynamics under environmental change, and supports hypothesis 1. It should be mentioned, however, that enzyme activity sometimes differed between identical pairings whose interaction outcome was the same under different environmental conditions (e.g. when *T. versicolor* and *H. fasciculare* deadlocked at 25 °C and in the field (Chapter 3)), suggesting that

interaction outcomes may not be the sole cause or effect of diverging secondary metabolite profiles.

9.1.2 Hypothesis 2: changes to spatial distributions and increased species diversity cause interaction outcomes and community dynamics to alter

It is known that the addition of a third competitor can cause interaction dynamics to change, often in an unpredictable manner (Toledo et al. 2016; Hiscox et al. 2017). However, changes in metabolic mechanisms during interactions of a community of wood decay fungi had not previously been assessed, so I addressed this knowledge gap by investigating multispecies interspecific interactions within novel ecologically realistic 3-dimesnional resources, and assessed metabolism during decomposition of those resources, with comparisons to 2-dimensional structures (Chapters 5,6,7,8).

Interactions that were transitive in 2-dimensional systems often became intransitive in the species richer 3-dimensional systems (Chapters 5,6). Territory fragmentation within the three species community caused the weakest competitors to be outcompeted, while coexistence of individuals occurred when the weakest competitor's territory was adjacent (i.e. spatial distribution was altered), thus supporting hypothesis 2. The mechanisms responsible for this emergent property were not clear at this stage, although it was hypothesised (hypothesis 3) that changes to secondary metabolite production were causal (Lindahl & Olsson 2004; Hiscox et al. 2010a; El Ariebi et al. 2016: Hiscox & Boddy 2017). Changes in secondary metabolite production by fungi whose combative abilities varied under different environmental conditions (Chapters 3,4), and changes in combative mechanisms by a fungus whose combative ability improved when occupying a larger adjacent territory (Chapters 6,7,8) support this (discussed in more detail in Section 9.1.3). The fact that spatial dynamics affect interactions is not a new discovery (White et al. 1998; Sturrock et al. 2002; Toledo et al. 2016; Hiscox et al. 2017), yet the

finding that differences arise between linear 2-dimensional set-ups and more heterogeneous 3-dimensional set-ups is novel. In addition, spatial heterogeneity in the form of vessel orientation caused interaction dynamics to alter: weaker competitors defended their territory more effectively when traversing vessels adjacent to their competitors (Chapter 5). Heterogeneity arising from the 3-dimensional nature of natural resources has been overlooked in previous studies, and investigations such as those in Chapters 3 and 4 are likely missing important ecological variables, such as structural diversity, that influence species interactions (Chapters 5,6).

9.1.3 Hypothesis 3: changes to metabolic strategies for antagonism and resource utilisation will reflect alterations to community dynamics

Pair-wise interactions are often used as predictors of community dynamics (Veech 2012; Maynard et al. 2017a; Maynard et al. 2017b). While caution should be taken when making such predictions, as an increase in species diversity can cause interactions to become unreflective of their pair-wise counterparts (Toledo et al. 2016; Hiscox et al. 2017; Chapters 5,6), predictions regarding more general community processes are still extremely useful, e.g. Chapters 3 and 4. VOCs that function primarily in warfare were produced in different quantities when fungi were interacting compared to monocultures, and when species combinations changed (Chapter 4). Ligninolytic enzyme production changed in a similar way indicating alteration in substrate utilisation (Chapter 3). As the production of secondary metabolites and outcomes of interactions are inherently linked (hypothesis 1: Chapters 3,4), it can be predicted from these pair-wise studies that alterations to secondary metabolism will reflect alterations to community dynamics, as either a cause or effect of each other. In community interactions, interaction dynamics altered with species diversity, territory fragmentation, and between 2- and 3-dimensional systems (Chapters 5,6). Changes to VOCs with antimicrobial properties (Ho et al. 2010; Tumen et al. 2013; Özer & Arin 2014) and resource-utilising enzymes reflected those alterations (Chapters 6,7). This

provides further evidence, supporting the predictions made from pair-wise studies (Chapters 3,4), and hypothesis 3, that the relationship between secondary metabolism and interaction outcomes is reflected by alterations to community dynamics. Additionally, the first metabolomics study ever to be performed on fungi during wood decay (Chapter 8), revealed that metabolites which specifically function in metabolic pathways associated with decomposition and antimicrobial activity changed when community dynamics were altered as a result of species diversity and territory fragmentation. The combined findings from Chapters 3, 4, 6, 7 and 8, therefore, provide undeniable evidence that changes to secondary metabolism and community dynamics reflect one another (hypothesis 3), as either a cause or effect of each other.

9.1.4 Driving the diversity-function relationship

Many studies have shown that species diversity in fungal communities promotes coexistence, leading to a positive diversity-function relationship, i.e. increased rate of decay (Nielsen et al. 2011; Maynard et al. 2017a; Maynard et al. 2017b), due to species complementarity and resource partitioning (Nielsen et al. 2011; Wagg et al. 2015). While effects induced by spatial distributions and species diversity were not directly translated into ecosystem services within the studies of this thesis (i.e. the rate of decay was not significantly affected), secondary metabolism was affected by abiotic conditions (Chapters 3,4), species diversity (Chapters 3,4,6,7,8), and differed between systems of 2- and 3-dimensions (Chapters 6,7,8). Crucially, the production of lignin and cellulose decaying enzymes was altered (Chapters 3,6), and production of intracellular metabolites that function in decomposition pathways changed (Chapter 8), indicating changes to the mechanistic utilisation of the lignocellulose substrate. Decay in the natural environment occurs over much larger time-scales than used here (Freschet et al. 2011), so it is probable that given a greater length of time spatial heterogeneity and species diversity would have resulted in changes to the rate of decomposition, given the fact that over

a short time-scale substrate utilisation was affected (Chapters 3,6,8). This is hugely important to forest dynamics, where the rate of nutrient cycling determines forest functioning (Hobbie 1992), and carbon released from organic substrates enters the carbon cycle, driving global change (Davidson & Janssens 2006).

9.2 Strengths and weaknesses in experimental design

The novel 3-dimensional systems pioneered in this thesis were a triumph in the exciting information regarding species interactions that they produced. The effect of species diversity and spatial distributions on interactions had been discerned previously (White et al. 1998; Sturrock et al. 2002; Toledo et al. 2016; Hiscox et al. 2017), but resource heterogeneity in the context of increased dimensionality had not been tested before. Comparisons of interaction dynamics in 3-dimensions did not reflect those in 2-dimensions, and emergent properties arose which mediated coexistence (Chapter 5), highlighting the importance of this pioneering experimental design for the ecologically relevant study of community dynamics. The traditional system of testing species interactions and community processes within 2-dimensional microcosms clearly overlooks crucial natural variables, and as such the 3-dimensional system is presented as a tractable model for the study of more general ecological community processes, not just for fungi.

The collection of a far wider range of VOCs (Chapters 4,7) than has previously been reported in fungi (Hynes et al. 2007; Evans et al. 2008; El Ariebi et al. 2016) provided a more accurate representation of the 'volatome' of these organisms and allowing more powerful analysis of the roles of VOCs during interactions. The use of the TD method of sampling, rather than SPME as before, increased sensitivity by 50-100 fold (Pfannkoch & Whitecavage 2000), and resulted in collection of a wider spectrum of carbon based compounds. Once compounds are collected, or metabolites extracted from biological material (Chapter 8), however, separation of those metabolites can be challenging. To date, there is no column material that is capable of the

separation of all metabolites, meaning those that are bound too strongly are consequently lost from the analysis (Viant & Sommer 2012). Furthermore, while identification of compounds separated through a GC-MS is relatively robust, LC-MS analyses are not yet sufficiently consistent enough across specific instrumentation types and laboratories, and collaborative inter-laboratory databases cannot be assembled and used for metabolite identification, as they are for GC-MS (Viant & Sommer 2012). This results in datasets with high levels of unidentified metabolites (as in Chapter 8), identification of which can be achieved by multiple fragmentation experiments and comparison to mass spectral trees (Peironcely et al. 2013), a process which is costly, and rarely performed on whole metabolomics datasets.

Production of metabolites that are involved in the biosynthesis pathways of antibacterial compounds (Chapter 8), and also a metabolite which functions within the bacterial PTS carbohydrate uptake system (Kotrba et al. 2001), were unexpected. Given the extensive functional genomics studies that have been performed on wood decay (Martinez et al. 2009; Eastwood et al. 2011; Floudas et al. 2012; Riley et al. 2014), it is unlikely that these metabolic pathways occur in fungi and have been overlooked. In the natural environment, bacteria live alongside fungi and sometimes even form symbiotic relationships (Nazir et al. 2014), so a more likely explanation is that bacteria are co-occurring with fungi in what we believed to be 'pure' fungal cultures. Fungal-associated bacteria have been found to impede the competitive ability of some hosts (Johnston 2017b), while protecting others from toxic compounds (Nazir et al. 2014). Thus, the potential presence of bacteria in the present study could have been affecting the combative abilities of fungi in a species-specific manner, influencing outcomes. Screening for bacteria in mixed microbial samples is commonly achieved by targeting the 16S rRNA gene by quantitative PCR (qPCR) (Oschsenreiter et al. 2003; Fierer et al. 2005), however, it has recently been discovered that commonly used bacterial primers co-amplify eukaryotic DNA when it is in abundance (Johnston 2017a). This poses a problem for the screening of fungal cultures, used in the present study, for bacterial DNA. Potential alternative screening methods

include microscopy (van Teeffelen et al. 2012), or culture based methods with the addition of fungicide (Balouiri et al. 2016), however the reliability of either method is debatable.

While all experiments within this thesis were successfully replicable with results relatively homogenous within replicates, it is important to note that repeatability of experimental results in fungal studies may not always be achieveable. Even under seemingly identical environmental conditions, interactions between the same combinations of fungi can resolve in different outcomes (Boddy 2000). For example, the interaction between *Peniophoroa lycii* and *T. versicolor* resulted in replacement of *P. lycii* in two out of 20 replicates, and replacement of *T. versicolor* in the remainder, despite environmental conditions being the same (Rayner et al. 1995). Fungi are extremely sensitive to very small environmental changes which may affect sporulation, biomass, enzyme production and combative abilities (Mora-Gomez et al. 2016). Consequently, care must be taken when comparing results of similar studies, as any differences/similarities in results may be due to micro-differences in environmental conditions of apparently identical expiermental systems.

9.3 Future research priorities

With the discovery that the relationship between interaction outcome and secondary metabolism is intrinsically affected by abiotic stressors, and that interaction dynamics in 3-dimensional systems are not reflective of those in pair-wise studies, emphasis should be placed on investigating the changing metabolism of communities under environmental change. Chapters 3 and 4 were instrumental in defining changes to secondary metabolites as a result of changing abiotic conditions, directly (via the production of lignocellulolytic enzymes; Chapter 3) and indirectly (the use of VOCs to influence outcomes, changing the suite of species-specific enzymes; Chapter 4) altering wood decay processes. Next, fungal communities in 3-dimensional systems (Chapter 5) should have their metabolic responses to environmental change assessed,

to provide an insight into how forest carbon dynamics are likely to change under future climate predictions (IPCC 2013).

Very few investigations into the intracellular regulation of interactions between wood decay fungi have ever been conducted (Peiris et al. 2008; Luo et al. 2017; Xu et al. 2018; Chapter 8), and Chapter 8 is the first time the metabolome of a decay fungus has actually been characterised during multi-species interactions in wood. Furthermore, transcriptomic and proteomic analyses are rather thin on the ground (Hiscox & Boddy 2017), and to my knowledge neither approach has been applied to community interactions of decay fungi. Combining the results of these powerful multi-omics platforms on interactions between communities of decay fungi would provide unrivalled explanations for the roles of genes, metabolites and proteins vital for interactions, and would be integral in unravelling the roles of species-interactions in decomposition processes. Greater transparency of results, and publication of large 'omics datasets globally, is vital if the potential of these new technological approaches is to be utilised fully. Information sharing will facilitate more comprehensive comparisons between systems and species, allowing deeper investigations into decomposition processes and forest dynamics than have ever been achieved before.

9.4 Conclusions

Metabolic processes during decomposition are altered as a result of competition, species diversity, abiotic stressors, and spatial distributions within resources. Furthermore, these factors are inherently linked to interaction outcome, with any one of them being the cause or effect of the outcome. Within the natural environment, individuals of a community are frequently encountering and interacting with each other, species richness constantly changes following interactions, environmental conditions fluctuate, and non-uniform 3-dimensional resources cause spatial patterning of individuals that arrive at the resource. The combined effects of these

factors influence secondary metabolism, and, therefore, influence the rate of decomposition and the release of organic carbon into the carbon cycle.

References

Abdalla, S.H.M. & Boddy, L. (1996) Effect of soil and litter type on outgrowth patterns of mycelial systems of *Phanerochaete velutina*. *Microbiology Ecology*, 20(3), 195-204.

A'Bear, A.D., Jones, T.H., Kandeler, E. & Boddy, L. (2014) Interactive effects of temperature and soil moisture on fungal-mediated wood decomposition and extracellular enzyme activity. *Soil Biology and Biochemistry*, 70, 151-158.

A'Bear, A.D., Murray, W., Webb, R., Boddy, L. & Jones, T.H. (2013) Contrasting effects of elevated temperature and invertebrate grazing regulate multispecies interactions between decomposer fungi. *PLoS One*, 8(10), e77610, doi: 10.1371/journal.pone.0077610.

Abraham, W.R. (2010) Bioactive sesquiterpenes produced by fungi, are they useful for humans as well? *Current Medicinal Chemistry*, 8, 583-606.

Ahearn, D.G., Crow, S.A., Simmons, R.B., Price, D.L., Mishra, S.K. & Pierson, D.L. (1997) Fungal colonisation of air filters and insulation in a mutli-story office building: Production of volatile organics. *Current Microbiology*, 35(5), 305-308.

Allison, S.D. & Tresedler, K.K. (2008) Warming and drying suppress microbial activity and carbon cycling in boreal forest soils. *Global Change Biology*, 14(12), 2898-2909.

Andrews, J.H. (1992) Fungal life-history strategies. In: *The Fungal Community*, 2nd Edition, (eds C.G. Carroll & D.T. Wicklow). Marcel Dekker, New York, USA, pp. 119-145.

Annamalai, N., Rajeswari, M.V. & Sivakumar, N. (2016) Cellobiohydrolases: Role, Mechanism, and Recent Developments. In: *Microbial Enzymes in Bioconversions of Biomass*, (eds. V.K. Gupta). Springer International Publishing, Switzerland. pp. 29-35.

Arnstadt, T., Hoppe, B., Kahl, T., Kellner, H., Krüger, D., Bauhus, J. & Hofrichter, M. (2016) Dynamics of fungal community composition, decomposition and resulting deadwood properties

in logs of *Fagus sylvatica*, *Picea abies* and *Pinus sylvestris*. *Forest Ecology and Management*, 382, 129-142.

Asensio, D., Peñuelas, J. Filella, I. & Llusià, J. (2007) On-line screening of soil VOCs exchange responses to moisture, temperature and root presence. *Plant and Soil*, 291(1-2), 249-261.

Baldrian, P. (2004) Increase of laccase activity during interspecific interactions of white-rot fungi. *FEMS Microbiology Ecology*, 50, 245-253.

Baldrian, P. (2006) Fungal laccases – occurrence and properties. *FEMS Microbiology Reviews*, 30, 215-242.

Baldrian, P. (2009) Microbial enzyme-catalyzed processes in soils and their analysis. *Plant, Soil and Environment*, 55(9), 370-378.

Baldrian, P. (2008) Wood-inhabiting ligninolytic basidiomycetes in soils: Ecology and constraints for applicability in bioremediation. *Fungal Ecology*, 1(1), 4-12.

Baldrian, P. & Gabriel, J. (2002) Copper and cadmium increase laccase activity in *Pleurotus ostreatus*. *FEMS Microbiology Letters*, 206, 69-74.

Baldrian, P., in der Wiesche, C., Gabriel, J., Nerud, F. & Zadražil, F. (2000) Influence of cadmium and mercury on activities of ligninolytic enzymes and degradation of ploycyclic aromatic hydrocarbons by *Pleurotus ostreatus*in soil. *Applied Environmental Microbiology*, 66(6), 2471-2478.

Baldrian, P. & Lindahl, B. (2011) Decomposition in forest ecosystems: after decades of research still novel findings. *Fungal Ecology*, 4(6), 359-361.

Baldrian, P., Šnajdr, J., Merhautová, V., Dobiášová, P., Cajthaml, T. & Valášková, V. (2013) Responses of the extracellular enzyme activities in hardwood forest to soil temperature and

seasonality and the potential effects of climate change. *Soil Biology and Biochemistry*, 56, 60-68.

Baldrian, P. & Valásková, V. (2008) Degradation of cellulose by basidiomycetous fungi. *FEMS Microbiology Review*, 32, 501-521.

Balouiri, M., Sadiki, M. & Ibnsouda, S.K. (2016) Methods for *in vitro* evaluating antimicrobial activity: A review. *Journal of Pharmaceutical Analysis*, 6(2), 71-79.

Behrendt, C.J. & Blanchette, R.A. (2001) Biological control of blue stain in pulpwood: mechanisms of control used by *Phlebiopsis gigantea. Holzforschung*, 55, 238–245.

Bell, L., Spadafora, N., Müller, C.T., Wagstaff, C. & Rogers, H. (2016) Use of TD-GC-TOF-MS to assess volatile composition during post-harvest storage in seven accessions of rocket salad (*Eruca sativa*). *Food Chemistry*, 194, 626-636.

Benjamini, Y. & Hochberg, Y. (1995) Controlling the false discovery rate – a practical and powerful approach to multiple testing. *Journal of the Royal Statistical Society Series B-Methodological*, 57, 289-300.

Benjamin, M.A., Zhioua, E. & Ostfeld, R.S. (2002) Laboratory and field evaluation of the entomopathogenic fungus *Metarhizium anisopliae* (Deuteromycetes) for controlling questing adult *Ixodes scapularis* (Acari: Ixodidae). *Journal of Medicinal Entomology*, 39(5), 723-728.

Bennett J.W., Hung R., Lee S. & Padhi S. (2012) 18 Fungal and Bacterial Volatile Organic Compounds: An Overview and Their Role as Ecological Signaling Agents. In: *Fungal Associations. The Mycota (A Comprehensive Treatise on Fungi as Experimental Systems for Basic and Applied Research)*, (eds. B. Hock). vol 9. Springer, Berlin, Germany.

Bertrand, S., Schumpp, O., Bohni, N., Bujard, A., Azzollini, A., Monod, M., Gindro, K. & Wolfender, J.-L. (2013) Detection of metabolite induction in fungal co-cultures on solid media by high-

throughput differential ultra-high pressure liquid chromatography–time-of-flight mass spectrometry fingerprinting. *Journal of Chromatography A*, 1292, 219-228.

Blanchette, R.A. (1995) Degradation of the lignocellulose complex in wood. *Canadian Journal of Botany*, 73, 999-1010.

Blanchette, R.A., Held, B.W., Jurgens, J.A., McNew, D.L., Harrington, T.C., Duncan, S.M., Farrell, R.L. (2004) Wood-rotting soft rot fungi in the historic expedition huts of Antarctica. *Applied Environmental Microbiology*, 70(3), 1328-1335.

Bleuler-Martinez, S., Schmieder, S., Aebi, M. & Künzler, M. (2012) Biotin-binding proteins in the defense of mushrooms against predators and parasites. *Applied and Environmental Microbiology*, 78(23), 8485-8487.

Boddy, L. (2000) Interspecific combative interactions between wood-decaying basidiomycetes. *FEMS Microbiology Ecology*, 31, 185-194.

Boddy, L. (2001) Fungal community decomposition processes in angiosperms: from standing tree to complete decay of coarse woody debris. *Ecological Bulletins*, 49, 43-56.

Boddy, L. & Abdalla, S.H.M. (1998) Development of *Phanerochaete velutina* mycelial cord systems: effect of encounter of multiple colonised wood resources. *FEMS Microbiology Ecology*, 25, 257-269.

Boddy, L. & Hiscox, J. (2016) Fungal Ecology: principles and mechanisms of colonization and competition by saprotrophic fungi. *Microbiology Spectrum*, 4(6), FUNK-0019-2016, doi: 10.1128/microbiolspec.FUNK-0019-2016.

Borjesson, T., Stollman, U., Adamek, P. & Kaspersson, A. (1989) Analysis of volatile compounds for detection of molds in stored cereals. *American Association of Cereal Chemists*, 66(4), 300-304.

Bourbonnais, R. & Paice, M.G. (1990) Oxidation of non-phenolic substrates. An expanded role for laccase in lignin biodegradation. *FEBS Letters*, 267, 99–102.

Brakhage, A.A. & Schroeckh, V. (2011) Fungal secondary metabolites – strategies to activate silent gene clusters. *Fungal Genetics and Biology,* 48, 15–22.

Brakhage, A.A. (2013) Regulation of fungal secondary metabolism. *Nature Reviews Microbiology*, 11, 21-32.

Brian, P.W. (1951) Antibiotics produced by fungi. *The Botanical Review*, 17(6), 357-430.

Brockhurst, M.A., Buckling, A. & Rainey, P.B. (2005) Spatial heterogeneity and the stability of host-parasite coexistence. *Journal of Evolutionary Biology*, 19, 374-379.

Broekaert, K., Heyndrick, M., Herman, L. Devlieghere, F. & Vlaemynck, G. (2013) Molecular identification of the microbiota of peeled and unpeeled brown shrimp (*Crangon crangon*) during storage on ice and at 7.5 °C. *Food Microbiology*, 36(2), 123-134.

Brown, M., Dunn, W.B., Dobson, P., Patel, Y., Winder, C.L., Francis-McIntyre, S., Begley, P., Carroll, K., Broadhurst, D., Tseng, A., Swainston, N., Spasic, I., Goodacre, R. & Kell, D.B. (2009) Mass spectrometry tools and metabolite-specific databases for molecular indentification in metabolomics. *Analyst*, 134(7), 1322-1332.

Calvo, A.M., Wilson, R.A., Bok, J.W. & Keller, N.P. (2002) Relationship between secondary metabolism and fungal development. *Microbiology and Molecular Biological Reviews*, 66(3), 447-459.

Cánovas, D., Studt, L., Marcos, A.T. & Strauss, J. (2017) High-throughput format for the phenotyping of fungi on solid substrates. *Scientific Reports*, 7, 4289, doi: 10.1038/s41598-017-03598-9.

Cardinale, B.J., Srivastava, D.S., Duffy, J.E., Wright, J.P., Downing, A.L., Sankaran, M. & Jouseau, C. (2006) Effects of biodiversity on the functioning of trophic groups and ecosystems. *Nature*, 443, 989-992.

Cardinale, B.J., Nelson, K. & Palmer, M.A. (2000) Linking species diversity to the functioning of ecosystems: on the importance of environmental context. *Oikos*, 91, 175–183.

Caruso, T., Hempel, S., Powell, J.R., Barto, E.K. & Rillig, M.C. (2012) Compositional divergence and convergence in arbuscular mycorrhizal fungal communities. *Ecology*, 93, 1115-1124.

Chappell, J. & Coates, R.M. (2010) Sesquiterpenes. In: *Comprehensive Natural Products II, Volume 1: Natural Products Structural Diversity-I Secondary Metabolites: Organization and Biosynthesis*, (eds. L. Mander & H.-W. Liu). Elsevier, Amsterdam, the Netherlands. pp 609-641.

Chen, W.P., Liu, L.L. & Yang, Y.Q. (1989) Synthesis and antifungal activity of N-(6,6-dimethyl-2-hepten-4-ynyl)-N-methyl-alpha-substituted -1-(4-substi tuted) naphthalenemethanamines. *Acta Pharmaceutica Sinica,* 24(12), 895-905.

Chet, I., Inbar, J. & Hader, Y. (1997) Fungal antagonists and mycoparasites. In: *The Mycota IV. Environmental and Microbial Relationships*, (eds. D.T. Wicklow & B. Soderstrom). Springer, Berlin, Germany. pp. 165-184.

Chitarra, G.S., Abee, T., Rombouts, F.M., Posthumus, M.A. & Dijksterhuis, J. (2004) Germination of *Penicillium paneum* conidia is regulated by 1-octen-3-ol, a volatile self-inhibitor. *Applied Environmental Microbiology*, 70(5), 2823-2829.

Ciesla, W.M. (2002) An Overview of Temperate Broadleaf Forests. In: *Non-Wood Forest Products from Temperate Broad-Leaved Trees*. Food and Agricultural Organisation of the United Nations, Rome, Italy. pp. 3-10.

Connolly, J.D. & Hill, R.A. (1991) Dictionary of Terpenoids. Chapman and Hall, London, UK.

Copeland, N., Cape, J.N., Nemitz, E. & Heal, M.R. (2014) Volatile organic compound speciation above and within a Douglas fir forest. *Atmospheric Environment*, 94, 86-95.

Crockatt, M.E., Pierce, G.I., Camden, R.A., Newell, P.M. & Boddy, L. (2008) Homokaryons are more combative than heterokaryons of *Hericium coralloides*. *Fungal Ecology*, 1(1), 40-48.

Cordero, P., Principe, A., Jofre, E., Mori, G. & Fischer, S. (2014) Inhibition of the phytopathogenic fungus *Fusarium proliferatum* by volatile compounds produced by *Pseudomonas*. *Archives of Microbiology,* 196(11), 803-809.

Crowther, T., Jones, T.H., Boddy, L. & Baldrian, P. (2011) Invertebrate grazing determines enzyme production by basidiomycete fungi. *Soil Biology and Biochemistry*, 42, 2060-2068.

Coates, D. & Rayner, A.D.M. (1985) Fungal population and community development in cut beech logs: 1. Establishment via the aerial cut surface. *New Phytologist*, 101, 153-171.

Cox, P.M., Betts, R.A., Jones, C.D., Spall, S.A. & Totterdell, I.J. (2000) Acceleration of global warming due to carbon-cycle feedbacks in a coupled climate model. *Nature*, 408, 184–187.

da Silva Coelho-Moreira, J., Maciel, G.M., Castoldi, R., da Silva Mariano, S., Inácio, F.D., Bracht, A. & Peralta, R.M. (2013) Involvement of lignin-modifying enzymes in the degradation of herbicides. In: *Herbicides - Advances in Research*, (eds. A. Price). In Tech, Croatia.

Daugherty, M.P. (2011) Host plan quality, spatial heterogeneity, and the stability of mite predator-prey dynamics. *Experimental and Applied Acarology*, 54, 311-322.

Davidson, E.A. & Janssens, I.A. (2006) Temperature sensitivity of soil carbon decomposition and feedbacks to climate change. *Nature*, 440, 165-173.

Davidson, P.M. (2001) Chemical preservatives and natural antimicrobial compounds. *Food Microbiology: Fundamentals and Frontiers*, (eds. M.P. Beuchat & L.R. Montville). ASM Press, Washington DC, USA. pp. 593-628.

Davies, G. & Henrissat, B. (1995) Structures and mechanisms of glycosyl hydrolases. *Structure*, 3(9), 853-9.

Davis, T.S., Crippen, T.L., Hofstetter, R.W. & Tomberlin, J.K. (2013) Microbial volatile emissions as insect semiochemicals. *Journal of Chemical Ecology*, 39(7), 840–859.

Deacon, J.W. (2013) Fungal Biology. John Wiley & Sons, New-Jersey, USA.

Deacon, L.J., Pryce-Miller, E.J., Frankland, J.C., Bainbridge, B.W., Moore, P.D. & Robinson, C.H. (2006) Diversity and function of decomposer fungi from a grassland soil. *Soil Biology Biochemistry*, 38, 7–20.

Debeljak, M. (2006) Coarse woody debris in virgin and managed forest. *Ecological Indicators*, 6, 733-742.

De Boer, W., Folman, L.B., Summerbell, R.C. & Boddy, L. (2005) Living in a fungal world: impact of fungi on soil bacterial niche development. *FEMS Microbiology Reviews*, 29(4), 795-811.

de Lima, P.F., Furlan, M.F., de Lima Ribeiro, F.A., Pascholati, S.F. & Augusto, F. (2015) *In vivo* determination of the volatile metabolites of saprotroph fungi by comprehensive two-dimensional gas chromatography. *Journal of Separation Science*, 38(11), 1924-1932.

Didham, R.K. (2010) Ecological consequences of habitat fragmentation. *eLS*, doi: 10.1002/9780470015902.a0021904.

Dimitrakopoulos, P.G. & Schmid, B. (2004) Biodiversity effects increase linearly with biotope space. *Ecology Letters*, 7, 574–583.

Doddapaneni, H., Chakraborty, R. & Yadav, J.S. (2005) Genome-wide structural and evolutionary analysis of the P450 monooxygenase genes (P450ome) in the white rot fungus *Phanerochaete chrysosporium*: Evidence for gene duplications and extensive gene clustering. *BMC Genomics*, 6, 92, doi: 10.1186/1471-2164-6-92.

Doddapaneni, H., Subramanian, V., Fu, B. & Cullen, D. (2013) A comparative genomic analysis of the oxidative enzymes potentially involved in lignin degradation by *Agaricus bisporus*. *Fungal Genetics and Biology,* 55, 22-31.

Donnelly, D.P. & Boddy, L. (2001) Mycelial dynamics during interactions between *Stropharia caerulea* and other cord-forming, saprotrophic basidiomycetes. *New Phytologist,* 151, 691-704.

Dosdall, R., Preuß, F., Hahn, V., Schlüter, R. Schauer, F. (2017) Decay of the water reed *Phragmites communis* caused by the white-rot fungus *Phlebia tremellosa* and the influence of some environmental factors. *Applied Microbiology and Biotechnology*, doi: 10.1007/s00253-017-8582-0.

Dunn, W.B. (2008) Current trends and future requirements for the mass spectrometric investigation of microbial, mammalian and plant metabolomes. *Physical Biology*, 5, 1-24.

Dunn, W.B., Broadhurst, D., Begley, P., Zelena, E., Francis-McIntyre, S., Anderson, N., Brown, M., Knowles, J.D., Halsall, A., Haselden, J.N., Nicholls, A.W., Wilson, I.D., Kell, D.B., Goodacre, R. & Human Serum Metabolome (HUSERMET) Consortium. (2011) Procedures for large-scale metabolic profiling of serum and plasma using gas chromatography and liquid chromatography coupled to mass spectrometry. *Nature Protocols*, 6, 1060, 1083.

Du, T., Shupe, T. & Hse, C.Y. (2011) Antifungal activities of three supercritical fluid extracted cedar oils. *Holzforschung*, 65(2), 277-284.

Eastwood, D.C., Floudas, D., Binder, M., Majcherczyk, A., Schneider, P., Aerts, A., Asiegbu, F.O., Baker, S.E., Barry, K., Bendiksby, M., Blumentritt, M., Coutinho, P.M., Cullen, D., de Vries, R.P., Gathman, A., Goodell, B., Henrissat, B., Ihrmark, K., Kauserud, H., Kohler, A., LaButti, K., Lapidus, A., Lavin, J.L., Lee, Y.H., Lindquist, E., Lilly, W., Lucas, S., Morin, E., Murat, C., Oguiza, J.A., Park, J., Pisabarro, A.G., Riley, R., Rosling, A., Salamov, A., Schmidt, O., Schmutz, J., Skrede, I., Stenlid, J., Wiebenga, A., Xie, X., Kues, U., Hibbett, D.S., Hoffmeister, D., Hogberg, N., Martin, F.,

Grigoriev, I.V. & Watkinson, S.C. (2011) The plant cell wall-decomposing machinery underlies the functional diversity of forest fungi. *Science*, 333, 762– 765.

Eichlerová, I., Homolka, L., Žifčáková, L., Lisá, L., Dobiášová, P. & Baldrian, P. (2015) Enzymatic systems involved in decomposition reflects ecology and taxonomy of saprotrophic fungi. *Fungal Ecology*, 13, 10-22.

Elamparithi, D., Mani, P. & Moorthy, V. (2014) Antimicrobial activity and GC-MS analysis of *Ocimun tenuiflorum* and *Acalypha hispida* extract against *Steptococcus pyogenes*. *Malaya Journal of Biosciences*, 1(4), 259-266.

El Ariebi, N., Hiscox, J., Scriven, S.A., Müller, C.T. & Boddy, L. (2016) Production and effects of volatile organic compounds during interspecific interactions. *Fungal Ecology*, 20, 144-154.

Ells, R., Kock, J.L.F., Albertyn, J. & Pohl, C.H. (2012), Arachidonic acid metabolites in pathogenic yeasts. *Lipids in Health and Disease*, 11, 100, doi: 10.1186/1476-511X-11-100.

Eriksson, K.L. & Bermek, H. (2016) Lignin, Lignocellulose, Ligninase. *Encyclopedia of Microbiology*, 3, 373-384.

Eriksson, K.L., Blanchette, R.A. & Ander, P. (1990) Biodegradation of lignin. In: *Microbial and Enzymatic Degradation of Wood and Wood components* (eds. K.L. Eriksson, R.A. Blanchette & P. Ander). Springer-Verlag, Berlin, Germany. pp. 225-333.

Evans, J.A., Eyre, C.A., Rogers, H.J., Boddy, L. & Müller, C.T. (2008) Changes in volatile production during interspecific interactions between four wood rotting fungi growing in artificial media. *Fungal Ecology*, 1, 57-68.

Eyre, C., Muftah, W., Hisocx, J., Hunt, J., Kille, P. Boddy, H.J. & Rogers, H.J. (2010) Microarray analysis of differential gene expression elicited in *Trametes versicolor* during interspecific mycelial interactions. *Fungal Biology*, 114, 646-660.

Faraldos, J.A., O'Maille, P.E., Dellas, N., Noel, J.P. & Coates, R.M. (2010) Bisabolyl-Derived Sesquiterpenes from Tobacco 5-Epi-aristolochene Synthase-Catalyzed Cyclization of (2Z,6E)-Farnesyl Diphosphate. *Journal of the American Chemical Society*, 132(12), 4281-4289.

Fawcett, R. & Collins-George, N. (1967) A filter-paper method for determining the moisture characteristics of soil. *Australian Journal of Experimental Agriculture and Animal Husbandry*, 7, 162-167

Fengel, D. & Wegener, G. (1984) *Wood: Chemistry, ultrastructure, reactions*. De Gruyter, Berlin, Germany.

Fernandez de Simon, B., Sanz, M., Cadahia, E., Esteruelas, E. & Minoz, A.M. (2014) Nontargeted GC–MS approach for volatile profile of toasting in cherry, chestnut, false acacia, and ash wood. *Journal of Mass Spectrometry*, 49(5), 353-370.

Fernández-Fueyo, E., Ruiz-Dueñas, F.J., Martínez, M.J., Romero, A., Hammel, K.E., Medrano, F.J. & Martínez, A.T. (2014) Ligninolytic peroxidase genes in the oyster mushroom genome: heterologous expression, molecular structure, catalytic and stability properties, and lignin-degrading ability. *Biotechnology for Biofuels*, 7(1), doi: 10.1186/1754-6834-7-2.

Fierer, N., Jackson, J.A., Vilgalys, R. & Jackson, R.B. (2005) Assessment of soil microbial community structure by use of taxon-specific quantitative PCR assays. *Applies and Environmental Microbiology*, 71(7), 4117-4120.

Floudas, D., Binder, M., Riley, R., Barry, K., Blanchette, R.A., Henrissat, B., Martinez, A.T., Otillar, R., Spatafora, J.W., Yadav, J.S., Aerts, A., Benoit, I., Boyd, A., Carlson, A., Copeland, A., Coutinho, P.M., de Vries, R.P., Ferreira, P., Findley, K., Foster, B., Gaskell, J., Glotzer, D., Gorecki, P., Heitman, P., Hesse, C., Hori, C., Igarashi, K., Jurgens, J.A., Kallen, N., Kersten, P., Kohler, A., Kues, U., Kumar, T.K.A., Kuo, A., LaButti, K., Larrondo, L.F., Lindquist, E., Ling, A., Lombard, V., Lucas, S., Lundell, T., Martin, R., McLaughlin, D.J., Morgenstern, I., Morin, E., Murat, R., Nagy, L.G.,

Nolan, M., Ohm, R.A., Patyshakuliyeva, A., Rokas, A., Ruiz-Duenas, F.J., Sabat, G., Salamov, A., Samejima, M., Schmutz, J., Slot, J.C., St. John, F., Stenlid, J., Sun, H., Sun, S., Syed, K., Tsang, A., Wiebenga, A., Young, D., Pisabarro, A., Eastwood, D.C., Martin, F., Cullen, D., Grigoriev, I.V. & Hibbett, D.S. (2012) The Paleozoic origin of enzymatic lignin decomposition reconstructed from 31 fungal genomes. *Science*, 336, 1715-1719.

Forest Europe. (2012) The Ministerial Conference on the Protection of Forests in Europe. URL: https://www.eea.europa.eu/data-and-maps/indicators/forest-deadwood-1/assessment-1#tab-related-briefings.

Forrester, I.T., Grabski, A.C., Burgess, R.R. & Leatham, G.F. (1988) Manganese, Mn-dependent peroxidases, and the biodegradation of lignin. *Biochemical and Biophysical Research Communications*, 157, 992-999.

Fox, E.M. & Howlett, B. (2008) Secondary metabolism: regulation and role in fungal biology. *Current Optionion in Microbiology*, 11, 481-497.

Freschet, G.T., Weedon, J.T., Aets, R., van Hal, J.R. & Cornelissen, J.H.C. (2011) Interspecific differences in wood decay rates: insights from a new short-term method to study long-term wood decomposition. *Journal of Ecology*, 100(1), 161-170.

Fukuda, H., Fujii, T. & Ogawa, T. (1984) Microbial Production of C3- and C4-Hydrocarbons under Aerobic Conditions. *Agricultural and Biological Chemistry*, 48(6), 1679-1682.

Gadd, G.M. (1999) Fungal production of citric and oxalic acid: Importance in metal speciation, physiology and biogeochemical processes. *Advances in Microbial Physiology*, 41, 47-92.

Gallien, L., Zimmermann, N.E., Levine, J.M. & Adler, P.B. (2017) The effects of intransitive competition on coexistence. *Ecology Letters*, 20, 791-800.

Garavaglia, S., Cambria, M.T., Miglio, M., Ragusa, S Iacobazzi, V., Palmieri, F., D'Ambrosio, C., Scaloni, A. & Rizzi, M. (2004) The structure of *Rigidoporus lignosus* laccase containing a full

complement of copper ions, reveals an asymmetrical arrangement for the T3 copper pair. *Journal of Molecular Biology*, 342(5), 1519-1531.

Garbelotto, M.M., Lee, H.K., Slaughter, G., Popenuck, T., Cobb, F.W. & Bruns, T.D. (1997) Heterokaryosis is not required for virulence of *Heterobasidion annosum. Mycologia*, 89, 92-102.

Geethalakshmi, R. & Sarada, D.V.L. (2013) Evaluation of antimicrobial and antioxidant activity of essential oil ot *Trianthema decandra* L.. *Journal of Pharmacy Research*, 6(1), 101-106.

Geris, R. & Simpson, T.J. (2009) Meroterpenoids produced by fungi. *Natural Products Reports*, 26, 1063-1094.

Glenn, J.K. & Gold, M.H. (1985) Purification and characterization of an extracellular Mn(II)-dependent peroxidase from the lignin-degrading basidiomycete, *Phanerochaete chrysosporium*. *Archives of Biochemistry and Biophysics,* 242, 329–341.

Goodell, B., Qian, Y. & Jellison, J. (2008) *Development of Commercial Wood Preservatives*. American Chemical Society, Washington DC, USA.

Goszczynski, S., Paszczynski, A., Pasti-Grigsby, M.B., Crawford, R.L. & Crawford, D.L. (1994) New pathway for degradation of sulfonated azo dyes by microbial peroxidases of *Phanerochaete chrysosporium* and *Streptomyces chromofuscus*. *Journal of Bacteriology*, 176, 1339–1347.

Grigoriev, I.V., Nikitin, R., Haridas, S., Kuo, A., Ohm, R., Otillar, R., Riley, R., Shabalov, A., Zhao, X., Korzeniewski, F., Smirnova, T., Nordberg, H., Dubchak, I. & Shabalov, I. (2014) MycoCosm portal: gearing up for 1000 fungal genomes. *Nucleic Acids Research*, 42, D699–D704.

Guillarme, D., Nguyen, D.T.T., Rudaz, S. & Veuthey, J.L. (2007) Recent developments in liquid chromatography-impact on qualitative and quantitative performance. *Journal of Chromatography A*, 1149, 20–29.

Gutierrez, A., del Rio, J.C., Martinez-Inigo, M., Martinez, M.J. & Martinez, A.T. (2002) Production of new unsaturated lipids during wood decay by ligninolytic basidiomycetes. *Applies and Environmental Microbiology*, 68(3), 1344-1350.

Halley, J.M., Robinson, C.H., Comins, H.N. & Dighton, J. (1996) Predicting straw decomposition by a 4-species fungal community – a cellular automaton model. *Journal of Applied Ecology*, 33, 493-507.

Hannula, S.E., de Boer, W., Baldrian, P. & van Veen, J.A. (2013) Effect of genetic modification of potato starch on decomposition of leaves and tubers and on fungal decomposer communities. *Soil Biology and Biochemistry*, 58, 88-98.

Hansen, C.A., Allison, S.D., Bradford, M.A., Wallenstein, M.D. & Treseder, K.K. (2008) Fungal taxa target different carbon sources in forest soil. *Ecosystems*, 11, 1157–1167.

Hansen, J., Ruedy, R., Sato, M. & Lo, K. (2006) *GISS Surface Temperature Analysis. Global Temperature Trends: 2005 Summation*. NASA Goddard Institute for Space Studies and Columbia University Earth Institute, New York, USA.

Henson, J.M., Butler, M.J. & Day, A.W. (1999) The dark side of the mycelium: melanins of phytopathogenic fungi. *Annual Review of Phytopathology*, 37, 447-471.

Hibbett, D.S., Binder, M., Bischoff, J.F., Blackwell, M., Cannon, P.F., Eriksson, O.E., Huhndorf, S., James, T., Kirk, P.M., Lücking, R., Lumbsch, H.T., Lutzoni, F., Matheny, P.B., McLaughlin, D.J., Powell, M.J., Redhead, S., Schoch, C.L., Spatafora, J.W., Stalpers, J.A., Vilgalys, R., Aime, C.M., Aptroot, A., Bauer, R., Begerow, D., Benny, G.L., Castlebury, L.A., Crous, P.W., Dai, Y., Gams, W., Geiser, D.M., Griffith, G.W., Gueidan, C., Hawksworth, D.L., Hestmark, G., Hosaka, K., Humber, R.A., Hyde, K.D., Ironside, J.E., Kõljalg, U., Kurtzman, C.P., Larsson, K.H., Lichtwardt, R., Longcore, J., Miadlikowska, J., Miller, A., Moncalvo, J.M., Mozley-Standridge, S., Oberwinkler, F., Parmasto, E., Reeb, V., Rogers, J.D., Roux, C., Ryvarden, L., Sampaio, J.P., Schüssler, A., Sugiyama, J., Thorn,

R.G., Tibell, L., Untereiner, W.A., Walker, C., Wang, Z., Weir, A., Weiss, M., White, M.M., Winka, K., Yao. Y.J. & Zhang, N. (2007) A higher-level phylogenetic classification of the Fungi. *Mycology Research*, 111, 509-547.

Hicks. J.K., Yu, J.-H., Keller, N.P. & Adams, T.H. (1997) *Aspergillus* sporulation and mycotoxin production both require inactivation of the FadA Gα protein-dependent signaling pathway. *The EMBO Journal*, 16(16), 4797-5148.

Higuchi, T. (1990) Lignin biochemistry: Biosynthesis and biodegradation. *Wood Science and Technology*, 24, 23-63.

Higuchi, T. (1993) Biodegradation mechanism of lignin by white-rot basidiomycetes. *Journal of Biotechnology*, 30, 1-8.

Higuchi, T. (1997) *Biochemistry and molecular Biology of Wood.* Springer-Verlag, London, UK.

Hiscox, J., Baldrian, P., Rogers, H.J. & Boddy, L. (2010a) Changes in oxidative enzyme activity during interspecific mycelial interactions involving the white-rot fungus *Trametes versicolor*. *Fungal Genetics and Biology*, 47(6), 562-571.

Hiscox, J. & Boddy, L. (2017) Armed and dangerous – Chemical warfare in wood decay communities. *Fungal Biology Reviews*, 31, 169-184.

Hiscox, J., Clarkson, G., Savoury, M., Powell, G., Savva, I., Lloyd, M., Shipcott, J., Choimes, A., Cumbriu, X.A. & Boddy, L. (2016a) Effects of pre-colonisation and temperature on interspecific fungal interactions in wood. *Fungal Ecology*, 21, 32-42.

Hiscox, J., Hibbert, C., Rogers, H.J. & Boddy, L. (2010b) Monokaryons and dikaryons of *Trametes versicolor*have similar combative, enzyme and decay ability. *Fungal Ecology*, 3(4), 347-356.

Hiscox, J., Savoury, M., Johnstone, S.R., Parfitt, D., Müller, C.T., Rodgers, H. & Boddy, L. (2016b) Location, location, location: priority effects in wood decay communities may vary between sites. *Environmental Microbiology*, 18, 1954-1969.

Hiscox, J., Savoury, M., Müller, C.T., Lindahl, B.D., Rogers, H.J. & Boddy, L. (2015b) Priority effects during fungal community establishment in beech wood. *The ISME Journal*, 9, 2246-2260.

Hiscox, J., Savoury, M., Toledo, S., Kingscott-Edmunds, J., Bettridge, A., Al Waili, N. & Boddy, L. (2017) Threesomes destabilise certain relationships: multispecies interactions between wood decay fungi in natural resources. *FEMS Microbiology Ecology,* 93, fix014, doi: 10.1093/femsec/fix014.

Hiscox, J., Savoury, M., Vaughan, I.P., Müller, C.T. & Boddy, L. (2015a) Antagonistic fungal interactions influence carbon dioxide evolution from decomposing wood. *Fungal Ecology*, 14, 24-32.

Hobbie, S.E. (1992) Effects of plant species on nutrient cycling. *Trends in Ecology and Evolution*, 7(10), 336-339.

Ho, C.L., Liao, P.C., Hsu, K.P., Wang, E.I., Dong, W.C. & Su, Y.C. (2010) Composition and antimicrobial and anti-wood-decay fungal activities of the leaf essential oils of *Machilus pseudolongifolia* from Taiwan. *Natural Products Communications*, 5(7), 1143-1146.

Ho, C.L., Liao, P.C., Wang, E.I. & Su, Y.C. (2011) Composition and antimicrobial activity of the leaf and twig oils of *Litsea acutivena* from Taiwan. *Natural Products Communications*, 6(11), 1755-1758.

Holighaus, G., Weißbecker, B., von Fragstein, M. & Schütz, S. (2014) Ubiquitous eight-carbon volatiles of fungi are infochemicals for a specialist fungivore. *Chemoecology*, 24(2), 57-66.

Holmer, L. & Stenlid, J. (1993) The importance of inoculum size for the competitive ability of wood decomposing fungi. *FEMS Microbiology Ecology*, 12, 169-179.

Holmes, E.E., Lewis, M.A., Banks, J.E. & Veit, R.R. (1994) Partial differential equations in ecology: Spatial interactions and population dynamics. *Ecology*, 75, 17-29.

Hori, C., Gaskell, J., Igarashi, K., Samejima, M., Hibbett, D., Henrissat, B. & Cullen, D. (2013) Genome wide analysis of polysaccharides degrading enzymes in 11 white- and brown-rot Polyporales provides insight into mechanisms of wood decay. *Mycologia*, 105(6), 1412-1427.

Horn S.J., Sikorski, P., Cederkvist, J.B., Vaaje-Kolstad, G., Sørlie, M., Synstad, B., Vriend, G., Vårum, K.M. & Eijsink, V.G.H. (2006) Costs and benefits of processivity in enzymatic degradation of recalcitrant polysaccharides. *PNAS*, 103(48), 18089-18094.

Horn, S.J., Vaaje-Kolstad, G., Westereng, B. & Eijsink, V.G.H. (2012) Novel enzymes for the degredation of cellulose. *Biotechnology for Biofuels*, 5, doi: 10.1186/1754-6834-5-45.

Huffaker, C.B. (1958) Experimental studies on predation: Dispersion factors and predator-prey oscillations. *Hilgardia*, 27(14), 343-383.

Humphrey, J.W., Sippola, A.L., Lemperiere, G., Dodelin, B., Alexander, K.N.A. & Butler, J.E. (2004). Deadwood as an indicator of biodiversity in European forests: from theory to operational guidance. *EFI-Proceedings*, 51, 193-206.

Humphris, S.N., Bruce, A., Buultjens, E. &Wheatley, R.E. (2001) The effects of volatile microbial seconday metabolites on protein synthesis in *Serpula lacrymans*. *FEMS Microbiology Letters*, 210, 215-219.

Hung, R., Lee, S. & Bennett, J.W. (2015) Fungal volatile organic compounds and their role in ecosystems. *Applied Microbiology and Technology*, 99, 3395–3405.

Hu, Q., Noll, R.J., Li, H., Makarov, A., Hardman, M. & Cooks, R.G. (2005) The Orbitrap: a new mass spectrometer. *Mass Spectrometry*, 40(4), 430-443.

Hynes, J., Müller, C.T., Jones, T.H. & Boddy, L. (2007) Changes in volatile production during the course of fungal mycelial interactions between *Hypholoma fasciculare*and *Resinicium bicolor*. *Journal of Chemical Ecology*, 33(1), 43-57.

Ichinose, H. (2013) Cytochrome P450 of wood-rotting basidiomycetes and biotechnological applications. *Biotechnology and Applied Biochemistry*, 60(1), 71-81.

Ikediugwu, F.E.O. (1976) The interface in hyphal interference by *Peniophora gigantea* against *Heterobasidion annosum. Transactions of the British Mycological Society,* 66, 291–296.

Ikediugwu, F.E.O., Dennis, C. & Webster, J. (1970) Hyphal interference by *Peniophora gigantea* against *Heterobasidion annosum. Transactions of the British Mycological Society,* 54, 307–309.

IPCC. (2007) *Climate Change 2007: The Physical Science Basis. Contribution of Working Group I to the Fourth Assessment Report of the Intergovernmental Panel on Climate Change*, (eds. S. Solomon, D. Qin, M. Manning, Z. Chen, M. Marquis, K.B. Averyt, M. Tignor & H.L. Miller). Cambridge University Press, UK. pp. 847-996.

IPCC. (2013) *Climate Change 2007: The Physical Science Basis. Contribution of Working Group I to the Fourth Assessment Report of the Intergovernmental Panel on Climate Change*, (eds. T.F. Stocker, D. Qin, G.K. Plattner, M. Tignor, S.K. Allen, J. Boschung, A. Nausels, Y. Xia, V. Bex & P.M. Midgley). Camdrige University Press, UK. pp. 1029-1136.

Isaka, M., Sappan, M., Supothina, S., Srichomthong, K., Komwijit, S. & Boonpratuang, T. (2017) Allicana sesquiterpenoids from submerged cultures of the basidiomycete Inonotus sp. BCC 22670. *Phytochemistry*, 136, 174-181.

Isidorov, V., Tyszkiewicz, Z. & Piroznikow, E. (2016) Fungal succession in relation to volatile organic compounds emissions from Scots pine and Norway spruce leaf litter-decomposing fungi. *Atmospheric Environment*, 131, 301-306.

Itoh, Y., Kodama, K., Furuya, K., Takahashi, S., Haneishi, T., Takiguchi, Y. & Arai, M. (1980) A new sesquiterpene antibiotic, heptelidic acid producing organisms, fermentation, isolation and characterisation. *Journal of Antibiotics*, 33(5), 468-473.

Janusz, G., Pawlik, A., Sulej, J., Świderska-Burek, U., Jarosz-Wilkolazka, A. & Paszczyński, A. (2017) Lignin degredation: microorganisms, enzymes involved, genomes analysis and evolution. *FEMS Microbiology Reviews*, 41(6), 941-962.

Jeleń, H.H. (2002) Volatile sesquiterpene hydrocarbons characteristic for *Penicillium roqueforti* strains producing PR toxin. *Journal of Agricultural Food and Chemistry*, 50(22), 6569-6574.

Johnston, S.R. (2017a) Bacterial qPCR primers co-amplify fungi. In: *Fungus-bacteria interactions in decomposing wood: unravelling community effects*, Cardiff University, UK.

Johnston, S.R. (2017b) The influence of migratory *Paraburkholderia* on growth and competiton of wood-decay fungi. In: *Fungus-bacteria interactions in decomposing wood: unravelling community effects*, Cardiff University, UK.

Johnston, S.R., Boddy, L. & Weightman, A.J. (2016) Bacteria in decomposing wood and their interactions with wood-decay fungi. *FEMS Microbiology Ecology*, 92(11), fiw179, doi: 10.1093/femsec/fiw179.

Jones, O.A.H., Maguire, M.H., Griffin, J.L., Dias, D.A., Spurgeon, D.J. & Svendsen, C. (2013) Metabolomics and its use in ecology. *Austral Ecology*, 38(6), 713-720.

Kaiserer, L., Oberparleiter, C., Weiler-Gorz, R., Burgstaller, W., Leiter, E. & Marx, F. (2003) Characterization of the *Penicillium chrysogenum* antifungal protein PAF. *Archives Microbiology*, 180(3), 204-210.

Zamocky, M., Furtmüller, P.G. & Obinger, C. (2009) Two distinct groups of fungal catalase/peroxidases. *Biochemisry Society Transactions*, 37, 772-7.

Zamocky, M., Gasselhuber, B., Furtmüller, P.G. & Obinger, C. (2014) Turning points in the evolution of peroxidase-catalase superfamily: molecular phyolgeny of hybrid heme peroxidases. *Cell Molecular Life Sciences*, 71, 468-469.

Kareiva, P. (1987) Habitat fragmentation and the stability of predator-prey interactions. *Nature*, 326, 388-390.

Kauserud, H., Saetre, G.P., Schmidt, O., Decock, C. & Schumacher, T. (2006) Genetic of self/nonself recognition in *Serpula lacrymans*. *Fungal Genetics and Biology*, 43, 503-510.

Keenan, R.J., Reams, G.A., Achard, F., de Freitas, V., Grainger, A. & Lindquist, E. (2015) Dynamics of global forest area: Results from the FAO Global Forest Resources Assessment 2015. *Forest Ecology and Management*, 352, 9-20.

Keller, N.P., Turner, G. & Bennett, J.W. (2005) Fungal secondary metabolism – from biochemistry to genomics. *Nature Reviews Microbiology*, 3, 937-947.

Kerr, B., Riley, M.A., Feldman, M.W. & Bohannan, B.J.M. (2002) Local dispersal promotes biodiversity in a real-life game of rock-paper-scissors. *Nature*, 418, 171-174.

Kind, T. & Fiehn, O. (2006) Metabolomic database annotations via query of elemental compositions: Mass accuracy is insufficient even at less than 1 ppm. *Bioinformatics*, 7, 234.

Kirk, T.K. & Farrell, R.L. (1987) Enzymatic "combustion": The microbial degredation of lignin. *Annual Review of Microbiology*, 41, 465-505.

Kirwan, J.A., Weber, R.J.M., Broadhurst, D.I. & Viant, M.R. (2014) Direct infusion mass spectrometry metabolomics dataset: a benchmark for data processing and quality control. *Scientific Data*, 1, 140012.

Kishimoto, K., Maysui, K., Ozawa, R. & Takabayashi, J. (2007) Volatile 1-octen-3-ol induces a defensive response in *Arabidopsis thaliana*. *Journal of General Plant Pathology*, 73(1), 35-37.

Klein, L.L., Li, L., Chen, H.-J., Curty, C.B., DeGoey, D.A., Grampovnik, D.J., Leone, C.L., Thomas, S.A., Yeung, C.M., Funk, K.W., Kishore, V., Lundell, E.O., Wodka, D., Meulbroek, J.A., Alder, J.D., Nilius, A.M., Lartey, P.A. & Plattner, J.J. (2000) Total synthesis and antifungal evaluation of cyclic aminohexapeptides. *Bioorganic & Medicinal Chemistry*, 8(7), 1677-1696.

Konayli, S., Ocak, M., Aliyazicioglu, R. & Karaoglu, S. (2009) Chemical analysis and biological activities of essential oils from trunk-barks of eight trees. *Asian Journal of Chemistry*, 21(4) 2684-2694.

Kong, C., Xu, X., Zhou, B., Hu, F., Zhang, C. & Zhang, M. (2004) Two compounds from allelopathic rice accession and their inhibitory activity on weeds and fungal pathogens. *Phytochemistry*, 65(8), 1123-1128.

Konuma, R., Umezawa, K., Mizukoshi, A., Kawarada, K. & Yoshida, M. (2015) Analysis of microbial volatile organic compounds produced by wood-decay fungi. *Biotechnology Letters*, 37(9), 1845-1852.

Korpi, A., Jarnberg, J. & Pasanen, A.L. (2009) Microbial volatile organic compounds. *Critical Reviews in Toxicology*, 39(2), 139-193.

Kotrba, P., Inui, M. & Yukawa, H. (2001) Bacterial phosphotransferase system (PTS) in carbohydrate uptake and control of carbon metabolism. *Journal of Bioscience and Bioengineering*, 92(6), 502-517.

Kraigher, H., Jurc, D., Kalan, P., Kutnar, L., Levanic, T., Rupel, M. & Smolej, I. (2002) Beech coarse woody debris characteristics in two virgin forest reserves in southern Slovenia. *Forestry Wood Science Technology*, 69, 91–134.

Kramer, R. & Abraham, W.-R. (2012) Volatile sesquiterpenes from fungi: what are they good for? *Phytochemistry Reviews*, 11, 15-37.

Kubicek, C.P. (1990) *Fungi and Lignocellulosic biomass*. Wiley-Blackwell, New-Jersey, USA.

Kudalkar, P., Strobel, G., Riyaz-Ul-Hassan, S., Geary, B. & Sears, J. (2012) *Muscodor sutura*, a novel endophytic fungus with volatile antibiotic activities. *Mycoscience*, 53(4), 319-325.

Kukula-Koch, W.A. & Widelski, J. (2017) Alkaloids. In: *Pharmacognosy: Fundamental, Applications and Strategies* (eds. S.B. McCreath & R. Delgoda). Academic Press, Elsevier, The Netherlands. pp 163-198.

Laird, R.A. & Schamp, B.S. (2006) Competitive intransitivity promotes species coexistence. *The American Naturalist*, 168, 182-193.

Lal, R. & Lorenz, K. (2012) Carbon Sequestration in Temperate Forests. In: *Recarbonization of the Biosphere*, (eds. R. Lal, K. Lorenz, R. Huttl, B. Schneider & J. von Braun). Springer, Dordrecht, The Netherlands. pp 187-201.

Laurance, W.F., Camargo, J.L.C., Luizão, R.C.C., Laurance, S.G., Pimm, S.L., Bruna, E.M., Stouffer, P.C., Williamson, G.B., Benitez-Malvido,J., Vasconcelos, H.L., Van Houtan, K.S., Zartman,C.E., Boyle, S.A., Didham, R.K., Andrade, A. & Lovejoy, T.E. (2011) The fate of Amazonian forest fragments: A 32-year investigation. *Biological Conservation*, 144, 56-67.

Leather, S.E., Baumgart, E.A., Evans, H.F. & Quicke, D.J. (2014) Seeing the trees for the wood – beech (*Fagus sylvatica*) decay fungal volatiles influence the structure of saproxylic beetle communities. *Insect Conservation and Diversity*, 7, 314-326.

Lee, S.-E., Park, B.-S., Kim, M.-K., Choi, W.-S., Kim, H.-T., Cho, K.-Y., Lee, A.-G. & Lee, H.-S. (2001) Fungicidal activity of pipernonaline, a piperidine alkaloid derived from long pepper, *Piper longum* L., against phytopathogenic fungi. *Crop Protection*, 20(6), 523-528.

Lee, S., Yap, M., Behringer, G., Hung, R. & Bennett, J. (2016) Volatile organic compounds emitted by *Trichoderma* species mediate plant growth. *Fungal Biology and Biotechnology*, 3(7), doi: 10.1186/s40694-016-0025-7.

Lemfack, M.C., Nickel, J., Dunkel, M., Preissner, R. & Piechulla, B. (2014) mVOC: a database of microbial volatiles. *Nucleic Acids Research*, 42(1), 744-788.

Lindahl, B.D. & Finlay, R.D. (2006) Activities of chitinolytic enzymes during primary and secondary colonisation of wood by basidiomycetes. *New Phytologist*, 169, 389-397.

Lindahl, B.D. & Olsson, S. (2004) Fungal translocation—creating and responding to environmental heterogeneity. *Mycologist*, 18, 79-88.

Liouane, K., Saidana, D., Edziri, H., Ammar, S., Chriaa, J., Mahjoub, M.A., Said, K. & Mighri, Z. (2010) Chemical composition and antimicrobial activity of extracts from *Gliocladium* sp. growing wild in Tunisia. *Medicinal Chemistry Research*, 19(8), 743-756.

Lippolis, V., Pascale, M., Cervellieri, S., Damascelli, A. & Visconti, A. (2014) Screening of deoxynivalenol contamination in durum wheat by MOS-based electronic nose and identification of the relevant pattern of volatile compounds. *Food Control*, 37, 263-271.

Ljunggren, J. (2015) *Biochemical Interactions of Some Saproxylic Fungi*. Mid Sweden Univiersity, Sweden.

López-Mondéjar, R., Ros, M. & Pascual, J.A. (2011) Mycoparasitism-related gene expression of *Trichoderma harzianum* isolates to evaluate their efficacy as biological control agents. *Biological Control*, 56(1), 59-66.

Lorito, M., Woo, S.L., Harman, G.E. & Monte, E. (2010) Translational research on *Trichoderma*: from 'omics to the field. *Annual Review of Phytopathology*, 48, 395–417.

Lovejoy, T.E., Bierregaard, R.O., Rylands, A.B., Malcolm, J.R., Quintela, C.E., Harper, L.H., Brown, K.S., Powell, A.H., Powell,G.V.N., Schubart, H.O.R. & Hays, M.B. (1986) Edge and other effects of isolation on Amazon forest fragments. In: *Conservation Biology: The Science of Scarcity and Diversity*, (eds M.E. Soulé). Sinauer, Massachusetts, USA. pp. 257-285.

Lowe, R.G., Lord, M., Rybak, K., Trengove, R.D., Oliver, R.P. & Solomon, P.S. (2009) Trehalose biosynthesis is involved in sporulation of *Stagonospora nodorum*. *Fungal Genetics Biology*, 46(5), 381-389.

Luckinbill, L.S. (1973) Coexistence in laboratory populations of *Paramecium aurelia* and its predator *Didinium nasutum*. *Ecology*, 54, 1320-1327.

Lundell, T.K., Mäkelä, M.R. & Hildén, K. (2010) Lignin-modifying enzymes in filamentous basidiomycetes – ecological, functional and phylogenetic review. *Journal of Basic Microbiology*, 50, 5-20.

Luo, F., Zhong, Z., Liu, L., Igarashi, Y., Xie, D. & Li, N. (2017) Metabolomic differential analysis of interspecific interactions among white rot fungi *Trametes versicolor*, *Dichomitus squalens* and *Pleurotus ostreatus*. *Scientific Reports*, 7, 5265, doi: 10.1038/s41598-017-05669-3.

Lynd, L.R., Weimer, P.J., van Zyl, W.H. & Pretorius, I.S. (2002) Microbial cellulose utilisation: fundamentals and biotechnology, *Microbiology and Molecular Biology Reviews*, 66(3), 506-577.

Mackie, A. & Wheatley, R.E. (1998) Effects and incidence of volatile organic compound interactions between soil bacterial and fungal isolates. *Soil Biology & Biochemistry*, 31, 375-385.

Maciel, M.J.M., Castro e Silva, A. & Ribeiro, H.C.T. (2010) Industrial biotechnological applications of ligninolytic enzymes of the basidiomycota: A review. *Electronic Journal of Biotechnology*, 13(6), doi: 10.2225/vol13-issue6-fulltext-2.

Mansour, A.B., Chtourou, F., Khbou, W., Flamini, G. & Bouaziz, M. (2017) Phenolic and volatile compounds of Neb Jmel olive oil cultivar according to their geographical origin using chemometrics. *European Food Research and Technology*, 243(3), 403-418.

Martínez, A.T., Speranza, M., Ruiz-Duenas, F.J., Ferreira, P., Guillén, F., Martínez, M.J., Gutiérrez, A. & del Rio, C.J. (2005) Biodegradation of lignocellulosics: microbial, chemical, and enzymatic aspects of the fungal attack of lignin. *International Microbiology*, 8, 195-204.

Martinez, D., Challacombe, J., Morgenstern, I., Hibbett, D., Schmoll, M., Kubicek, C.P., Ferreira, P., Ruiz-Duenas, F.J., Martinez, A.T., Kersten, P., Hammel, K.E., Vanden Wymelenberg, A., Gaskell, J., Lindquist, E., Sabat, G., Bondurant, S.S., Larrondo, L.F., Canessa, P., Vicuna, R., Yadav, J., Doddapaneni, H., Subramanian, V., Pisabarro, A.G., Lavín, J.L., Oguiza, J.A., Master, E., Henrissat, B., Coutinho, P.M., Harris, P., Magnuson, J.K., Baker, S.E., Bruno, K., Kenealy, W., Hoegger, P.J., Kües, U., Ramaiya, P., Lucas, S., Salamov, A., Shapiro, H., Tu, H., Chee, C.L., Misra, M., Xie, G., Teter, S., Yaver, D., James, T., Mokrejs, M., Pospisek, M., Grigoriev, I.V., Brettin, T., Rokhsar, D., Berka, R. & Cullen, D. (2009) Genome, transcriptome, and secretome analysius of wood decay fyngus *Postia placenta* supports unique mechanisms of lignocellulose conversion. *Proceedings of the National Academy of Sciences*, 10, 1954-1959.

Martin, P.H., Nabuurs, G-J., Aubinet, M., Karjalainen, T., Vine, E.L., Kinsman, J. & Heath, L.S. (2001) Carbon sinks in temperate forests. *Annual Review of Energy and the Environment*, 26, 435-465.

Makarov, A. (2000) Electrostatic axially harmonic Orbital trapping: A high-performance technique of mass analysis. *Analytical Chemistry*, 72(6), 1156-1162.

Makarov, A., Denisov, E., Lange, O. & Horning, S. (2006) Dynamic range of mass accuracy in LTQ Orbitrap hybrid mass spectrometer. *Journal of the American Society for Mass Spectrometry*, 17(7), 977-982.

Makarov, A. & Scigelova, M. (2010) Coupling liquid chromatography to Orbitrap mass spectrometry. *Journal of Chromatography A*, 1217(25), 3938-3945.

Martíinez, A.T., Speranza, M., Ruiz-Duenas, F.J., Ferreira, P., Camarero, S., Guillen, F., Martíinez, M.J., Gutierrez, A. & Del Rıo, J.C. (2005) Biodegradation of lignocellulosics: microbial, chemical, and enzymatic aspects of the fungal attack of lignin. *International Microbiology*, 8,195–204.

Martinez, D., Challacombe, J., Morgenstern, I., Hibbett, D., Schmoll, M., Kubicek, C.P., Ferreira, P., Ruiz-Duenas, F.J., Martinez, A.T., Kersten, P., Hammel, K.E., Vanden Wymelenberg, A., Gaskell, J., Lindquist, E., Sabat, G., Bondurant, S.S., Larrondo, L.F., Canessa, P., Vicuna, R., Yadav, J., Doddapaneni, H., Subramanian, V., Pisabarro, A.G., Lavín, J.L., Oguiza, J.A., Master, E., Henrissat, B., Coutinho, P.M., Harris, P., Magnuson, J.K., Baker, S.E., Bruno, K., Kenealy, W., Hoegger, P.J., Kües, U., Ramaiya, P., Lucas, S., Salamov, A., Shapiro, H., Tu, H., Chee, C.L., Misra, M., Xie, G., Teter, S., Yaver, D., James, T., Mokrejs, M., Pospisek, M., Grigoriev, I.V., Brettin, T., Rokhsar, D., Berka, R. & Cullen, D. (2009) Genome, transcriptome, and secretome analysius of wood decay fyngus *Postia placenta* supports unique mechanisms of lignocellulose conversion. *Proceedings of the National Academy of Sciences*, 10, 1954-1959.

Maynard, D.S., Bradford, M.A., Linder, D.L., van Diepen, L.T.A., Frey, S.D., Glaeser, J.A. & Crowther, T.W. (2017a) Diversity begets diversity in competition for space. *Nature Ecology & Evolution*, 1, 0156, doi: 10.1038/s41559-017-0156.

Maynard, D.S., Crowther, T.W. & Bradford, M.A. (2017b) Competitive networkdetermines the direction of the diversity-function relationship. *PNAS*, 114(43), doi: 10.1073/pnas.1712211114.

McQuilken, M.P., Gemmel, J., Hill, R.A. & Whipps, J.M. (2003) Production of macrosphelide A by the mycoparasite *Coniothyrium minitans*. *FEMS Microbiological Letters*, 219, 27-31.

Merganičová, K., Merganič, J., Svoboda, M., Bače, R. & Šebeň, V. (2012) Deadwood in Forest Ecosystems. In: *Forest Ecosystems – More than Just Trees*, (eds. J.A. Blanco & Y.H. Lo). InTech Book. pp. 81-108.

Micheluz, A., Manente, S., Rovea, M., Slanzi, D., Varese, G.C., Ravagnan, G. & Formenton, G. (2016) Detection of volatile metabolites of moulds isolated from a contaminated library. *Journal of Microbiological Methods*, 128, 34-41.

Minerdi, D., Bossi, S., Gullino, M.L. & Garibaldi, A. (2008) Volatile organic compounds: a potential direct long-distance mechanism for antagonistic action of *Fusarium oxysporum* strain MSA 35. *Environmental Microbiology*, 11(4), 844-854.

Modiya, P.R. & Patel, C.N. (2012) Synthesis and screening of antibacterial and antifungal activity of 5-chloro-1,3-benzoxazol-2(3 h)-one derivatives. *Organic and Medicinal Chemistry Letters*, 2, 29, doi: 10.1186/2191-2858-2-29.

Mora-Gomez, J., Elosegi, A., Duarte, S., Cassio, F., Pascoal, C. & Romani, A.M. (2016) Differences in the sensitivity of fungi and bacteria to season and invertebrates affect leaf litter decomposition in a Mediterranean stream. *FEMS Microbiology Ecology*, 92(8), fiw121.

Morath, S.U., Hung, R. & Bennett, J.W. (2012) Fungal volatile organic compounds: A review with emphasis on their biotechnological potential. *Fungal Biology Reviews*, 26, 73-83.

Mun, A.P. & Prewitt, L. (2011) Antifungal activity of organic extracts from *Juniperus virginiana* heartwood against wood decay fungi. *Forest Products Journal*, 61(6), 443-449.

Narukawa, Y. & Yamamoto, S. (2002) Effects of dwarf bamboo (Sasa sp.) and forest floor microsites on conifer seedling recruitment in a subalpine forest, Japan. *Forest Ecology and Management*, 163, 61-70.

Nazir, R., Tazetdinova,D.I. & van Elsas, J.D. (2014) *Burkholderia terrae* BS001 migrates proficiently with diverse fungal hosts through soil and provides protection from antifungal agents. *Frontiers in Microbiology*, 11(5), 598, doi: 10.3389/fmicb.2014.00598.

Nevell, T.P. & Zeronian, S.H. (1985) *Cellulose Chemistry and Its Applications.* Ellis Horwood, Chichester, UK.

Ngo, T.T. & Lenhoff, H.M. (1980) A sensitive and versatile chromogenic assay for peroxidase and peroxidase-coupled reactions. *Analytical Biochemistry*, 105, 389–397.

Nguyen, L.N., Hai, F.I., Yang, S., Kang, J., Leusch, F.D.L., Roddick, F., Price, W.E. & Nghiem, L.D. (2013) Removal of trace organic contaminants by an MBR comprising a mixed culture of bacteria and white-rot fungi. *Bioresource Technology*, 148, 234-241.

Nielsen, U.N., Ayres, E., Wall, D.H. & Bardgett, R.D. (2011) Soil biodiversity and carbon cycling: a review and synthesis of studies examining diversity-function relationships. *European Journal of Soil Science* 62, 105-116.

Ochsenreiter, T., Selezi, D., Quaiser, A., Bonch-Osmolovskaya, L. & Schleper, C. (2003) Diversity and abundance of *Crenarchaeota* in terrestrial habitats studies by 16S RNA surveys and real time PCR. *Environmental Microbiology*, 5(9), 787-797.

Özer, N. & Arin, L. (2014) Evaluation of fungal antagonists to control black mold disease under field conditions and to induce the accumulation of antifungal compounds in onion following seed and set treatment. *Crop Protection*, 65, 21-28.

Pagans, E., Font, X. & Sánchez, A. (2006) Emission of volatile organic compounds from composting of different solid wastes: abatement by biofiltration. *Journal of Hazard Materials*, 131, 179-186.

Pan, Z., Jin, S., Zhang, X., Zheng, S., Han, S. Pan, L. & Lin, Y. (2016) Biocatalytic behavior of a new *Aspergillus niger* whole-cell biocatalyst with high operational stability during the synthesis of green biosolvent isopropyl esters. *Journal of Molecular Catalysis B: Enzymatic*, 131, 10-17.

Passardi, F., Bakalovic, N., Teixeira, F.K., Margis-Pinheiro, M., Penel, C. & Dunand, C. (2007) Prokaryotic origins of the non-animal peroxidase superfamily and organelle-mediated transmission to eukaryotes. *Genomics*, 89, 567–579.

Paszczynski, A., Huynh, V.-B. & Crawford, R. (1985) Enzymatic activities of an extracellular, manganese-dependent peroxidase from *Phanerochaete chrysosporium. FEMS Microbiology Letters*, 29, 37–41.

Patil, R.S., Ghormande, V. & Deshpande, M.V. (2000) Chitinolytic enzymes: an exploration. *Enzyme and Microbial Technology*, 26, 473-483.

Peiris, D., Dunn, W.B., Brown, M., Kell, D.B., Roy, I. & Hedger, J.N. (2008) Metabolite profiles of interacting mycelial fronts differ for pairings of the wood decay basidiomycete fungus, *Stereum hirsutum* with its competitors *Coprinus micaceus* and *Coprinus disseminatus*. *Metabolomics*, 4, 52-62.

Peironcely, J.E., Rojas-Cherto, M., Tas, A., Vreeken, R., Reijmers, T., Coulier, L. & Hankemeier, T. (2013) Automated pipeline for *de novo* metabolite identification using mass-spectrometry-based metabolomics. *Analytical Chemistry*, 85, 3575-3583.

Pérez-Boada, M., Ruiz-Dueñas, F.J., Pogni, R., Basosi, R., Choinowski, T., Martínez, M.J., Piontek, K. & Martínez, A.T. (2005) Versatile peroxidase oxidation of high redox potential aromatic compounds: site-directed mutagenesis, spectroscopic and crystallographic investigation of three long-range electron transfer pathways. *Journal of Molecular Biology*, 354(2), 385-402.

Pernak, J., Zabielska-Matejuk, J., Kropacz, A. & Foksowicz-Flaczyk, J. (2004) Ionic liquids in wood preservation. *Holzforschung*, 58(3), doi: 10.1515/HF.2004.044.

Peršoh, D (2015). Plant-associated fungal communities in the light of meta'omics. *Fungal Diversity*, 75, 1-25.

Pfannkoch, E. & Whitecavage, J. (2000) Comparison of the sensitivity of static headspace GC, solid phase microextraction, and direct thermal extraction for analysis of volatiles in solid matrices. In: *AppNote 6/2000*. Gerstel GmbH & Co. KG, Mulheim an der Ruhr, Germany.

Polizzi, V., Adams, A., Malysheva, S.V., De Saeger, S., Van Peteghem, C., Moretti, A., Picco, A.M. & De Kimpe, N. (2012) Identification of volatile markers for indoor fungal growth and chemotaxonomic classification of Aspergillus species. *Fungal Biology*, 116(9), 941-953.

Pollegioni, L., Tonin, F. & Rosini, E. (2015) Lignin-degrading enzymes. *The FEBS Journal*, 282, 1190-1213.

Popova, M., Trusheva, B., Gyosheva, M., Tsvetkova, I. & Bankova, V. (2009) Antibacterial triterpenes from the threatened wood-decay fungus *Fomitopsis rosea*. *Fitoterapia*, 80(5), 263-266.

Post, W.M., Emanuel, W.R., Zinke, P.J. & Stangenberger, A.G. (1982) Soil carbon pool and world life zones. *Nature*, 298, 156-159.

Qadri, M., Nalli, Y., Jain, S.K., Chaubey, A., Ali, A., Strobel, G.A., Vishwakarma, R.A. & Riyaz-Ul-Hassan, S. (2017) An insight into the secondary metabolism of *Muscodor yucatanesis*: Small-molecue epigenetic modifiers induce expression of secondary metabolism-related genes and production of mew metabolites in the endophyte. *Microbial Ecology*, 73(4), 954-965.

Rapior, S., Konska, G., Guillot, J., Andary, C. & Bessiere, J.M. (2000) Volatile composition of *Laetiporus sulphurous*. *Cryptogamie Mycologie*, 21, 67-72.

Rayner, A.D.M. (1991) The challenge of the individualistic mycelium. *Mycologica*, 83, 48-71.

Rayner, A.D.M. & Boddy, L. (1988) *Fungal Decomposition of Wood: Its Biology and Ecology*. John Wiley and Sons, Chichester, UK.

Rayner, A.D.M., Boddy, L. & Dowson, C.G. (1987) Temporary parasitism of *Coriolus* spp. by *Lenzites betulina* a strategy for domain capture in wood decay fungi. *FEMS Microbiology Ecology*, 45, 53–58.

Rayner, A.D.M., Griffith, G.S. & Ainsworth, A.M. (1995) Mycelial interconnectedness. In: *The Growing Fungus*. Chapman and Hall, London, Uk. pp. 20-40.

Raza, W., Yang, X., Wu, H., Wang, Y., Xu, Y. & Shen, Q. (2009) Isolation and characterisation of fusaricidin-type compound-producing strain of *Paenibacillus polymyxa*SQR-21 active

against *Fusarium oxysporum* f.sp. *nevium*. *European Journal of Plant Pathology*, 125(3), 471-483.

R Core Team. (2014) R: a Language and Environment for Statistical Computing. *R Foundation for Statistical Computing*. Vienna, Austria. http://www.R-project.org/.

Read, D.J. & Perez-Moreno, J. (2003) Mycorrhizas and nutrient cycling in ecosystems: a journey towards relevance? *New Phytologist*, 157, 475–492.

Redfern, D.B., Pratt, J.E., Gregory, S.C. & Macaskill, G.A. (2001) Natural infection of Sitka spruce thinning stumps in Britain by spores of *Heterobasidion annosum* and long-term survival of the fungus. *Forestry,* 74, 53-71.

Reichenbach, T., Mobilia, M. & Frey, E. (2007) Mobility promotes and jeopardizes biodiversity in rock-paper-scissors games. *Nature*, 448, 1046-1049.

Reyes, F., Villanueva, P., Alfonso, C. (1990) Comparative study of acid alkaline phosphatase during the autolysis of filamentous fungi. *Letters in Applied Microbiology*, 10, 175-177.

Riley, R., Salamova, A., Brown. D,. Nagy, L., Floudas, D., Held, B., Levasseur, A., Lombard, V., Morin, E., Otillar, R., Lindquist, E., Sun, H., LaButti, K., Schmutz, J., Jabbour, D., Luo, H., Baker, S., Pisabarro, A., Walton, J., Blanchette, R., Henrissat, B., Martin, F., Cullen, D., Hibbett, D. & Grigoriev, I. (2014) Extensive sampling of basidiomycete genomes demonstrates inadequacy of the white-rot/brown-rot paradigm for wood decay fungi. *PNAS*, 111(27), 9923-9928.

Rineau, F., Shah, F., Smits, M.M. Persson, P., Johansson, T., Carleer, R., Troein, C. & Tunlid, A. (2013) Carbon availability triggers the decomposition of plant litter and assimilation of nitrogen by an ectomycorrhizal fungus. *The ISME Journal*, 7, 2010-2022.

Rivas da Silva, A.C., Lopes, P.M., Barros de Azevedo, M.M., Costa, D.C.M., Alviano, C.S. & Alviano, D.S. (2012) Biolgical activities of a-pinene and β-pinene enantiomers. *Molecules*, 17, 6305-6316.

Roberts, L.D., Souza, A.L., Gerszten, R.E. & Clish, C.B. (2013) Targeted metabolomics. *Current Protocols in Molecular Biology*, 30, 1-24.

Rodakiewicz-Nowak, J., Jarosz-Wilkolazka, A. & Luterek, J. (2006) Catalytic activity of versatile peroxidase from *Bjerkandera fumosa* in aqueous solutions of water-miscible organic solvents. *Applied Catalysis A: General*, 308, 56-61.

Rosecke, J., Pietsch, M. & Konig, W.A. (2000) Volatile constitutents of wood-rotting basidiomycetes. *Phytochemistry*, 54, 747-750.

Rouches, E., Dignac, M.F., Zhou, S. & Carrere, H. (2017) Pyrolysis-GC-MS to assess the fungal pretreatment efficiency for wheat straw anaerobic digestion. *Journal of Analytical and Applied Pyrolysis*, 123, 409-418.

Ruiz-Dueñas, F.J., Camarero, S., Pérez-Boada, M, Martínez, M.J. & Martínez, A.T. (2001) A new versatile peroxidase from *Pleurotus*. *Biochemical Society Transactions*, 29, 116-122.

Ruiz- Dueñas, F.J., Guillén, F., Camarero, S., Pérez-Boada, M., Martínez, M.J. & Martínez, A.T. (1999) Regulation of Peroxidase Transcript Levels in Liquid Cultures of the Ligninolytic Fungus *Pleurotus eryngii*. *Applied Environmental Microbiology*, 65(10), 4458-4463.

Ruiz-Dueñas, F.J. & Martínez, Á.T. (2009) Microbial degredation of lignin: how a bulky recalcitrant polymer is efficiently recycled in nature and how we can take advantage of this. *Microbial Biotechnology*, 2(2), 164-177.

Sánchez-Fernández, R.E., Diaz, D., Duarte, G., Lappe-Oliveras, P. Sanchez, S. & Macias-Rubalcava, M.L. (2016) Antifungal Volatile Organic Compounds from the Endophyte *Nodulisporium* sp. Strain GS4d2II1a: a Qualitative Change in the Intraspecific and Interspecific Interactions with *Pythium aphanidermatum*. *Microbial Ecology*, 71(2), 347-364.

Santhanam, N., Badri, D.V., Decker, S.R., Manter, D.K. Reardon, K.F. & Vivanco, J.M. (2012) Lignocellulose decomposition by microbial secretions. In: *Secretions and Exudates in Biological Systems*, (eds. M.J. Vivanco & F. Baluška). Springer, Heidelberg, Germany. pp 125-153.

Sanyal, A., Rautaray, D., Bansal, V., Ahmad, A. & Sastry, M. (2005) Heavy-metal remediation by a fungus as a means of production of lead and cadmium carbonate crystals. *American Chemical Society*, 21(16), 7220-7224.

Savel'eva, E.I., Gavrilova, O.P. & Gagkaeva, Y.Y. (2014) Study of the composition of volatile organic compounds emitted by the filamentous fungus *Fusarium culmorum*by gas chromatography-mass spectrometry combined with solid phase microextraction. *Russian Journal of General Chemistry*, 84(13), 2603-2610.

Schade, G.W. & Custer, T.G. (2004) OVOC emissions from agricultural soil in northern Germany during the 2003 European heat wave. *Atmospheric Environment*, 38(36), 6105-6114.

Schaeffer, T.L., Cantwell, S.G., Brown, J.L., Watt, D.S. & Fall, R.R. (1979) Microbial growth on hydrocarbons: Terminal branching inhibits biodegradation. *Applied and Environmental Microbiology*, 38(4), 742-746.

Schalchli, H., Hormazabal, E., Becerra, J., Birkett, M., Alvear, M. Vidal, J. & Quiroz, A. (2011) Antifungal activity of volatile metabolites emitted by mycelial cultures of saprophytic fungi. *Chemistry and Ecology*, 27(6), 503-513.

Schmidt-Dannert, C. (2015) Biosynethesis of terpenoid natural products in fungi. In: *Biotechnology of Isoprenoids*, (eds. J. Schrader & J. Bohlmann). Advances in Biochemical Engineering/Biotechnology, Springer. pp. 19-62.

Schoeman, M.W., Webber, J.F. & Dickinson, D.J. (1996) The effect of diffusible metabolites of *Trichoderma harzianum* on in vitro interactions between basidiomycete isolates at two different temperature regimes. *Mycological Research*, 100, 1454-1458.

Schwarze, F.W.M.R., Jauss, F., Spencer, C., Hallam, C. & Schubert, M. (2012) Evaluation of an antagonistic *Trichoderma* strain for reducing the rate of wood decomposition by the white rot fungus *Phellinus noxius*. *Biological Control*, 61(2), 160-168.

Sen, S., Dehingia, M., Talukdar, N.C. & Khan, M. (2017) Chemometric analysis reveals links in the formation of fragrant bio-molecules during agarwood (*Aquilaria malaccensis*) and fungal interactions. *Scientific Reports*, 7, doi:10.1038/srep44406.

Sharip, N.S., Ariffin, H., Hassan, M.A., Nishida, H. & Shirai, Y. (2016) Characterization and application of bioactive compounds in oil palm mesocarp fiber superheated steam condensate as an antifungal agent. *Royal Society of Chemistry*, 6, 84672-84683.

Siddoquee, S. (2014) Recent Advancements on the Role and Analysis of Volatile Compounds (VOCs) from *Trichoderma*. In: *Biotechnology and Biology of Trichoderma*, (eds. V.G. Gupta, M. Schmoll, A. Herrera-Estrella, R.S. Upadhyay, I. Druzhinina & M. Tuohy). Elsivier, Amsterdam, the Netherlands. pp 139-175.

Sigoillot, J.-C. Berrin, J.-G., Bey, M., Lessage-Meessen, L., Levasseur, A., Lomascolo, A., Record, E. & Uzan-Boukhris, E. (2012) Fungal strategies for lignin degradation. In: *Lignins: Biosynthesis, Biodegradation and Bioengineering*, (eds. L. Jouanin & C. Lapierre). Elsevier, London, UK. pp. 263-308.

Silar, P. (2005) Peroxide accumulation and celldeath in filamentous fungi induced by contact with a contestant. *Mycological Research*, 109, 137-149.

Singh, S.B., Lal, S.P., Pant, S. & Kulshrestha, G. (2008) Degradation of atrazine by an acclimatized soil fungal isolate. *Journal of Environmental Science and Health, Part B*, 43(1), 27-33.

Sinha, M., Sorensen, A., Ahamed, A. & Ahring, K. (2015) Production of hydrocarbons by *Aspergillus carbonarius* ITEM 5010. *Fungal Biology*, 119(4), 274-282.

Šnajdr, J., Dobiášová, P., Vetrovský, T., Valášková, V., Alawi, A., Boddy, L & Baldrian, P. (2011) Saprotrophic basidiomycete mycelia and their interspecific interactions affect the spatial distribution of extracellular enzymes in soil. *FEMS Microbiology Ecology*, 78(1), 80-90.

Soidrou, S.H., Farah, A., Satrani, B., Ghanmi, M., Jennan, S., Hassane, S.O.S., Lachkar, M., El Abed, S., Ibnsouda Koraichi, S. & Bousya, D. (2013) Fungicidal activity of four essential oils from *Piper capense*, *Piper borbonense* and *Vetiveria zizanoides* growing in Comoros against fungi decay wood. *Journal of Essential Oil Reasearch*, 25(3), doi: 10.1080/10412906.2013.767758.

Sonnenbichler, J., Jurgen, D. & Peipp, H. (1994) Secondary fungal metabolites and their biological activities, V. Investigations concerning the induction of the biosynthesis of toxic secondary metabolites in basidiomycetes. *Journal of Biological Chemistry*, 375, 71-79.

Spadafora, N., Paramithiotis, S., Drosinos, E., Cammarisano, L., Rogers, H. & Müller, C.T. (2016) Detection of Listeria monocytogenes in cut melon fruit using analysis of volatile organic compounds. *Food Microbiology*, 54, 52-59.

Splivallo, R., Novero, M., Bertea, C.M., Bossi, S. & Bonfante, P. (2007) Truffle volatiles inhibit growth and induce an oxidative burst in *Arabidopsis thaliana*. *New Phytologist*, 175(3), 417-424.

Spry, C., Kirk, K. & Saliba, K.J. (2008) Coenzyme A biosynthesis: an antimicrobial drug target. *FEMS Microbiology Reviews*. 32(1), 56-106.

Stein, S.E. (2011) https://www.nist.gov/sites/default/files/documents/srd/NIST1a11Ver2-0Man.pdf.

Strobel, G.A., Knighton, B., Kluck, K., Ren, Y., Livinghouse, T., Griffin, M., Spakowicz, D. & Sears, J. (2008) The production of myco-diesel hydrocarbons and their derivatives by the endophytic fungus *Gliocladium roseum* (NRRL 50072). *Microbiology*, 154(11), 3319-3328.

Sturrock, C.J., Ritz, K., Samson, W.B., Bown, J.L., Staines, H.J., Palfreyman, J.W., Crawford, J.W. & White, N.A. (2002) The effects of fungal inoculum arrangement (scale and context) on emergent community development in an agar model system. *FEMS Microbiology Ecology*, 39, 9–16.

Sun, D., Meng, J., Liang, H., Yang, E., Huang, Y., Chen, W., Jiang, L., Lan, Y., Zhang, W. & Gao, J. (2015) Effect of volatile organic compounds absorbed to fresh biochar on survival of *Bacillus mucilaginosus* and structure of soil microbial communities. *Journal of Soils and Sediments*, 15(2), 271-281.

Suwannarach, N. Bussaban, B., Nuangmek, W., Pithakpol, W., Jirawattanakul, B., Matsui, K. & Lumyong, S. (2016) Evaluation of *Muscodor suthepensis* strain CMU-Cib462 as a postharvest biofumigant for tangerine fruit rot caused by *Penicillium digitatum*. *Science of Food and Agriculture*, 96(1) 339-345.

Swain, S.S., Paidesetty, S.K. & Padhy, R.N. (2017) Antibacterial, antifungal and antimycobacterial compounds from cyanobacteria. *Biomedicine and Pharmacotherapy*, 90, 760-776.

Tan, K.-C., Trengove, R.D., Maker, G.L., Oliver, R.P. & Solomon, P.S. (2009) Metabolite profiling identifies themycotoxin alternariol in the pathogen *Stagonospora nodorum*. *Metabolomics*, 5(3), 330-335.

Tang, J.D., Parker, L.A., Perkins, A.D., Sonstegard, T.S., Schroeder, S.G., Nicholas, D.D. & Diehl, S.V. (2013) Gene expression analysis of copper tolerance and wood decay in the brown rot fungus *Fibroporia radiculosa*, *Applied Environmental Microbiology*, 79(5), 1523-1533.

Teste, F.P., Simard, S.W., Durall, D.M., Guy, R.D., Jones, M.D. & Schoonmaker, A.L. (2009) Access to mycorrhizal networks and roots of trees: importance for seedling survival and resource transfer. *Ecology*, 90(10), 2808-2822.

Tien, M. & Kirk, T.K. (1983) Lignin-degrading enzyme from the hymenomycete *Phanerochaete chrysosporium* Burds. *Science*, 221, 661-663.

Toledo, S., Hiscox, J., Savoury, M. & Boddy, L. (2016) Multispecies interactions between wood decay basidiomycetes. *Journal of Fungal Research*, doi: 10.13341/j.jfr.2014.2059.

Toljander, Y.K., Lindahl, B.J.D, Holmer, L. & Högberg, N.O.S. (2006) Environmental fluctuations facilitate species co-existence and increase decomposition in communities of wood decay fungi.. *Oecologia*, 148, 625–631.

Tolstikov, V.V., Lommen, A., Nakanishi, K., Tanaka, N. & Fiehn, O. (2003) Monolithic silica-based capillary reversed-phase liquid chromatography/electrospray mass spectrometry for plant metabolomics. *Analytical Chemistry*, 75, 6737–6740.

Tumen, I., Eller, F.J., Clausen, C.A. & Teel, J.A. (2013) Antifungal activity of heartwood extracts from three *Juniperus* species. *BioResources*, 8(1), 12-20.

Tuor, U., Winterhalter, K. & Fiechter, A. (1995) Enzymes of white-rot fungi involved in lignin degredation and ecological determinants for wood decay. *Journal of Biotechnology*, 41, 1-17.

Usha Nandhini, S., Sangareshwari, S. & Kumari, L. (2015) Gas chromatography-mass spectrometry analysis of bioactive constituents from the marine *Streptomyces*. *Asian Journal of Pharmaceutical and Clinical Research*, 8(2), 0974-2441.

Valášková, V., Šnajdr, J., Bittner, B., Cajthaml, T., Merhautová, V., Hofrichter, M. & Baldrian, P. (2007) Production of lignocellulose-degrading enzymes and degradation of leaf litter by saprotrophic basidiomycetes isolated from a *Quercus petraea* forest. *Soil Biology & Biochemistry*, 39, 2651-2660.

Van Der Wal, A., Gunnewiwk, P.J.A.K., Cornelissen, J.H.C., Crowther, T.W. & De Boer, W. (2016) Patterns of natural fungal community assembly during initial decay of coniferous and broadleaf tree logs. *Ecosphere*, doi: 10.1002/ecs2.1393.

Van Teeffelen, S., Shaevitz, J.W. & Gitai, Z. (2012) Image analysis in fluorescence microscopy: Bacterial dynamics as a case study. *Bioassays*, 34(5), 427-436.

Veech, J.A. (2012) A probabilistic model for analysing species co-occurrence. *Global Ecology and Biogeography,* 22, 252-260.

Venugopal, P., Junninen, K., Linnakoski, R., Edman, M. & Kouki, J. (2016) Climate and wood quality have decayer-specific effects on fungal wood decomposition. *Forest Ecology and Management*, 360, 341-351.

Viant, MR., Rosenblum, E.S. & Tjeerdema, R.S. (2003) NMR-based metabolomics: A powerful approach for characterizing the effects of environmental stressors on organism health. *Environmental Science and Technology*, 37, 4982-4989.

Viant, M.R. & Sommer, U. (2012) Mass spectrometry based environmental metabolomics: a primer and review. *Metabolomics*, 9, 144-158.

Viiri, H., Annila, E., Kitunen, V. & Niemela, P. (2001) Induced responses in stilbenes and terpenes in fertilized Norway spruce after inoculation with blue-stain fungus *Ceratocystis polonica*. *Tree – Structure and Function*, 15, 112-122.

Wagg, C., Barendregt, C., Jansa, J. & van der Heijden, M.G.A. (2015) Complementarity in both plant and mycorrhizal fungal communities are not necessarily increased by diversity in the other. *Journal of Ecology*, 103, 1233-1244.

Walters, D., Raynor, L., Mitchell, A., Walker, R. & Walker, K. (2004) Antifungal activity of four fatty acids against plant pathogenic fungi. *Mycopathologia*, 157(1), 87-90.

Wang, J., Li, S., Freitag, C., Morrell, J.J. & Karchesy, J.J. (2012) Antifungal activities of four cedar foliage oils to wood stain or decay fungi. *Advanced Materials*, 365, 375-381.

Wang, L., Wu, S., Chen, Y., Yu, Y., Yang, L., Li, S. & Li, Z. (2009) Studies on the secondary metabolites of endophytic fungus *Epicoccum* sp. isolated from *Azadirachta indica. Tianran Chanwu Yanjiu Yu Kaifa*, 21(6), 916-918.

Wang, R.W., Dunn, D.W., Luo, J., He, J.Z. & Shi, L. (2015) The importance of spatial heterogeneity and self-restraint on mutualism stability – a quantitative review. *Scientific Reports*, doi: 10.1038/srep14826.

Wang, T.J., Larson, M.G., Vasan, R.S., Cheng, S., Rhee, E.P., McCabe, E., Lewis, G.D., Fox, C.S., Jacques, P.F., Fernandez, C., O'Donnell, C.J., Carr, S.A., Mootha, V.K., Florez, J.C., Souza, A., Melander, O., Clish, C.B. & Gerszten, R.E. (2011) Metabolite profiles and the risk of developing diabetes. *Nature Medicine*, 17(4), 448-453.

Warneke, C., Karl, T., Judmaier, H., Hansel, A., Jordan, A., Lindinger, W. & Crutzen, P.J. (1999) Acetone, methanol, and other partially oxidized volatile organic emissions from dead plant matter by abiological processes: Significance for atmospheric HO_x chemistry. *Global Biogeochemical Cycles*, 13(1), 9-17.

Warne, M., Lenz, E.M., Osborn, D., Weeks, J.M. & Nicholson, J.K. (2000) An NMR-based metabonomic investigation of the toxic effects of 3-trifluromethyl-aniline on the earthworm *Eisenia veneta*. *Biomarkers*, 5(1), 56-72.

Weber, R.J.M. & Viant, M.R. (2010) MI-Pack: Increased confidence of metabolite identification in mass spectra by integrating accurate masses and metabolic pathways. *Chemometrics and Intelligent Laboratory Systems*, 104, 75-82.

Werner, T. (2010) Next generation sequencing in functional genomics. *Briefings in Bioinformatics*, 11(5), 499-511.

Wheatley, R.E. (2002) The consequences of volatile organic compound mediated bacterial and fungal interactions. *Antonie Leeuwenhoek*, 81, 357-364.

Whipps, J.M. (1987) Effect of media on growth and Interactions between a range of soil-borne glasshouse pathogens and antagonistic fungi. *New Phytologist*, 107, 127-142.

White, N.A. (2003) The Importance of Wood-Decay Fungi in Forest Ecosystems. In: *Fungal Biotechnology in Agricultural, Food and Environmental Applications*, (eds. D.K. Arora, P.D. Bridge & D. Bhatnagar), Marcel Dekker, New York, USA. pp. 375-391.

White, N.A., Sturrock, C., Ritz, K., Samson, W.B., Bown, J., Staines, H.J., Palfreyman, J.W. & Crawford, J. (1998) Interspecific fungal interactions in spatially heterogeneous systems. *FEMS Microbiology Ecology*, 27, 21–32.

Wihlborg, R., Pippitt, D. & Marsili, R. (2008) Headspace sorptive extraction and GC-TOFMS for the identification of volatile fungal metabolites. *Journal of Microbiological Methods*, 75(2) 244-250.

Wilkens, S. (2015) Structure and mechanism of ABC transporters. *F1000 Prime Reports*, 7, 14, doi: 10.12703/P7-14.

Williams, E.N.D., Todd, N.K. & Rayner, A.D.M. (1981) Spatial development of populations of *Coriolus versicolor. New Phytologist*, 89, 307-319.

Wong, D.W. (2009) Structure and action mechanism of ligninolytic enzymes. *Applied Biochemistry and Biotechnology*, 157, 174-209.

Woodward, S. & Boddy, L. (2008) Interactions between saprotrophic fungi. In: *Ecology of Saprotrophic Basidiomycetes*, (eds. L. Boddy, J.C. Frankland & P. van West). Elsevier, Amsterdam. pp. 123-139.

Xia, J. & Wishart, D.S. (2016) Using MetaboAnalyst 3.0 for Comprehensive Metabolomics Data Analysis Current Protocols in Bioinformatics, 55: 14.10.1-14.10.91.

Xu, J., Zhang, J., Yuan, Y., Yang, X. & Ming, J. (2015) effects of different culture media on aroma components pf *Pleurotus ostreatus*. *Food Science*, 36(4), 86-91.

Xu, X.-Y., Shen, X.-T., Yuan, X.-J., Zhou, Y.-M., Fan, H., Zhu, L.-P. Du, F.-Y., Sadilek, M., Yang, J., Qiao, B. & Yang, S. (2018) Metabolomics investigation of an association of induced features and corresponding fungus during the co-culture of *Trametes versicolor* and *Ganoderma applanatum*. *Frontiers in Microbiology*, 8, 2647, doi: 10.3389/fmicb.2017.02647.

Yan, C., Yu, J.X., Xing, T. & Qing, C.X. (2008) Comparison of volatile components from *Marchantia convolute* obtained by microwaves extraction and phytosol extraction. *Journal of the Chilean Chemical Society*, 53(2), 1518-1522.

Yang, Y.S., Zhou, J.T., Lu, H., Yuan, Y.L. & Zhao, L.H. (2011) Isolation and characterization of a fungus *Aspergillus* sp. strain F-3 capable of degrading alkali lignin. *Biodegradation*, 22(5), 1017-1027.

Yim, G., Wang, H H. & Davies, J. (2007) Antibiotics as signalling molecules. *Philosophical Transactions of the Royal Society* of London, 362, 1195–1200.

Zamocky, M., Furtmüller, P.G. & Obinger, C. (2009) Two distinct groups of fungal catalase/peroxidases. *Biochemical Society Transactions*, 37, 772–777.

Zamocky, M., Gasselhuber, B., Furtmuller, P.G. & Obinger, C. (2014) Turning points in the evolution of peroxidase-catalase superfamily: molecular phylogeny of hybrid heme peroxidases. *Cellular and Molecular Life Sciences*, 71(23), 4681–96.

Zhang, A., Sun, H., Xu, H., Qiu, S. & Wang, X. (2013) Cell metabolomics. *Omics*, 17(10), 495-501.

Yelle, D.J., Wei, D., Ralph, J. & Hammel, K.E. (2011) Multidimensional NMR analysis reveals truncated lignin structures in wood decayed by the brown rot basidiomycete *Postia placenta*. *Environmental Microbiology*, 13(4), 1091-1100.

Yu, Y., Yanquing, Z., Yelin, Z., Zuo, J., Ma, Fuying., Yang, X., Zhang, X. & Wang, Y. (2013) Improving the conversion of biomass in catalytic fast pyrolysis via white-rot fungal pretreatment. *Bioresource Technology*, 134, 198-203.

Yu, Z., Shi, G., Sun, Q., Jin, H., Teng, Y., Tao, K., Zhou, G., Liu, W., Wen, F. & Hou, T. (2009) Design, synthesis and in vitro antibacterial/antifungal evaluation of novel 1-ethyl-6-fluoro-1,4-dihydro-4-oxo-7(1-piperazinyl)quinoline-3-carboxylic acid derivatives. *European Journal of Medicinal Chemistry*, 44(11), 4726-4733.

Zerinque, H.J. & Bhatnagar, D. (1994) Effects of neem leaf volatiles on submerged cultures of aflatoxigenic *Aspergillus parasiticus*. *Applied and Environmental Microbiology*, 60(10), 3543-3547.

Appendix 1: Chapter 2 supplementary material

S 2.1 Studying volatile organic compounds

The most widely used method of fungal VOC sampling involves collection with either active or passive sorbent sampling from ambient air followed by solid phase microextraction (SPME) (Korpi et al. 2009; Stoppacher et al. 2010; Hynes et al. 2007; Evans et al. 2008; Zang & Li 2010; El Ariebi et al. 2016). SPME was first introduced in the 1990's as a quicker method of VOC sampling than had previously been reported, with increased sensitivity by the incorporation of extraction, pre-concentration and sample introduction into a single step (Arthur & Pawliszyn 1990). Briefly, SPME is achieved by the coating of a fiber in a stationary phase and placement into an aqueous sample allowing the partitioning of analytes into the stationary phase where they are thermally desorbed onto a column in a gas chromatograph. The main variable affecting the efficiency of SPME extraction is the coating phase of the SPME fiber, the selection of which is dependent on the polarity of VOCs being assessed. Polydimethylsiloxane (PDMS) and carboxen-PDMS coated fibers are most suited to nonpolar compound extraction whereas polyacrylate and divinylbenzene (DVB) fibers are more efficient in the extraction of polar compounds. Carboxylic compounds, ketones, alcohols and other compounds, however, are bipolar, so duel fiber coatings such as a mixture of PDMS and DVB may be better in those instances (Balasubramanian & Panigrahi 2011).

Dynamic headspace sampling technique is another name for purge and trap sampling which transfers sample VOCs to a solvent trap (usually Tenax®, silica gel or activated charcoal) following continual purging of the extracted sample with inert gas (usually helium or nitrogen) (Wang et al. 2016). It is an improvement on the previously used SPME method by its superior absorption of a far wider range of compounds. It is a sampling method that has been particularly useful for the identification of marker-indicators in the food processing industry (Spadafora et al. 2016; Bell et al. 2016).

A major challenge in VOC quantification is the identification of extracted compounds. There is currently no standard method for the analysis of VOCs, but many methods exist such as secondary electrospray ionization mass spectrometry (SESI-MS) proton transfer reaction mass spectrometry (PTR-MS) and ion mobility spectrometry (IMS), but the most widely used analytical method is high resolution gas chromatography and mass spectrometry (GC-MS) (Wang et al. 2016). Gas chromatography (GC) utilizes the vaporization of compounds at the GC injection port and is a powerful analytical technique for compound identification, especially when coupled with mass spectrometry (MS) (Wang et al. 2016). Compounds are identified using either a database or library of mass spectra, or by the comparison of spectra and retention times with those of known standards. High-resolution mass spectrometry, most notably, time-of-flight (TOF) mass spectrometry is increasingly being used to further improve the identification of complex compounds, however, one limitation of GC–MS is that it cannot be used for the identification of novel compounds (Morath et al. 2012).

S 2.2 Instrumentation for the study of metabolomics

The first spectroscopy tool used in the field, NMR, is easily automated, capable of quantitative analysis and is highly reproducible between laboratories. It is limited, however, by its lower sensitivity compared to MS instruments (Viant & Sommer 2012). MS is most commonly coupled with GC or liquid chromatography (LC) to separate metabolites, one of a variety of ion sources is used to form ions with the native metabolites, including electron impact (EI) and electron spray ionization (ESI), and finally metabolites are analysed by, for example, TOF, triple quadrupole (QQQ), Orbitrap and Fourier transform ion cyclotron resonance (FT-ICR) (Dunn 2008; Viant & Sommer 2012). More detailed discussion of the full array of analytical tools in metabolomics is beyond the scope of this review, and instead focus will be placed on LC-MS coupled with Orbitrap, analytical tools which have been used within the studies of this thesis (Chapter 8).

LC-MS is commonly used in both targeted (measuring defined groups of biochemically annotated metabolites) and untargeted (analysis of the full complement of measureable analytes within a sample, including chemical unknowns) metabolomics (Roberts et al. 2013). It is more sensitive than GC-MS and NMR due to smaller capillary columns (Tolstikov et al. 2013), but higher sensitivity can often come at a cost to chromatogram resolution. The introduction of ultra-high performance LC-MS (UHPLC-MS), therefore, was revolutionary in its high sensitivity ability whilst also retaining a respectable resolution and expedited analysis by the use of more evenly shaped columns with smaller particles (Guillarme et al. 2007). A major disadvantage of LC-MS, and untargeted metabolomics in general, is the relatively low metabolite identification ability which is limited further in LC-MS studies by high inconsistency of analyses across different instrument types (Viant & Sommer 2012). That being said, given that ultra-high performance metabolomics has never before been applied to wood decay fungi, the potential for novel discoveries regarding the physiology of these organisms during decay processes is huge.

Orbitrap technology was first described in 2000 (Makarov 2000) and now represents one of the most widely used analytical tools in the field of metabolomics (Makarov & Scigelova 2010). Though diverse in their specific instrument components, Orbitrap mass analysers all contain an external injection device which traps a large quantity of ions in a gas-filled curved quadrupole, termed the C-trap, from which they are injected into the Orbitrap analyser. Here, a central electrode rapidly increases its voltage causing the ions to assume a circular trajectory around it, and their axial oscillations and the frequency of their oscillations are detected (Makarov & Scigelova 2010). Subsequently, a fast Fourier transform (FT) determines the mass-charge ratio (*m/z*) of the ions from the frequency of their axial oscillations (Hu et al. 2005), from which metabolite identifications can be made. Orbitrap spectrometers have an impressively higher *m/z* accuracy than other available mass spectrometers (Makarov et al. 2006), placing them at the forefront of their field in terms of structural elucidation of uncharacterised metabolites (Makarov & Scigelova 2010). Care must be taken when characterising novel compounds,

however, as other characteristics such as isotopic patterns and Lewis and Senior chemical rules must be taken into account for accurate metabolite annotation (Kind & Fiehn 2006).

Appendix 2: Chapter 3 supplementary material

Supplementary Table 3.1 Regions of blocks from 15 °C, 25 °C and field experiments that were assayed for enzymes. Blocks were chosen based on results from re-isolation onto agar.

Supplementary Table 3.1

Interaction	15C				25C				Field			
	Outcome	Day	Rep ID	Region	Outcome	Day	Rep ID	Region	Outcome	Day	Rep ID	Region
T. versicolor vs. H. fasciculare	Initial deadlock	14 d	8	IZ	Initial deadlock	14 d	1	IZ	Initial deadlock	14 d	1643	IZ
			7				17				1648	
			21				22				1655	
			9			28 d	18				1656	
			15				20				1660	
	PR of *T. versicolor*	28 d	20	2	PR of *H. fasciculare*	14 d	3	3	PR of *T. versicolor*	56 d	1642	2
			23	1			23	3			1657	2
			24	2		28 d	16	3		84 d	1646	2
		56 d	17	1			6	4			1649	2
			19	1		84 d	15	4			1663	1
	R of *T. versicolor*	56 d	16	1	Late deadlock	56 d	14	IZ	Late deadlock	56 d	1647	IZ
		84 d	11				21				1651	
			12				9				1652	
			13			84 d	8			-	-	-
			22				19			-	-	-
T. versicolor vs. P. velutina	Initial deadlock	14 d	23	IZ	Initial deadlock	1 d	?	IZ	Initial deadlock	14 d	1700	IZ
			24				?				1712	
			8				?				1697	
			20			14 d	15				1690	
		28 d	6				17				1711	
	PR of *T. versicolor*	14 d	22	2	PR of *P. velutina*	14 d	20	3	PR of *T. versicolor*	28 d	1694	2
		28 d	9	2			2	4			1707	2
		56 d	11	1			6	3		56 d	1709	2
			15	2		28 d	1	3			1713	2
			13	2			3	4			-	-
	Late deadlock	56 d	10	IZ	R of *P. velutina*	28 d	18	4	R of *T. versicolor*	84 d	1692	1
		84 d	16			56 d	16				1695	
			17			84 d	9				1703	
			18				8				1710	
			19				12				1714	

Supplementary Table 3.2 Interaction outcomes (A), score of combative ability (B) and % density loss (C). (A) Interaction outcomes are defined as R, replacement of competitor by *T. versicolor*; PR, partial replacement of competitor by *T. versicolor*; D, deadlock; pr, partial replacement of *T. versicolor* by competitor; r, complete replacement of *T. versicolor* by competitor. (B) *T. versicolor* score of combative ability calculated as total territory occupied over all interaction pairings, normalised to the number of replicates performed. (C) % density loss of blocks at the end of interactions.

A

T. versicolor	**Competitor**	**Interaction treatment**					
		15C	**25C**	**Field**	**Young Tv Old comp**	**Old Tv young comp**	**Old Tv old comp**
Heterokaryon	*V. comedens*	PR	R(4)	PR(2) D(1)	PR(5)	R(1) PR(1) D(1)	R(2) PR(1) D(1)
Heterokaryon	*C. puteana*	D	R(2) PR(2) D(1)	R(2) PR(1) D(1)	R(3)	R(5)	R(5)
Heterokaryon	*B. adusta*	D	D(3) PR(1) r (1)	D(4)	-	-	-
Heterokaryon	*P. ostreatus*	PR	R(3) PR(1)	D(1)	-	-	-
Heterokaryon	*H. fasciculare*	pr	D(3) PR(1) r(1)	pr(3) D(1)	D(4) pr(1)	r(3) pr(2)	r(3) pr(2)
Heterokaryon	*P. velutina*	pr	R(3) D(1)	r(5)	R(3)	D(2) r(2)	R(2)
Homokaryon	*V. comedens*	D(3) PR(1)	R(4)	D(3)	-	-	-
Homokaryon	*C. puteana*	R(1) PR(1) D(1) pr(1) r(1)	R(1) D(1)	PR(2) pr(1)	-	-	-

Supplementary Table 3.2 *Continued*

B

T. versicolor	**Competitor**	**Interaction treatment**					
		15C	**25C**	**Field**	**Young Tv Old comp**	**Old Tv young comp**	**Old Tv old comp**
Heterokaryon	*V. comedens*	309	339	277	263	279	293
Heterokaryon	*C. puteana*	367	348	280	366	393	373
Heterokaryon	*B. adusta*	209	171	196	-	-	-
Heterokaryon	*P. ostreatus*	310	314	295	-	-	-
Heterokaryon	*H. fasciculare*	116	225	173	196	97	145
Heterokaryon	*P. velutina*	159	284	125	300	116	275
Homokaryon	*V. comedens*	228	351	245	-	-	-
Homokaryon	*C. puteana*	228	259	245	-	-	-

C

T. versicolor	**Competitor**	**Interaction treatment**					
		15C	**25C**	**Field**	**Young Tv Old comp**	**Old Tv young comp**	**Old Tv old comp**
Heterokaryon	*V. comedens*	14.15	14.72	8.99	12.85	10.82	13.65
Heterokaryon	*C. puteana*	11.71	18.07	7.65	22.76	3.15	15.94
Heterokaryon	*B. adusta*	14.51	5.36	4.93	-	-	-
Heterokaryon	*P. ostreatus*	8.39	4.23	13.47	-	-	-
Heterokaryon	*H. fasciculare*	10.89	7.07	4.08	-	10.52	6.16
Heterokaryon	*P. velutina*	11.10	-6.81	6.77	2.59	17.03	2.73
Homokaryon	*V. comedens*	3.24	8.11	8.68	-	-	-
Homokaryon	*C. puteana*	15.48	12.53	5.83	-	-	-

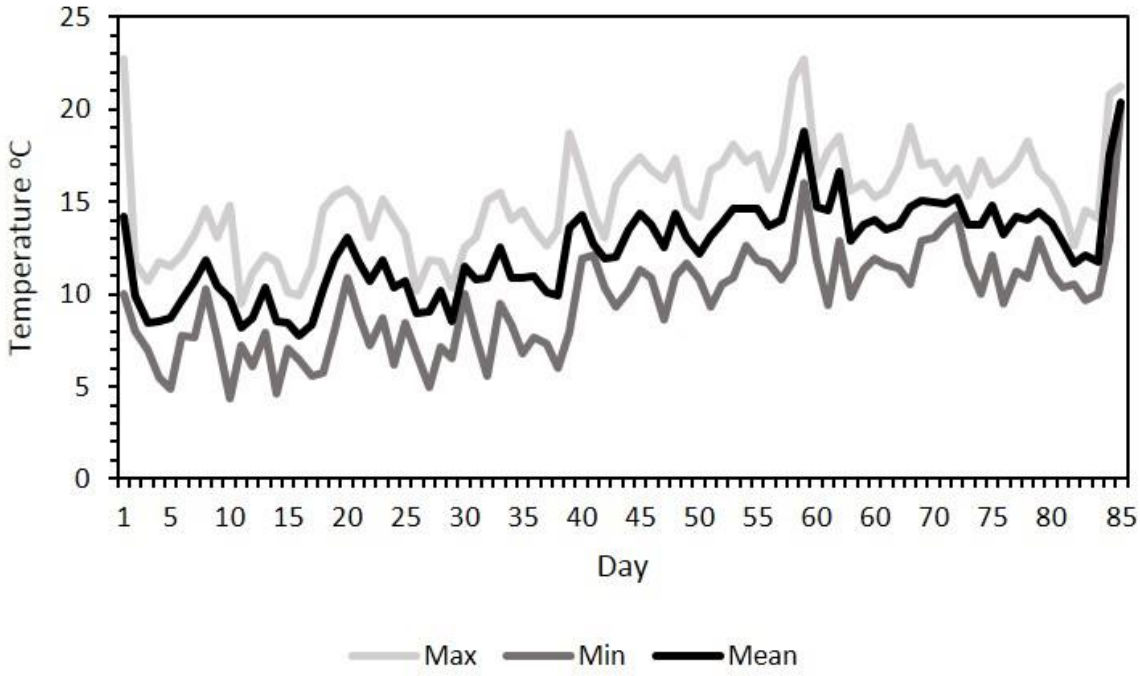

Supplementary Figure 3.1 Mean, maximum and minimum temperatures (°C) recorded in the field by data loggers (3 replicates; TinyTag, UK). Data were recorded every hour from the start of the experiment for 84 d (4th May 2015 – 28th July 2015).

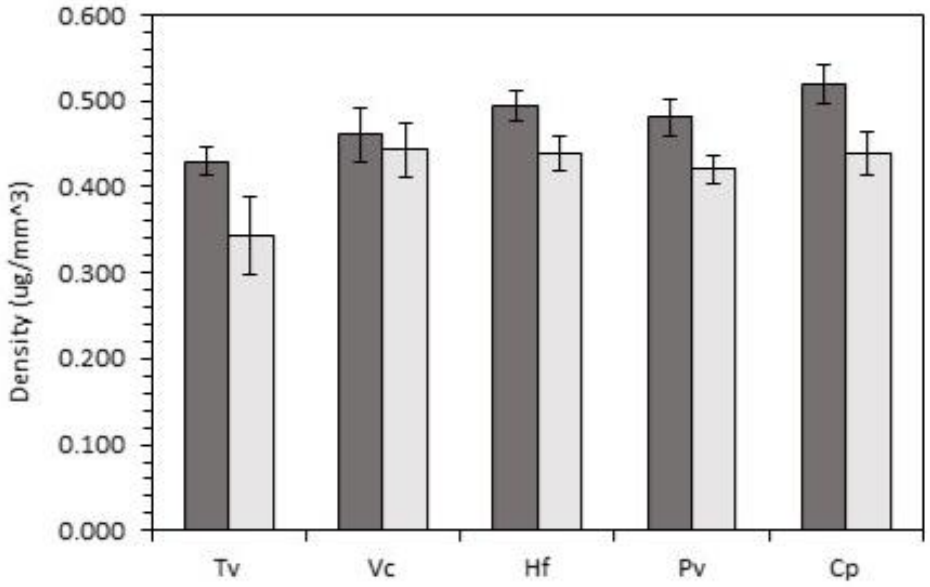

Supplementary Figure 3.2 Density (ug/mm^3) of wood blocks sacrificed after pre-colonisation for 12 weeks (dark grey) and 24 weeks (pale grey). Bars represent the mean of 10 replicates with 95% confidence intervals. Tv: *T. versicolor*; Vc: *V. comedens*; Hf: *H. fasciculare*; Pv: *P. velutina*; Cp: *C. puteana*.

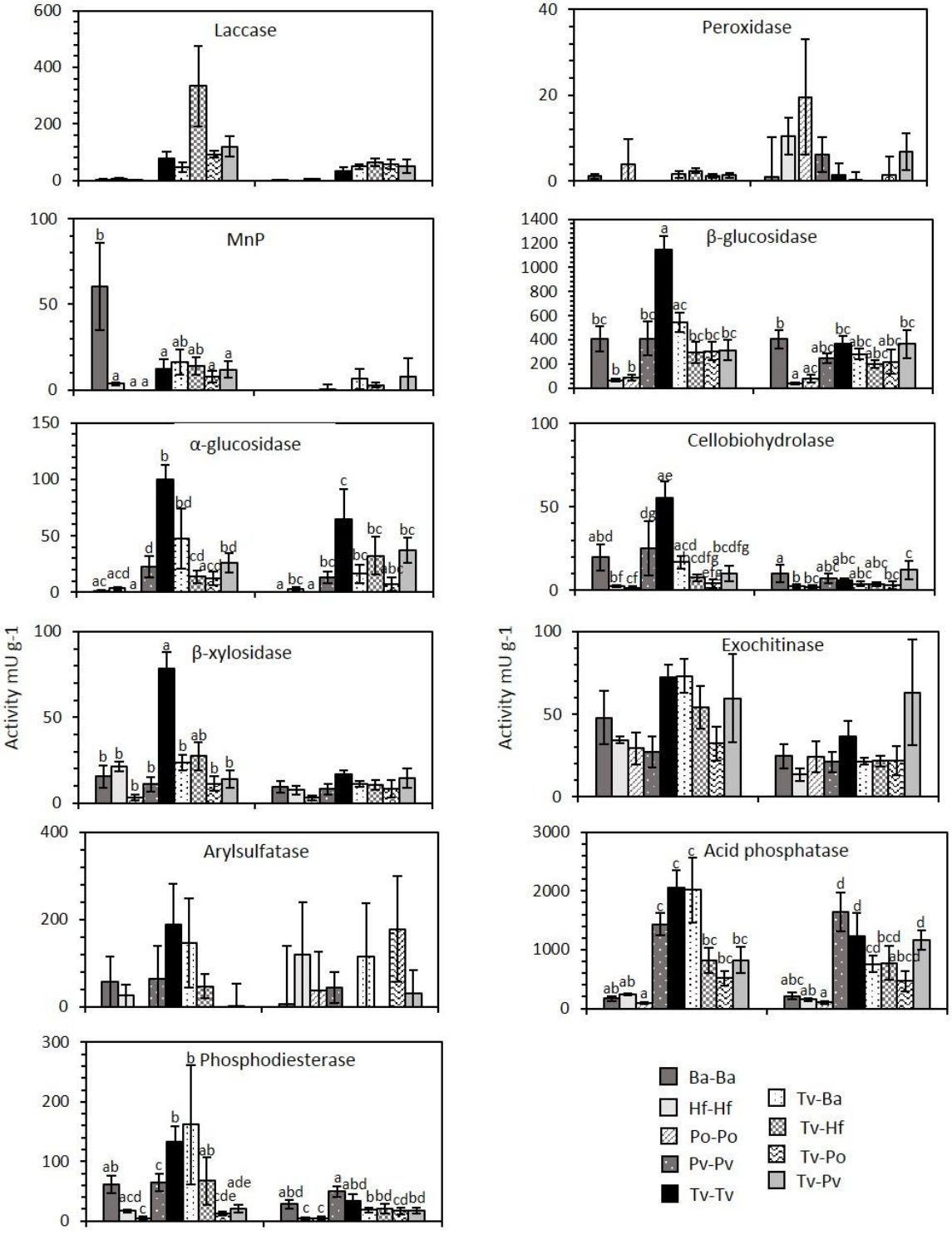

Supplementary Figure 3.3 Extracellular enzyme activity from the pooled interaction zone of interacting wood blocks from the field and at 15 °C controlled laboratory conditions. Bars are the mean activity of 5 replicates ± SEM. Different letters indicate a significant (P < 0.05) difference in activity between pairings. Statistical comparisons are made separately for each enzyme and condition, and no letters indicates no significant differences (p > 0.05).

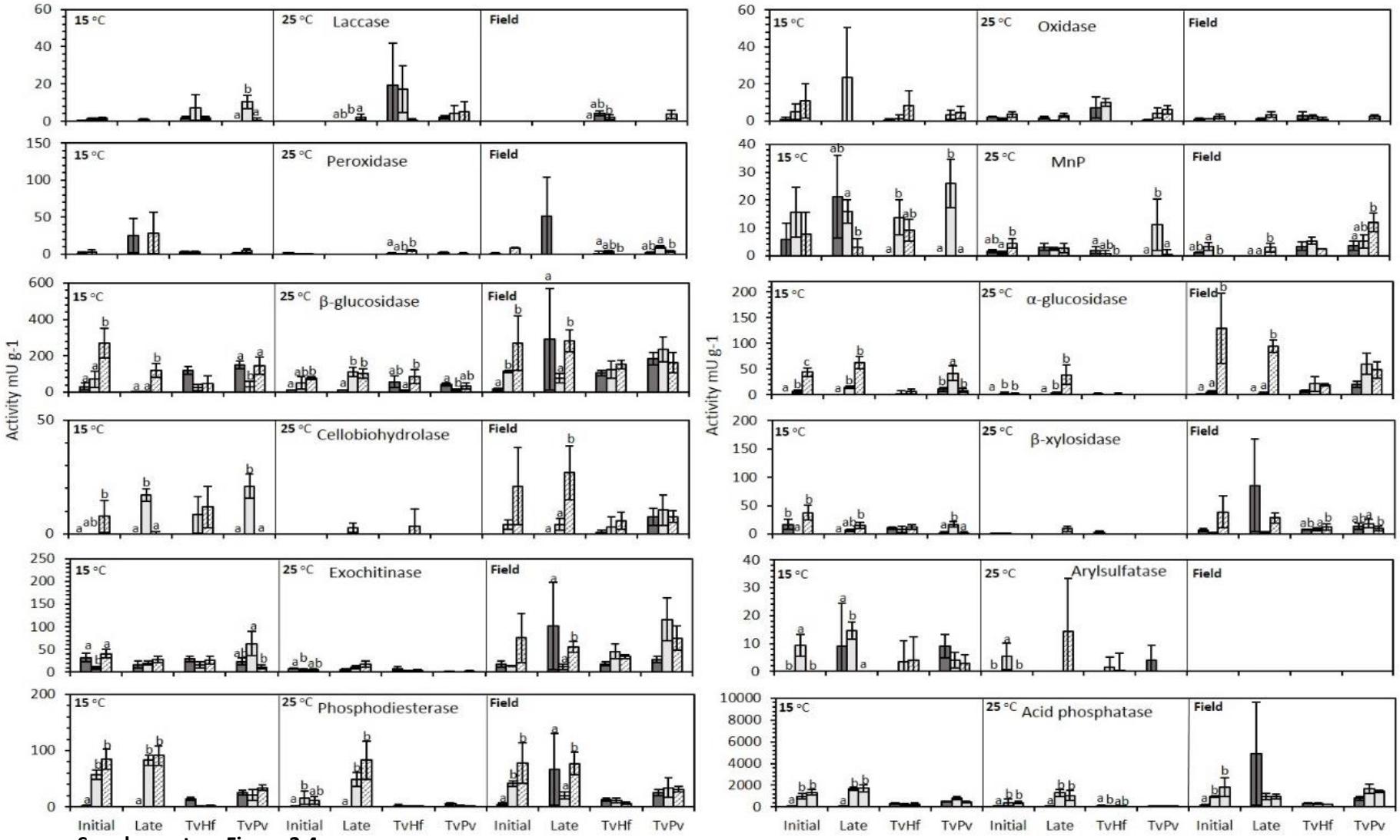

Supplementary Figure 3.4

Supplementary Figure 3.4 Extracellular enzyme activity of interactions with *T. versicolor* (Tv) against *H. fasciculare* (Hf) and *P. velutina* (Pv) at 15 °C, 25 °C and in the field. For self-pairings, assays were performed on the pooled interaction zone of each pairing initially and late into the experiment, and dark grey bars represent *H fasiculare* self-pairings, light grey represent *P. velutina* and stripped bars represent the activity of *T. versicolor* self-pairings. For interspecific interactions, assays were performed on pooled regions of each pairing at different time points based on the interaction outcome at that time point and bars represent activity for each outcome, shown chronologically from left to right (see Supplementary Table 3.1 for details). Bars are the mean activity of 5 replicates ± SEM. Different letters indicate a significant ($p < 0.05$) difference in activity between pairings. Statistical comparisons are made separately for each enzyme, pairing and condition, and no letters indicates no significant differences ($p > 0.05$).

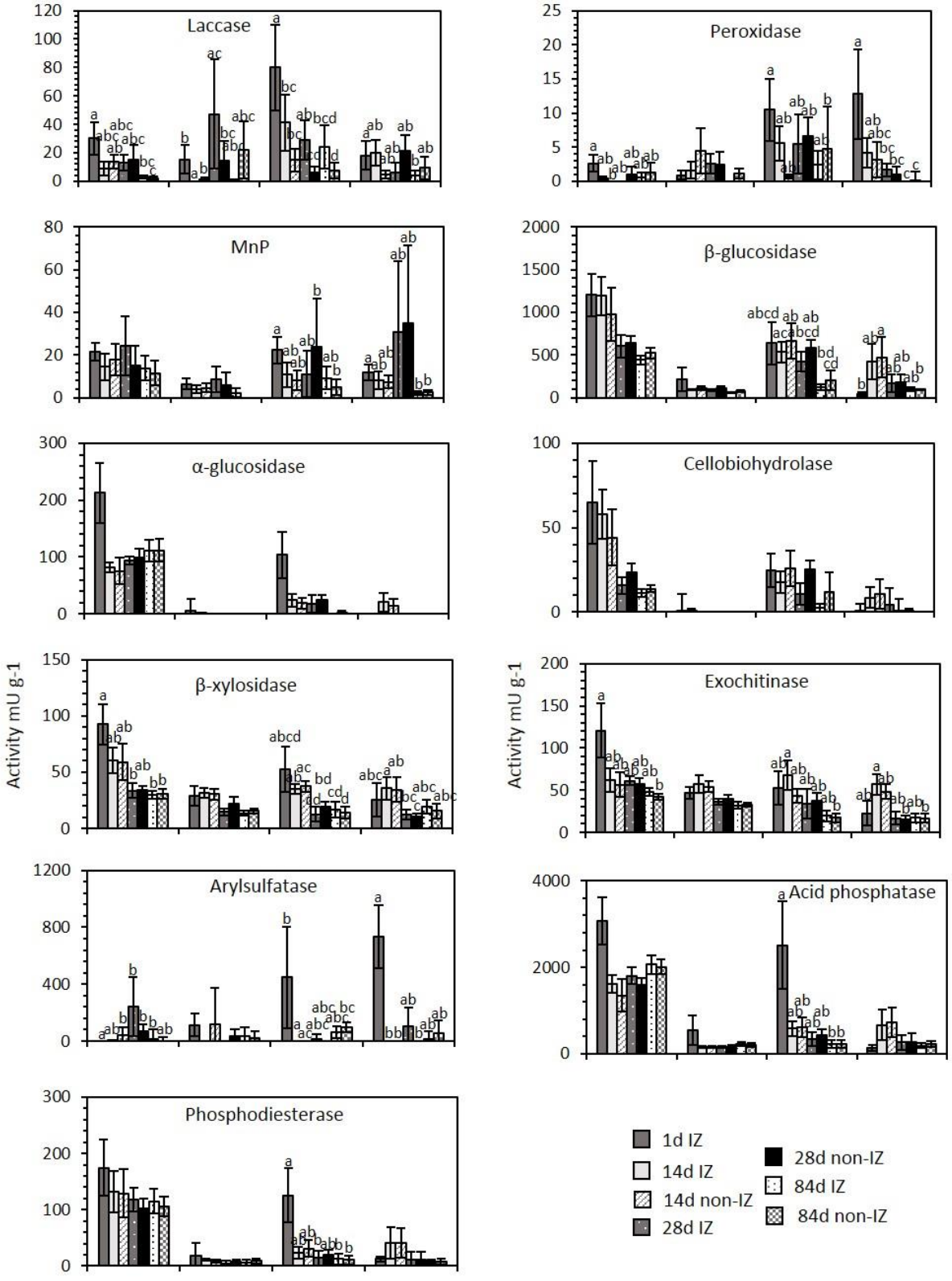

Supplementary Figure 3.5

Supplementary Figure 3.5 Extracellular enzyme activity of different regions of the interaction with *T. versicolor* (Tv) against *H. fasciculare* (Hf) over 84d at 15 °C. Regions include the pooled interaction zone (IZ) and non-interaction (non-IZ) of self-pairings, and the *T. versicolor* block and *H. fasciculare* block IZ and non-IZ separately at 1 d, 14 d, 28 d and 84 d after interaction set-up. Square brackets indicate side of the interactions assayed. Bars are the mean activity of 5 replicates ± SEM. Statistical comparisons are made separately for each enzyme and pairing. Different letters indicate a significant ($p < 0.05$) difference in activity between regions and no letters indicates no significant differences ($p > 0.05$).

Appendix 3: Chapter 4 supplementary material

Supplementary Table 4.1 Density (ug/mm^3) of wood blocks sacrificed after pre-colonisation for 3 months or 6 months. Values are the mean of 10 replicates with a 95% confidence interval.

	Density (ug/mm3)		95% Confidence interval	
	3	6	3	6
T. versicolor	0.429	0.343308	0.01628457	0.046464944
V. comedens	0.461	0.442888	0.03172123	0.030397699
H. fasciculare	0.495	0.43913	0.01727569	0.020668685
P. velutina	0.481	0.420459	0.02152249	0.015603607
C. puteana	0.519997	0.440069	0.02246578	0.025316329

Supplementary Table 4.2 Average percentage abundance from three replicates of each compound detected in interactions at 15 °C 1 d, 14 d and 28 d after interaction set-up, ± SEM. nd denotes compounds that were below to level of detection. Statistical differences were calculated for each compound and interaction separately, different letters indicate significant differences ($p < 0.05$) between means. Putative identification of compounds are given in Table 4.2. Tv: *T. versicolor*; Ba: *B. adusta*; Cp: *C. puteana*; Hf: *H. fasciculare*; Po: *P. ostreatus*; Pv: *P. velutina*; Vc: *V. comedens*.

Available online at:

https://www.dropbox.com/s/abu912dgipddea7/Supplementary%20Table%204.2.xlsx?dl=0

Supplementary Table 4.3 Significant compounds (ANOVA: $p < 0.05$) in the 15 °C temperature experiment across the entire data set (A), at 1 d (B), 14 d (C) and 28 d (D) after interaction set up, identified from the OPLS-DA modelled covariance and correlation (S-plot). The test statistic f value, p value and 5% Benjamini-Hochberg false discovery rate (FDR) correction is given. Compounds are listed in order of significance.

Available online at:

https://www.dropbox.com/s/kohyviofppix1wv/Supplementary%20Table%204.3.xlsx?dl=0

Supplementary Table 4.4 Average percentage abundance from three replicates of each compound detected in interactions at 25 °C 1 d, 14 d and 28 d after interaction set-up, ± SEM. nd denotes compounds that were below to level of detection. Statistical differences were calculated for each compound and interaction separately, different letters indicate significant differences ($p < 0.05$) between means. Putative identification of compounds are given in Table 4.2. Tv: *T. versicolor*; Ba: *B. adusta*; Cp: *C. puteana*; Hf: *H. fasciculare*; Po: *P. ostreatus*; Pv: *P. velutina*; Vc: *V. comedens*.

Available online at:

https://www.dropbox.com/s/wm7awmzgzp3tee7/Supplementary%20Table%204.4.xlsx?dl=0

Supplementary Table 4.5 Significant compounds (ANOVA: $p < 0.05$) in the 25 °C temperature experiment across the entire data set (A), at 1 d (B), 14 d (C) and 28 d (D) after interaction set up, identified from the OPLS-DA modelled covariance and correlation (S-plot). The test statistic f value, p value and 5% Benjamini-Hochberg false discovery rate (FDR) correction is given. Compounds are listed in order of significance.

Available online at:

https://www.dropbox.com/s/ckzvg7j6ezbqdxc/Supplementary%20Table%204.5.xlsx?dl=0

Supplementary Table 4.6 Average percentage abundance from three replicates of each compound detected in interactions with different pre-colonisation lengths 1 d, 14 d and 28 d after interaction set-up, ± SEM. nd denotes compounds that were below to level of detection. Statistical differences were calculated for each compound and interaction separately, different letters indicate significant differences ($p < 0.05$) between means. Putative identification of compounds are given in Table 4.2. Tv: *T. versicolor*; Ba: *B. adusta*; Cp: *C. puteana*; Hf: *H. fasciculare*; Po: *P. ostreatus*; Pv: *P. velutina*; Vc: *V. comedens*. Numbers indicate pre-colonisation length (three or six months).

Available online at:

https://www.dropbox.com/s/sucue9zz7iyyq58/Supplementary%20Table%204.6.xlsx?dl=0

Supplementary Table 4.7 Significant compounds (ANOVA: $p < 0.05$) in the pre-colonisation length experiment across the entire data set (A), at 1 d (B), 14 d (C) and 28 d (D) after interaction set up, identified from the OPLS-DA modelled covariance and correlation (S-plot). The test statistic f value, p value and 5% Benjamini-Hochberg false discovery rate (FDR) correction is given. Compounds are listed in order of significance.

Available online at:

https://www.dropbox.com/s/qx3e5p0sa2rdq1p/Supplementary%20Table%204.7.xlsx?dl=0

Supplementary Table 4.8 SEM of the abundancies of chosen compounds in pair-wise interactions at 15 °C (A), 25 °C (B) and in the pre-colonisation length experiment (C). Tv: *T. versicolor*; Ba: *B. adusta*; Cp: *C. puteana*; Hf: *H. fasciculare*; Po: *P. ostreatus*; Pv: *P. velutina*; Vc: *V. comedens*. Numbers in (B) indicate pre-colonisation length (3 or 6 months). Mean abundancies of 3 replicates are shown in Figure 4.3.

A

	C3			C4		
	1d	14d	28d	1d	14d	28d
Ba-Ba	1482.078	-	-	288.3415	-	-
Cp-Cp	766.981	-	-	662.3124	-	-
Hf-Hf	1144.26	134.283	-	11167.96	1449.411	-
Po-Po	1110.415	-	-	0	-	-
Pv-Pv	5047.938	463.7759	-	8414.771	827.0563	-
Tv-Tv	7569.309	1926.742	-	14327.38	3528.873	575.8243
Vc-Vc	9554.705	735.8245	-	12912.18	3329.11	5121.175
Tv-Ba	13972.7	330.9786	-	18950.93	-	-
Tv-Cp	5705.209	723.0108	294.2015	9433.496	1436.378	294.5907
Tv-Hf	827.0327	576.7829	-	1732.21	1285.531	-
Tv-Po	2977.001	-	-	3936.12	-	-
Tv-Pv	1682.584	329.863	-	1373.305	311.7116	391.2233
Tv-Vc	-	-	-	23859.07	-	569.5151

B

	C3			C4		
	1d	14d	28d	1d	14d	28d
Ba-Ba	5582.399	-	-	10122.11	96.04454	-
Cp-Cp	709.5949	974.823	-	267.8276	1005.875	-
Hf-Hf	277.8633	-	-	3306.993	317.1762	2201.471
Po-Po	-	-	-	-	-	-
Pv-Pv	1776.64	-	-	3883.414	1391.303	-
Tv-Tv	8022.994	321.7383	306.571	12729.09	604.9823	329.2152
Vc-Vc	-	766.0868	-	-	1220.48	-
Tv-Ba	2717.439	445.9511	-	5875.422	892.1561	-
Tv-Cp	56.01578	-	276.0193	229.7008	-	282.607
Tv-Hf	-	5290.977	-	-	8940.647	1700.268
Tv-Po	1520.674	-	21.09553	3717.193	171.6859	268.6245
Tv-Pv	1906.697	526.1706	402.5208	3796	1583.116	370.4463
Tv-Vc	-	-	557.1602	-	-	1010.222

Supplementary Table 4.8 *Continued*

C

	C3			C4		
	1d	14d	28d	1d	14d	28d
Hf6-Hf6	-	-	-	408.564	1755.226	-
Pv6-Pv6	-	-	-	-	-	-
Tv6-Tv6	329.9772	652.5792	375.0973	1019.705	1684.785	390.7868
Vc6-Vc6	3403.676	458.0799	239.4796	8965.649	2215.99	1213.638
Tv3-Hf6	1987.742	-	-	5507.116	230.7483	813.3741
Tv3-Pv6	469.4583	-	487.3581	1871.753	-	728.3035
Tv3-Vc6	2166.579	1704.127	-	5765.071	3446.595	1173.315
Tv6-Hf3	3271.709	872.3261	-	5115.16	1726.626	-
Tv6-Pv3	4630.059	443.904	-	7931.11	1609.33	857.0784
Tv6-Vc3	4642.162	1167.987	191.1665	7719.611	1014.135	665.3757
Tv6-Hf6	4677.801	341.1986	-	7545.615	764.8135	-
Tv6-Pv6	5386.576	970.7621	-	8481.562	1110.72	-
Tv6-Vc6	3238.686	3036.819	383.3919	3790.535	4339.213	752.1022

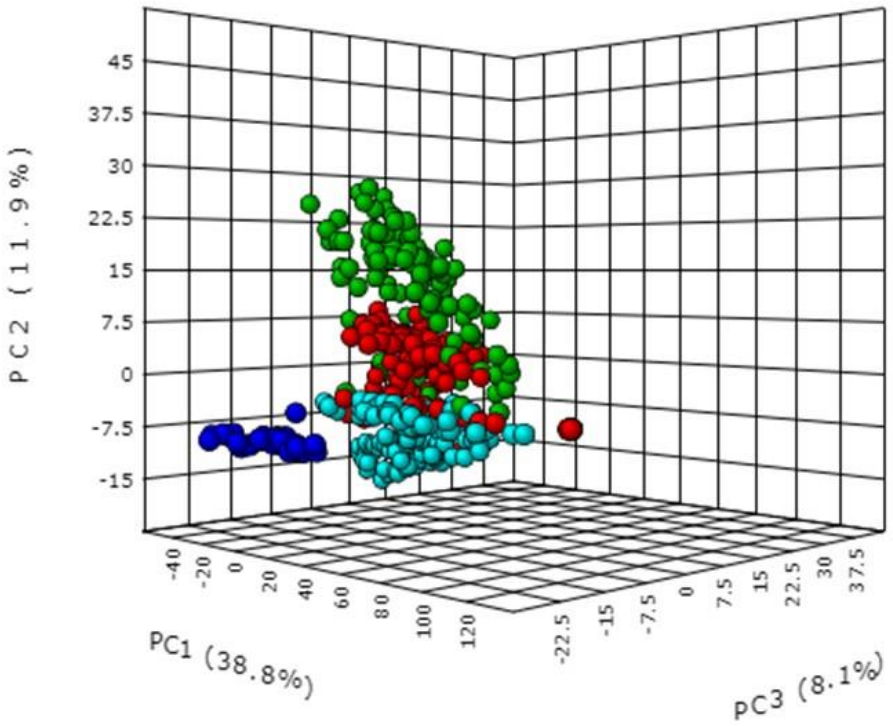

Supplementary Figure 4.1 3-D trajectory PCA plot showing QC clustering. Plot is derived from PCA of GC/MS spectra of all self-pairings and interspecific interactions at 15 °C (red), 25 °C (green) and with different pre-colonisation lengths (turquoise), and C8-C20 alkane standard QCs are shown (blue). The QC clustering indicated that the data was of sufficient quality to continue analysis. Subsequently, QCs were removed from the matrix and further statistical analysis carried out on the standardised binned data.

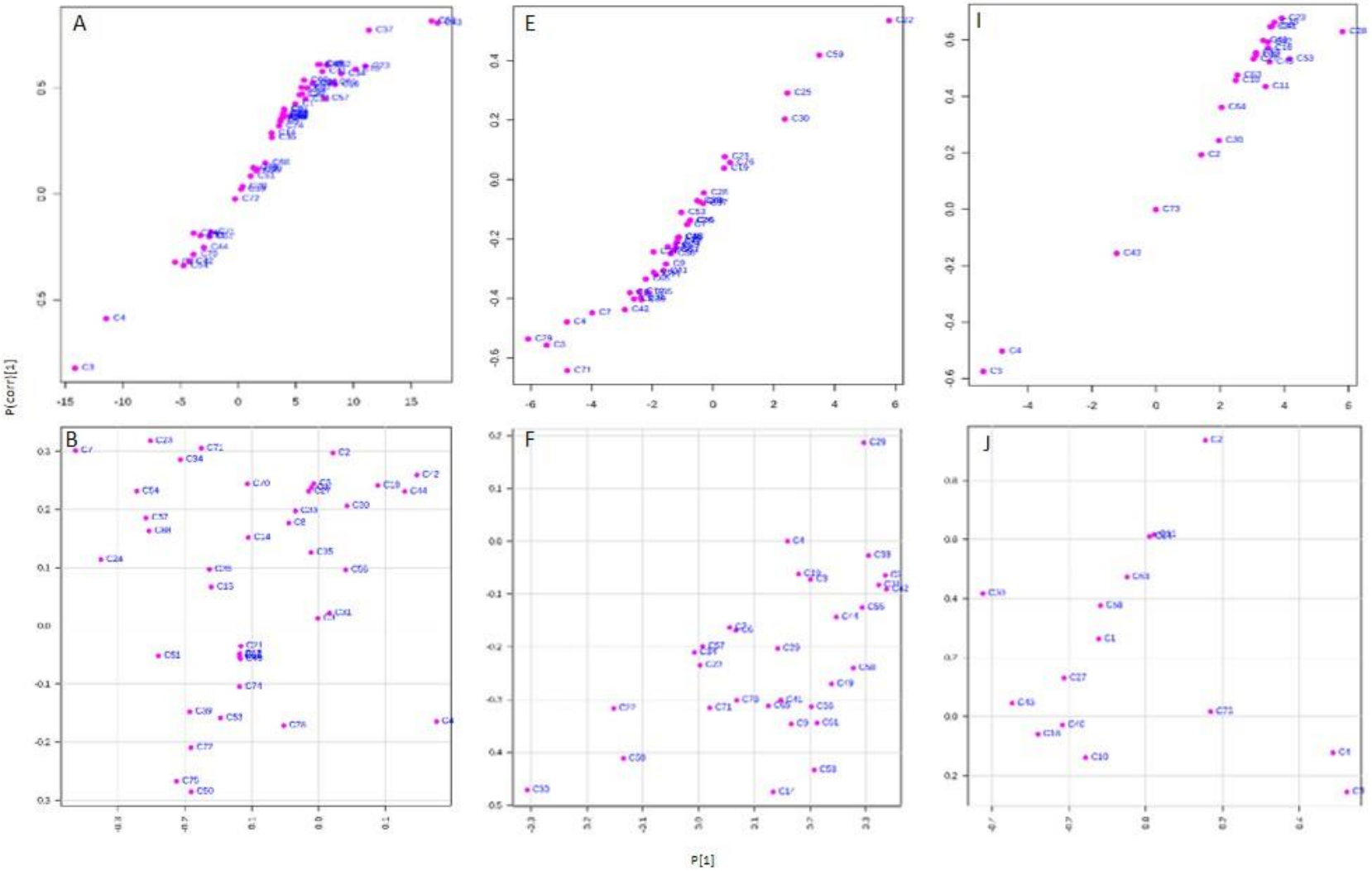

Supplementary Figure 4.2

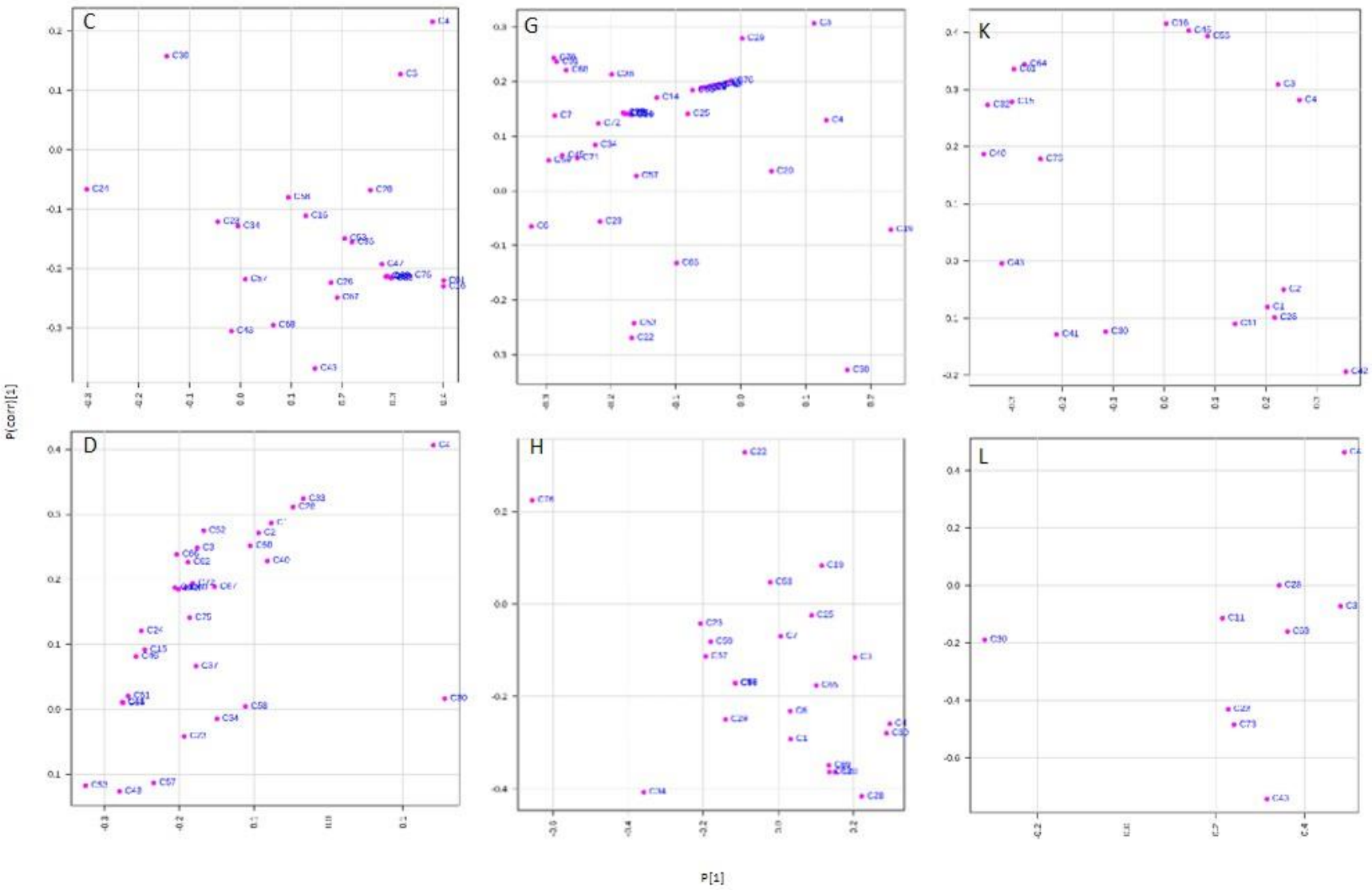

Supplementary Figure 4.2 *Continued*

Supplementary Figure 4.2 OPLS-DA loading plots of GC/MS mass spectra. A-D show the significant features (compounds) contributing to the separation of sample groups in the scores plots of 15 °C experimental samples in Figure 4.1A-D; E-H shows significant features contributing to the separation between sample groups in the scores plots of 25 °C experimental samples (Figure 4.1E-H); and I-L shows significant features contributing to the separation between sample groups in the scores plots of the pre-colonisation length experiment (Figure 4.2A-D). Features are labelled as per compounds in Table 4.2. Data were acquired from three independent biological replicates.

Appendix 4: Chapter 5 supplementary material

Supplementary Table 5.1 Fungal species, strain identification, and isolation information of experimental species.

Species	Ecological role	Strain ID	Source	Isolated
Stereum gausapatum	Primary coloniser	Sg1	Fruit body tissue	Unknown
Stereum hirsutum	Early secondary coloniser	ShSS1	Fruit body tissue	April 2011
Trametes versicolor	Early secondary coloniser	Tv CCJH1	Fruit body tissue	March 2011

Supplementary Table 5.2 Outcomes of mycelia interactions. Final occupant is expressed as an estimate of the percentage (to the nearest whole number) of each block occupied by individuals at the end of the experiment based on re-isolation outgrowth and normalised to the number of replicates. *Denotes interactions where vessels are laid parallel (5). Tv: *T. versicolor*, Sh: *S. hirsutum*, Sg: *S. gausapatum*.

		Final occupant of block (%)								
	Pattern	Block 1	Block 2	Block 3	Block 4	Block 5	Block 6	Block 7	Block 8	Block 9
(1) Pair-wise	a	Tv(100)	Tv(100)							
	a*	Tv(100)	Tv(75), Sg(25)							
	b	Tv(100)	Tv(72), Sh(28)							
	b*	Tv(100)	Tv(20), Sh(80)							
	c	Sg(100)	Sh(100)							
	c*	Sg(100)	Sh(100)							
(2) Three-way	d	Tv(100)	Tv(100)	Tv(19), Sh(81)						
	d*	Tv(100)	Tv(100)	Tv(13), Sh(87)						
	e	Tv(100)	Tv(100)	Tv(90), Sh(10)						
	e*	Tv(100)	Tv(100)	Tv(10), Sh(90)						
	f	Sg(100)	Tv(19), Sh(81)	Tv(100)						
	f*	Tv(15), Sg(85)	Tv(20), Sh(80)	Tv(100)						
(3) Nine-block	g	Tv(100)	Tv(85), Sh(15)	Tv(70), Sg(30)	Tv(65), Sh(35)	Tv(83), Sg(17)	Tv(100)	Tv(93), Sh(7)	Tv(100)	Tv(61), Sh(39)
	g*	Tv(100)	Tv(56), Sh(44)	Tv(90), Sg(10)	Tv(35), Sh(65)	Tv(52), Sg(48)	Tv(100)	Tv(69), Sg(29), Sh(2)	Tv(100)	Tv(29), Sh(71)
	h	Tv(100)	Tv(100)	Tv(54), Sh(46)	Tv(100)	Tv(80), Sh(20)	Tv(73), Sg(27)	Tv(66), Sh(34)	Tv(100)	Tv(100)
	h*	Tv(92), Sg(8)	Tv(100)	Tv(34), Sg(33), Sh(33)	Tv(100)	Tv(17), Sh(83)	Tv(75), Sg(25)	Tv(33), Sh(67)	Tv(67), Sg(33)	Tv(100)
	i	Tv(100)	Tv(92), Sh(8)	Tv(100)	Tv(92), Sh(8)	Tv(100)	Tv(83), Sh(17)	Tv(100)	Tv(96), Sh(4)	Tv(42), Sh(58)
	i*	Tv(86), Sh(14)	Tv(84), Sh(16)	Tv(100)	Tv(88), Sh(12)	Tv(100)	Tv(72), Sh(28)	Tv(100)	Tv(83), Sh(17)	Tv(69), Sh(31)

Supplementary Table 5.2 *Continued*

		Final occupant of block (%)											
	Pattern	Block 1	Block 2	Block 3	Block 4	Block 5	Block 6	Block 7	Block 8	Block 9	Block 10	Block 11	Block 12
(4) 27-block	j	Tv(83), Sh(17)	Tv(90), Sg(10)	Tv(100)	Tv(98), Sg(2)	Tv(100)	Tv(61), Sh(39)	Tv(100)	Tv(91), Sh(9)	Tv(55), Sg(45)	Tv(100)	Tv(100)	Tv(74), Sh(27)
	k	Tv(55), Sh(45)	Tv(100)	Tv(100)	Tv(100)	Tv(100)	Tv(70), Sh(30)	Tv(100)	Tv(90), Sh(10)	Tv(38), Sg(62)	Tv(100)	Tv(85), Sh(15)	Tv(50), Sg(50)
	l	Tv(100)	Tv(100)	Tv(100)	Tv(100)	Tv(100)	Tv(100)	Tv(100)	Tv(100)	Tv(100)	Tv(100)	Tv(100)	Tv(100)
(6) Nine-block	m	Sg(89), Sh(11)	Tv(67), Sg(11), Sh(22)	Tv(100)	Sg(100)	Tv(100)	Tv(78), Sh(22)	Sg(100)	Tv(60), Sh(40)	Tv(100)			
	n	Tv(10), Sg(90)	Tv(100)	Tv(66), Sh(34)	Tv(10), Sg(90)	Tv(80), Sh(20)	Tv(100)	Tv(10, Sg(90)	Tv(100)	Tv(45), Sh(55)			
(7) 27-block	o	Tv(100)	Tv(100)	Tv(100)	Tv(90), Sh(10)	Tv(100)	Tv(100)	Tv(100)	Tv(100)	Tv(100)	Tv(93), Sh(7)	Tv(100)	Tv(100)
	p	Tv(92), Sh(7)	Tv(100)	Tv(88), Sh(12)	Tv(100)	Tv(100)	Tv(100)	Tv(79), Sh(21)	Tv(100)	Tv(98), Sh(2)	Tv(100)	Tv(100)	Tv(100)

	Pattern	**Block 13**	**Block 14**	**Block 15**	**Block 16**	**Block 17**	**Block 18**	**Block 19**	**Block 20**	**Block 21**	**Block 22**	**Block 23**	**Block 24**	**Block 25**	**Block 26**	**Block 27**
(4)	j	Tv(100)	Tv(96), Sh(4)	Tv(95), Sg(5)	Tv(94), Sh(6)	Tv(100)	Tv(100)	Tv(100)	Tv(70), Sg(5), Sh(25)	Tv(46), Sg(54)	Tv(69), Sg(5), Sh(26)	Tv(76), Sg(24)	Tv(100)	Tv(99), Sg(1)	Tv(100)	Tv(81), Sh(19)
	k	Tv(100)	Tv(100)	Tv(100)	Tv(85), Sg(16)	Tv(100)	Tv(100)	Tv(100)	Tv(100)	Tv(80), Sh(20)	Tv(100)	Tv(95), Sh(5)	Tv(63, Sg(20), Sh(17)	Tv(88), Sh(12)	Tv(100)	Tv(100)
	l	Tv(100)	Tv(100)	Tv(100)	Tv(100)	Tv(100)	Tv(88), Sg(12)	Tv(100)	Tv(100)	Tv(100)	Tv(100)	Tv(100)	Tv(13), Sg(87)	Tv(100	Tv(100)	Tv(100)
(7)	o	Tv(100)	Tv(100)	Tv(100)	Tv(97), Sh(3)	Tv(100)	Tv(75), Sh(25)	Sg(100)	Sg(100)	Sg(100)	Sg(100)	Sg(100)	Sg(100)	Sg(100)	Sg(100)	Sg(100)
	p	Tv(84), Sh(16)	Tv(100)	Tv(68), Sh(32)	Tv(100)	Tv(98), Sh(2)	Tv(100)	Sg(100)	Sg(100)	Sg(100)	Sg(100)	Sg(100)	Sg(100)	Sg(100)	Sg(100)	Tv(5), Sg(95)

Supplementary Table 5.3 Mean % weight loss after 119 d of blocks following interactions between *T. versicolor*, *S. hirsutum* and *S. gausapatum*. The mean % weight loss of all blocks within an interaction colonised by individual species is given, as well as the mean total % weight loss for each interaction. Interactions are coded as per Fig. 1. * Denotes parallel vessel orientation.

	Mean % weight loss			
Interaction	*T. versicolor*	*S. hirsutum*	*S. gausapatum*	Total % loss
a	15.50	-	28.48	43.98
a*	19.17	-	25.01	44.18
b	19.19	12.93	-	32.12
b*	13.71	12.93	-	26.64
c	-	2.21	9.86	12.07
c*	-	2.21	11.80	14.01
d	9.89	-1.16	11.41	20.14
d*	17.03	15.40	20.61	53.04
e	27.91	17.76	24.39	70.05
e*	21.30	9.41	30.53	61.24
f	17.10	11.58	11.58	40.27
f*	21.20	15.93	10.01	47.15
g	17.32	17.68	24.77	59.78
g*	22.75	11.95	23.38	58.08
h	22.01	15.10	28.85	65.96
h*	27.93	17.06	28.66	73.65
i	17.33	11.90	18.45	47.68
i*	22.62	11.44	19.31	53.36
j	14.08	22.87	18.90	55.85
k	8.65	19.02	15.55	43.22
l	9.93	14.43	20.52	44.89
m	26.48	26.35	15.94	68.76
n	29.78	19.38	21.04	70.19
o	15.18	15.42	18.94	49.54
p	25.21	20.73	20.98	66.92

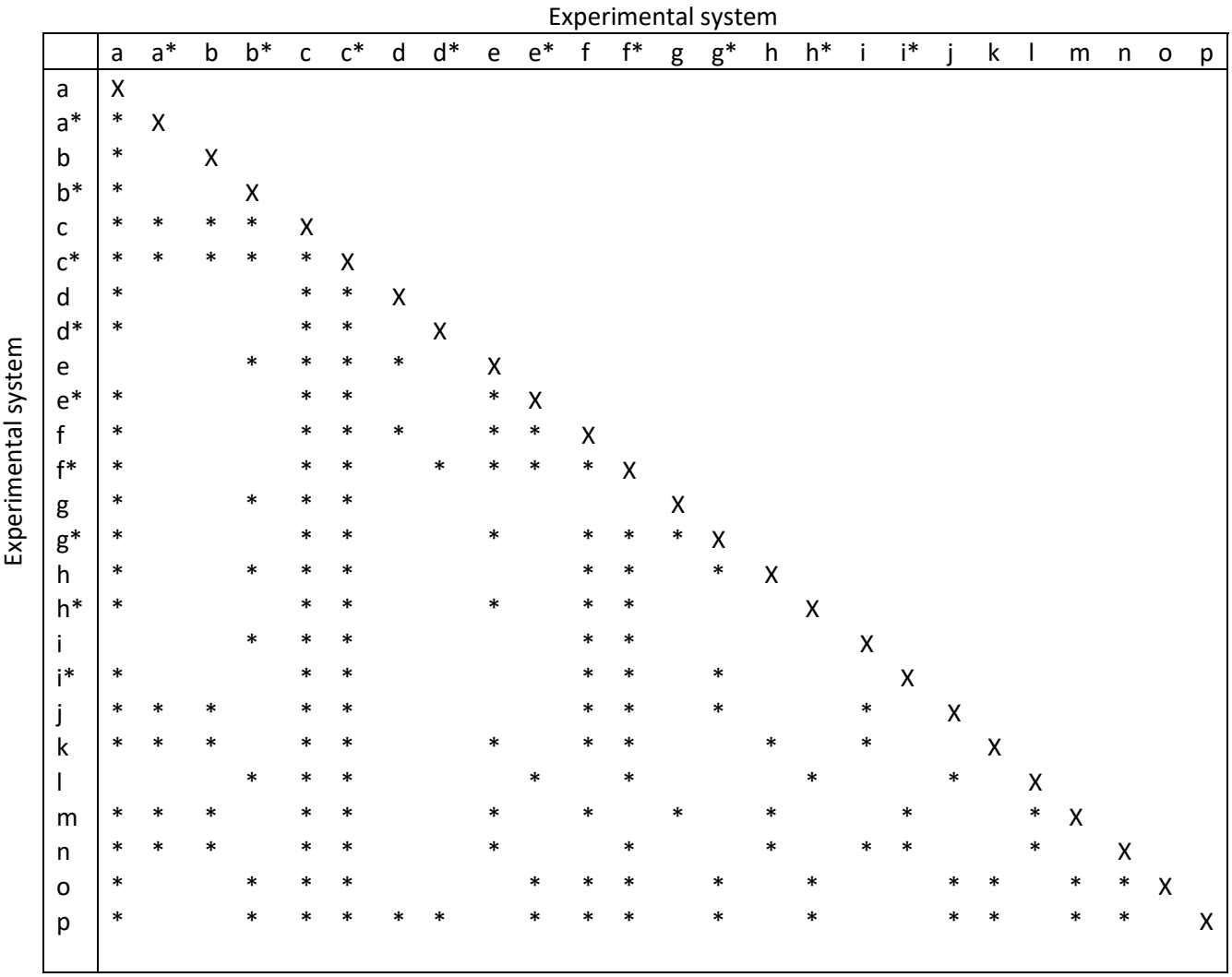

Supplementary Figure 5.1 Significant differences of species combative abilities between difference interactions. Experimental systems are labelled as in Figure 1 and (*) represents systems with vessels laid parallel. (*) within the matrix represents a significant difference ($p < 0.05$) between group means.

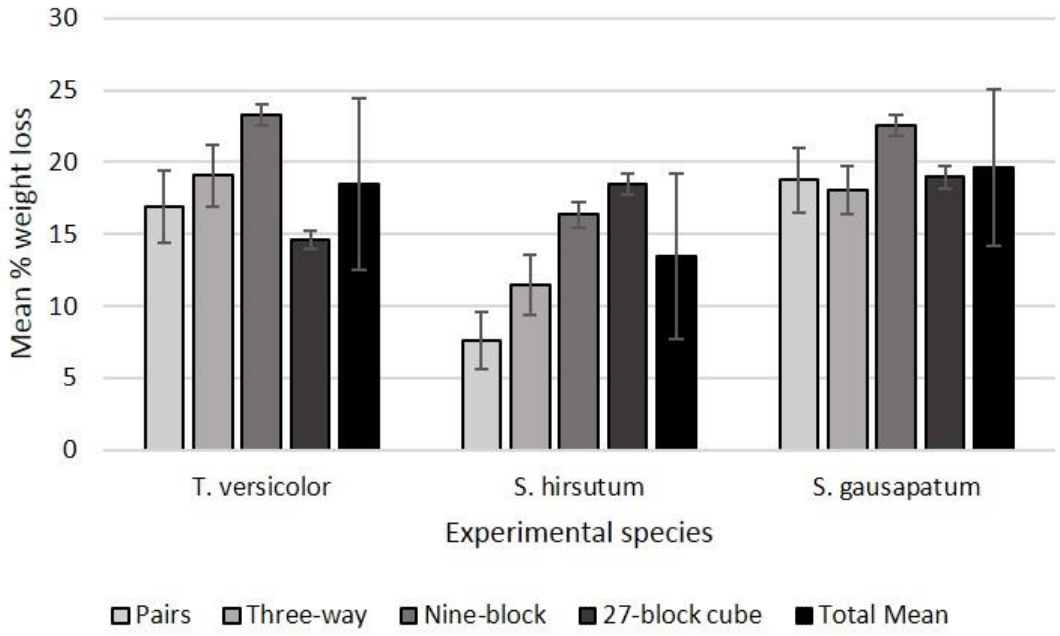

Supplementary Figure 5.2 Mean % weight loss of blocks colonised by individual fungi in pair-wise, three-block, nine-block and 27-block interactions. Error bars denote SEM.

Appendix 5: Chapter 6 supplementary material

Supplementary Table 6.1 Identity of blocks in pair-wise and 27-block interactions used for enzyme assays. Dark grey indicates *V. comedens* colonised blocks that were used for assays, and pale grey indicates *T. versicolor* colonised blocks used for assays. Numbers indicate block position within interactions. Vc: *V. comedens*, Hf: *H. fasciculare*, Tv: *T. versicolor*, self-cubes: 27-block cubes comprising each species singly, wall cubes: 27-block interactions where *V. comedens* occupied a larger adjacent volume, dispersal cubes: 27-block interactions where all fungi were evenly dispersed and no two blocks of the same species were in contact.

Interaction	Block number																										
	1	2	3	4	5	6	7	8	9	10	11	12	13	14	15	16	17	18	19	20	21	22	23	24	25	26	27
Vc-Hf	Vc	Hf																									
Vc-Tv	Vc	Tv																									
Tv-Hf	Tv	Hf																									
Tv-Tv	Tv	Tv																									
Vc-Vc	Vc	Vc																									
Hf-Hf	Hf	Hf																									
Tv self-cubes	Tv1	Tv2	Tv3	Tv4	Tv5	Tv6	Tv7	Tv8	Tv9	Tv10	Tv11	Tv12	Tv13	Tv14	Tv15	Tv16	Tv17	Tv18	Tv19	Tv20	Tv21	Tv22	Tv23	Tv24	Tv25	Tv26	Tv27
Hf self-cubes	Hf1	Hf2	Hf3	Hf4	Hf5	Hf6	Hf7	Hf8	Hf9	Hf10	Hf11	Hf12	Hf13	Hf14	Hf15	Hf16	Hf17	Hf18	Hf19	Hf20	Hf21	Hf22	Hf23	Hf24	Hf25	Hf26	Hf27
Vc self-cubes	Vc1	Vc2	Vc3	Vc4	Vc5	Vc6	Vc7	Vc8	Vc9	Vc10	Vc11	Vc12	Vc13	Vc14	Vc15	Vc16	Vc17	Vc18	Vc19	Vc20	Vc21	Vc22	Vc23	Vc24	Vc25	Vc26	Vc27
Wall cubes	Hf1	Tv2	Hf3	Tv4	Hf5	Tv6	Vc7	Vc8	Vc9	Tv10	Hf11	Tv12	Hf13	Tv14	Hf15	Vc16	Vc17	Vc18	Hf19	Tv20	Hf21	Tv22	Hf23	Tv24	Vc25	Vc26	Vc27
Dispersal cubes	Hf1	Vc2	Tv3	Vc4	Tv5	Hf6	Tv7	Hf8	Vc9	Vc10	Tv11	Hf12	Tv13	Hf14	Vc15	Hf16	Vc17	Tv18	Tv19	Hf20	Vc21	Hf22	Vc23	Tv24	Vc25	Tv26	Hf27

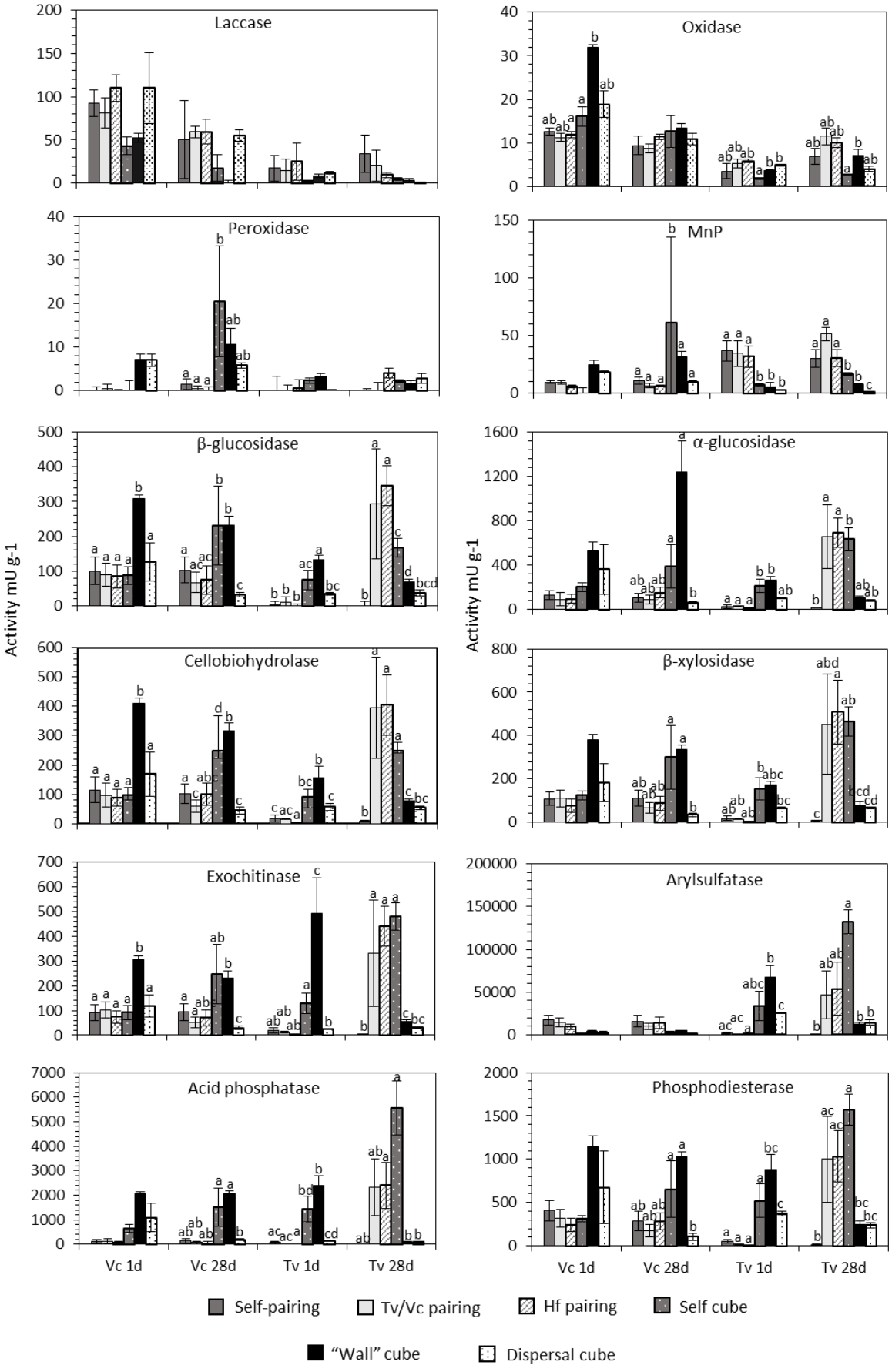

Supplementary Figure 6.1

Supplementary Figure 6.1 Extracellular enzyme activity in *V. comedens* (Vc) and *T. versicolor* (Tv) blocks from pair-wise and 27-block interactions 1 d and 28 d after interaction set up. Bars are the mean activity of five and 15 replicates in pair-wise and 27-block interactions respectively ± SEM. Different letters indicate a significant difference ($p > 0.05$) in activity between interactions. Statistical comparisons were made separately for each enzyme, competitor and time point, and no letters indicates no significant differences ($p > 0.05$).

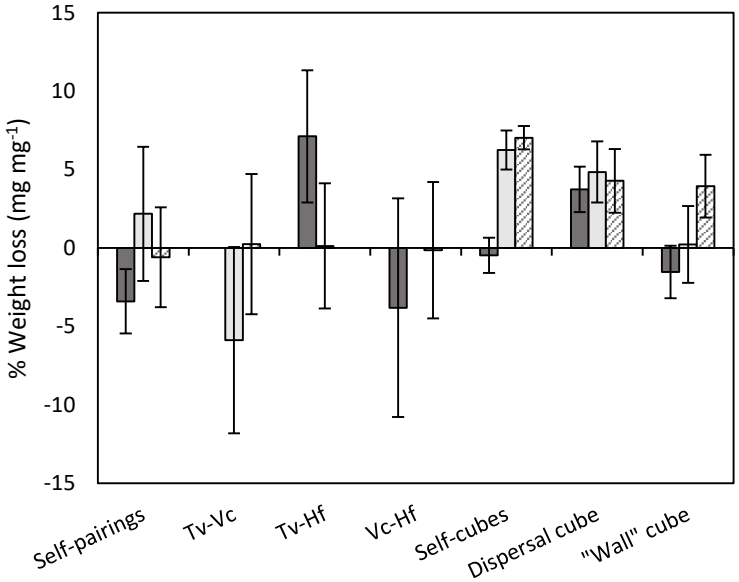

Supplementary Figure 6.2 Percentage weight loss of individual species blocks after 28 d compared to weight at the start of the experiment. Bars are the mean of all blocks per species per interaction sampled, with SEM. Dark grey: *H. fasciculare* (Hf); pale grey: *T. versicolor* (Tv); stripped: *V. comedens* (Vc).

Appendix 6: Chapter 7 supplementary material

Supplementary Table 7.1 Significant compounds (ANOVA: $p < 0.05$) in pair-wise experimental samples identified from the OPLS-DA modelled covariance and correlation (loadings plot). The test statistic f value, *p* value and 5% Benjamini-Hochberg false discovery rate (FDR) correction is given. Compounds are listed in order of significance.

	f value	*p* value	-log10(*p* value)	FDR
c21	200.95	7.70E-21	20.113	2.85E-19
c57	168.5	6.16E-20	19.21	1.14E-18
c5	144.69	3.71E-19	18.431	4.57E-18
c45	134.88	8.46E-19	18.073	7.82E-18
c55	127.46	1.64E-18	17.784	1.22E-17
c29	123.33	2.42E-18	17.617	1.49E-17
c14	114.83	5.58E-18	17.253	2.95E-17
c64	111.89	7.56E-18	17.121	3.50E-17
c25	101.89	2.25E-17	16.647	9.21E-17
c43	101.03	2.49E-17	16.604	9.21E-17
c10	94.18	5.64E-17	16.249	1.90E-16
c60	88.482	1.16E-16	15.934	3.59E-16
c59	85.626	1.70E-16	15.768	4.85E-16
c41	83.236	2.37E-16	15.626	5.84E-16
c48	83.229	2.37E-16	15.626	5.84E-16
c4	82.101	2.77E-16	15.557	6.17E-16
c38	81.853	2.87E-16	15.542	6.17E-16
c27	81.549	3.00E-16	15.523	6.17E-16
c8	74.435	8.62E-16	15.065	1.68E-15
c35	72.233	1.22E-15	14.914	2.23E-15
c3	72.005	1.26E-15	14.898	2.23E-15
c28	71.327	1.41E-15	14.851	2.37E-15
c19	71.061	1.47E-15	14.832	2.37E-15
c18	66.244	3.30E-15	14.482	5.08E-15
c9	65.441	3.79E-15	14.421	5.62E-15
c63	63.089	5.77E-15	14.239	8.22E-15
c33	58.37	1.40E-14	13.852	1.93E-14
c42	55.866	2.32E-14	13.635	3.06E-14
c36	53.222	4.02E-14	13.395	5.13E-14
c62	51.6	5.72E-14	13.243	7.05E-14
c13	47.599	1.43E-13	12.846	1.70E-13
c47	43.17	4.28E-13	12.369	4.95E-13
c32	42.414	5.22E-13	12.283	5.85E-13
c54	31.57	1.38E-11	10.86	1.50E-11
c51	31.252	1.54E-11	10.812	1.63E-11
c17	28.386	4.40E-11	10.357	4.52E-11
c65	27.854	5.40E-11	10.268	5.40E-11

Supplementary Table 7.2 Significant compounds (ANOVA: $p < 0.05$) in 27-block experimental samples identified from the OPLS-DA modelled covariance and correlation (loadings plot). The test statistic f value, *p* value and 5% Benjamini-Hochberg false discovery rate (FDR) correction is given. Compounds are listed in order of significance.

	f value	*p* value	-log10(*p* value)	FDR
c60	789.62	1.64E-23	22.784	7.72E-22
c29	282.4	4.49E-19	18.348	1.06E-17
c44	164.13	9.49E-17	16.023	1.49E-15
c49	142.04	3.92E-16	15.407	4.60E-15
c4	117.26	2.55E-15	14.593	2.40E-14
c22	114.86	3.12E-15	14.505	2.45E-14
c3	111.47	4.18E-15	14.379	2.77E-14
c63	110.11	4.71E-15	14.327	2.77E-14
c24	107.47	5.97E-15	14.224	3.12E-14
c12	101.4	1.05E-14	13.978	4.94E-14
c34	88.02	4.14E-14	13.383	1.77E-13
c25	80.785	9.49E-14	13.023	3.72E-13
c27	77.446	1.43E-13	12.846	5.15E-13
c20	75.957	1.72E-13	12.765	5.77E-13
c28	75.087	1.92E-13	12.717	6.02E-13
c6	66.15	6.48E-13	12.188	1.80E-12
c66	66.12	6.51E-13	12.187	1.80E-12
c56	59.527	1.77E-12	11.751	4.63E-12
c13	57.995	2.27E-12	11.643	5.63E-12
c2	57.371	2.52E-12	11.598	5.73E-12
c51	57.277	2.56E-12	11.592	5.73E-12
c46	55.921	3.22E-12	11.493	6.80E-12
c62	55.715	3.33E-12	11.478	6.80E-12
c26	52.702	5.64E-12	11.249	1.10E-11
c31	51.07	7.60E-12	11.119	1.43E-11
c5	49.779	9.67E-12	11.014	1.75E-11
c30	47.623	1.47E-11	10.833	2.56E-11

Supplementary Table 7.2 *Continued*

	f value	p value	-log10(p value)	FDR
c23	46.587	1.81E-11	10.743	2.93E-11
c39	43.987	3.10E-11	10.509	4.85E-11
c65	42.196	4.57E-11	10.34	6.92E-11
c61	42	4.77E-11	10.322	7.01E-11
c14	40.633	6.49E-11	10.187	9.25E-11
c50	39.763	7.94E-11	10.1	1.10E-10
c11	38.735	1.01E-10	9.9943	1.36E-10
c41	37.216	1.47E-10	9.8331	1.92E-10
c40	36.628	1.70E-10	9.7691	2.16E-10
c59	34.234	3.17E-10	9.4984	3.93E-10
c57	33.176	4.24E-10	9.3731	5.10E-10
c53	30.065	1.04E-09	8.9825	1.22E-09
c21	23.946	8.06E-09	8.0938	9.24E-09
c67	21.377	2.19E-08	7.6589	2.45E-08
c7	15.472	3.50E-07	6.4565	3.82E-07
c37	15.267	3.91E-07	6.408	4.18E-07
c18	12.171	2.48E-06	5.6052	2.59E-06
c52	11.094	5.16E-06	5.2876	5.27E-06
c8	5.5994	0.000662	3.1792	0.000662

Supplementary Table 7.3 Average percentage abundance from 3 replicates of each compound detected in pair-wise interactions, ± SEM. Nd denotes compounds that were below the level of detection. Statistical differences were calculated for each compound and interaction separately and different letters indicate significant differences ($p < 0.05$) between means. Putative identification of compounds are given in Table 7.1. Tv: *T. versicolor*; Hf: *H. fasciculare*; Vc: *V. comedens.*

	Tv-Tv		Vc-Vc		Tv-Vc		Hf-Vc		Hf-Hf		Tv-Hf	
	1 d	28 d	1 d	28 d	1 d	28 d	1 d	28 d	1 d	28 d	1 d	28 d
c2	nd^a	nd^a	nd^a	nd^a	nd^a	nd^a	nd^a	nd^a	nd^a	0.3±0.1^a	nd^a	nd^a
c3	nd^a	nd^a	nd^a	nd^a	nd^a	nd^a	nd^a	nd^a	nd^a	0.8±0.1^b	nd^a	nd^a
c4	nd^a	nd^a	nd^a	nd^a	nd^a	4.5±2.2^b	nd^a	nd^a	nd^a	7.8±0.1^b	nd^a	1.5±1.0^b
c5	nd^a	nd^a	nd^a	nd^a	62.3±8.3^a	13.7±5.7^a	nd^a	nd^a	nd^a	73.7±0.1^b	83.1±7.4^b	4.3±3.2^a
c8	nd^a	1.3±0.3^b	nd^a	nd^a	0.1±0.0^a	0.4±0.1^b	nd^a	1.5±0.2^b	nd^a	0.7±0.2^b	nd^a	1.6±0.7^b
c9	nd^a	nd^a	nd^a	nd^a	nd^a	nd^a	nd^a	nd^a	nd^a	nd^a	0.4±0.2^b	nd^a
c10	nd^a	12.5±3.8^b	nd^a	nd^a	nd^a	nd^a	nd^a	nd^a	nd^a	nd^a	nd^a	nd^a
c13	nd^a	nd^a	nd^a	nd^a	nd^a	3.3±1.6^b	nd^a	nd^a	nd^a	nd^a	nd^a	nd^a
c14	nd^a	nd^a	nd^a	23.1±6.5^b	nd^a	nd^a	nd^a	nd^a	nd^a	nd^a	nd^a	nd^a
c17	nd^a	nd^a	nd^a	nd^a	nd^a	nd^a	nd^a	0.5±0.4^a	nd^a	nd^a	0.5±0.1^b	nd^a
c18	nd^a	22.1±5.2^b	4.5±0.7^b	nd^a	nd^a	5.3±2.1^b	33.3±33.3^b	1.3±0.4^a	nd^a	nd^a	nd^a	nd^a
c19	nd^a	nd^a	nd^a	nd^a	nd^a	2.9±1.4^b	nd^a	nd^a	nd^a	nd^a	nd^a	nd^a
c21	nd^a	6.3±0.8^b	nd^a	11.2±1.7^b	nd^a	4.9±0.5^b	nd^a	15.4±1.7^b	nd^a	6.6±1.7^b	nd^a	13.5±2.8^b
c25	nd^a	21.9±4.4^b	nd^a	nd^a	nd^a	nd^a	nd^a	1.2±0.6^b	nd^a	nd^a	nd^a	nd^a
c27	nd^a	nd^a	nd^a	nd^a	nd^a	4.6±1.7^b	nd^a	nd^a	nd^a	nd^a	nd^a	nd^a
c28	nd^a	nd^a	nd^a	nd^a	nd^a	1.0±0.3^b	nd^a	nd^a	nd^a	nd^a	nd^a	nd^a
c29	nd^a	19.5±1.7^b	95.0±0.8^b	nd^a	nd^a	3.9±1.5^b	nd^a	9.1±4.2^b	88.4±3.3^b	nd^a	nd^a	8.2±4.8^b
c32	nd^a	nd^a	nd^a	nd^a	0.3±0.1^b	nd^a	nd^a	nd^a	nd^a	nd^a	nd^a	nd^a

Supplementary Table 7.3 *Continued*

	Tv-Tv		Vc-Vc		Tv-Vc		Hf-Vc		Hf-Hf		Tv-Hf	
	1 d	28 d	1 d	28 d	1 d	28 d	1 d	28 d	1 d	28 d	1 d	28 d
c33	nd[a]	0.1±0.0[a]	nd[a]	nd[a]	nd[a]	nd[a‡]	nd[a]	nd[a]	nd[a]	nd[a]	nd[a]	nd[a]
c35	nd[a]	nd[a]	nd[a]	nd[a]	nd[a]	0.4±0.2[b]	nd[a]	nd[a]	nd[a]	0.9±0.1[b]	nd[a]	nd[a]
c36	nd[a]	nd[a]	nd[a]	nd[a]	nd[a]	nd[a]	nd[a]	nd[a]	nd[a]	0.1±0.0[b]	nd[a]	nd[a]
c38	nd[a]	nd[a]	nd[a]	nd[a]	0.6±0.2[b]	nd[a]	nd[a]	nd[a]	nd[a]	nd[a]	nd[a]	nd[a]
c41	nd[a]	nd[a]	nd[a]	nd[a]	nd[a]	27.1±14.1[b]	nd[a]	9.6±2.4[b]	nd[a]	nd[a]	nd[a]	8.5±4.5[b]
c42	nd[a]	nd[a]	0.2±0.1[b]	nd[a]	nd[a]	nd[a]	nd[a]	nd[a]	nd[a]	nd[a]	nd[a]	nd[a]
c43	nd[a]	nd[a]	nd[a]	nd[a]	5.6±1.5[b]	nd[a]	nd[a]	nd[a]	nd[a]	nd[a]	nd[a]	nd[a]
c45	nd[a]	nd[a]	nd[a]	nd[a]	11.8±4.6[b]	nd[a]	nd[a]	nd[a]	nd[a]	nd[a]	6.2±1.9[b]	nd[a]
c47	nd[a]	2.6±1.5[b]	nd[a]	nd[a]	nd[a]	nd[a]	nd[a]	nd[a]	nd[a]	nd[a]	nd[a]	nd[a]
c48	nd[a]	nd[a]	nd[a]	nd[a]	0.5±0.1[b]	nd[a]	nd[a]	nd[a]	nd[a]	nd[a]	nd[a]	nd[a]
c51	nd[a]	nd[a]	nd[a]	nd[a]	nd[a]	nd[a]	nd[a]	nd[a]	nd[a]	nd[a]	1.0±0.5[b]	nd[a]
c54	nd[a]	4.2±2.7[b]	nd[a]	2.0±0.5[b]	0.3±0.0[a]	5.0±2.5[b]	nd[a]	1.6±1.2[a]	nd[a]	1.7±0.4[b]	0.1±0.1	4.1±1.7[b]
c55	nd[a]	nd[a]	nd[a]	5.1±2.2[b]	nd[a]	4.6±2.1[b]	nd[a]	33.0±7.8[b]	nd[a]	nd[a]	nd[a]	18.6±8.7[b]
c57	nd[a]	6.6±2.2[b]	nd[a]	56.9±7.7[b]	nd[a]	14.0±5.4[b]	nd[a]	18.7±4.8[b]	nd[a]	7.0±1.6[b]	nd[a]	36.2±12.1[b]
c58	nd[a]	nd[a]	nd[a]	nd[a]	0.1±0.0[a]	nd[a]	nd[a]	nd[a]	nd[a]	nd[a]	nd[a]	nd[a]
c59	nd[a]	nd[a]	nd[a]	nd[a]	nd[a]	1.5±0.4[b]	nd[a]	4.9±0.8[b]	nd[a]	0.2±0.1[b]	nd[a]	2.3±1.2[b]
c60	nd[a]	nd[a]	nd[a]	nd[a]	nd[a]	nd[a]	nd[a]	nd[a]	11.6±3.3[b]	nd[a]	nd[a]	nd[a]
c62	nd[a]	nd[a]	nd[a]	nd[a]	nd[a]	nd[a]	nd[a]	nd[a]	nd[a]	0.1±0.0[b]	nd[a]	nd[a]
c63	nd[a]	nd[a]	nd[a]	nd[a]	nd[a]	nd[a]	nd[a]	nd[a]	nd[a]	0.2±0.0[b]	nd[a]	nd[a]
c64	nd[a]	nd[a]	nd[a]	nd[a]	18.2±4.4[b]	nd[a]	nd[a]	nd[a]	nd[a]	nd[a]	8.8±6.0[b]	nd[a]
c65	nd[a]	0.6±0.2[a]	nd[a]	nd[a]	0.3±0.2[a]	0.5±0.1[a]	nd[a]	1.0±0.5[a]	nd[a]	nd[a]	nd[a]	nd[a]

Supplementary Table 7.4 Average percentage abundance from 3 replicates of each compound detected in 27-block interactions, ± SEM. Nd denotes compounds that were below the level of detection. Statistical differences were calculated for each compound and interaction separately, different letters indicate significant differences ($p < 0.05$) between means and (‡) indicates a significant difference between corresponding "wall" and dispersal cube sample groups. Putative identification of compounds are given in Table 7.1. Tv: *T. versicolor*; Hf: *H. fasciculare*; Vc: *V. comedens*.

	Hf cube		Tv cube		Vc cube		Wall cube		Dispersal cube	
	1 d	28 d	1 d	28 d	1 d	28 d	1 d	28 d	1 d	28 d
c1	nd^{a}	nd^{a}	nd^{a}	nd^{a}	0.1±0.0^{b}	nd^{a}	nd^{a}	nd^{a}	nd^{a}	nd^{a}
c2	nd^{a}	nd^{a}	0.9±0.1^{b}	nd^{a}	0.2±0.1^{b}	nd^{a}	1.3±0.1^{a}	0.5±0.1^{a}	0.6±0.1^{a}	0.9±0.4^{a}
c3	nd^{a}	nd^{a}	3.8±0.5^{b}	nd^{a}	15.8±0.4^{b}	0.6±0.1^{a}	9.8±1.2^{b}	0.5±0.1^{a}	6.2±0.6^{b}	0.3±0.1^{a}
c4	1.4±0.4	1.6±0.5	19.8±0.9^{b}	nd^{a}	10.7±0.6^{a}	6.5±1.1^{a}	nd^{a‡}	11.3±0.7^{b‡}	21.6±1.5^{b‡}	1.7±0.5^{a‡}
c5	29.1±1.2	21.8±7.1	39.3±2.2^{b}	nd^{a}	51.4±2.6^{a}	64.2±6.1^{a}	60.0±0.5^{a}	46.0±2.6^{a‡}	45.6±4.5^{b}	4.2±0.9^{a‡}
c6	nd^{a}	nd^{a}	0.2±0.3^{a}	nd^{a}	nd^{a}	nd^{a}	0.5±0.2^{b}	nd^{a}	0.7±0.3^{b}	nd^{a}
c7	nd^{a}	nd^{a}	0.1±0.0^{a}	nd^{a}	0.0±0.0^{a}	nd^{a}	0.1±0.0^{b}	nd^{a‡}	0.1±0.0^{a}	0.1±0.1^{a‡}
c8	0.8±0.0	nd^{a}	0.1±0.0^{a}	nd^{a}	nd^{a}	1.8±0.8^{a}	0.1±0.0^{a}	0.1±0.1^{a}	0.1±0.1^{a}	0.0±0.0^{a}
c11	nd^{a}	nd^{a}	nd^{a}	nd^{a}	nd^{a}	0.1±0.0^{a}	0.1±0.0^{b}	nd^{a}	0.0±0.0^{a}	nd^{a}
c12	nd^{a}	nd^{a}	3.5±0.6^{b}	nd^{a}	0.0±0.0^{a}	nd^{a}	4.1±0.7^{b‡}	nd^{a}	nd^{a‡}	nd^{a}
c13	nd^{a}	nd^{a}	nd^{a}	nd^{a}	0.3±0.1^{a}	nd^{a}	1.1±0.7^{a}	1.8±0.6^{a}	1.4±0.3^{a}	4.8±0.4^{a}
c14	1.0±0.2	nd^{a}	0.1±0.0^{a}	nd^{a}	0.1±0.0^{a}	nd^{a}	0.2±0.1^{b}	nd^{a}	0.1±0.1^{b}	nd^{a}
c15	1.5±0.4	nd^{a}	nd^{a}	nd^{a}	nd^{a}	nd^{a}	nd^{a}	nd^{a}	nd^{a}	nd^{a}
c16	nd^{a}	nd^{a}	nd^{a}	nd^{a}	0.1±0.0^{a}	nd^{a}	0.4±0.1^{b}	nd^{a}	nd^{a}	nd^{a}
c18	nd^{a}	nd^{a}	nd^{a}	nd^{a}	nd^{a}	nd^{a}	0.1±0.1^{a‡}	0.3±0.1^{a‡}	nd^{a‡}	nd^{a‡}
c20	3.3±0.4	nd^{a}	0.2±0.0^{a}	nd^{a}	0.2±0.0^{b}	nd^{a}	0.7±0.2^{b‡}	nd^{a}	nd^{a‡}	nd^{a}
c21	32.7±7.7	0.6±0.3	2.2±0.7^{b}	nd^{a}	4.2±0.4^{a}	12.9±2.5^{a}	1.0±0.2^{a}	5.5±1.3^{a‡}	4.5±1.3^{b}	0.3±0.0^{a‡}
c22	nd^{a}	24.3±6.2	0.3±0.1^{a}	nd^{a}	nd^{a}	nd^{a}	0.3±0.0^{b}	nd^{a}	0.2±0.0^{b}	nd^{a}
c23	nd^{a}	0.3±0.1	nd^{a}	nd^{a}	nd^{a}	nd^{a}	nd^{a}	nd^{a‡}	nd^{a}	0.1±0.1^{b‡}
c24	nd^{a}	nd^{a}	2.2±0.4^{b}	nd^{a}	nd^{a}	nd^{a}	1.6±0.5^{b}	nd^{a}	1.5±0.3^{b}	nd^{a}
c25	0.5±0.1	5.5±2.0	0.0±0.0^{a}	nd^{a}	nd^{a}	nd^{a}	nd^{a}	nd^{a}	nd^{a}	nd^{a}
c26	nd^{a}	nd^{a}	0.2±0.1^{a}	nd^{a}	nd^{a}	nd^{a}	0.3±0.1^{b}	nd^{a}	0.1±0.0^{b}	nd^{a}
c27	nd^{a}	nd^{a}	nd^{a}	nd^{a}	0.1±0.0^{a}	0.4±0.2^{a}	nd^{a‡}	5.2±1.8^{b}	0.1±0.0^{a‡}	24.3±0.5^{b}
c28	nd^{a}	nd^{a}	nd^{a}	nd^{a}	nd^{a}	nd^{a}	nd^{a}	nd^{a‡}	nd^{a}	0.7±0.0^{b‡}
c29	10.2±2.3	17.9±0.8	nd^{a}	nd^{a}	1.8±0.1^{a}	13.5±3.9^{b}	nd^{a}	26.1±1.7^{b}	nd^{a}	46.7±0.7^{b}
c30	nd^{a}	nd^{a}	nd^{a}	nd^{a}	nd^{a}	nd^{a}	nd^{a}	0.4±0.2^{b‡}	nd^{a}	nd^{a‡}
c31	nd^{a}	nd^{a}	nd^{a}	nd^{a}	0.4±0.1^{b}	nd^{a}	nd^{a}	nd^{a}	nd^{a}	nd^{a}
c33	nd^{a}	nd^{a}	nd^{a}	nd^{a}	nd^{a}	nd^{a}	nd^{a}	0.0±0.0^{a}	nd^{a}	nd^{a}

Supplementary Table 7.4 *Continued*

	Hf cube		Tv cube		Vc cube		Wall cube		Dispersal cube	
	1 d	28 d	1 d	28 d	1 d	28 d	1 d	28 d	1 d	28 d
c37	nd[a]	nd[a]	0.0±0.0[a]	nd[a]	0.1±0.0[a]	nd[a]	0.3±0.0[b]	nd[a]	0.1±0.1[b]	nd[a]
c39	nd[a]	nd[a]	0.5±0.2[a]	nd[a]	nd[a]	nd[a]	nd[a]	nd[a]	nd[a]	nd[a]
c40	0.3±0.0	nd[a]	0.1±0.0[a]	nd[a]	0.1±0.0[a]	nd[a]	0.1±0.0[b]	nd[a]	0.1±0.0[b]	nd[a]
c41	10.1±3.7	5.2±1.9	3.2±2.0[b]	nd[a]	3.4±1.7[b]	nd[a]	nd[a‡]	nd[a‡]	0.7±0.7[a‡]	1.4±0.4[a‡]
c44	nd[a]	nd[a]	14.2±3.2[b]	nd[a]	nd[a]	nd[a]	7.3±1.0[b]	nd[a]	10.3±2.8[b]	nd[a]
c46	1.5±0.4	nd[a]	0.1±0.0[a]	nd[a]	nd[a]	nd[a]	0.3±0.1[b]	nd[a]	0.1±0.1[b]	nd[a]
c49	nd[a]	nd[a]	5.2±1.0[b]	nd[a]	nd[a]	nd[a]	0.4±0.8[b]	nd[a]	2.9±0.5[b]	nd[a]
c50	nd[a]	nd[a]	nd[a]	nd[a]	0.0±0.0[a]	nd[a]	nd[a]	nd[a]	nd[a]	nd[a]
c51	nd[a]	nd[a]	0.3±0.1[a]	nd[a]	nd[a]	nd[a]	1.1±0.6[b]	nd[a]	1.0±0.3[b]	nd[a]
c52	nd[a]	nd[a]	0.1±0.1[a]	nd[a]	nd[a]	nd[a]	0.1±0.0[b]	nd[a‡]	0.0±0.0[a]	0.0±0.0[a‡]
c53	nd[a]	nd[a]	0.3±0.1[a]	nd[a]	nd[a]	nd[a]	0.2±0.1[b]	nd[a]	0.1±0.0[b]	nd[a]
c56	5.9±3.3	nd[a]	nd[a]	nd[a]	1.4±0.7[b]	nd[a]	nd[a]	nd[a]	nd[a]	nd[a]
c57	1.0±0.4	12.7±1.6	0.6±0.2[a]	nd[a]	0.1±0.0[a]	1.4±0.4[b]	nd[a‡]	0.5±0.3[b]	0.3±0.2[a‡]	3.2±1.1[b]
c59	0.6±0.5	nd[a]	nd[a]	nd[a]	nd[a]	nd[a]	nd[a]	nd[a‡]	nd[a]	0.1±0.0[b‡]
c60	nd[a]	10.0±0.2	0.7±0.1[b]	nd[a]	nd[a]	nd[a]	0.9±0.0[a]	1.7±0.2[a‡]	0.5±0.1[a]	6.3±0.6[b‡]
c61	nd[a]	nd[a]	nd[a]	nd[a]	0.2±0.1[b]	nd[a]	nd[a]	nd[a]	nd[a]	nd[a]
c62	0.0±0.0	nd[a]	nd[a]	nd[a]	0.8±0.0[b]	nd[a]	nd[a]	0.1±0.0[b]	nd[a]	0.2±0.1[b]
c63	nd[a]	nd[a]	nd[a]	nd[a]	2.1±0.1[b]	nd[a]	1.6±0.2[b‡]	nd[a]	nd[a‡]	nd[a]
c65	nd[a]	nd[a]	0.0±0.0[a]	nd[a]	0.3±0.0[b]	nd[a]	0.1±0.0[b‡]	nd[a‡]	0.8±0.2[a‡]	4.6±1.0[a‡]
c66	nd[a]	nd[a]	0.2±0.0[a]	nd[a]	nd[a]	nd[a]	0.3±0.0[b]	nd[a]	0.1±0.0[b]	nd[a]
c67	nd[a]	nd[a]	0.2±0.1[a]	nd[a]	nd[a]	nd[a]	nd[a]	nd[a]	nd[a]	nd[a]

Supplementary Table 7.5 SEM of the abundancies of highly significant compounds pair-wise interactions (A), and 27-block interactions (B) 1 d and 28 d after interaction set up. (C). Hf: *H. fasciculare*, Tv: *T. versicolor*, Vc: *V. comedens*. Mean abundancies of 3 replicates are shown in Figure 7.2 (A) and Figure 7.3 (B).

A

	c5	c21	c29	c45	c55	c57
Hf-Hf 1d	-	-	549.67	-		
Hf-Hf 28d	1014.51	837.80	-	-		329.32
Tv-Tv 1d	-	-	-	-		
Tv-Tv 28d	-	188.39	603.32	-		604.11
Vc-Vc 1d	-	-	2035.23	-		
Vc-Vc 28d	-	1570.07	-	-	257.46	3589.35
Tv-Hf 1d	7957.03	-	1558.65	-		
Tv-Hf 28d	369.73	1560.15	502.53	-	2458.43	1500.11
Hf-Vc 1d	-	-	-	-		
Hf-Vc 28d	-	692.46	137.03	-	1353.48	634.25
Tv-Vc 1d	2564.86	-	-	638.78		
Tv-Vc 28d	751.91	1344.13	386.00	-	970.60	3904.26

B

	c60	c29	c44	c49	c4	c22
Wall cubes 1d	82.52	-	2591.59	3096.92	-	131.39
Wall cubes 28d	365.08	2118.75	-	-	2284.37	-
Dispersal cubes 1d	862.38	0.00	8367.56	3251.92	5491.58	1217.65
Dispersal cubes 28d	977.33	1604.95	-	-	631.80	-
Hf cubes 1d	-	192.80	-	-	804.10	-
Hf cubes 28d	176.08	413.51	-	-	525.78	1227.77
Tv cubes 1d	2341.99	-	9622.61	5897.43	7496.74	1753.32
Tv cubes 28d	3498.64	-	-	-	-	-
Vc cubes 1d	-	976.24	-	-	1041.49	-
Vc cubes 28d	-	898.32	-	-	2097.16	-

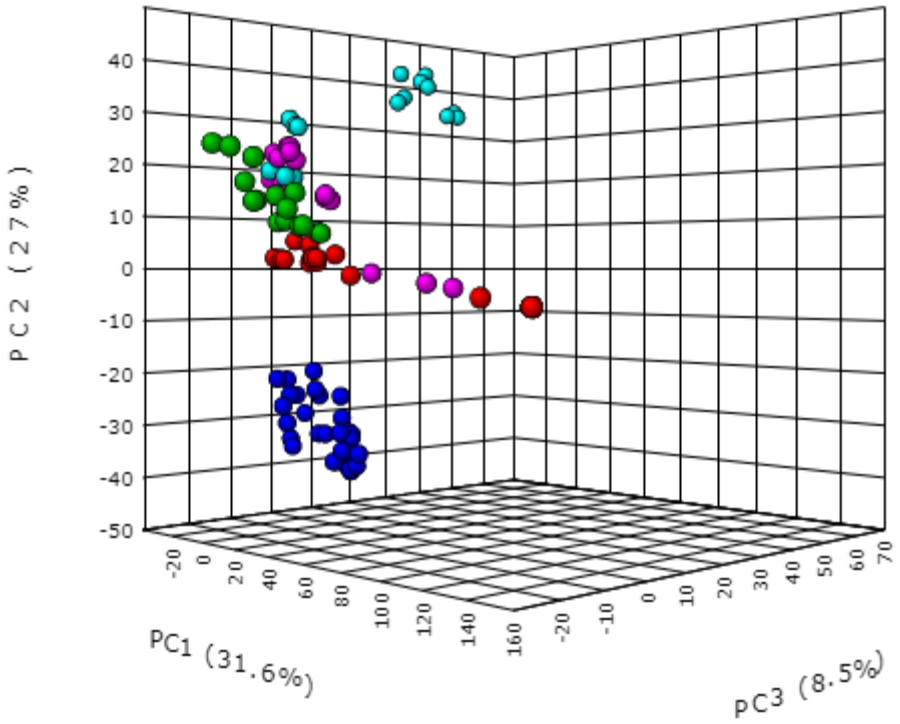

Supplementary Figure 7.1 3-D trajectory PCA plot showing quality control (QC) clustering. Plot is derived from PCA of GC/MS spectra of all pair-wise interactions 1d (red) and 28 d (green) after interaction set up, and 27-block interactions 1 d (turquoise) and 28 d (pink) after interaction set up, and C8-C20 alkane standard QCs are shown (blue). The QC clustering indicated that the data were of sufficient quality to continue analysis. Subsequently, QCs were removed from the matrix and further statistical analysis carried out on the standardised binned data.

Appendix 7: Chapter 8 supplementary material

Supplementary Table 8.1 Identity of blocks in pair-wise and 27-block interactions used for enzyme assays. Shading indicates *T. versicolor* colonised blocks that were used for metabolomics analysis. Numbers indicate block position within interactions. Vc: *V. comedens*, Hf: *H. fasciculare*, Tv: *T. versicolor*, self-cubes: 27-block cubes comprising each species singly, wall cubes: 27-block interactions where *V. comedens* occupied a larger adjacent volume, dispersal cubes: 27-block interactions where all fungi were evenly dispersed and no two blocks of the same species were in contact.

Interaction	Block number																										
	1	2	3	4	5	6	7	8	9	10	11	12	13	14	15	16	17	18	19	20	21	22	23	24	25	26	27
Vc-Hf	Vc	Hf																									
Vc-Tv	Vc	Tv																									
Tv-Hf	Tv	Hf																									
Tv-Tv	Tv	Tv																									
Vc-Vc	Vc	Vc																									
Hf-Hf	Hf	Hf																									
Tv self-cubes	Tv1	Tv2	Tv3	Tv4	Tv5	Tv6	Tv7	Tv8	Tv9	Tv10	Tv11	Tv12	Tv13	Tv14	Tv15	Tv16	Tv17	Tv18	Tv19	Tv20	Tv21	Tv22	Tv23	Tv24	Tv25	Tv26	Tv27
Hf self-cubes	Hf1	Hf2	Hf3	Hf4	Hf5	Hf6	Hf7	Hf8	Hf9	Hf10	Hf11	Hf12	Hf13	Hf14	Hf15	Hf16	Hf17	Hf18	Hf19	Hf20	Hf21	Hf22	Hf23	Hf24	Hf25	Hf26	Hf27
Vc self-cubes	Vc1	Vc2	Vc3	Vc4	Vc5	Vc6	Vc7	Vc8	Vc9	Vc10	Vc11	Vc12	Vc13	Vc14	Vc15	Vc16	Vc17	Vc18	Vc19	Vc20	Vc21	Vc22	Vc23	Vc24	Vc25	Vc26	Vc27
Wall cubes	Hf1	Tv2	Hf3	Tv4	Hf5	Tv6	Vc7	Vc8	Vc9	Tv10	Hf11	Tv12	Hf13	Tv14	Hf15	Vc16	Vc17	Vc18	Hf19	Tv20	Hf21	Tv22	Hf23	Tv24	Vc25	Vc26	Vc27
Dispersal cubes	Hf1	Vc2	Tv3	Vc4	Tv5	Hf6	Tv7	Hf8	Vc9	Vc10	Tv11	Hf12	Tv13	Hf14	Vc15	Hf16	Vc17	Tv18	Tv19	Hf20	Vc21	Hf22	Vc23	Tv24	Vc25	Tv26	Hf27

Supplementary Table 8.2 Fold changes of the 35 most significant metabolites (ANOVA: $p < 0.001$) produced by *T. versicolor* (Tv) when paired against *H. fasciculare* (Hf). Fold changes are calculated as the ratio of the metabolite intensity (mean of 5 biological replicates) between the *T. versicolor* self-pairing after 1 d, and the *T. versicolor* and *H. fasiculare* interaction 1 d and 28 d after interaction set up. Log_2 of the fold change was calculated for enhanced visualisation of the largest intensity differences (positive and negative values represent increased and decreased production respectively). For metabolites that have been putatively identified, KEGG registry numbers and ion forms are given. Full metabolic peak list with fold changes between each pair-wise group is given in Supplementary Table 8.6.

				Fold change (FC)			
				Tv-Hf 1 d		Tv-Hf 28 d	
Metabolite	**m/z**	**Kegg number**	**Ion form**	**FC**	**log_2(FC)**	**FC**	**log_2(FC)**
Swainsonine	174.11	C10173	1 [M+H]+	-0.14	-2.86+4.53i	1.39	0.47
?	192.12	-	-	-0.38	-1.38+4.53i	1.53	0.61
Pantothenol	206.14	C05944	[M+H]+	-0.43	-1.20+4.53i	1.52	0.6
?	306.26	-	-	-0.44	-1.18+4.53i	1.48	0.57
?	160.10	-	-	0.06	-3.97	1.32	0.4
17beta-Hydroxyestr-4-en-3-one cyclopentanepropionate	399.29	C14603	[M+H]+	-0.05	-4.27+4.53i	1.28	0.35
?	348.27	-	-	-0.31	-1.70+4.53i	1.31	0.38
?	350.29	-	-	-0.18	-2.44+4.53i	1.38	0.47
?	370.26	-	-	-0.39	-1.34+4.53i	1.46	0.54
?	290.23	-	-	-0.29	-1.77+4.53i	1.37	0.45
?	141.02	-	-	0.57	-0.81	1.15	0.21
?	307.27	-	-	-0.05	-4.20+4.53i	1.41	0.5
?	318.23	-	-	-0.24	-2.07+4.53i	1.43	0.51

Retronecine	156.10	C06177	[M+H]+	0.19	-2.41	1.24	0.31
?	262.20	-	-	-0.17	-2.53+4.53i	1.36	0.44
?	162.11	-	-	0.24	-2.04	1.22	0.28
?	334.29	-	-	-0.39	-1.38+4.53i	1.46	0.55
?	158.09	-	-	0.18	-2.45	1.3	0.38
?	330.26	-	-	-0.28	-1.83+4.53i	1.52	0.6
?	272.22	-	-	0.07	-3.91	1.25	0.33
?	163.11	-	-	0.29	-1.81	1.21	0.28
?	190.11	-	-	0.25	-1.99	1.28	0.35
N2-Acetyl-L-aminoadipate semialdehyde	188.09	C12988	[M+Na]+	0.01	-6.33	1.28	0.36
(S)-5-Oxo-2,5-dihydrofuran-2-acetate	143.03	C14610	[M+H]+	0.63	-0.66	1.14	0.19
?	414.28	-	-	-0.01	-7.38+4.53i	1.2	0.26
?	376.30	-	-	-0.17	-2.54+4.53i	1.29	0.36
Hydroxyatrazine	220.12	C06552	[M+2Na-H]+	-0.07	-3.82+4.53i	1.29	0.37
Atraton	234.13	C19098	[M+Na]+	-0.16	-2.68+4.53i	1.35	0.43
?	304.21	-	-	-0.09	-3.51+4.53i	1.37	0.45
?	335.30	-	-	-0.19	-2.42+4.53i	1.45	0.54
?	276.22	-	-	-0.14	-2.80+4.53i	1.24	0.31
?	328.25	-	-	0.23	-2.13	1.11	0.14
?	238.11	-	-	0.17	-2.53	1.34	0.42
?	304.25	-	-	-0.27	-1.87+4.53i	1.41	0.49
Xylobiose	305.08	C01630	[M+Na]+	0.4	-1.34	1.12	0.17

Supplementary Table 8.3 Fold changes of the 35 most significant metabolites (ANOVA: $p < 0.001$) produced by *T. versicolor* when arranged in 27-block assemblages. Fold changes are calculated as the ratio of the metabolite intensity (mean of 15 replicates: 5 biological replicates x 3 pseudoreplicates) between 27-block cubes comprised solely of *T. versicolor* after 1 d, and each 27-block spatial arrangement 1 d and 28 d after interaction set up. Log_2 of the fold change was calculated for enhanced visualisation of the largest intensity differences (positive and negative values represent increased and decreased production respectively). Wall cube: 27-block assemblages where *V. comedens* occupied a larger adjacent volume, Dispersal cube: 27-block assemblages where the three fungi were dispersed. For metabolites that have been putatively identified, KEGG registry numbers and ion forms are given. Full metabolic peak list with fold changes between each community assemblage is given in Supplementary Table 8.7.

Supplementary Table 8.3

				Fold change (FC)							
				Wall cube 1 d		Dispersal cube 1 d		Wall cube 28 d		Dispersal cube 28 d	
Metabolite	**m/z**	**KEGG number**	**Ion form**	**FC**	**log_2(FC)**	**FC**	**log_2(FC)**	**FC**	**log_2(FC)**	**FC**	**log_2(FC)**
1-Guanidino-1-deoxy-scyllo-inositol	244.09	C04280	[M+Na]+	8.24	3.04	5.17	2.37	7.68	2.94	1.56	0.64
Methylazoxymethanol	113.03	C02390	[M+Na]+	3.24	1.7	2.46	1.3	2.9	1.53	1.34	0.43
?	203.14	-	-	5.65	2.5	4.01	2	4.97	2.31	1.68	0.75
D-Lysopine	219.13	C04020	[M+H]+	5.85	2.55	4.12	2.04	5.16	2.37	1.69	0.76
dethiobiotin	237.12	C01909	[M+H]+	6.62	2.73	4.61	2.21	5.81	2.54	1.81	0.85
(+)-trans-alpha-Irone	247.13	C11350	[M+(41K)]+	6.94	2.8	4.81	2.27	6.1	2.61	1.84	0.88
Luciduline	248.12	C09872	[M+(41K)]+	3.65	1.87	2.82	1.5	3.15	1.66	1.5	0.58
3-Hydroxyhexobarbital	253.12	C03068	[M+H]+	5.43	2.44	3.95	1.98	4.7	2.23	1.73	0.79
?	290.17	-	-	5	2.32	3.52	1.82	4.48	2.16	1.52	0.61
?	302.21	-	-	6.15	2.62	4.18	2.06	5.55	2.47	1.61	0.68
Terbucarb	318.17	C19129	[M+2Na-H]+	6.77	2.76	4.67	2.22	5.98	2.58	1.79	0.84
17beta-Amino-5alpha-androstan-11beta-ol	332.22	C15356	[M+(41K)]+	6.57	2.72	4.53	2.18	5.83	2.54	1.75	0.8
?	390.19	-	-	7.67	2.94	5.21	2.38	6.8	2.77	1.87	0.9
?	231.17	-	-	5.72	2.52	3.97	1.99	5.11	2.35	1.61	0.69
?	245.18	-	-	6.74	2.75	4.64	2.22	5.97	2.58	1.77	0.83
?	374.23	-	-	7.08	2.82	4.83	2.27	6.29	2.65	1.79	0.84
4,4a,5,6,7,8-Hexahydro-6-(p-hydroxyphenyl)-2(3H)-naphthalenone	265.12	C14898	[M+H]+	5.43	2.44	3.72	1.89	4.92	2.3	1.51	0.59
?	343.20	-	-	5.69	2.51	4.04	2.02	4.99	2.32	1.7	0.77

Supplementary Table 8.3 *Continued*

?	274.17	-	-	4.59	2.2	3.27	1.71	4.12	2.04	1.47	0.56
1-epi-Fortimicin B	371.23	C17978	[M+Na]+	4.23	2.08	3.12	1.64	3.72	1.9	1.5	0.59
?	246.19	-	-	8.5	3.09	5.67	2.5	7.59	2.92	1.92	0.94
?	318.20	-	-	5.66	2.5	3.92	1.97	5.07	2.34	1.59	0.67
?	362.19	-	-	6.19	2.63	4.35	2.12	5.43	2.44	1.75	0.81
(+)-7-Isojasmonic acid	233.11	C16317	[M+2Na-H]+	6.04	2.59	4.24	2.09	5.31	2.41	1.73	0.79
?	232.17	-	-	5.72	2.52	3.9	1.96	5.17	2.37	1.54	0.63
?	260.16	-	-	5.76	2.53	4.11	2.04	5.03	2.33	1.73	0.79
?	288.20	-	-	8.31	3.06	5.83	2.54	7.14	2.83	2.18	1.12
17beta-Nitro-5alpha-androstane	346.20	C15281	[M+(41K)]+	5.72	2.52	3.99	2	5.09	2.35	1.63	0.7
Propafenone	382.16	C07381	[M+(41K)]+	4.61	2.2	3.27	1.71	4.14	2.05	1.47	0.55
?	316.19	-	-	9.63	3.27	6.83	2.77	8.11	3.02	2.52	1.33
Amprotropine	348.18	C11760	[M+(41K)]+	6.6	2.72	4.46	2.16	5.94	2.57	1.66	0.73
?	294.14	-	-	4.78	2.26	3.45	1.79	4.22	2.08	1.56	0.64
Serratine	320.14	C09901	[M+(41K)]+	3.51	1.81	2.59	1.37	3.17	1.66	1.34	0.42
?	302.21	-	-	6.44	2.69	4.44	2.15	5.72	2.52	1.72	0.78
?	175.12	-	-	5.2	2.38	3.85	1.94	4.45	2.15	1.75	0.81

Supplementary Table 8.4 Fold changes of the 35 most significant metabolites (ANOVA: $p < 0.001$) between 27-block cubes where *V. comedens* occupied a larger adjacent volume, and 27-block cubes where all three fungi were evenly dispersed. Fold changes are calculated as the ratio of the metabolite intensity between the two assemblages (mean of 15 replicates: 5 biological replicates x 3 pseudoreplicates), after 1 d and 28 d. Log_2 of the fold change was calculated for enhanced visualisation of the largest intensity differences (positive and negative values represent increased and decreased production respectively). For metabolites that have been putatively identified, KEGG registry numbers and ion forms are given. Full metabolic peak list with fold changes between each community assemblage is given in Supplementary Table 8.8.

Supplementary Table 8.4

1 d						28 d					
Metabolite	**m/z**	**KEGG number**	**Ion form**	**FC**	**log_2(FC)**	**Metabolite**	**m/z**	**KEGG number**	**Ion form**	**FC**	**log_2(FC)**
?	271.0052	-	-	1.99	1	Decylubiquinol	365.1921	C15495	[M+(41K)]+	0.62	-0.69
?	272.0087	-	-	1.96	0.97	D-Thevetose	201.0727	C16287	[M+Na]+	1.81	0.86
Miserotoxin	290.0845	C08507	[M+Na]+	0.63	-0.67	Anisomycin	266.1394	C11281	[M+H]+	1.9	0.93
S-Succinyldihydrolipoamide	346.0534	C01169	[M+K]+	2.47	1.3	?	272.0812	-	-	1.6	0.68
GMP	364.0646	-	[M+H]+	2.33	1.22	Spironolactone	439.1914	C07310	[M+Na]+	1.78	0.83
?	151.1475	-	-	0.28	-1.82	?	504.3727	-	-	2.17	1.12
11-Dehydro-thromboxane B2	391.2077	C05964	[M+Na]+	0.52	-0.94	?	629.1464	-	-	0.68	-0.57
AMP	348.0692	-	[M+H]+	2.2	1.14	?	143.1171	-	-	1.51	0.6
Gabaculine	140.0701	C12110	[M+Na]+	1.4	0.49	N6-Acetyl-L-lysine	189.1236	C02727	[M+H]+	1.39	0.47
?	162.1117	-	-	0.66	-0.61	?	204.1224	-	-	1.97	0.98
?	303.2093	-	-	1.61	0.69	Mannopine	311.1454	C16692	[M+H]+	2.08	1.06
Spirasine I	378.2043	C08710	[M+Na]+	1.68	0.75	?	547.1425	-	-	0.76	-0.39
?	249.0216	-	-	1.62	0.7	5'-Phosphoribostamycin	573.1585	C18004	[M+K]+	0.71	-0.5
?	198.1228	-	-	0.51	-0.98	?	403.0996	-	-	0.73	-0.45
L-alpha-Acetyl-N-normethadol	380.1809	C16661	[M+(41K)]+	1.6	0.68	?	127.1112	-	-	1.62	0.7
?	507.1108	-	-	0.69	-0.54	4alpha-formyl-4beta-methyl-5alpha-cholesta-8,24-dien-3beta-ol	427.3556	C15808	[M+H]+	2.63	1.39
?	295.1599	-	-	1.47	0.56	?	471.1107	-	-	1.28	0.35

Supplementary Table 8.4 *Continued*

Nicotinamide	123.0549	C00153	[M+H]+	0.59	-0.76	S-Formylmycothiol	515.155	C06718	[M+H]+	0.73	-0.46
Hydnocarpic acid	293.171	-	[M+(41K)]+	0.58	-0.78	?	548.1451	-	-	0.75	-0.42
?	380.1791	-	-	1.39	0.48	?	341.0836	-	-	1.12	0.17
N-Ethylmaleimide	126.0546	C02441	[M+H]+	1.35	0.43	?	404.1032	-	-	0.7	-0.52
?	246.1882	-	-	1.66	0.73	?	759.2146	-	-	0.61	-0.71
Homocystine	269.0626	C00155	[M+H]+	0.71	-0.5	?	285.0211	-	-	1.29	0.37
?	270.0656	-	-	0.69	-0.54	?	334.0752	-	-	2.04	1.03
?	302.2058	-	-	1.59	0.67	3-ketolactose	363.0891	C05403	[M+Na]+	1.19	0.25
CMP	324.0591	C00055	[M+H]+	2.25	1.17	Mitomycin	375.0887	C06681	[M+Na]+	1.19	0.25
?	360.2121	-	-	1.88	0.91	?	487.1057	-	-	1.25	0.32
?	374.2277	-	-	1.56	0.64	?	205.1239	-	-	1.74	0.8
Spiredine	394.1617	C08711	[M+(41K)]+	1.53	0.62	?	267.1571	-	-	1.89	0.92
Undecanoic acid	231.1329	C17715	[M+2Na-H]+	2.11	1.08	?	367.0996	-	-	0.74	-0.44
?	245.1849	-	-	1.56	0.64	Tributyrin	325.161	C13870	[M+Na]+	1.43	0.52
?	267.1344	-	-	1.72	0.78	Coumatetralyl	333.0721	C16806	[M+(41K)]+	1.93	0.95
(-)-Laudanidine	366.167	C09555	[M+Na]+	1.46	0.54	?	339.0682	-	-	0.75	-0.41
4,4-(Diphenylethenylidene)bis[N,N-dimethylbenzenamine]	419.2466	-	[M+H]+	1.49	0.58	Bis-D-fructose 2',1:2,1-dianhydride	347.0939	C04333	[M+Na]+	1.47	0.56
?	390.1875	-	-	1.61	0.69	?	134.1169	-	-	0.32	-1.64

Supplementary Table 8.5 Fold changes of the 35 most significant metabolites (ANOVA: $p < 0.001$) between *T. versicolor* self-pairings and 27-block community assemblages. Fold changes are calculated as the ratio of the metabolite intensity between *T. versicolor* self-pairings after 1 d (mean of 5 replicates), and each 27-block spatial arrangement 1 d and 28 d after interaction set up (mean of 15 replicates: 5 biological replicates x 3 pseudoreplicates). Log_2 of the fold change was calculated for enhanced visualisation of the largest intensity differences (positive and negative values represent increased and decreased production respectively). Wall cube: 27-block assemblages where *V. comedens* occupied a larger adjacent volume, Dispersal cube: 27-block assemblages where the three fungi were dispersed. For metabolites that have been putatively identified, KEGG registry numbers and ion forms are given. Full metabolic peak list with fold changes between each pair-wise group and community assemblage is given in Supplementary Table 8.9.

Supplementary Table 8.5

				Fold change (FC)							
				Wall cube 1 d		Dispersal cube 1 d		Wall cube 28 d		Dispersal cube 28 d	
Metabolite	m/z	KEGG number	Ion form	FC	log_2(FC)	FC	log_2(FC)	FC	log_2(FC)	FC	log_2(FC)
Deoxynupharidine	274.1389	C09945	[M+2K-H]+	0.54	-0.88	0.72	-0.47	0.6	-0.74	0.67	-0.59
Swainsonine	174.1119	C10173	1 [M+H]+	2.96	1.57	3.45	1.79	4.18	2.06	2.23	1.16
?	267.1571	-	-	0.69	-0.54	0.47	-1.09	0.33	-1.61	0.83	-0.27
?	536.3613	-	-	0.59	-0.77	0.74	-0.44	0.62	-0.68	0.7	-0.52
Fructoselysine	309.166	C16488	[M+H]+	0.67	-0.59	0.51	-0.98	0.37	-1.44	0.8	-0.31
AMP, AMP group, dGMP	348.0692	C00020	[M+H]+	1.52	0.6	2.64	1.4	3	1.59	1.16	0.21
L-alpha-Acetyl-N,N-dinormethadol	366.166	C16662	[M+(41K)]+	1.53	0.61	1.93	0.95	2.17	1.12	1.28	0.36
?	304.2107	-	-	14.11	3.82	13.85	3.79	18.17	4.18	9.79	3.29
?	216.6255	-	-	1.78	0.83	2.11	1.08	2.42	1.28	1.46	0.55
CMP	324.0591	C00055	[M+H]+	1.19	0.25	1.97	0.98	2.16	1.11	1	-0.01
?	520.3674	-	-	0.5	-1.01	0.75	-0.41	0.63	-0.67	0.62	-0.69
?	160.0958	-	-	2.64	1.4	2.64	1.4	3.18	1.67	2.09	1.07
?	204.1224	-	-	0.8	-0.33	0.61	-0.72	0.51	-0.97	0.9	-0.16
1-Guanidino-1-deoxy-scyllo-inositol	244.0908	C04280	[M+Na]+	1.74	0.8	2.44	1.29	2.8	1.49	1.38	0.46
S-Succinyldihydrolipoamide	346.0534	C01169	[M+K]+	1.69	0.76	2.93	1.55	3.36	1.75	1.25	0.33
?	171.0743	-	-	1.37	0.45	1.5	0.59	1.65	0.72	1.22	0.29
1,16-dihydroxyhexadecane	299.218	-	[M+(41K)]+	0.42	-1.24	0.65	-0.62	0.5	-1.01	0.58	-0.79

Supplementary Table 8.5 *Continued*

?	285.1667	-	-	0.75	-0.41	0.54	-0.9	0.42	-1.26	0.87	-0.2
GMP	364.0646	C00144	[M+H]+	1.21	0.27	1.93	0.95	2.11	1.08	1.02	0.03
?	526.3592	-	-	2.44	1.29	2.54	1.35	3.04	1.61	1.95	0.96
?	227.1615	-	-	0.55	-0.88	0.75	-0.42	0.63	-0.67	0.66	-0.59
?	120.1013	-	-	0.33	-1.6	0.54	-0.89	0.35	-1.51	0.52	-0.95
?	268.1605	-	-	0.76	-0.39	0.52	-0.95	0.4	-1.33	0.88	-0.18
Pantothenol	206.1381	C05944	[M+H]+	2.8	1.49	3.57	1.84	4.3	2.1	2.07	1.05
Mannopine	311.1454	C16692	[M+H]+	0.75	-0.41	0.55	-0.86	0.43	-1.21	0.87	-0.21
?	471.1107	-	-	0.99	-0.02	0.83	-0.26	0.8	-0.32	1.02	0.02
?	281.0625	-	-	0.75	-0.41	0.72	-0.47	0.63	-0.66	0.84	-0.25
?	119.1255	-	-	0.89	-0.17	0.67	-0.58	0.59	-0.75	0.96	-0.05
?	190.1066	-	-	1.3	0.38	1.75	0.81	1.92	0.94	1.12	0.17
?	341.0836	-	-	0.91	-0.14	0.83	-0.26	0.79	-0.34	0.95	-0.07
Cytosine	112.0502	C00380	[M+H]+	2.25	1.17	3	1.59	3.54	1.82	1.71	0.77
?	103.0402	-	-	1.2	0.27	0.94	-0.09	0.97	-0.05	1.18	0.24
?	188.1379	-	-	1.87	0.9	1.26	0.33	1.45	0.53	1.68	0.75
Atraton	234.1325	C19098	[M+Na]+	-184.65	7.53+4.53i	-183.89	7.52+4.53i	-245.65	7.94+4.53i	-122.89	6.94+4.53i
?	205.1239	-	-	0.83	-0.26	0.71	-0.5	0.63	-0.67	0.91	-0.14

Supplementary Table 8.6 Full ANOVA model results of pair-wise interaction data. Pair-wise comparisons were made between (1) *T. versicolor* (Tv) self-pairings and interspecific interactions; (2) 1 d and 28 d; and (3) *T. versicolor* self-pairings and interspecific interactions after 1 d and after 28 d. The *p*-value and adjusted *p*-value (q-value) is given for each metabolite in each comparison and metabolites are ranked in order of significane. The fold change (FC) of metabolite intensity between comparisons, and $\log_2$(FC) is shown. Putative annotations of metabolites (MI-pack software version 2 beta and comparison to the KEGG database) are given.

Available online at:

https://www.dropbox.com/s/cdfkxm25havrkkr/Supplementary%20Table%208.6.xlsx?dl=0

Supplementary Table 8.7 Full ANOVA model results of 27-block cubes data. Pair-wise comparisons were made between (1) cubes comprised solely of *T. versicolor* and community interaction cubes; (2) 1 d and 28 d; and (3) cubes comprised solely of *T. versicolor* and community interaction cubes after 1 d and after 28 d. The *p*-value and adjusted *p*-value (q-value) is given for each metabolite in each comparison and metabolites are ranked in order of significane. The fold change (FC) of metabolite intensity between comparisons, and $\log_2$(FC) is shown. Putative annotations of metabolites (MI-pack software version 2 beta and comparison to the KEGG database) are given.

Available online at:

https://www.dropbox.com/s/czovs2kuqna0olo/Supplementary%20Table%208.7.xlsx?dl=0

Supplementary Table 8.8 Full ANOVA model results of 27-block cube data. Pair-wise comparisons were made between all cube assemblages (cubes comprised solely of *T. versicolor*, cubes where *V. comedens* occupied a larger adjacent volune, cubes where all three fungi were evenly dispersed) after 1 d and after 28 d. The *p*-value and adjusted *p*-value (q-value) is given for each metabolite in each comparison and metabolites are ranked in order of significane. The fold change (FC) of metabolite intensity between comparisons, and $\log_2$(FC) is shown. Putative annotations of metabolites (MI-pack software version 2 beta and comparison to the KEGG database) are given.

Available online at:

https://www.dropbox.com/s/9817rtu028sspp9/Supplementary%20Table%208.8.xlsx?dl=0

Supplementary Table 8.9 Full ANOVA model results of *T. versicolor* self-pairings and 27-block community assemblage data. Pair-wise comparisons were made between (1) *T. versicolor* self-pairings and community interaction cubes; (2) 1 d and 28 d; and (3) c *T. versicolor* self-pairings and community interaction cubes after 1 d and after 28 d. The *p*-value and adjusted *p*-value (q-value) is given for each metabolite in each comparison and metabolites are ranked in order of significane. The fold change (FC) of metabolite intensity between comparisons, and $\log_2$(FC) is shown. Putative annotations of metabolites (MI-pack software version 2 beta and comparison to the KEGG database) are given.

Available online at:

https://www.dropbox.com/s/hbqs0od657oxyim/Supplementary%20Table%208.9.xlsx?dl=0

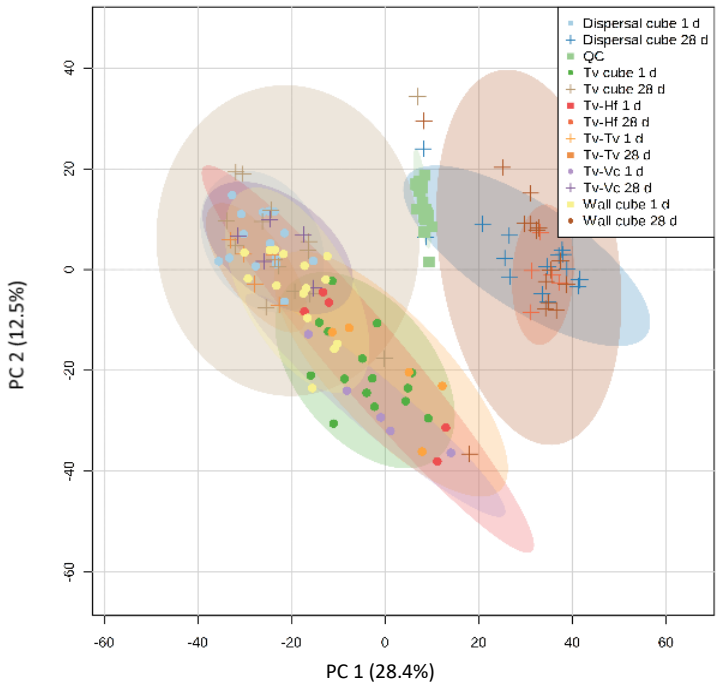

Supplementary Figure 8.1 PCA scores plot with QC clustering. Plot is derived from PCA of the UHPLC-MS spectra of all pair-wise and 27-block interactions, 1 d (circles) and 28 d (crosses) after interaction set up. QCs (squares) are closely clustered with a median RSD of 11.15 % indicating high quality of the data. QCs were subsequently removed from the matrix and ASCA performed on the standardised binned data.